

C(sp³)–H Activation *via* Dehydrogenation of Cyclic
and Heterocyclic Alkanes by Single-Site Iridium
Pincer Ligated Complexes

Thesis by
Zainab Ahmed Al-Saihati

In Partial Fulfillment of the Requirements for
the degree of
Doctor of Philosophy

The logo for the California Institute of Technology (Caltech), featuring the word "Caltech" in a bold, orange, sans-serif font.

CALIFORNIA INSTITUTE OF TECHNOLOGY
Pasadena, California

2020
(Defended May 29th, 2020)

© [2020]

Zainab Ahmed Al-Saihati
ORCID: 0000-0002-3837-9736

Dedicated To my Mom and Dad, my Husband Abdulaziz, and my son Talal

<3

ACKNOWLEDGEMENTS

Caltech is truly a special place filled with people that are eager to learn and are hungry for knowledge. The excellent resources provided by Caltech to conduct research at a top level has also added to the depth of my experience. I feel honored to have been part of the community at Caltech, a community that has motivated me to continuously learn and grow.

I would like to express my deepest gratitude to my co-advisors **Professor Robert H. Grubbs** and **Professor Brian M. Stoltz**. I feel deeply privileged to have spent the last five years being co-advised not only by one renowned scientist and mentor, but by two.

I would like to thank **Professor Robert H. Grubbs (Bob)**, for providing me the opportunity to join his lab and conduct research under his mentorship. His approach granted me the appropriate degrees of freedom to work on areas that deeply interested me and sparked my passionate curiosity. His mentorship has crafted me into an independent scientist and thinker. Additionally, Bob has been incredibly supportive with his advice and willingness to answer my questions. I deeply respect Bob not only for being an intelligent chemist and a Nobel Laureate, but also for being very humble and grounded, which truly reflects how wonderful he is as an advisor and as a person. I have enjoyed all of the stories he has shared with me, in addition to his deep knowledge about science.

I would also like to thank **Professor Brian M. Stoltz** for being my co-advisor through my PhD career and for being a great mentor. Brian always encouraged me to push my boundaries and think of chemistry deeply and science more broadly. Brian's passion about chemistry truly comes through and has always inspired and motivated me to become a better and well-rounded scientist. When in doubt about chemistry or even myself, Brian

possessed a special power that always made me feel better and ready to embark on the next step whenever I talked to him.

Beyond my scientific journey, Bob and Brian have also supported me personally, particularly when I became pregnant during my graduate research. I was overwhelmed by how supportive they were and how much they cared about me and my safety. I'm forever grateful for them because honestly, they truly made every impediment through the PhD journey easier to overcome.

I would like to thank **Professor Theodor Agapie** and **Professor David A. Tirrell** for being very supportive members of my committee, and for asking difficult questions that allowed me to think critically about the quality of the work I presented. They helped me seek answers to important problems and I have always valued their input and advice during our meetings. I would also like to thank Professor Sarah E. Reisman for her feedback and comments during the joint Stoltz/Reisman group meetings that made me think beyond the scope of work I do. She was also very supportive and helpful when we discussed life/work balance issues. She shared with me valuable information about childcare for my son, which I deeply appreciate.

I extend my gratitude to Caltech's staff that work hard every day to ensure that our daily routine work and research runs smoothly. In particular, I would like to thank Alison Ross for her logistical and emotional support during stressful periods through my PhD journey. I am also thankful to Elizabeth Callihan for providing me a private office to use as a lactation room for my son. I'm also grateful for Linda Syme, Lynne Martinez, and

Beth Marshall for their continuous support and promptness when scheduling meetings with my advisors.

I'm very grateful to Dr. Scott Virgil, Dr. David Vander Velde, Rick Gerhat, Naseem Torian, and Dr. Mona Shahgholi for maintaining instrumentation and glassware. They are truly outstanding resources to Caltech's scientific community and I highly appreciate their commitment and support when needed.

It has been a pleasure to work with everyone in the Grubbs lab and I have learned at least one thing from each member I overlapped with, which reflects how helpful and supportive everyone was. I would not be here today without **Dr. Michael Haibach's** (Mike) and **Dr. Nicholas Swisher's** (Nick) help and mentorship at the beginning of my PhD career. Mike helped me start my PhD research and guided me through the experiments with patience. He addressed all of my questions and since my research background was from a different field, his approach and manner were much appreciated. I've enjoyed our friendship outside of the lab by participating in group hikes and adventures that he so thoughtfully arranged. Likewise, I would like to thank Nick for the intellectual discussions and advice he provided me. I enjoyed his company in the lab and it was nice to have someone working with especially during late nights. I would also like to thank **Dr. Jeong Hoon Ko**, **Dr. Yan Xu**, and **Dr. William Wolf** for all their help, support, and friendship during the last two years of my PhD journey. I enjoyed and learned from all the scientific discussions we've had.

In addition, I would like to thank Dr. Michael Schulz, Dr. TP Lin, Dr. Patrick Montgomery, Dr. Karthish Manthiram, Dr. Chris Marotta, Dr. Noah Fine Nathel, Dr. Jiaming Li, Dr. Allegra Liberman-Martin, Dr. Sankarganesh Krishnamoorthy, Dr. Carl Blumenfeld, Dr. Tonia Ahmed, Dr. Julian Edward, and Quan Gan for their help, support, and friendship through my PhD journey. I would like to especially thank Dr. Crystal Chu, Dr. Lauren Rosebrugh, and Dr. Alice Chang for making my time in the Grubbs lab enjoyable. I have enjoyed our friendship and our time outside the lab whether it be dining out, making Sunday brunches, getting massages, or just complaining about life. I would like to thank past and current members of the Grubbs lab and everyone I overlapped with during my time at Caltech. I would also like to thank the Stoltz lab members for always helping me and answering any questions I had. I would like to especially thank my cohort from the Stoltz lab: Fa Ngamnithiporn, Carina Jette, Dr. Eric Alexy, and Chris Reimann. I'm also thankful for the friendships I made at Caltech and I'm grateful for getting to know Siobhan MacArdle, Elise Tookmanian, Katherine Rinaldi, Alex Sorum, Alexandra Barth, Jeremy Tran, and Joey Messenger, and Faisal Alshafei.

Being part of Women in Chemistry (**WiC**) club was enjoyable and purposeful. I was honored to be a committee member of **WiC** for two years and I enjoyed networking with and meeting aspiring women in the field. I also learned a lot from the intellectual discussions and events we organized relating to women issues in STEM. I also enjoyed hosting IOS seminars for one year and learning about the amazing science that takes place at Caltech.

My experience at Caltech made me grow as a scientist and as a person. I'm grateful to my employer **Saudi Aramco** for fully sponsoring me throughout the whole PhD journey at Caltech and for providing financial and logistical support. They have truly shown me that they care about their employees by continuously being in contact with me and following up on my progress at Caltech. In addition, especially during COVID-19 pandemic, they have extended their support by contacting me on weekly basis to ensure that my family and I are safe. They also provided me with all the supplies I needed to feel safe including masks and sanitizers, at a time where the rest of the world is running out of. I'm thankful to my mentor at Saudi Aramco, **Dr. David McLeary**, whom I worked with prior to joining Caltech. Dr. McLeary always pushed me to excel and I appreciate his belief in me. He taught me how to conduct fundamental research at the highest level and set high standards for me. He supported me at my career in Saudi Aramco, leveraged my knowledge about the oil and gas industry, and also encouraged and guided me when applying to graduate schools.

Beyond the scientific community, first and foremost, I'm deeply grateful to **my parents** who are the reason I started my journey at Caltech. Since a young age, my parents always supported and loved me for who I am. At a time where women were dictated by a male legal guardian in Saudi Arabia, **my dad** granted me freedom to travel and explore the world through the lens of my eye. He always believed in me and trusted that I'd do what's right for me. **My mom**, who is the kindest and most giving person I've ever known in my life, instilled the love of learning in me since I was young. She taught me that the sky is my limit and that there is nothing I can't do if I set my mind to it. She is also the person

that calms me down when I'm extremely stressed and the one I find comfort in. Because of my parents, I embarked on my first major life journey at The University of Texas at Austin (UT Austin) on my own and my success is forever indebted to their support. They have truly given me wings to fly, roots to come back to, and reasons to stay at home.

I am immensely thankful and grateful to my husband, **Abdulaziz**, who is the reason why I'm finishing my PhD today. Abdulaziz supported me in every step of my PhD journey, especially during stressful times. Writing my thesis during quarantine because of COVID-19 pandemic, has been especially challenging with a teething 10-month old baby. But Abdulaziz made every part of it easier. He's shown me that not only he is a wonderful husband, but also a great father who I could depend to take care of our son Talal at times like this when I'm extremely busy. He's shown me that he is the strength I lean on, the shoulder I cry on, the ears that always listen to me, and the soul that has given me light. Abdulaziz is the reason why I wake up with a smile every day, and I would not have finished my PhD journey without him by my side. Abdulaziz is my best friend, the love of my life, and the best father to our son. We are very fortunate to have found each other and I am looking forward to experiencing the next chapter of our life together. I love you.

I am forever grateful for my son **Talal** who has chosen me to be his mother and given me purpose in life. His smile motivated me every day to finish the last bits of my PhD journey. Talal was born 9 weeks premature and struggled in his first two months of life, but he has shown me what it means to be strong and resilient. He has shown me what it means to love unconditionally and to enjoy precious moments in life. I love you Talal,

and I will always support the person you will grow into and become. I will always remember to fight like a preemie, just like you did.

I would like to thank each one of my siblings: Jumana, Rami, Ali, Bayan, Rabie, and Bandar. Growing up in a large family has taught me that it's okay to be different but that it is also important to accept one another. Each one of us have developed different views of life and it's amazing how much we've learned from each other. I've learned from **Jumana** to be bold, enjoy life and celebrate it, and to defy society norms. I've learned from **Rami** to set high standards for myself, challenge my comfort zone, and support my family. I've learned from **Ali** to extremely appreciate our roots and where we come from, to value our culture, and to be persistent. Growing up, **Bayan** is two years older than me and was my partner in crime and the sibling that I spent time with the most, and she was also the one that I knew I could count on. I learned from her to be courageous and strong, to be adventurous, and to always be motivated. Rabie and Bandar are my younger siblings and have become very close to me in the recent years. I learned from **Rabie** what it means to be humble and kind, to love one another, and to be patient during stressful times. I learned from **Bandar** to fight for what I want, to be perseverant, and to critically think about life choices. Every one of them have supported me while being away from home and I'm grateful and proud to be their sibling. I would like to especially thank **my sisters** who are strong beautiful women and shaped the woman I am today. I'm also thankful to Rami's wife, my sister in-law **Hanadi**, who has always been kind and supportive, and is a wonderful and a patient mother to my three beautiful and mischievous nephews **Faris**,

Yousef, and **Ahmed**. I'm thankful to everyone in my extended family including my aunts, uncles, and cousins for all their love and support.

I'm thankful to my **in-laws**, especially **Abdulaziz's parents (Uncle Abdullah and Auntie Shaikhah)** who have supported us throughout the years we've been married. I've learned from my in-laws what it means to value family and support one another. I'm grateful for their support and that I have an amazing second family. Thank you **Areej** and **Medhat**, **Najeeb** and **Nour**, **Sol** and **Nu**, **Elaf** and **Khaled**, **Ali** and **Afnan**, and sweet **Asma** for all your support.

I'm also thankful to all my friends I've made outside Caltech that supported me through this journey. I'm especially thankful to **Lubna Barghouty**, who is an aspiring geophysicist, a wonderful mother, and just a brilliant person. I'm very lucky that our paths crossed and that I call her my best friend. She is a person that I look up to and taught me what it means to be hard working. I'm very thankful to all her support throughout my journey at UT Austin and at Caltech, she always reminded me to believe in myself and to trust my potential. I'm also thankful to my childhood best friend **Ghadeer Al-Awami**, who throughout the years have been there for me no matter how far apart we were. I've known Ghadeer since first grade and I'm lucky we maintained our friendship until this day. I'm also thankful to her family who extended their support when I was at UT Austin and treated me like their own daughter. I'm thankful to **Emily Andry** who has shown me how to live life and embrace it. She is truly a kind and genuine person and I'm lucky to have known her. Her joyous smile and positive soul always encouraged me and supported me even when in doubt about myself.

My PhD journey at Caltech has been challenging and rewarding at the same time.

And it would not have been half as wonderful without the support I received from everyone around me from all over the world. I'm extremely grateful for all the love and support I received from everyone, whether be it a text, a call, a visit, or just a positive thought. Thank you from the bottom of my heart to all of you.

ABSTRACT

The direct dehydroaromatization of C(sp³)–H alkanes may seem conceptually simple but in fact is a challenging transformation. Industrially practiced methods utilize energy-intensive processes operating at high pressures and temperatures due to the requirement of such conditions to overcome the endergonic and unreactive nature of alkanes. **Chapter 1** briefly discusses early and recent achievements in the field of alkanes dehydrogenation by Ir pincer ligated complexes. While there has been great advancement in the dehydrogenation transformation recently, the direct dehydroaromatization of heterocyclic substrates generating functionalized aromatics is significantly underdeveloped. In **Chapter 2**, we successfully extended the applicability of Ir-catalyzed dehydrogenation systems using pincer ligated complexes on a diverse collection of heterocyclic alkanes with functionalities known to be strongly coordinating and poorly compatible with (PCP)–Ir type catalysts. Carbo- and heteroarenes containing oxygen and nitrogen can be synthesized in moderate to excellent yields up to 99%, and the reaction tolerates functional groups such as bromides and fluorides. In **Chapter 3**, we demonstrate the efficient disproportionation of cycloalkenes to the corresponding arenes and cycloalkanes with up to 100% conversion, which has been a long-standing challenge in the field of pincer-ligated Ir-catalyzed dehydrogenation studies. For example, 1-cyclohexene was disproportionated to benzene and cyclohexane and 1-4-vinyl-1-cyclohexene was disproportionated to ethylbenzene and ethylcyclohexane. We also demonstrate that a key mechanistic feature of our system is a lack of catalyst inhibition by arenes. In addition, our method is advantageous to previous reports as no sacrificial olefin is used, thereby circumventing the requirement for exogenous hydrogen acceptors. Our studies presented in **Chapter 2** and **Chapter 3** provides a novel

and a complementary pathway to access important aromatic building blocks and may help create alternative routes to complex molecules *via* late stage dehydrogenation without the need of stoichiometric oxidants.

PUBLISHED CONTENT AND CONTRIBUTIONS

Zainab A. Al-Saihati[†], Michael C. Haibach, Brian M. Stoltz, and Robert H. Grubbs.
“C(sp³)–H Dehydroaromatization of Cyclic and Heterocyclic Alkanes *via* Iridium Pincer
Ligated Complexes” **2020** (Submitted).

[†]ZAS led the project design, experimental work, data acquisition and analysis, and manuscript preparation and writing. This work is discussed in Chapter 2 and 3 and related appendices.

TABLE OF CONTENTS

Dedication	iii
Acknowledgements	iv
Abstract	xiii
Published Content and Contributions	xv
Table of Contents	xvi
List of Figures	xxiii
List of Schemes	xxx
List of Tables	xxxvi
List of Abbreviations	xl
Chapter 1:	1
<i>Alkane C(sp³)-H Dehydrogenation Catalyzed by Single-Site Iridium Catalysis</i>	
1.1 Introduction	1
1.2 Challenges of C(sp ³)-H Alkanes Dehydrogenation	4
1.3 Early Examples of C(sp ³)-H Dehydrogenation Using Iridium Homogeneous Catalysts.....	7
1.4 Recent Examples of C(sp ³)-H Dehydrogenation Using Iridium Pincer Ligated Complexes	9
1.5 Pincer-Ligated Iridium-Catalyzed C(sp ³)-H Dehydrogenation Mechanism	12
1.6 Conclusions	14

1.7 Notes and References	16
Chapter 2:	22
<i>C(sp³)-H Dehydroaromatization of Cyclic and Heterocyclic Alkanes Catalyzed by Iridium Pincer Ligated Complexes</i>	
2.1 Introduction	22
2.2 Related Literature.....	23
2.3 Iridium Pincer Ligated Complexes Synthesis and Application on COA/TBE System.....	29
2.3.1 Synthesis of (<i>t</i> -Bu ⁴ PCP)-Ir Complex c3	29
2.3.2 Synthesis of (<i>t</i> -Bu ⁴ POCOP)-Ir Complex c13/c13a	31
2.3.3 Synthesis of (<i>i</i> -Pr ⁴ PSCOP)-Ir Complex c22	32
2.3.4 Synthesis of (<i>i</i> -Pr ⁴ Anthraphos)-Ir Complex c24	34
2.3.5 COA/TBE Transfer Dehydrogenation System and Reaction Set-Up Investigation.....	35
2.4 Transfer Dehydrogenation of Heterocyclic Alkanes Catalyzed by Iridium Pincer Ligated Complexes	39
2.4.1 6-Methoxy-1,2,3,4-Tetrahydronaphthalene Transfer Dehydrogenation	39
2.4.2 Indane Transfer Dehydrogenation.....	44
2.4.3 6-Methoxy-1,2,3,4-Tetrahydroquinoline Transfer Dehydrogenation	48
2.4.4 7-Bromo-1,2,3,4-Tetrahydroisoquinoline Transfer Dehydrogenation	51
2.4.5 Tetralone Derivatives Transfer Dehydrogenation	54
2.4.6 Acenaphthene Transfer Dehydrogenation	60

2.5 Summary and Conclusions	64
2.6 Notes and References	67
Appendix 1:	76
<i>Experimental Section and Spectra Related to Chapter 2</i>	
A1.1 Materials and Methods	76
A1.2 Known Iridium Pincer Ligated Complexes General Synthesis	
Procedure	79
A1.2.2 Synthesis of (<i>t</i> -Bu ⁴ PCP)IrHCl c3 and (<i>t</i> -Bu ⁴ PCP)IrH ₄ c3b Complexes	79
A1.2.2 Synthesis of (<i>t</i> -Bu ⁴ POCOP)IrHCl c13 and (<i>t</i> -Bu ⁴ POCOP)IrC ₂ H ₄ c13a Complexes	81
A1.3 Notes and References	82
A1.4 Relevant Spectra	83
Appendix 2:	97
<i>C(sp³)-H Dehydrogenation Attempts of Challenging Heterocyclic Alkanes by Iridium Pincer Ligated Complexes</i>	
A2.1 Introduction	97
A2.2 Attempts to Transfer Dehydrogenation Piperidine and N-Methylpiperidine.....	98
A2.3 Attempts to Transfer Dehydrogenate Five-Membered Ring Derivatives	100
A2.3.1 Investigations of 5-Methoxy-1-Indanone Transfer Dehydrogenation.....	101
A2.3.2 Investigations of 1-Chlorocyclopentene Transfer Dehydrogenation.....	102

A2.3.3 Investigations of 5-Iodo-2,3-Dihydrobenzofuran Transfer Dehydrogenation	102
A2.3.4 Investigation of 4-Aminoindan Transfer Dehydrogenation	103
A2.4 Attempts to Transfer Dehydrogenate Carbonyl Containing Cyclic Alkane Derivatives	104
A2.4.1 Investigations of 7-Bromo-1-Tetralone Transfer Dehydrogenation	105
A2.4.2 Investigations of Tetrahydrothiopyran-4-one Transfer Dehydrogenation	106
A2.4.3 Investigations of 4 Methoxy 5,6,7,8-Tetrahydronaphthalene -1-Carbaldehyde Transfer Dehydrogenation	107
A2.4.4 Investigations of 8-Fluoro-1-Benzosuberone Transfer Dehydrogenation	107
A2.4.5 Investigations of 5,6,7,8-Tetrahydro-2-Naphthoic Acid Transfer Dehydrogenation	109
A2.4.6 Investigations of 1-Acetylcyclohexene Transfer Dehydrogenation	110
A2.4.7 Synthesis of 3-(4-Bromo-2-Fluorophenyl)Cyclohexan-1-one and Transfer Dehydrogenation Attempts	111
A2.4.8 Investigations of 6-Methoxy-3,4-Dihydronaphthalen-1(2H) -one Transfer Dehydrogenation	112
A2.5 Attempts to Transfer Dehydrogenate Cyclohexyl Derivatives	113
A2.5.1 Investigations of 1,4-Thioxane Transfer Dehydrogenation	114
A2.5.2 Investigations of 2-Cyclohexene-1-Acetonitrile Transfer Dehydrogenation	115
A2.5.3 Investigations of Phenylcyclohexane Transfer Dehydrogenation	116

A2.5.4 Investigations of 1-Bromo-4-Cyclohexylbenzene Transfer Dehydrogenation.....	116
A2.5.5 Investigations of 3-Bromo-Cyclohexene Transfer Dehydrogenation.....	117
A2.5.6 Investigations of Chlorocyclohexane Transfer Dehydrogenation.....	118
A2.5.7 Investigations of 1-(Trimethylsiloxy)Cyclohexene Transfer Dehydrogenation.....	119
A2.5.8 Investigations of Julolidine Transfer Dehydrogenation ..	120
A2.5.9 Investigations of Paroxetine Transfer Dehydrogenation.	120
A2.6 Summary and Conclusions.....	122
A2.7 Notes and References	125
Appendix 3:	127
<i>Experimental Section and Spectra Relevant to Appendix 2</i>	
A3.1 Materials and Methods.....	127
A3.2 General Procedure for Dehydrogenation Reactions.....	129
A3.3 Synthesis Procedure of 3-(4 Bromo-2-Fluorophenyl) Cyclohexan-1-one.....	130
A3.4 ¹ H NMR Spectra of Reactions.....	131
Appendix 4:	145
<i>Progress Toward the Synthesis of a Novel Asymmetric NHC-Phosphonite Hybrid Pincer Ligand</i>	
A4.1 Introduction.....	145
A4.2 Related Literature	147
A4.3 Synthesis of ^t -Bu ² Mes-NHCCOP Ligand	149

A4.4 Summary and Future Work.....	150
A4.5 Notes and References	152
A4.6 Experimental Section and Spectra	153
A4.6.1 Materials and Methods	153
A4.6.2 General Procedure of $t\text{-Bu}^2\text{Mes-NHCCOP}$ Ligand 91 Synthesis.....	154
A4.6.3 NMR Spectra	157
Chapter 3:	163
<i>$C(sp^3)\text{-H}$ Dehydroaromatization of 1-Cyclohexene and 4-Vinyl-1-Cyclohexene via Disproportionation Catalyzed by Ir Pincer Ligated Complexes</i>	
3.1 Introduction	163
3.2 Related Literature.....	164
3.3 1-Cyclohexene Disproportionation by Iridium Pincer Ligated Complexes.....	169
3.4 4-Vinyl-1-Cyclohexene Disproportionation by Complex ($t\text{-Bu}^4\text{POCOP}$)–Ir.....	175
3.5 Summary and Conclusions	177
3.6 Notes and References	180
Appendix 5:	182
<i>Experimental Section and Spectra Related to Chapter 6</i>	
A5.1 Materials and Methods.....	182
A5.2 Relevant Spectra.....	185

Comprehensive Bibliography	200
---	------------

About the Author	215
-------------------------------	------------

LIST OF FIGURES

Chapter 1

ALKANE C(SP³)-H DEHYDROGENATION BY SINGLE-SITE METAL CATALYSIS

Figure 1.1 Most Important Building Blocks and Current Industrial Production ..	2
Figure 1.2 Substituted Aromatics in Drugs and Industrial Synthesis	3
Figure 1.3 Examples of Presented Work in Chapters 2 and 3.....	4
Figure 1.4 σ -Bonds vs. π -Bonds Molecular Orbitals	5
Figure 1.5 Thermodynamic Equilibrium Conversion of n-Alkane Dehydrogenation	6
Figure 1.6 Recent Developments in Iridium Pincer Complexes.....	11

Chapter 2

C(SP³)-H DEHYDROAROMATIZATION OF CYCLIC AND HETEROCYCLIC ALKANES CATALYZED BY IRIIDIUM PINCER LIGATED COMPLEXES

Figure 2.1 Ir Pincer Ligated Complexes Utilized as Dehydrogenation Catalysts	24
Figure 2.2 (a) ³¹ P NMR of (t-Bu ⁴ PCP)IrHCl c3 Before the Reaction (b) ³¹ P NMR of (t-Bu ⁴ PCP)IrHCl c3 After Heating the Reaction Mixture in Table 2.1 Entry 7.....	38
Figure 2.3 Temperature Effect on (t-Bu ⁴ POCOP)-Ir c13 Catalytic Activity as Dehydrogenation Catalyst of 6-Methoxy-1,2,3,4-Tetrahydronaphthalene 10 ..	44

Appendix 1

EXPERIMENTAL SECTION AND SPECTRA RELEVANT TO CHAPTER 2

Figure A1.1 ¹ H NMR (400 MHz, C ₆ D ₆) of Complex c3a	83
---	----

Figure A1.2 ^1H NMR (400 MHz, C_6D_6) of Complexes c3/c3b	84
Figure A1.3 ^{31}P NMR (400 MHz, C_6D_6) of Complex c3a	85
Figure A1.4 ^{31}P NMR (400 MHz, C_6D_6) of Mixture of Complexes c3/c3b	85
Figure A1.5 ^1H NMR (400 MHz, C_6D_6) of Ligand 3	86
Figure A1.6 ^{31}P NMR (400 MHz, C_6D_6) of Ligand 3	87
Figure A1.7 ^1H NMR (400 MHz, C_6D_6) of Ligand c13	88
Figure A1.8 ^{31}P NMR (400 MHz, C_6D_6) of Complex c13	89
Figure A1.9 ^{31}P NMR (400 MHz, C_6D_6) of Complex c13a	89
Figure A1.10 Table 2.3 Entry 6 ^1H NMR	90
Figure A1.11 GC Spectra of 10 Crude Reaction	90
Figure A1.12 Table 2.4 Entry 8 ^1H NMR	91
Figure A1.13 GC Spectra of 12 Crude Reaction	91
Figure A1.14 Table 2.5 Entry 5 ^1H NMR	92
Figure A1.15 GC Spectra of 14 Crude Reaction	92
Figure A1.16 Table 2.6 Entry 4 ^1H NMR	93
Figure A1.17 GC Spectra of 16 Crude Reaction	93
Figure A1.18 Table 2.7 Entry 4 ^1H NMR	94
Figure A1.19 GC Spectra of 18 Crude Reaction	94
Figure A1.20 Table 2.8 Entry 9 ^{19}F NMR	95
Figure A1.21 GC Spectra of 20 Crude Reaction	95
Figure A1.22 Table 2.9 Entry 3 ^1H NMR	96
Figure A1.23 GC Spectra of 22 Crude Reaction	96

Appendix 2

C(SP³)-H DEHYDROGENATION ATTEMPTS OF CHALLENGING HETEROCYCLIC ALKANES BY IRIIDIUM PINCER LIGATED COMPLEXES

Figure A2.1 Complex (*t*-Bu₄PCP)-Ir **c3** Chemical Structure 100

Figure A2.2 Summary of Investigated Substrate Scope in Appendix 2..... 124

Appendix 3.....

EXPERIMENTAL SECTION AND SPECTRA RELEVANT TO APPENDIX 2

Figure A3.1 Table A2.1 Entry 1 Crude Reaction of Piperidine 131

Figure A3.2 Table A2.1 Entry 5: Crude Reaction of Piperidine 131

Figure A3.3 Table A2.1 Entry 6: Crude Reaction of Piperidine 132

Figure A3.4 Scheme A2.1: Crude Reaction of N-Methylpiperidine 132

Figure A3.5 Scheme A2.2: Crude Reaction of 5-Methoxy-1-Indanone 133

Figure A3.6 Scheme A2.3: Crude Reaction of 1-Chlorocyclopentene 133

Figure A3.7 Table A2.2 Entry 1: Crude Reaction of 5-Iodo-
2,3-Dihydrobenzofuran 134

Figure A3.8 Table A2.2 Entry 2: Crude Reaction of 5-Iodo-
2,3-Dihydrobenzofuran..... 134

Figure A3.9 Scheme A2.4: Crude Reaction of 4-Aminoindan 135

Figure A3.10 Scheme A2.5: Crude Reaction of 7-Bromo-1-Tetralone 135

Figure A3.11 Scheme A2.7: Crude Reaction of Tetrahydrothiopyran-4-one 136

Figure A3.12 Scheme A2.8: Crude Reaction of 4-Methoxy-5,6,7,8-
Tetrahydronaphthalene-1-Carbaldehyde..... 136

Figure A3.13 Scheme A2.9: Crude Reaction of 8-Fluoro-1-Benzosuberone 137

Figure A3.14 Scheme A2.10: Crude Reaction of 5,6,7,8-Tetrahydro-2-Naphthoic Acid	137
Figure A3.15 Scheme A2.11: Crude Reaction of 1-Acetylcyclohexene	138
Figure A3.16 Scheme A2.12: ¹ H NMR of Synthesized 3-(4-Bromo-2-Fluorophenyl)Cyclohexan-1-one	138
Figure A3.17 Scheme A2.13: Crude Reaction of 3-(4-Bromo-2-Fluorophenyl)Cyclohexan-1-one	139
Figure A3.18 Scheme A2.14: Crude Reaction of 6-Methoxy-3,4-Dihydronaphthalen-1(2H)-one	139
Figure A3.19 Scheme A2.15: Crude Reaction of 1,4-Thioxane	140
Figure A3.20 Scheme A2.16: Crude Reaction of 2-Cyclohexene-1-Acetonitrile	140
Figure A3.21 Scheme A2.17: Crude Reaction of Phenylcyclohexane	141
Figure A3.22 Scheme A2.18: Crude Reaction of 1-Bromo-4-Cyclohexylbenzene	141
Figure A3.23 Scheme A2.19: Crude Reaction of 3-Bromocyclohexene	142
Figure A3.24 Scheme A2.20: Crude Reaction of 3-Bromocyclohexene	142
Figure A3.25 Schemes A2.21 and A2.22: Crude Reaction of Chlorocyclohexane	143
Figure A3.26 Schemes A2.23: 1-(Trimethylsiloxy)Cyclohexene	143
Figure A3.27 Scheme A2.24: Crude Reaction of Unreacted Julolidine	144
Figure A3.28 Scheme A2.25: Crude Reaction of Paroxetine	144

Appendix 4

PROGRESS TOWARD THE SYNTHESIS OF A NOVEL ASYMMETRIC NHC-PHOSPHONITE HYBRID Pincer LIGAND

Figure A4.1 Various Reported Ir Pincer Ligated Complexes	146
Figure A4.2 Proposed Novel Asymmetric NHC-Phosponite Complex (<i>t</i> -Bu ₂ Mes_NHCCOP)–Ir c31	147
Figure A4.3 ¹ H NMR (400 MHz, Chloroform- <i>d</i>) of 88	157
Figure A4.4 ¹³ C NMR (101 MHz, Chloroform- <i>d</i>) of 88	158
Figure A4.5 ¹ H NMR (400 MHz, DMSO- <i>d</i> ₆) of 90	159
Figure A4.6 ¹³ C NMR (101 MHz, DMSO- <i>d</i> ₆) of 90	160
Figure A4.7 ¹ H NMR (400 MHz, C ₆ D ₆ - <i>d</i>) of 91	161
Figure A4.8 ³¹ P NMR (162 MHz, Benzene- <i>d</i> ₆) of 91	162

Chapter 3

C(SP³)–H DEHYDROAROMATIZATION OF 1-CYCLOHEXDENE AND 4-VINYL- 1-CYCLOHEXENE VIA DISPROPORTIONATION CATALYZED BY IR Pincer LIGATED COMPLEXES

Figure 3.1 1-Cyclohexene Disproportionation Conversion by Complex (<i>t</i> -Bu ₄ POCOP)–Ir c13	175
--	-----

Appendix 5

EXPERIMENTAL SECTION AND SPECTRA RELEVANT TO CHAPTER 3

Figure A5.1 Table 3.2 Entry 3 ¹ H NMR	185
Figure A5.2 GC Spectra of 77 Crude Reaction	185
Figure A5.3 Table 3.3 Entry 1 (AVG 77 Conversion) ¹ H NMR	186

Figure A5.4 Table 3.3 Entry 2 (AVG 77 Conversion) ^1H NMR.....	186
Figure A5.5 Table 3.3 Entry 3 (AVG 77 Conversion) ^1H NMR.....	187
Figure A5.6 Table 3.3 Entry 4 (AVG 77 Conversion) ^1H NMR.....	187
Figure A5.7 Table 3.3 Entry 5 (AVG 77 Conversion) ^1H NMR.....	188
Figure A5.8 Table 3.3 Entry 6 (AVG 77 Conversion) ^1H NMR.....	188
Figure A5.9 Table 3.3 Entry 7 (AVG 77 Conversion) ^1H NMR.....	189
Figure A5.10 Table 3.3 Entry 8 (AVG 77 Conversion) ^1H NMR.....	189
Figure A5.11 Table 3.3 Entry 9 (AVG 77 Conversion) ^1H NMR.....	190
Figure A5.12 Table 3.3 Entry 10 (AVG 77 Conversion) ^1H NMR.....	190
Figure A5.13 (Spiked With 50% Benzene) @ 0 Min ^1H NMR.....	191
Figure A5.14 Table 3.3 Entry 1 (Spiked With 50% Benzene) ^1H NMR.....	191
Figure A5.15 Table 3.3 Entry 2 (Spiked With 50% Benzene) ^1H NMR.....	192
Figure A5.16 Table 3.3 Entry 3 (Spiked With 50% Benzene) ^1H NMR.....	192
Figure A5.17 Table 3.3 Entry 4 (Spiked With 50% Benzene) ^1H NMR.....	193
Figure A5.18 Table 3.3 Entry 5 (Spiked With 50% Benzene) ^1H NMR.....	193
Figure A5.19 Table 3.3 Entry 6 (Spiked With 50% Benzene) ^1H NMR.....	194
Figure A5.20 Table 3.3 Entry 7 (Spiked With 50% Benzene) ^1H NMR.....	194
Figure A5.21 Table 3.3 Entry 8 (Spiked With 50% Benzene) ^1H NMR.....	195
Figure A5.22 Table 3.3 Entry 9 (Spiked With 50% Benzene) ^1H NMR.....	195
Figure A5.23 Table 3.3 Entry 10 (Spiked With 50% Benzene) ^1H NMR.....	196
Figure A5.24 Table 3.3 Entry 11 (Spiked With 50% Benzene) ^1H NMR.....	196
Figure A5.25 Table 3.3 Entry 12 (Spiked With 50% Benzene) ^1H NMR.....	197
Figure A5.26 Table 3.3 Entry 13 (Spiked With 50% Benzene) ^1H NMR.....	197
Figure A5.27 Table 3.4 Entry 3 ^1H NMR.....	198

Figure A5.28 GC Spectra of **81** Crude Reaction..... 198

Figure A5.29 Scheme 3.7 ^1H NMR of Crude Reaction 199

LIST OF SCHEMES

Chapter 1

ALKANE $C(SP^3)$ -H DEHYDROGENATION BY SINGLE-SITE METAL CATALYSIS

Scheme 1.1 Representative Bond Dissociation Energies of Alkanes	6
Scheme 1.2 First Reported Stoichiometric Alkane Dehydrogenation Examples by Crabtree.....	8
Scheme 1.3 Example of COA/TBE Dehydrogenation by Felkin	8
Scheme 1.4 Selected Recent Examples of <i>n</i> -Alkanes Dehydrogenation.....	11
Scheme 1.5 Mechanism for $(t\text{-Bu}_4\text{PCP})\text{-Ir}$ -Catalyzed Dehydrogenation of COA	13
Scheme 1.6 Mechanism for Pincer Iridium-Catalyzed Dehydrogenation of <i>n</i> -Alkanes	14

Chapter 2

$C(SP^3)$ -H DEHYDROAROMATIZATION OF CYCLIC AND HETEROCYCLIC ALKANES CATALYZED BY Iridium Pincer Ligated Complexes

Scheme 2.1 Selected Examples of Cyclic Ethers Transfer Dehydrogenation Ir Complexes	25
Scheme 2.2 Pincer-Ligated Ir Catalysis Inhibition by Coordination of Product.....	26
Scheme 2.3 Selected Examples of Amines Transfer Dehydrogenation.....	27
Scheme 2.4 The Only Example of Dehydrogenating Heteroatomic Substrates by $(t\text{-Bu}_4\text{POCOP})\text{-Ir } \mathbf{c13}$	27

Scheme 2.5 Transfer Dehydrogenation of Broad Range of Substrates with Functional Groups by Ir Pincer Ligated Complexes.....	28
Scheme 2.6 Synthesis of (<i>t</i> -Bu ₄ PCP)–Ir Complex c3	30
Scheme 2.7 Synthesis of (<i>t</i> -Bu ₄ POCOP)–Ir Complex c13a	32
Scheme 2.8 Synthesis of (<i>i</i> -Pr ₄ PSCOP)–Ir Complex c22	33
Scheme 2.9 Synthesis of (<i>i</i> -Pr ₄ Anthraphos)–Ir Complex c24	35
Scheme 2.10 Transfer Dehydrogenation of 6-Methoxy-1,2,3,4-Tetrahydronaphthalene Catalyzed by Ir Pincer Ligated Complexes.....	40
Scheme 2.11 Transfer Dehydrogenation of Indane Catalyzed by Complex (<i>i</i> -Pr ₄ Anthraphos)–Ir c24	47
Scheme 2.12 Transfer Dehydrogenation of 6-Methoxy-1,2,3,4-Tetrahydroquinoline d by Complex (<i>i</i> -Pr ₄ PSCOP)–Ir c22	51
Scheme 2.13 Selected Examples of Brominated Isoquinoline Synthetic Utility.....	52
Scheme 2.14 Industrial Methods for the Synthesis of α -Naphthol	55
Scheme 2.15 Selected Examples of 1-Tetralone Dehydrogenation.....	55
Scheme 2.16 Selected Examples Manifesting Acenaphthylene Synthetic Utility.....	61
Scheme 2.17 Selected Methods of Acenaphthylene Synthesis.....	62

Appendix 1

EXPERIMENTAL SECTION AND SPECTRA RELEVANT TO CHAPTER 2

Appendix 2

C(SP³)-H DEHYDROGENATION ATTEMPTS OF CHALLENGING HETEROCYCLIC ALKANES BY IRIIDIUM Pincer LIGATED COMPLEXES

Scheme A2.1 Attempts to Transfer Dehydrogenate N-Methylpiperidine by Complex (t-Bu ₄ POCOP)-Ir c13	100
Scheme A2.2 Attempts to Transfer Dehydrogenate 5-Methoxy-1-Indanone by Complex (t-Bu ₄ POCOP)-Ir c13	101
Scheme A2.3 Attempts to Transfer Dehydrogenate 1-Chlorocyclopentene by Complex (t-Bu ₄ POCOP)-Ir c13	102
Scheme A2.4. Attempts to Transfer Dehydrogenate 4-Aminoindan by Complex (t-Bu ₄ POCOP)-Ir c13	104
Scheme A2.5 Attempts to Transfer Dehydrogenate 7-Bromo-1-Tetralone by Complex (t-Bu ₄ POCOP)-Ir c13	105
Scheme A2.6 Debromination of 7-Bromo-1-Tetralone and Transfer Dehydrogenation by Complex (t-Bu ₄ POCOP)-Ir c13	106
Scheme A2.7 Attempts to Transfer Dehydrogenate Tetrahydrothiopyran-4-one by Complex (t-Bu ₄ POCOP)-Ir c13	106
Scheme A2.8 Attempts to Transfer Dehydrogenate 4-Methoxy-5,6,7,8-Tetrahydronaphthalene-1-Carbaldehyde by Complex (t-Bu ₄ POCOP)-Ir c13	108
Scheme A2.9 Attempts to Transfer Dehydrogenate 8-Fluoro-1-Benzosuberone by Complex (t-Bu ₄ POCOP)-Ir c13	108
Scheme A2.10 Attempts to Transfer Dehydrogenate 5,6,7,8-Tetrahydro-2-Naphthoic Acid by Complex (t-Bu ₄ POCOP)-Ir c13	109

Scheme A2.11 Attempts to Transfer Dehydrogenate 1-Acetylcyclohexene by Complex (<i>t</i> -Bu ₄ POCOP)—Ir c13	110
Scheme A2.12 3-(4-Bromo-2-Fluorophenyl)Cyclohexan-1-one Synthesis via Rhodium Catalyzed 1,4-Conjugate Addition.....	111
Scheme A2.13 3-(4-Bromo-2-Fluorophenyl)Cyclohexan-1-one Transfer Dehydrogenation Attempts by Complex (<i>t</i> -Bu ₄ POCOP)—Ir c13	112
Scheme A2.14 6-Methoxy-3,4-Dihydronaphthalen-1(2H)-one Transfer Dehydrogenation Attempts by Complex (<i>t</i> -Bu ₄ POCOP)—Ir c13	113
Scheme A2.15 1,4-Thioxane Transfer Dehydrogenation Attempts by Complex (<i>t</i> -Bu ₄ POCOP)—Ir c13	114
Scheme A2.16 2-Cyclohexene-1-Acetonitrile Transfer Dehydrogenation Attempts by Complex (<i>t</i> -Bu ₄ POCOP)—Ir c13	115
Scheme A2.17 Phenylcyclohexane Transfer Dehydrogenation Attempts by Complex (<i>t</i> -Bu ₄ POCOP)—Ir c13	116
Scheme A2.18 1-Bromo-4-Cyclohexylbenzene Transfer Dehydrogenation Attempts by Complex (<i>t</i> -Bu ₄ POCOP)—Ir c13	117
Scheme A2.19 3-Bromocyclohexene Transfer Dehydrogenation Attempts by Complex (<i>t</i> -Bu ₄ POCOP)—Ir c13	118
Scheme A2.20 3-Bromocyclohexene Reaction with Benzene without an Ir Complex	118
Scheme A2.21 Chlorocyclohexane Transfer Dehydrogenation Attempts by Complex (<i>t</i> -Bu ₄ POCOP)—Ir c13	119
Scheme A2.22 Chlorocyclohexane Decomposition to 1-Cyclohexene During Transfer Dehydrogenation Attempts.....	119

Scheme A2.23 1-(Trimethylsiloxy)Cyclohexene Transfer Dehydrogenation Attempts by Complex $(t\text{-Bu}_4\text{POCOP})\text{-Ir } \mathbf{c13}$	120
Scheme A2.24 Julolidine Transfer Dehydrogenation Attempts by Complex $(t\text{-Bu}_4\text{POCOP})\text{-Ir } \mathbf{c13}$	121
Scheme A2.25 Paroxetine Transfer Dehydrogenation Attempts by Complex $(t\text{-Bu}_4\text{POCOP})\text{-Ir } \mathbf{c13}$	121

Appendix 3

EXPERIMENTAL SECTION AND SPECTRA RELEVANT TO APPENDIX 2

Appendix 4

PROGRESS TOWARD THE SYNTHESIS OF A NOVEL ASYMMETRIC NHC-PHOSPHONITE HYBRID Pincer LIGAND

Scheme A4.1 Reported NHC-Phosphonite Complex $(t\text{-Bu}_2n\text{-BuNHCCOP})\text{-Ir } \mathbf{c32}$ by Braunstein	148
Scheme A4.2 Synthesis of Novel Asymmetric NHC-Phosphonite Complex $(t\text{-Bu}_2\text{Mes-NHCCOP})\text{-Ir } \mathbf{c32}$	150

Chapter 3

$C(\text{SP}^3)\text{-H}$ DEHYDROAROMATIZATION OF 1-CYCLOHEXENE AND 4-VINYLL-1-CYCLOHEXENE VIA DISPROPORTIONATION CATALYZED BY IR Pincer LIGATED COMPLEXES

Scheme 3.1 Important Aromatics Industrial Production	164
---	-----

Scheme 3.2 Styrene Formation via Ethylbenzene Transfer

Dehydrogenation by Complex (*t*-Bu₄PCP)–Ir **c3** 165

Scheme 3.3 *p*-Xylene Formation as a Minor Product via Dehydrogenation by

Complex (*i*-Pr₄Anthraphos)–Ir **c24** 166

Scheme 3.4 Reported Studies of Benzene Formation via Dehydrogenation

by Ir Pincer Ligated Complexes 167

Scheme 3.5 Only Reported Studies of Ethylbenzene Formation via

Dehydrogenation by Ir Pincer Ligated Complexes 168

Scheme 3.6 Our Work in Cyclohexenyl Derivatives Dehydrogenation by Ir

Pincer Ligated Complexes 169

Scheme 3.7 1-Cyclohexene Disproportionation Pathway 173**Scheme 3.8** Attempts to Transfer Dehydrogenate Ethylbenzene to Styrene 177**Scheme 3.9** Plausible Reaction Pathway of 4-Vinyl-1-Cyclohexene

Disproportionation 177

Scheme 3.10 Industrially Relevant Disproportionation via Dehydrogenation

Forming Benzene and Ethylbenzene by Complex (*t*-Bu₄POCOP)–Ir **c13** 179

Appendix 5**EXPERIMENTAL SECTION AND SPECTRA RELEVANT TO CHAPTER 3**

LIST OF TABLES

Chapter 1

ALKANE C(SP³)-H DEHYDROGENATION BY SINGLE-SITE METAL CATALYSIS

Chapter 2

C(SP³)-H DEHYDROAROMATIZATION OF CYCLIC AND HETEROCYCLIC ALKANES CATALYZED BY Iridium Pincer Ligated Complexes

Table 2.1 COA/TBE Transfer Dehydrogenation Reactions with Complexes (t-Bu ₄ PCP)-Ir c3 and (t-Bu ₄ POCOP)-Ir c13	36
Table 2.2 Catalyst and Acceptor Screening of 6-Methoxy-1,2,3,4-Tetrahydronaphthalene Transfer Dehydrogenation	41
Table 2.3 Reaction Optimization of 6-Methoxy-1,2,3,4-Tetrahydronaphthalene Transfer Dehydrogenation Using Complex (t-Bu ₄ POCOP)-Ir c13	43
Table 2.4 Transfer Dehydrogenation of Indane to Indene by Complex (t-Bu ₄ POCOP)-Ir c13	46
Table 2.5 Transfer Dehydrogenation of 6-Methoxy-1,2,3,4-Tetrahydroquinoline by Complex (t-Bu ₄ POCOP)-Ir c13	49
Table 2.6 Transfer Dehydrogenation of 7-Bromo-1,2,3,4-Tetrahydroisoquinoline by Complex (t-Bu ₄ POCOP)-Ir c13	54
Table 2.7 Transfer Dehydrogenation of 1-Tetralone by Complex (t-Bu ₄ POCOP)-Ir c13	57
Table 2.8 Transfer Dehydrogenation of 7-Fluoro-1-Tetralone Transfer Dehydrogenation by Ir Pincer Ligated Complexes	59

Table 2.9 Transfer Dehydrogenation of Acenaphthene using (<i>t</i> -Bu ₄ POCOP)–Ir c13 and (<i>i</i> -Pr ₄ PSCOP)–Ir c122	63
Table 2.10 Successfully Optimized Studied Dehydroaromatized Substrates by Ir Pincer Ligated Complexes	66

Appendix 1

EXPERIMENTAL SECTION AND SPECTRA RELEVANT TO CHAPTER 2

Table A1.1 ZAS2 General Method Temperature Ramping Program for 10, 14, 16, 18, 20, and 22 Transfer Dehydrogenation.....	77
Table A1.2 ZAS_INDANE Method GC Temperature Ramping Program for Indane 12 to Indene 13 Transfer Dehydrogenation	77
Table A1.3 Inlet Parameters used in All Methods	78

Appendix 2

C(SP³)–H DEHYDROGENATION ATTEMPTS OF CHALLENGING HETEROCYCLIC ALKANES BY IRIIDIUM PINCER LIGATED COMPLEXES

Table A2.1 Investigated Conditions of Piperidine Transfer Dehydrogenation Attempts by Ir Pincer Ligated Complexes.....	99
Table A2.2 Investigated Conditions of 5-Iodo-2,3-Dihydrobenzofuran Transfer Dehydrogenation by Ir Pincer Ligated Complexes	103

Appendix 3

EXPERIMENTAL SECTION AND SPECTRA RELEVANT TO APPENDIX 2

Table A3.1 ZAS2 General Method Temperature Ramping Program for The Investigated Substrates in Appendix 2	128
Table A3.2 Inlet Parameters used in All Methods	128

Appendix 4

PROGRESS TOWARD THE SYNTHESIS OF A NOVEL ASYMMETRIC NHC-PHOSPHONITE HYBRID Pincer LIGAND

Chapter 3

C(SP³)-H DEHYDROAROMATIZATION OF 1-CYCLOHEXENE AND 4-VINYL-1-CYCLOHEXENE VIA DISPROPORTIONATION CATALYZED BY IR Pincer LIGATED COMPLEXES

Table 3.1 1-Cyclohexene Disproportionation Investigated by Ir Pincer Ligated Complexes	170
Table 3.2 Optimizing 1-Cyclohexene Disproportionation by Complex (t-Bu ⁴ POCOP)-Ir c13	172
Table 3.3 Kinetics Investigation of 1-Cyclohexene Disproportionation by Complex (t-Bu ⁴ POCOP)-Ir c13	174
Table 3.4 Optimizing 4-Vinyl-1-Cyclohexene Disproportionation by Complex (t-Bu ⁴ POCOP)-Ir c13	176

Appendix 5**EXPERIMENTAL SECTION AND SPECTRA RELEVANT TO CHAPTER 3**

Table A5.1 ZAS_Cyclohexene General Method Temperature Ramping Program for 1-Cyclohexene (77) Disproportionation.....	183
Table A5.2 ZAS2 General Method Temperature Ramping Program for 4-Vinyl-1-Cyclohexene (81) Disproportionation.....	183
Table A5.3 Inlet Parameters used in All Methods	184

LIST OF ABBREVIATIONS

°C	degrees Celsius
Å	Ångstrom
Ac	acetyl
AcOH	acetic acid
APCI	atmospheric pressure chemical ionization
app	apparent
aq	aqueous
Ar	aryl
atm	atmosphere
Bn	benzyl
Boc	<i>tert</i> -butyloxycarbonyl
bp	boiling point
br	broad
Bu	butyl
Bz	benzoyl
<i>c</i>	concentration for specific rotation measurements (g/100 mL)
ca.	about (Latin circa)
CAN	ceric ammonium nitrate
calc'd	calculated

cat.	catalyst
cm ⁻¹	wavenumber(s)
Cp	cyclopentadienyl
Cy	cyclohexyl
d	doublet
D	deuterium
DCE	1,2-dichloroethane
DDQ	2,3-dichloro-5,6-dicyano- <i>p</i> -benzoquinone
DFT	density functional theory
DME	1,2-dimethoxyethane
DMF	<i>N,N</i> -dimethylformamide
DTBP	Di- <i>tert</i> -butyl peroxide
e.g.,	for example (Latin <i>exempli gratia</i>)
EI+	electron impact
EPR	electron paramagnetic resonance
equiv.	equivalent(s)
ESI	electrospray ionization
Et	ethyl
EtOAc	ethyl acetate
Exs	excess
EWG	electron withdrawing group
FAB	fast atom bombardment
g	gram(s)

GC	gas chromatography
gCOSY	gradient-selected correlation spectroscopy
h	hour(s)
HEX	1-Hexene
HMBC	heteronuclear multiple bond correlation
HMPA	hexamethylphosphoramide
HPLC	high-performance liquid chromatography
HRMS	high-resolution mass spectroscopy
HSQC	heteronuclear single quantum correlation
Hz	hertz
<i>i</i> -Pr	isopropyl
i.e.,	that is (Latin id est)
IPA	isopropanol, 2-propanol
IR	infrared (spectroscopy)
<i>J</i>	coupling constant
K	Kelvin(s) (absolute temperature)
KC ₈	potassium intercalated graphite
kcal	kilocalorie
KHMDS	potassium hexamethyldisilazide
KIE	kinetic isotope effect
L	liter; ligand
LDA	lithium diisopropylamide
LG	leaving group

lit.	literature value
m	multiplet; milli
<i>m</i>	meta
M	metal; molar; molecular ion
<i>m/z</i>	mass-to-charge ratio
Me	methyl
mg	milligram(s)
MHz	megahertz
Min	minute(s)
MM	mixed method
Mol.	mole(s)
MOM	methoxymethyl acetal
Mp	melting point
Ms	methanesulfonyl (mesyl)
MS	molecular sieves
n	nano
N	normal
<i>n</i> -Bu	butyl
NBS	<i>N</i> -bromosuccinimide
NBE	Norbornene
NMR	nuclear magnetic resonance
Nu	nucleophile
<i>o</i>	ortho

<i>p</i>	para
Pd/C	palladium on carbon
Ph	phenyl
pH	hydrogen ion concentration in aqueous solution
Pin	2,3-dimethylbutane-2,3-diol (pinacol)
Piv	trimethylacetyl, pivaloyl
<i>p</i> K _a	<i>p</i> K for association of an acid
ppm	parts per million
PPTS	pyridinium <i>p</i> -toluenesulfonate
Pr	propyl
Py	pyridine
q	quartet
R	generic for any atom or functional group
Ref.	reference
rt	retention time
<i>R</i> _f	retention factor
s	singlet or strong or selectivity factor
sat.	saturated
t	triplet
<i>t</i> -Bu	<i>tert</i> -butyl
TBDPS	<i>tert</i> -butyldiphenylsilyl
TBHP	<i>tert</i> -butyl hydroperoxide
TBME	<i>tert</i> -butyl methyl ether

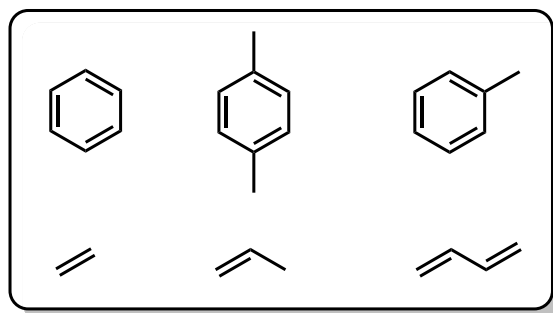
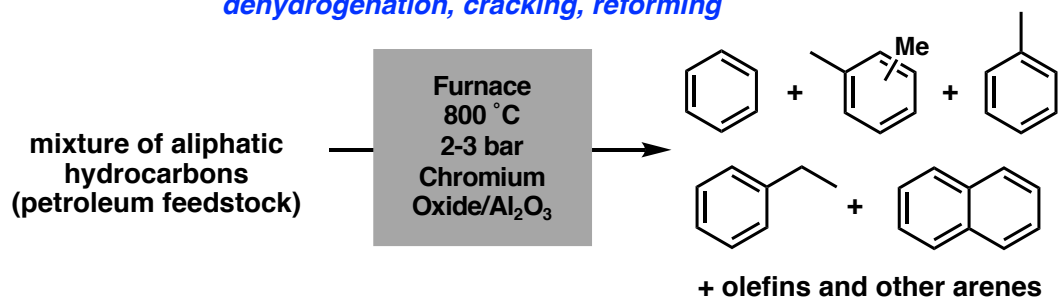
TBS	<i>tert</i> -butyldimethylsilyl
TBE	<i>tert</i> -butylethylene
TES	triethylsilyl
TFA	trifluoroacetic acid
THF	tetrahydrofuran
TIPS	triisopropylsilyl
TLC	thin-layer chromatography
TMS	trimethylsilyl
TOF	time-of-flight
Tol	tolyl
t_R	retention time
Ts	<i>p</i> -toluenesulfonyl (tosyl)
UV	ultraviolet
v/v	volume to volume
w	weak
w/v	weight to volume
X	anionic ligand or halide
λ	wavelength
μ	micro

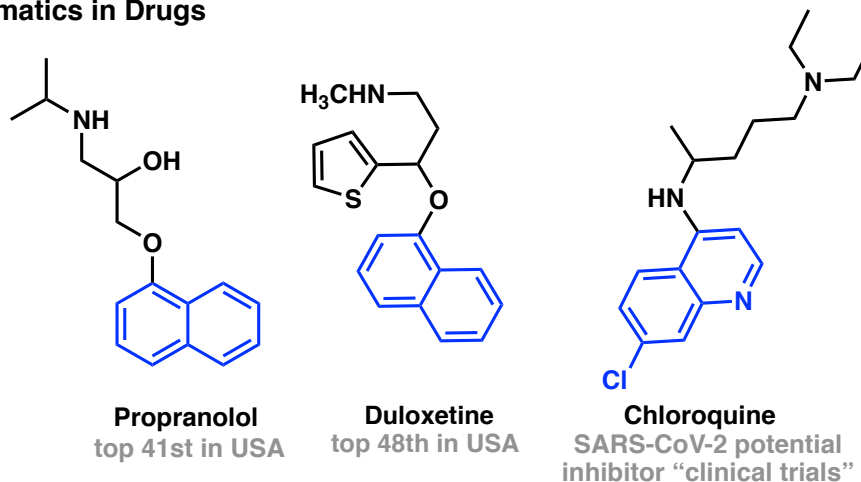
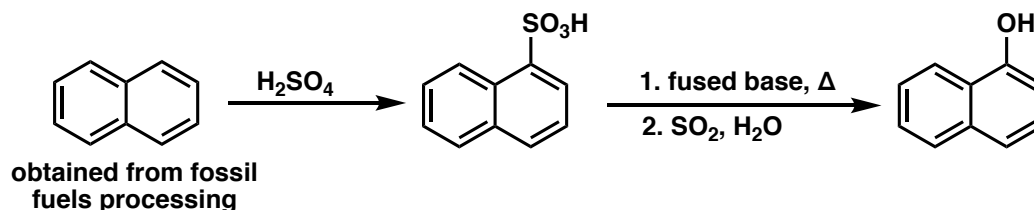
CHAPTER 1

ALKANE C(SP³)-H DEHYDROGENATION CATALYZED BY SINGLE-SITE IRIIDIUM CATALYSIS

1.1 INTRODUCTION

Olefins and aromatics are common cores in organic chemistry and serve as building blocks for the synthesis of complex molecules in pharmaceuticals and polymers. In addition, benzene, toluene, and xylenes are among the six most important feedstock chemicals that are not naturally occurring (Figure 1.1a).¹ The current industrial production of these building blocks is through dehydrogenating aliphatic hydrocarbons from crude oil feedstock using heterogeneous catalysts, which is an energy-intensive process operating at high pressures up to 60 bar and temperatures up to 900 °C (Figure 1.1b).² Additionally, isomerization occurs at such high temperatures, which lowers product selectivity making such processes inefficient.

a. Six Most Important Building Blocks from Fossil Resources**b. Industrial Process for Unsubstituted Aromatics Production***dehydrogenation, cracking, reforming***Figure 1.1** Most Important Building Blocks and Current Industrial Production

a. Aromatics in Drugs**b. An Example of Industrial Methods for Substituted Aromatics Production****Figure 1.2** Substituted Aromatics in Drugs and Industrial Synthesis

In addition, functionalized aromatics are of great synthetic utility in a wide variety of organic reactions, complex molecules, and pharmaceuticals. Propranolol, duloxetine, and chloroquine are among various important drugs that contain substituted aromatics in their structure (Figure 1.2a).³⁻⁸ However, synthesis of substituted aromatics and fused arenes can be cumbersome due to requiring harsh conditions such as strong acidic environments or highly toxic chemicals with large amounts of waste.⁹ For example, 1-naphthol compounds are synthesized industrially from either sulfonated naphthalene or nitrated naphthalene, which requires using concentrated sulfuric acid or toxic nitration conditions at high pressures in addition to requiring multiple-step reactions (Figure 1.2b).¹⁰⁻¹²

Hence, there is a great interest in developing and identifying methods for the synthesis of substituted and unsubstituted aromatics with milder conditions. Ideally, such a method would occur under acid-free and redox-neutral conditions, and would tolerate a much broader range of functional groups, making itself attractive for fine chemical manipulation. Dehydrogenating C(sp³)-H alkanes using homogenous transition metal catalysis could ideally be used to generate functionalized aromatic systems such as quinolines and naphthalenes from aliphatic precursors, which is the focus of our work in the subsequent chapters (Figure 1.3).

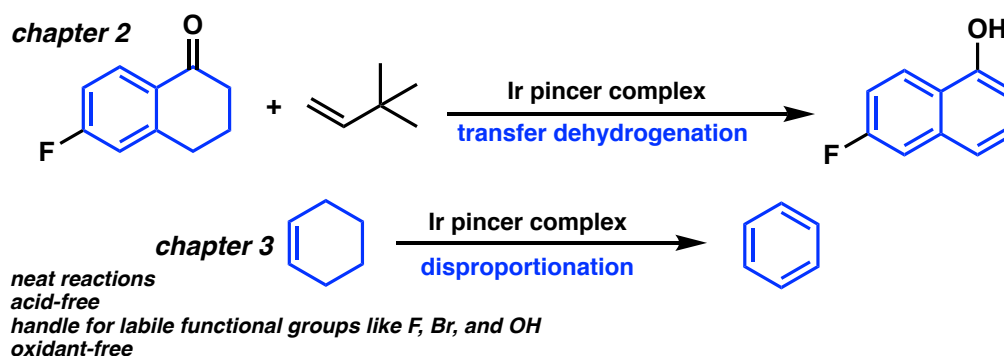


Figure 1.3 Examples of Presented Work in Chapters 2 and 3

1.2 CHALLENGES OF C(SP³)-H ALKANES DEHYDROGENATION

While alkanes dehydrogenation seems a conceptually simple process, C(sp³)-H activation is very challenging due to the chemical inertness of alkanes. Olefins and alkynes are good nucleophiles because they have the ability to donate or accept π -electrons, which can lead to metal-ligand π -backbonding (Figure 1.4). To the contrary, alkanes have strong,

localized C-C and C-H sigma bonds and coordinate weakly to metals with bond enthalpies of < 15 kcal/mol. making them poor nucleophiles and difficult to activate.¹³⁻¹⁵

Generally, C-H bonds in alkanes have high bond dissociation energies (BDE), in the range of 90-100 kcal/mol.⁹ Activating terminal C-H bonds in alkanes are preferred, but differing BDE between secondary and primary alkanes can affect the selectivity of the reaction, which imposes an additional challenge. Generally, terminal C-H positions have higher BDEs than internal positions (Scheme 1.1).^{1, 16} However, terminal C-H bond activation using transition-metal complexes is generally kinetically and thermodynamically favorable over secondary and tertiary C-H bonds.¹⁰⁻¹² One explanation for this observation is the bulky ligands around the metal center make C-H metal coordination more facile on the terminal position. In less sterically encumbered complexes, this effect may not be as strong and must be monitored.

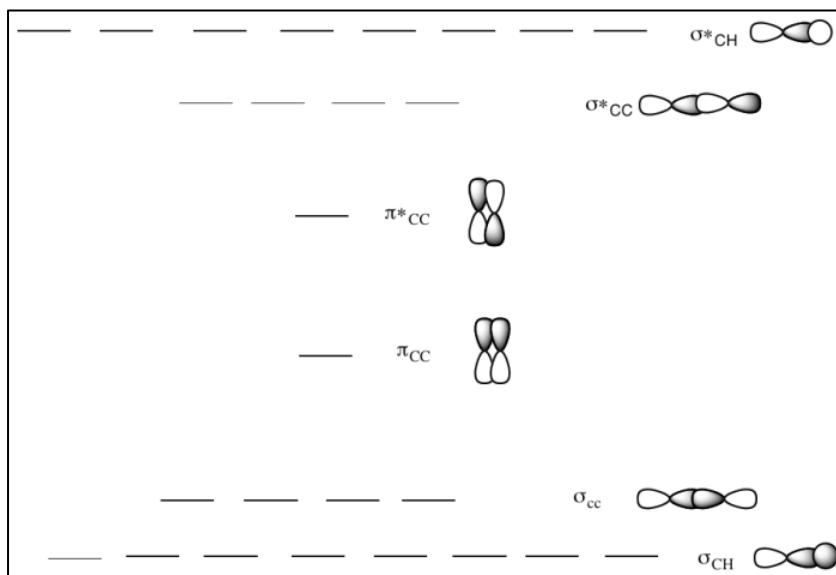
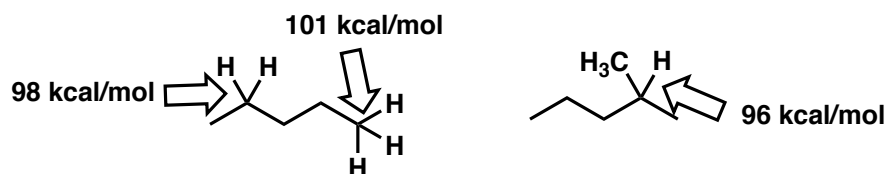
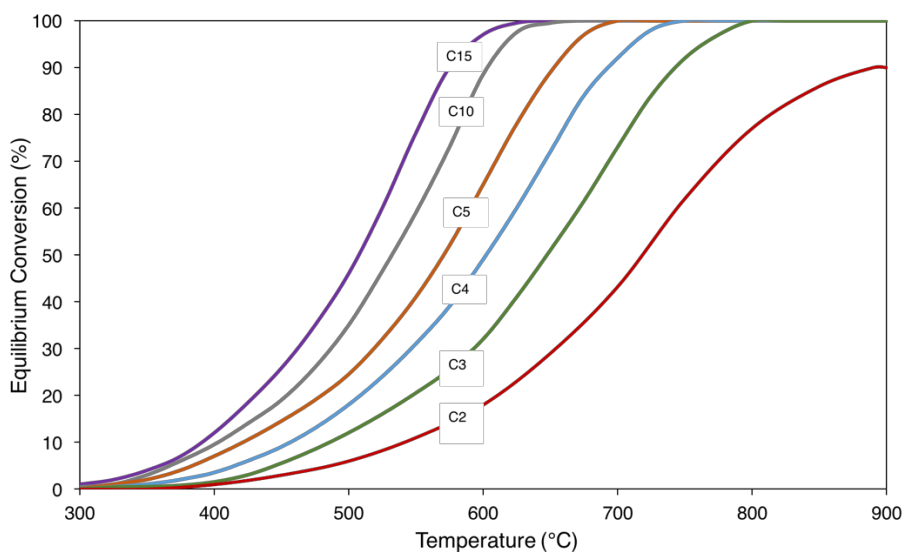


Figure 1.4 σ -Bonds vs. π -Bonds Molecular Orbitals

Scheme 1.1 Representative Bond Dissociation Energies of Alkanes

In addition, specific to C(sp³)-H dehydrogenation process, the chemical inertness increases as the hydrocarbon chain length decreases due to thermodynamic equilibrium, making it even more challenging to convert small chain alkanes to alkenes (Figure 1.5).¹⁷⁻¹⁹ Hence, high temperatures are necessary in dehydrogenation because one needs to amplify the entropic term to offset the strong endergonic nature of dehydrogenation.

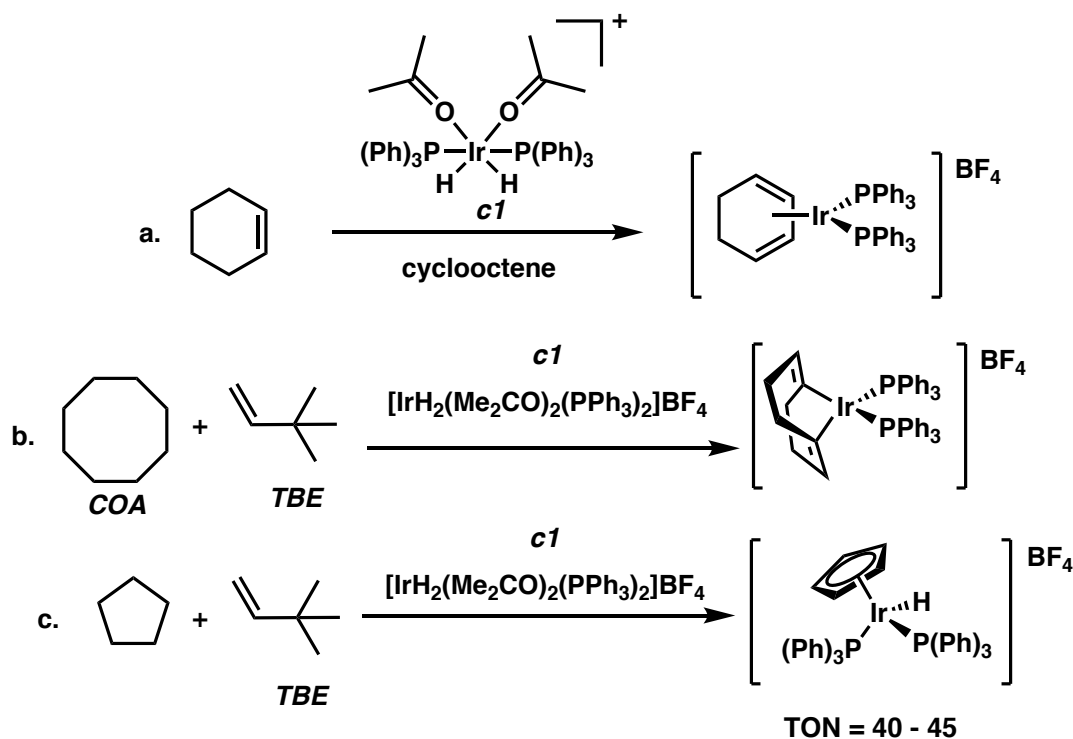
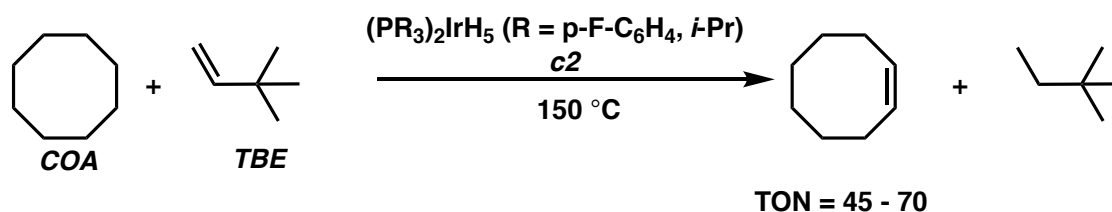
Furthermore, strong binding of the α -olefin or arene products to homogeneous catalysis can generate either a π -complex or a vinyl hydride with the catalyst, and thus dehydrogenation products may inhibit their catalytic activity.²⁴

**Figure 1.5** Thermodynamic Equilibrium Conversion of *n*-Alkane Dehydrogenation¹⁷

1.3 EARLY EXAMPLES OF C(SP³)-H DEHYDROGENATION USING IRIIDIUM HOMOGENEOUS CATALYSTS

Alkane dehydrogenation has received increased attention over the last decade due to the synthetic versatility of olefins and aromatics. However, this conceptually simple process is difficult to implement in practice due to the requirement of activation of strong C-H bonds. Hence, most of the reported systems require a sacrificial olefin that serves as a hydrogen acceptor to render the overall reaction exothermic.²⁰ Crabtree and co-workers reported the first example of stoichiometric alkane dehydrogenation using the cationic Ir(III) complex [(acetone)₂(PPh₃)₂-IrH₂]⁺ **c1** with cyclohexane yielding a 1,3-cyclohexadiene-Ir complex (Scheme 1.2a). More significantly, two important findings of the Crabtree studies were that cyclopentane and cyclooctane (**COA**) were dehydrogenated to cyclopentadienyl hydride and 1,5-cyclooctadiene complexes, respectively, in the presence of 3,3-dimethyl-1-butene commercially known as *t*-butylethylene (**TBE**) (Scheme 1.2b/1.2c).^{19, 21-22}

Concurrently but independently, Felkin and co-workers reported the dehydrogenation of cycloalkanes using Re and Ir metal complexes. Felkin reported the transfer dehydrogenation of the **COA/TBE** system by complex (*i*-Pr³P)₂-IrH₅ **c2** with turnover numbers (TONs) up to 70 when increasing reaction temperature to 150 °C (Scheme 1.3).²³⁻²⁴

Scheme 1.2 First Reported Stoichiometric Alkane Dehydrogenation Examples by Crabtree**Scheme 1.3** Example of COA/TBE Dehydrogenation by Felkin

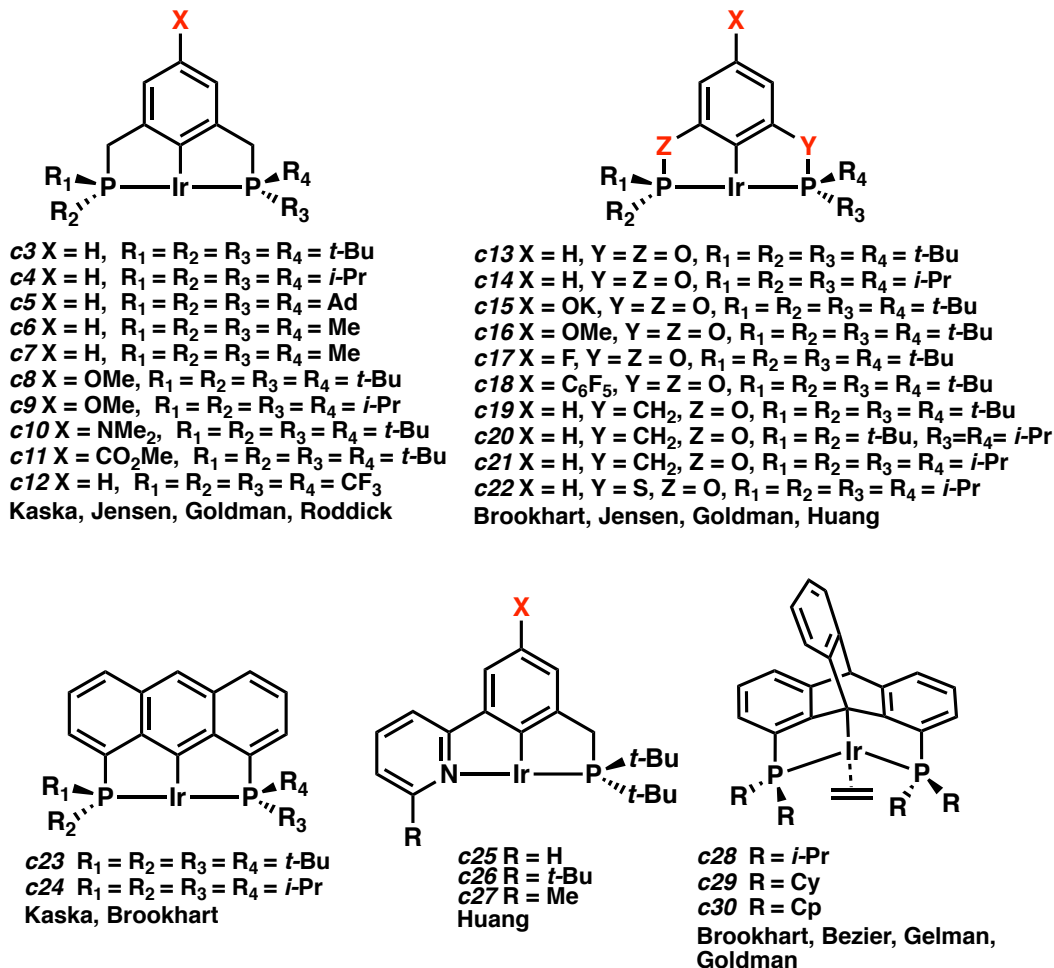
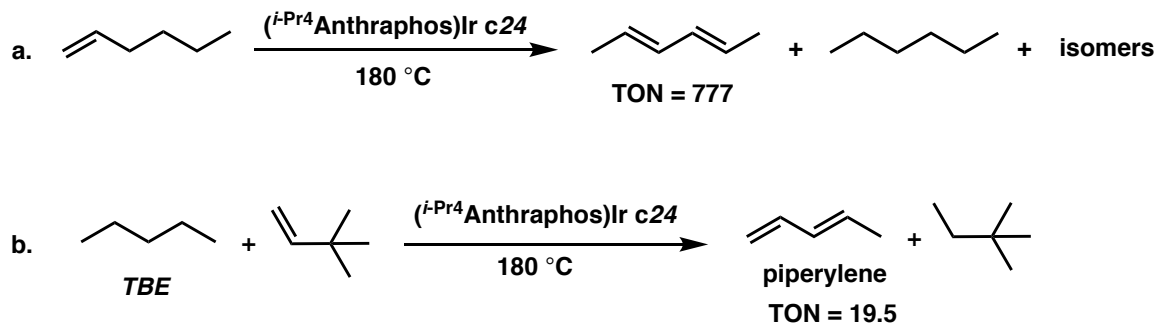
In addition, it has been shown that **TBE** is an effective hydrogen acceptor compared to ethylene or styrene because it offers great steric bulk that prevents strong coordination to the metal center and inhibiting catalysis. **TBE** also lacks allylic hydrogens so no allylic complex can irreversibly form and no isomers can be generated at the required temperatures for dehydrogenation *via* hydrogen migrations.

The transfer dehydrogenation reaction of **TBE/COA** has a substantial negative enthalpy (ca. -7 kcal/mol) due to the low dehydrogenation enthalpy of **COA** (+22.4 kcal/mol) relative to other alkanes (ca. 30 kcal/mol).²⁰ Hence, the **TBE/COA** system soon became the benchmark reaction for screening conditions and catalysis at play in transfer dehydrogenation studies.

1.4 RECENT EXAMPLES OF C(SP³)-H DEHYDROGENATION USING Iridium Pincer Ligated Complexes

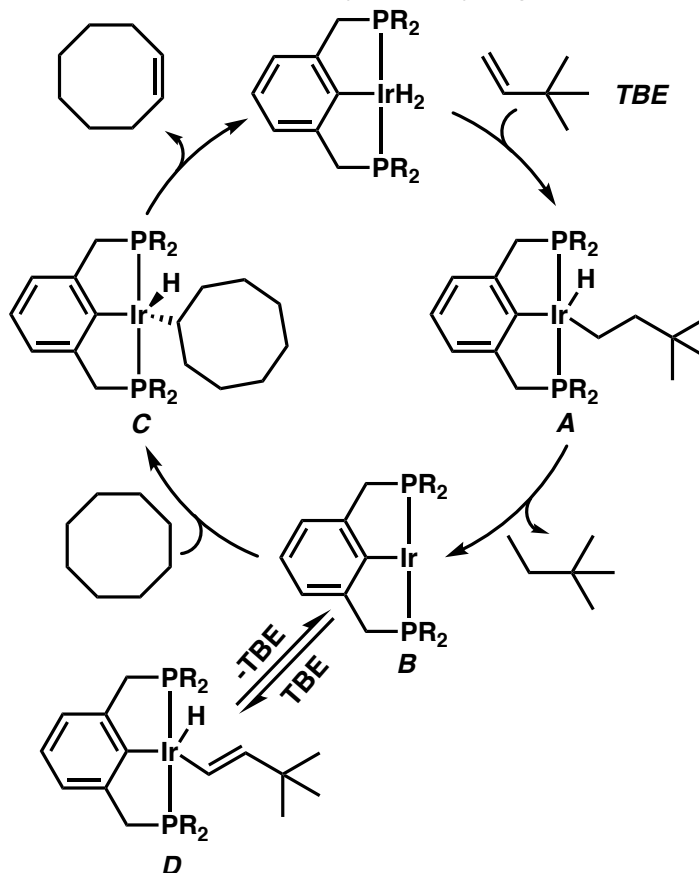
Most of the early examples of studied complexes showed poor thermal stability at the temperatures needed to achieve reasonable reaction rates. Pincer ligated complexes, however, were found to be thermally stable at these elevated temperatures, making them useful for this transformation.²⁵ These complexes are stable due to the tridentate coordination of ligands with the metal center. In 1996, Jensen and co-workers reported the first thermally stable pincer ligated complex used as dehydrogenation catalysts, (*t*-Bu⁴PCP)-Ir **c3**.²⁶⁻²⁷ Complex **c3** proved to be robust and reactive when employed on the **COA/TBE** system, yielding a maximum of 230 TONs.^{26, 28-29} Since then, variations of complex **c3** have been reported with different aryl backbones, various linkers, and ligating groups (Figure 1.6).³⁰⁻⁵² That being said, it was found that varying the electronics around the metal center is not as effective as varying the geometry around the metal center in improving catalytic activity.⁴² The complexes that showed high catalytic activity in most reactions were (*t*-Bu⁴POCOP)-Ir **c13**, (*i*-Pr⁴PSCOP)-Ir **c22**, and (*i*-Pr⁴anthrphos)-Ir **c24**.

While most of the previous studies focused on investigating these Ir pincer ligated complexes as dehydrogenation catalysts on the **COA/TBE** system, there were several studies that investigated other substrates. In 2012, Brookhart and co-workers reported the disproportionation of 1-hexene to 2,4-hexadiene and *n*-hexane using different Ir pincer ligated complexes. It was found that the (*i*-Pr⁴anthrphos)-Ir complex **c24** had the highest catalytic activity generating 777 TONs (Scheme 1.4a).⁵³ In a subsequent study, Brookhart and co-workers reported the synthesis of piperylene from *n*-pentane. Complex **c24** resulted in the highest activity generating 19.5 TONs even with employing **TBE** as the H₂ acceptor. One possible explanation for the lower catalytic activity of complex **c24** is that binding affinity of the product increases as the hydrocarbon chain length becomes smaller (Scheme 1.4b).⁵⁴ These examples demonstrate how catalytic activity vary significantly depending on the substrate investigated for dehydrogenation, even if it is only a change in carbon chain length.

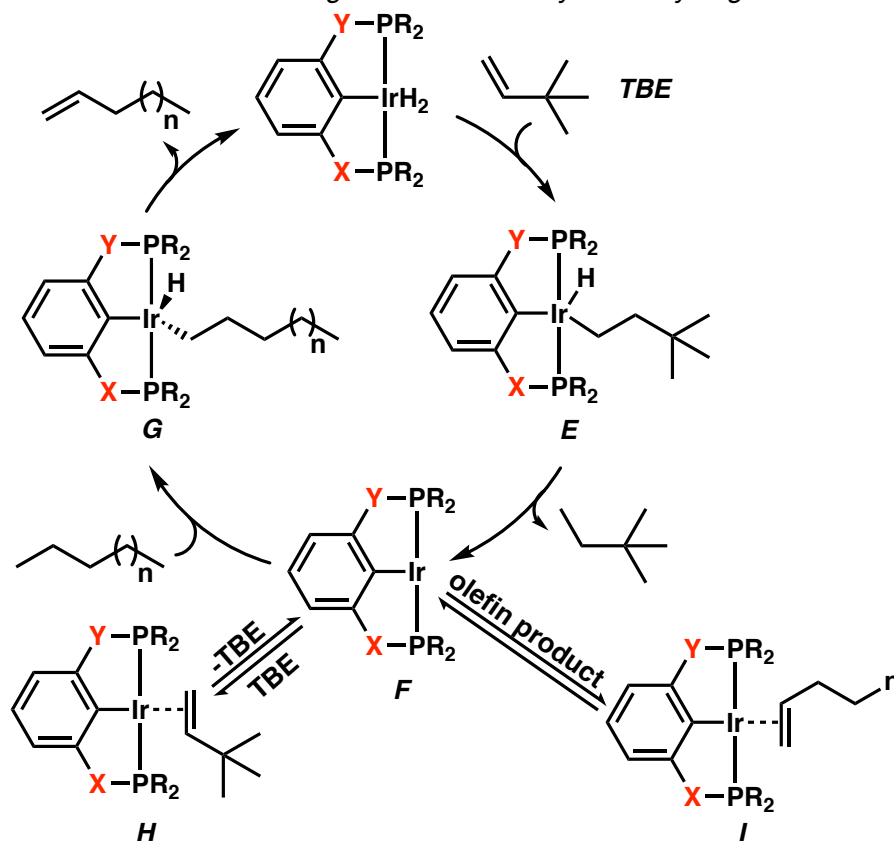
**Figure 1.6** Recent Developments in Iridium Pincer Ligated Complexes**Scheme 1.4** Selected Recent Examples of *n*-Alkanes Dehydrogenation

1.5 Pincer-Ligated Iridium-Catalyzed C(sp³)-H Dehydrogenation Mechanism

The widely accepted mechanism for the (*t*-Bu⁴PCP)-Ir **c3** catalytic dehydrogenation of the **COA/TBE** system occurs *via* an Ir(III)/Ir(I) catalytic cycle (Scheme 1.5).⁵⁵⁻⁵⁷ The first step of the catalytic cycle starts with the insertion of **TBE** followed by a reductive elimination to generate the catalytically active 14-electron three-coordinate Ir(I) species **B**. Then an oxidative addition of **COA** followed by a β -hydride elimination furnishes the dehydrogenated product to close the catalytic cycle (Scheme 1.5). The resting state for (*t*-Bu⁴PCP)-Ir **c3** at low concentrations of **TBE** is believed to be the Ir(III) hydrido-vinyl complex **D**.

Scheme 1.5 Mechanism for (*t*-Bu⁴PCP)-Ir-Catalyzed Dehydrogenation of COA

In the case of *n*-alkane dehydrogenation systems, it is envisioned to have a similar mechanistic pathway as the COA/TBE dehydrogenation system (Scheme 1.6). However, there is an additional inhibition pathway by the α -olefin product because it strongly binds to the active complex **B**. While the dehydrogenation cycle is similar for the various catalysts, the resting states are believed to vary for complexes other than (*t*-Bu⁴PCP)-Ir **c3**, which require less sterically demanding olefin acceptor. For example, the (*t*-Bu⁴POCOP)-Ir **c13** resting state is believed to be the alkene complex **H** and **I** and the rate determining step would be the release of the alkene.⁵⁵

Scheme 1.6 Mechanism for Pincer-Ligated Iridium-Catalyzed Dehydrogenation of *n*-Alkanes

1.6 CONCLUSIONS

Substantial progress has been achieved in the field of homogeneous catalytic alkane dehydrogenation using Ir pincer ligated complexes. Kaska, Jensen, Goldman, Brookhart, Huang, and others reported a variety of pincer ligated complexes including (*t*-Bu⁴PCP)–Ir **c3**, (*t*-Bu⁴POCOP)–Ir **c13**, (*i*-Pr⁴PSCOP)–Ir **c22**, and (*i*-Pr⁴anthraphos)–Ir **c24** that were shown to be highly effective transfer dehydrogenation catalysts. However, most of the reported examples focus on dehydrogenating the COA/TBE system or dehydrogenating unfunctionalized

normal and cyclic alkanes to olefins. The field of dehydrogenating functionalized substrates that could lead to important building blocks is lacking and remains significantly underdeveloped due to the strong coordination of many functionalities to metal centers leading to catalysis inhibition. Hence, our work in the subsequent chapters focuses on investigating dehydrogenating a diverse collection of substrates by Ir pincer ligated complexes with an emphasis on a variety of functional groups that are known to be strongly coordinating and poorly compatible with (PCP)-Ir type catalysts.

1.7 NOTES AND REFERENCES

1. Gunnoe, B. T. In *Alkane C-H Activation Activation By Single-Site Metal Catalysis*, 1 ed.; Perez, P. J., Ed. Springer Netherlands: Dordrecht, 2012; pp 1-15.
2. Chenier, P. J., *Survey of Industrial Chemistry*. 3 ed.; Springer US: New York, 2002; p XV, 515.
3. Wang, M.; Cao, R.; Zhang, L.; Yang, X.; Liu, J.; Xu, M.; Shi, Z.; Hu, Z.; Zhong, W.; Xiao, G., *Cell Res.* **2020**, 30 (3), 269-271.
4. Holshue, M. L.; DeBolt, C.; Lindquist, S.; Lofy, K. H.; Wiesman, J.; Bruce, H.; Spitters, C.; Ericson, K.; Wilkerson, S.; Tural, A.; Diaz, G.; Cohn, A.; Fox, L.; Patel, A.; Gerber, S. I.; Kim, L.; Tong, S.; Lu, X.; Lindstrom, S.; Pallansch, M. A.; Weldon, W. C.; Biggs, H. M.; Uyeki, T. M.; Pillai, S. K., *N. Engl. J. Med.* **2020**, 382 (10), 929-936.
5. Cortegiani, A.; Ingoglia, G.; Ippolito, M.; Giarratano, A.; Einav, S., *J. Crit. Care* **2020**.
6. Bymaster, F. P.; Beedle, E. E.; Findlay, J.; Gallagher, P. T.; Krushinski, J. H.; Mitchell, S.; Robertson, D. W.; Thompson, D. C.; Wallace, L.; Wong, D. T., *Bioorg. Med. Chem. Lett.* **2003**, 13 (24), 4477-4480.
7. Wong, D. T.; Robertson, D. W.; Bymaster, F. P.; Krushinski, J. K.; Reid, L. R., *Life Sci.* **1988**, 43 (24), 2049-2057.
8. Black, J. W.; Crowther, A. F.; Shanks, R. G.; Smith, L. H.; Dornhorst, A. C., *The Lancet* **1964**, 283 (7342), 1080-1081.

9. He, X.; Zheng, Y.-W.; Lei, T.; Liu, W.-Q.; Chen, B.; Feng, K.; Tung, C.-H.; Wu, L.-Z., *Catalysis Science & Technology* **2019**, 9 (13), 3337-3341.
10. Stevens Donna, G. H. H., Marshall B. Pearlman Phenols From Aromatic Sulfonic, Sulfamic, and Sulfone Compounds. April 22, 1958.
11. E.W. Schoeffel, D. M. B. Naphthalene. August 28, 1956.
12. Franzen, H.; Kempf, H., *Berichte der deutschen chemischen Gesellschaft* **1917**, 50 (1), 101-104.
13. Sun, X.-Z.; Grills, D. C.; Nikiforov, S. M.; Poliakoff, M.; George, M. W., *Journal of the American Chemical Society* **1997**, 119 (32), 7521-7525.
14. Hall, C.; Perutz, R. N., *Chemical Reviews* **1996**, 96 (8), 3125-3146.
15. Brown, C. E.; Ishikawa, Y.; Hackett, P. A.; Rayner, D. M., *Journal of the American Chemical Society* **1990**, 112 (7), 2530-2536.
16. Luo, Y.-R., Handbook of Bond Dissociation Energies in Organic Compounds. CRC Press: Boca Raton, 2003.
17. Treccani, Refining and Petrochemicals. In *Encyclopedia of Hydrocarbons*, Amadei, C., Ed. 2009; Vol. 2, p 668.
18. Crabtree, R. H., *Chemical Reviews* **2010**, 110 (2), 575-575.
19. Crabtree, R. H.; Mihelcic, J. M.; Quirk, J. M., *Journal of the American Chemical Society* **1979**, 101 (26), 7738-7740.
20. Michael Findlater, J. C., Alan S. Goldman, Maurice Brookhart. In *Alkane C-H Activation Activation By Single-Site Metal Catalysis*, 1 ed.; Perez, P. J., Ed. Springer Netherlands: Dordrecht, 2012; pp 113-141.

21. Crabtree, R. H.; Mellea, M. F.; Mihelcic, J. M.; Quirk, J. M., *Journal of the American Chemical Society* **1982**, 104 (1), 107-113.
22. Crabtree, R. H.; Demou, P. C.; Eden, D.; Mihelcic, J. M.; Parnell, C. A.; Quirk, J. M.; Morris, G. E., *Journal of the American Chemical Society* **1982**, 104 (25), 6994-7001.
23. Baudry, D.; Ephritikhine, M.; Felkin, H.; Holmes-Smith, R., *J. Chem. Soc., Chem. Commun.* **1983**, (14), 788-789.
24. Baudry, D.; Ephritikhine, M.; Felkin, H., *J. Chem. Soc., Chem. Commun.* **1980**, (24), 1243-1244.
25. M. Jensen, C., *Chem. Commun.* **1999**, (24), 2443-2449.
26. Gupta, M.; Hagen, C.; Kaska, W. C.; Cramer, R. E.; Jensen, C. M., *Journal of the American Chemical Society* **1997**, 119 (4), 840-841.
27. Gupta, M.; C. Kaska, W.; M. Jensen, C., *Chem. Commun.* **1997**, (5), 461-462.
28. Gupta, M.; Hagen, C.; Flesher, R. J.; Kaska, W. C.; Jensen, C. M., *Chem. Commun.* **1996**, (17), 2083-2084.
29. Kumar, A.; Bhatti, T. M.; Goldman, A. S., *Chemical Reviews* **2017**, 117 (19), 12357-12384.
30. Yao, W.; Zhang, Y.; Jia, X.; Huang, Z., *Angewandte Chemie International Edition* **2014**, 53 (5), 1390-1394.
31. Jia, X.; Zhang, L.; Qin, C.; Leng, X.; Huang, Z., *Chem. Commun.* **2014**, 50 (75), 11056-11059.

32. Brayton, D. F.; Beaumont, P. R.; Fukushima, E. Y.; Sartain, H. T.; Morales-Morales, D.; Jensen, C. M., *Organometallics* **2014**, 33 (19), 5198-5202.
33. Bézier, D.; Brookhart, M., *ACS Catalysis* **2014**, 4 (10), 3411-3420.
34. Shi, Y.; Suguri, T.; Dohi, C.; Yamada, H.; Kojima, S.; Yamamoto, Y., *Chemistry – A European Journal* **2013**, 19 (32), 10672-10689.
35. Nawara-Hultsch, A. J.; Hackenberg, J. D.; Punji, B.; Supplee, C.; Emge, T. J.; Bailey, B. C.; Schrock, R. R.; Brookhart, M.; Goldman, A. S., *ACS Catalysis* **2013**, 3 (11), 2505-2514.
36. Musa, S.; Ackermann, L.; Gelman, D., *Adv. Synth. Catal.* **2013**, 355 (14-15), 3077-3080.
37. Romm, D. G. a. R. In *Organometallic Pincer Chemistry*, Gerard Van Koten, D. M., Ed. Springer-Verlag Berlin Heidelberg: Heidelberg, 2013; pp 289-317.
38. Dobereiner, G. E.; Yuan, J.; Schrock, R. R.; Goldman, A. S.; Hackenberg, J. D., *Journal of the American Chemical Society* **2013**, 135 (34), 12572-12575.
39. Punji, B.; Emge, T. J.; Goldman, A. S., *Organometallics* **2010**, 29 (12), 2702-2709.
40. Huang, Z.; Rolfe, E.; Carson, E. C.; Brookhart, M.; Goldman, A. S.; El-Khalafy, S. H.; MacArthur, A. H. R., *Adv. Synth. Catal.* **2010**, 352 (1), 125-135.
41. Ahuja, R.; Punji, B.; Findlater, M.; Supplee, C.; Schinski, W.; Brookhart, M.; Goldman, A. S., *Nat. Chem.* **2010**, 3, 167.

42. Kundu, S.; Choliy, Y.; Zhuo, G.; Ahuja, R.; Emge, T. J.; Warmuth, R.; Brookhart, M.; Krogh-Jespersen, K.; Goldman, A. S., *Organometallics* **2009**, 28 (18), 5432-5444.
43. Huang, Z.; Brookhart, M.; Goldman, A. S.; Kundu, S.; Ray, A.; Scott, S. L.; Vicente, B. C., *Adv. Synth. Catal.* **2009**, 351 (1-2), 188-206.
44. Azerraf, C.; Gelman, D., *Organometallics* **2009**, 28 (22), 6578-6584.
45. Kuklin, S. A.; Sheloumov, A. M.; Dolgushin, F. M.; Ezernitskaya, M. G.; Peregudov, A. S.; Petrovskii, P. V.; Koridze, A. A., *Organometallics* **2006**, 25 (22), 5466-5476.
46. Zhu, K.; Achord, P. D.; Zhang, X.; Krogh-Jespersen, K.; Goldman, A. S., *Journal of the American Chemical Society* **2004**, 126 (40), 13044-13053.
47. Morales-Morales, D.; Redón, R. o.; Yung, C.; Jensen, C. M., *Inorg. Chim. Acta* **2004**, 357 (10), 2953-2956.
48. Göttker-Schnetmann, I.; White, P. S.; Brookhart, M., *Organometallics* **2004**, 23 (8), 1766-1776.
49. Göttker-Schnetmann, I.; White, P.; Brookhart, M., *Journal of the American Chemical Society* **2004**, 126 (6), 1804-1811.
50. Göttker-Schnetmann, I.; Brookhart, M., *Journal of the American Chemical Society* **2004**, 126 (30), 9330-9338.
51. Haenel, M. W.; Oevers, S.; Angermund, K.; Kaska, W. C.; Fan, H.-J.; Hall, M. B., *Angewandte Chemie International Edition* **2001**, 40 (19), 3596-3600.
52. Liu, F.; S. Goldman, A., *Chem. Commun.* **1999**, (7), 655-656.

53. Lyons, T. W.; Guironnet, D.; Findlater, M.; Brookhart, M., *Journal of the American Chemical Society* **2012**, 134 (38), 15708-15711.
54. Kundu, S.; Lyons, T. W.; Brookhart, M., *ACS Catalysis* **2013**, 3 (8), 1768-1773.
55. Akshai Kumar, A. S. G. In *The Privileged Pincer-Metal Platform: Coordination Chemistry & Applications*, Gerard Van Koten, R. A. G., Ed. Springer, Cham: Cham, 2015; Vol. 54, pp 307-334.
56. Renkema, K. B.; Kissin, Y. V.; Goldman, A. S., *Journal of the American Chemical Society* **2003**, 125 (26), 7770-7771.

CHAPTER 2

C(SP³)-H DEHYDROAROMATIZATION OF CYCLIC AND HETEROCYCLIC ALKANES CATALYZED BY Iridium Pincer LIGATED COMPLEXES

2.1 INTRODUCTION

Functionalized aromatic skeletons constitute a large variety of important organic compounds' substructures and serve as building blocks for the synthesis of complex molecules in pharmaceuticals and monomers for the production of polymers. As noted in Chapter 1, the synthesis of substituted aromatics and fused arenes can be cumbersome, often requiring harsh conditions such as strongly acidic environments or highly toxic chemicals that generate large amounts of waste. Hence, there is a great interest in developing and identifying methods for the synthesis of substituted and unsubstituted aromatics under milder conditions.

While the previous chapter discussed the substantial efforts in the past twenty years on C(sp³)-H dehydrogenation by Ir pincer ligated complexes, only a few examples reported the direct dehydroaromatization of heteroatomic hydrocarbons precursors. Additionally, the scope of such reactions is fairly narrow due to the Lewis basic nature of the heteroatoms, particularly by binding of dehydrogenated functionalized species to (PCP)-Ir type catalysts.¹

The purpose of the work presented in this chapter is to first expand the scope of dehydroaromatization beyond hydrocarbon substrates to generate heteroaromatics with an emphasis on a variety of functional groups that are known to be poorly compatible and strongly coordinating with (PCP)-Ir type catalysts, including halogens, ketones, arenes, and ethers. Second, we want to explore the effects of steric crowding on the ability of Ir pincer ligated complexes to accomplish these transformations.

2.2 RELATED LITERATURE

Since the first reports of Jensen and co-workers of the “parent catalyst” complex (*t*-Bu⁴PCP)-Ir **c3** for transfer dehydrogenating the cyclooctane/3,3-dimethyl-1-butene (COA/TBE) system²⁻³ many studies have utilized Ir pincer ligated complexes for dehydrogenating alkanes to alkenes.²⁻⁸ Amongst the different variations of complex **c3** reported, complexes (*t*-Bu⁴POCOP)-Ir **c13**, (*i*-Pr⁴PSCOP)-Ir **c22**, and (*i*-Pr⁴anthraphos)-Ir **c24** have been shown to exhibit high catalytic activity as dehydrogenation catalysts (Figure 2.1).

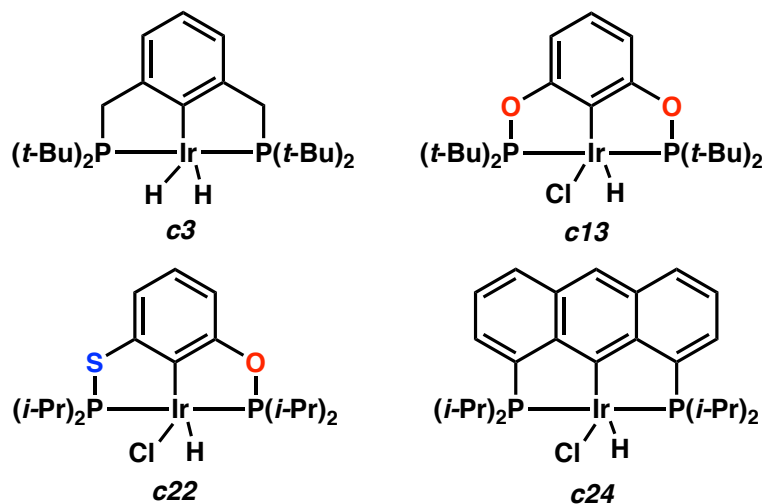
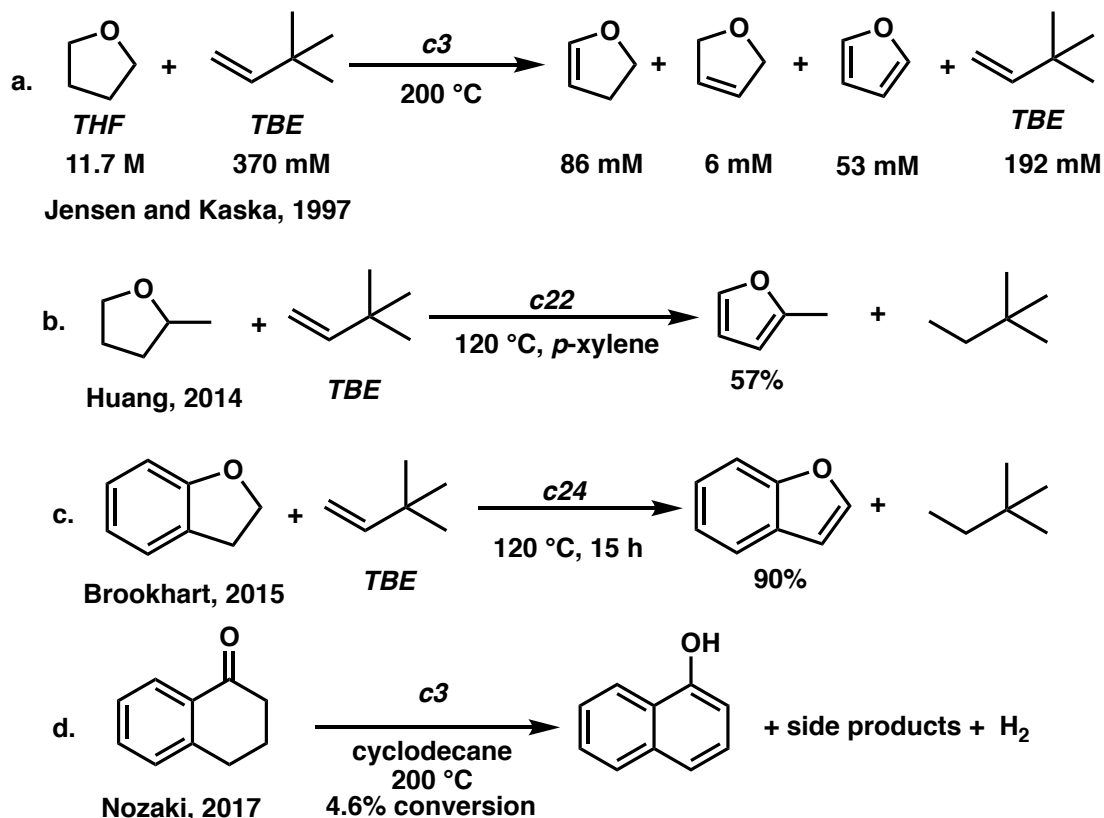


Figure 2.1 Ir Pincer Ligated Complexes Utilized as Dehydrogenation Catalysts

However, only a few studies have investigated the direct dehydroaromatization of heteroatom substituted alkanes by Ir pincer ligated complexes due to significant product inhibition by coordination to the Ir metal center. Early reports by Jensen and Kaska and co-workers in 1997 reported low activity of complex $(t\text{-Bu}_4\text{PCP})\text{-Ir}$ **c3** to catalyze the transfer dehydrogenation of tetrahydrofuran (THF) and using TBE as the H_2 acceptor (Scheme 2.1a).^{1, 8}

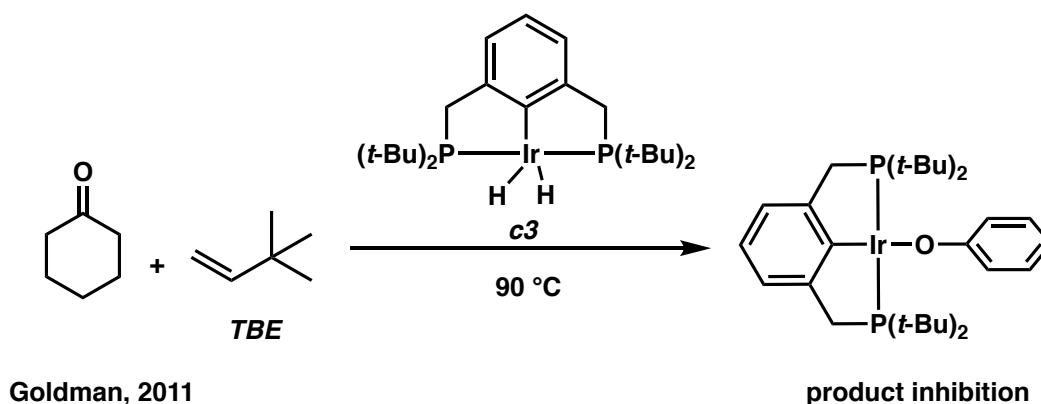
Scheme 2.1 Selected Examples of Cyclic Ethers Transfer Dehydrogenation Ir Complexes



Even though this reaction is thermodynamically favorable, only partial hydrogenation of **TBE** occurred to yield 14% of furan, demonstrating the difficulty of such reactions. Further investigations using Ir pincer ligated complexes for dehydrogenating THF were not reported for over a decade afterward. Later in 2014, Huang and co-workers reported the transfer dehydrogenation of a broad scope of cyclic ethers including THF using (*i*-Pr⁴PSCOP)-Ir **c22** (Scheme 2.1b).⁵ Later, Brookhart and Nozaki and co-workers reported dehydrogenation of linear and cyclic ethers using (*i*-Pr⁴anthraphos)-Ir **c24** and other variations of Ir pincer ligated complexes, and only limited examples exhibited the direct dehydroaromatization from its alkane precursor substrate (Scheme 2.1c/Scheme 2.1d).⁹⁻¹⁰

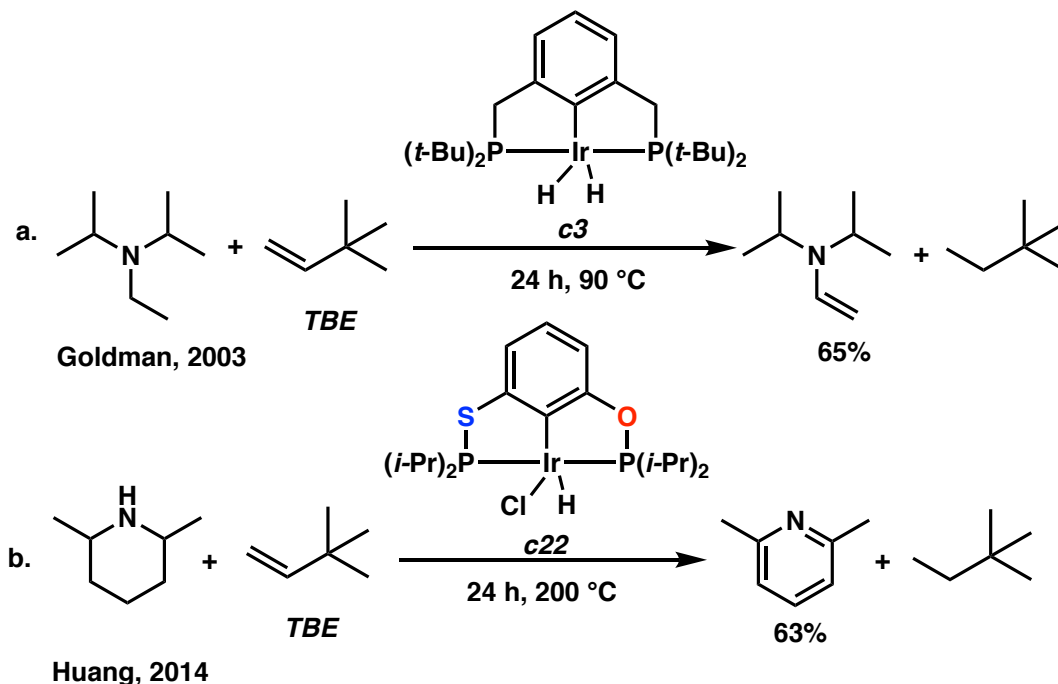
Goldman and co-workers attempted the transfer dehydrogenation of cyclohexanone using complex $(t\text{-Bu}_4\text{PCP})\text{-Ir}$ **c3** and found that catalysis was greatly inhibited by coordination of the phenol product (Scheme 2.2).¹¹

Scheme 2.2 Pincer-Ligated Ir Catalysis Inhibition by Coordination of Product

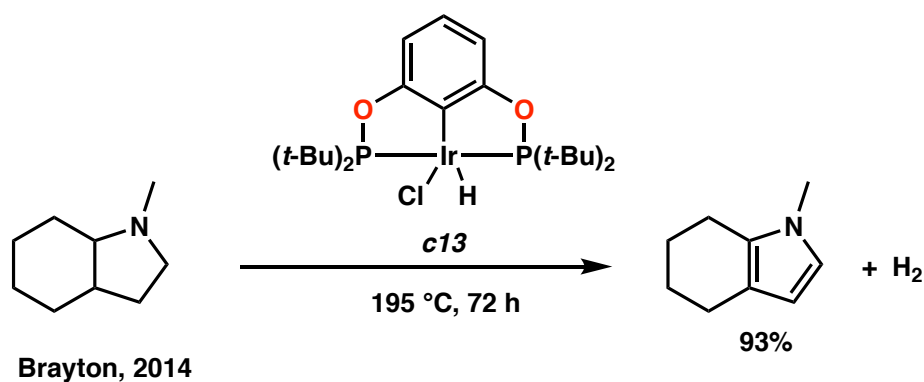


Other than oxygenated substrates, Goldman and Huang and co-workers also reported the dehydrogenation of amines using complexes $(t\text{-Bu}_4\text{PCP})\text{-Ir}$ **c3** and $(t\text{-Pr}_4\text{PSCOP})\text{-Ir}$ **c22** (Scheme 2.3).^{5, 12-13} The only report for complex $(t\text{-Bu}_4\text{POCOP})\text{-Ir}$ **c13** as a dehydrogenation catalyst for functionalized substrates has been on indolic and carbazolic derivatives in the context of hydrogen storage by Brayton and co-workers in 2014 (Scheme 2.4).¹⁴

Scheme 2.3 Selected Examples of Amines Transfer Dehydrogenation



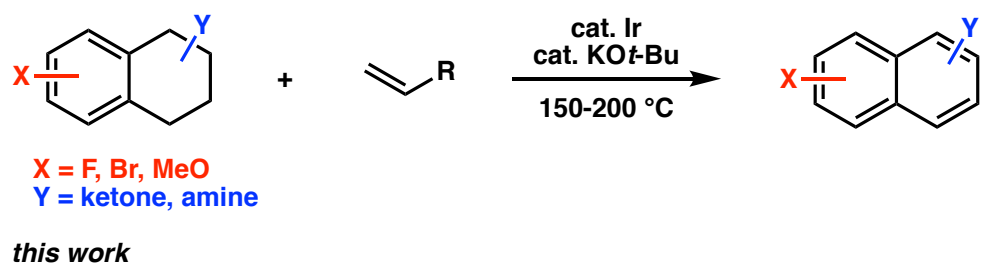
Scheme 2.4 The Only Example of Dehydrogenating Heteroatomic Substrates by $(t\text{-Bu}_4\text{POCOP})\text{-Ir c13}$



While these examples show significant achievements in the past twenty years, to date the direct dehydroaromatization of substrates containing a diverse collection of functional groups remains limited and significantly underdeveloped, mainly due to strong coordination

and product inhibition. Hence the purpose of this study is to investigate Ir pincer ligated complexes as dehydrogenation catalysts to access substituted fused aromatics with an emphasis on tolerating diverse functional groups (Scheme 2.5). This study presents novel and complementary routes to complex molecules *via* late stage dehydrogenation without the need of lengthy synthetic sequences, which would be useful for pharmaceuticals as well as materials applications.

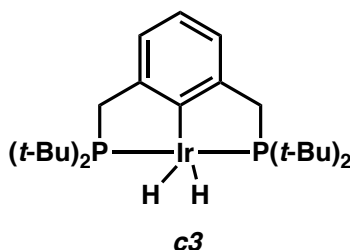
Scheme 2.5 Transfer Dehydrogenation of Broad Range of Substrates with Functional Groups by Ir Pincer Ligated Complexes



2.3 IRIDIUM Pincer Ligated Complexes Synthesis and Application on COA/TBE System

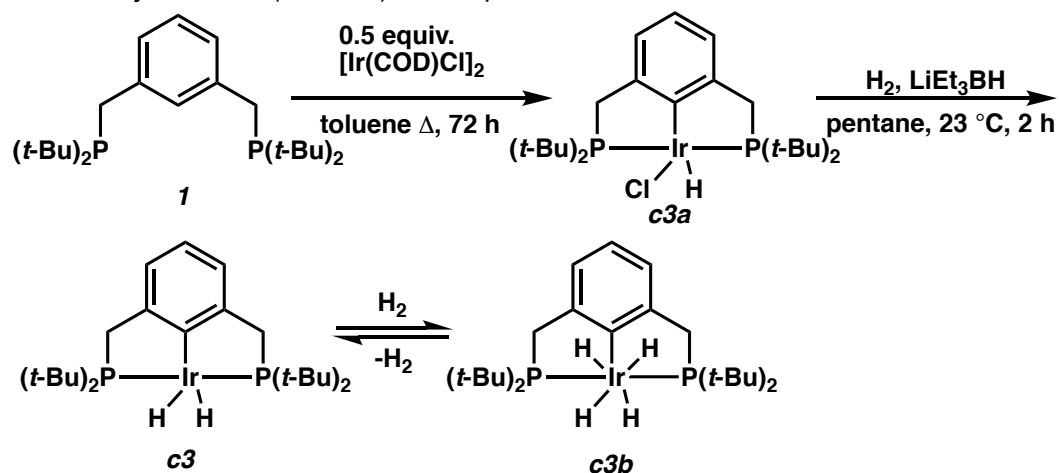
The synthetic routes toward four known complexes, (t -Bu⁴PCP)-Ir **c3**, (t -Bu⁴POCOP)-Ir **c13**, (i -Pr⁴PSCOP)-Ir **c22**, and (i -Pr⁴anthrathos)-Ir **c24**, are discussed in this section.

2.3.1 Synthesis of (t -Bu⁴PCP)-Ir Complex **c3**



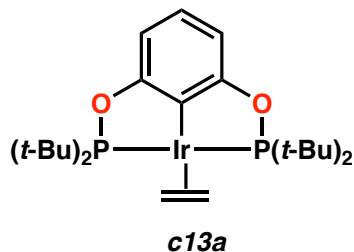
Jensen and co-workers first reported complex (t -Bu⁴PCP)-Ir **c3**, which is referred to as the “parent catalyst.”³ Complex **c3** achieved a maximum turnover numbers (TONs) of 230 on the **COA/TBE** system and was found to exhibit a low catalytic activity when dehydrogenating n -alkanes.¹⁵ Although other complexes such as (i -Pr⁴PSCOP)-Ir **c22** performed better when applied on the **COA/TBE** system (maximum of 2,900 TONs)⁵, complex **c3** was synthesized to replicate the transfer dehydrogenation results of the **COA/TBE** system as a control experiment before attempting to dehydrogenate alternative systems.

Scheme 2.6 Synthesis of $(t\text{-Bu}^4\text{PCP})\text{-Ir}$ Complex **c3**



The hydrido chloride complex **c3a** was first synthesized from metalating the commercially available 2,6-Bbis[(di-*t*-butylphosphino)methyl]phenyl ligand (**1**) in refluxing toluene under an argon atmosphere (Scheme 2.6).^{2-3, 16} The diagnostic NMR signals for complex **c3a** are the hydride shift observed at -42.50 ppm in the ^1H NMR spectrum and the phosphines signal observed at 67.09 ppm in the ^{31}P NMR spectrum. Then, complex **c3a** was treated with LiEt_3BH under an H_2 atmosphere generating the dihydride $(t\text{-Bu}^4\text{PCP})\text{-IrH}_2$ complex **c3**. It was found that the tetrahydride $(t\text{-Bu}^4\text{PCP})\text{-IrH}_4$ complex **c3b** was in equilibrium with complex **c3** and the diagnostic ^1H NMR shift for complex **c3b** was observed at -9.11 ppm. The energy barrier for the interconversion between the tetrahydride and dihydride species is almost negligible and the dehydrogenative catalytic activity for the dihydride and tetrahydride complexes are believed to be similar.^{12, 17} Hence, for consistency, we will refer to the mixture of these complexes as $(t\text{-Bu}^4\text{PCP})\text{-Ir}$ **c3**.

2.3.2 Synthesis of (t -Bu⁴POCOP)-Ir Complex **c13**/**c13a**

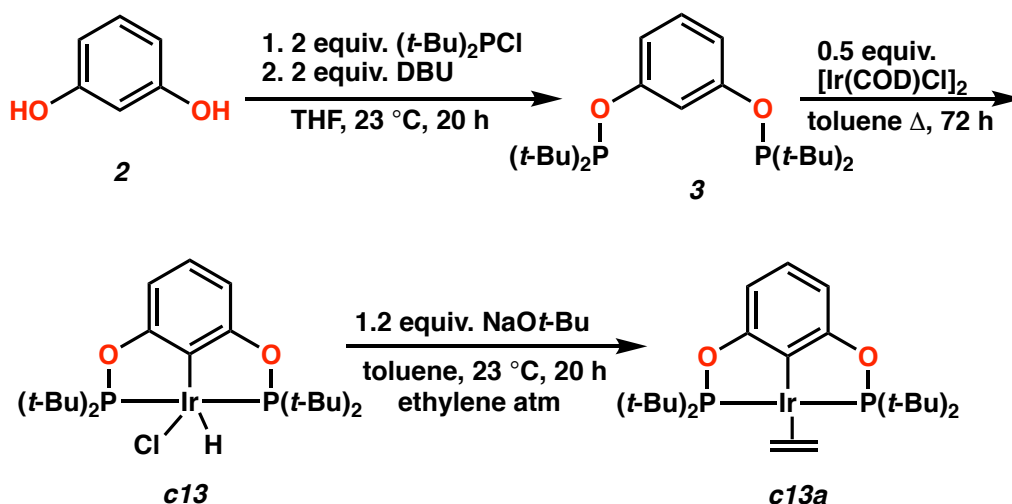


Complex (t -Bu⁴POCOP)-Ir **c13a** was first reported by Brookhart and co-workers.¹⁸⁻²¹ Notably, complex **c13a** showed higher activity compared to the parent catalyst **c3** by achieving a maximum of turnover frequency (TOF) of 6,900 h⁻¹ when applied on the COA/TBE dehydrogenation system. This complex has been shown to exhibit higher activity when dehydrogenating cycloalkanes relative to *n*-alkanes. Since we are interested in developing a method to directly dehydroaromatize heterocyclic alkanes, it is of interest to synthesize the (t -Bu⁴POCOP)-Ir complex **c13a**.^{1, 15}

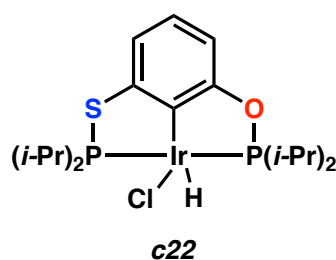
The t -Bu⁴POCOP ligand **2** was synthesized from treating resorcinol (**1**) with (t -Bu)₂PCl, and DBU (Scheme 2.7). The diagnostic signal of the t -Bu⁴POCOP ligand **2** is the phosphinite shift at 153.22 ppm in ³¹P NMR spectrum. Ligand **2** was then cyclometalated with half an equivalent of [Ir(COD)Cl]₂ in refluxing toluene under an argon atmosphere to obtain the t -Bu⁴POCOP hydrido chloride complex **c13**. It is worth noting that unlike most pincer ligated-Ir complexes, **c13** is air stable. The diagnostic NMR signals of **c13** are the hydride shift at -40.69 ppm in the ¹H NMR spectrum and the phosphinite shift at 175.34 ppm in the ³¹P NMR spectrum. Lastly, the ethylene complex **c13a** was generated by treating **c13** with NaOt-Bu under an ethylene atmosphere overnight. The diagnostic ³¹P NMR shift for

the phosphinite was observed at 181.00 ppm. Both **c13** and **c13a** are active precatalysts and believed to be similar in transfer dehydrogenation systems.

Scheme 2.7 Synthesis of $(t\text{-Bu}^4\text{POCOP})\text{-Ir}$ Complex **c13a**



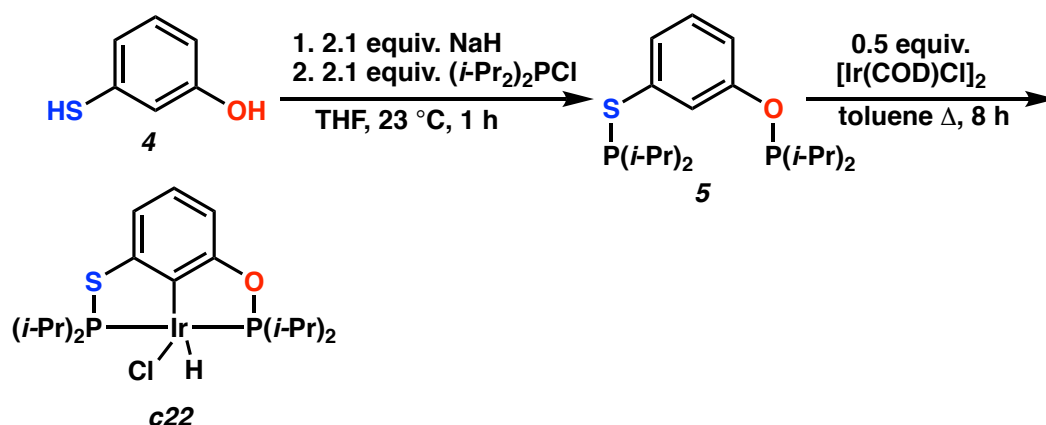
2.3.3 Synthesis of $(i\text{-Pr}^4\text{PSCOP})\text{-Ir}$ Complex **c22**



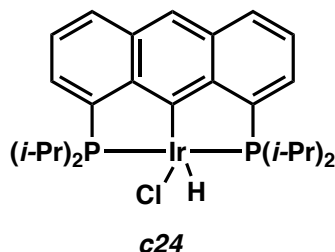
Complex $(i\text{-Pr}^4\text{PSCOP})\text{-Ir}$ **c22** was first reported by Huang and co-workers in 2014.⁵ Complex **c22** exhibited high catalytic activity on the **COA/TBE** system and generated a maximum TONs of 5901 in 7.5 h. Given its high catalytic activity, we were interested to test it and investigate it on underexplored systems for dehydrogenation. This complex was synthesized by Dr. Michael Haibach in the Grubbs group following literature protocols

(Scheme 2.8).⁵ Similar to the previous complexes, the PSCOP ligand **5** was first synthesized from deprotonating meta-mercaptophenol (**4**) with NaH followed by diphosphorylation with $(i\text{-Pr}_2)_2\text{PCl}$. The characteristic phosphinite shift is expected at 150.40 ppm and the phosphine sulfide shift is expected at 68.70 ppm in the ^{31}P NMR spectrum. Then the obtained ligand **5** was cyclometalated with half an equivalent of $[\text{Ir}(\text{COD})\text{Cl}]_2$ in refluxing toluene affording complex **c22**. The diagnostic NMR signal of **22** is the hydride shift and expected at -37.06 ppm in the ^1H NMR spectrum.

Scheme 2.8 Synthesis of $(i\text{-Pr}_4\text{PSCOP})\text{-Ir}$ Complex **c22**

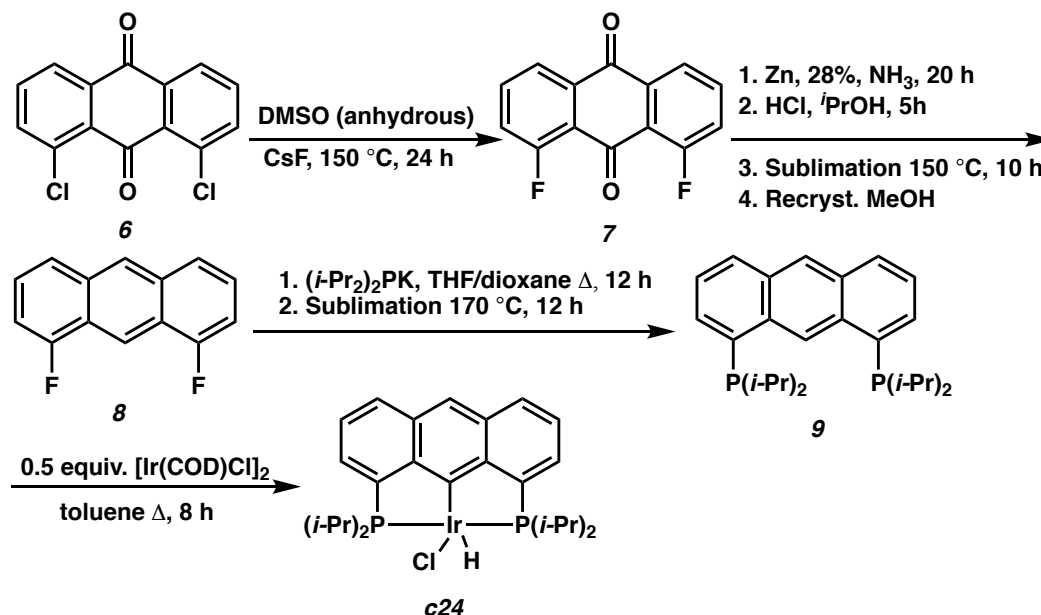


2.3.4 Synthesis of (i -Pr⁴Anthraphos)-Ir Complex **c24**



Complex (i -Pr⁴anthraphos)-Ir **c24** was first reported by Haenel *et al.* in 2001 for alkanes dehydrogenation.²² Complex **c24** was found to have higher thermal stability (up to 250 °C) relative to other Ir pincer ligated complexes and exhibited high catalytic activity when used as a dehydrogenation catalyst on the COA/TBE system. This complex was synthesized by Dr. Michael Haibach following literature protocols (Scheme 2.9).²³⁻²⁴ The anthraphos ligand **9** was first synthesized from commercially available 1,8-dichloroanthraquinone (**6**) followed by fluorination generating **7** and then reduction to 1,8-difluoroanthracene (**8**). Then **8** was treated with (i -Pr₂)₂PK affording the desired anthraphos ligand **9**. Finally, cyclometallation with half an equivalent of [Ir(COD)Cl]₂ in refluxing toluene generates the desired complex **c24**. The diagnostic NMR signals of **24** are the hydride shift expected at -35.90 ppm in the ¹H NMR spectrum and the phosphine shift expected at 61.00 ppm in the ³¹P NMR spectrum.²³

Scheme 2.9 Synthesis of (*i*-Pr⁴Anthraphos)-Ir Complex **c24**

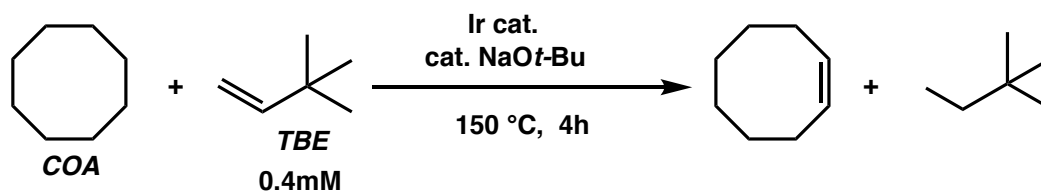


2.3.5 COA/TBE Transfer Dehydrogenation System and Reaction Set-Up Investigation

After synthesizing complexes (*t*-Bu⁴PCP)-Ir **c3** and (*t*-Bu⁴POCOP)-Ir **c13**, dehydrogenation reactions were performed on the **COA/TBE** system to validate the complexes activity as dehydrogenation catalysts.

Following the Jensen and Brookhart transfer dehydrogenation of **COA/TBE** system published procedures we tested the complexes in a degassed 0.4 mM stock solution under an argon atmosphere and the reaction mixture was prepared in a sealed vial inside the glovebox (setup a).^{3, 19} The transfer dehydrogenation of **COA/TBE** system was first investigated with the parent complex (*t*-Bu⁴PCP)-Ir **c3** using the hydrogenated version and precatalyst (Table 2.1 entry 1 and 2). Only 7.0 and 64.8 TONs were obtained and 16.2% to 17.6% of **TBE** was hydrogenated.

Table 2.1 COA/TBE Transfer Dehydrogenation Reactions with Complexes (*t*-Bu₄PCP)-Ir **c3 and (*t*-Bu₄POCOP)-Ir **c13****



entry	cat.	loading (mol.%)	TON	TBE conv.	set up ^a
1	(c3)IrH ₂	0.11	7.0	16.2%	a
2	(c3)IrHCl	0.08	64.8	17.6%	a
3	(c3)IrH ₂	0.18	9.4	30.4%	b
4	(c3)IrH ₂	0.14	12.5	25.7%	b
5	(c3)IrHCl	0.15	24.8	15.9%	b
6	(c3)IrHCl	0.11	20.9	27.2%	c
7	(c3)IrHCl	0.13	28.3	28.2%	d
8	(c13)Ir(C ₂ H ₂)	0.09	13.2 ^b	11.3%	a
9	(c13)Ir(C ₂ H ₂)	0.22	23.5	35.4%	b
10	(c13)Ir(C ₂ H ₂)	0.15	24.7	26.8%	b
11	(c13)Ir(C ₂ H ₂)	0.14	11.4	22.5%	c
12	(c13)IrHCl	0.15	5.3	13.8%	c
13	(c13)IrHCl	0.34	11.4	28.3%	c

[a] set up conditions: a = sealed vial, b = sealed vial with new **COA**, c = sealed Schlenk pressure flask with new **COA** + **TBE**, d = J. Young Tube with new **COA** + **TBE**. [b] reaction was run overnight.

Then, we investigated complex (*t*-Bu₄POCOP)-Ir **c13** catalytic activity using the ethylene species. Only 13.2 TONs were achieved and **TBE** was partially hydrogenated (Table 2.1 entry 8). In contrast to the literature reports, these complexes exhibited low

catalytic activity and the results were not consistent with literature values. A new **COA/TBE** stock solution was prepared and reaction mixtures were mixed in a sealed vial inside an argon glovebox (setup b). The obtained TONs with setup b with complexes **c3** and **c13** were again very low and exhibited low catalytic activity (Table 2.1 entries 3-5, and 9-10).

The dehydrogenation reactions of **COA/TBE** run at 150 °C, and there is a possibility that the vial cap was not sealing properly due to the high vapor pressure from the reaction mixture. Hence, a new reaction setup was investigated that replaced the sealed vial with a sealed Schlenk pressure flask (setup c). The transfer dehydrogenation of **COA/TBE** system was tested with setup c using complexes **c3** and **c13** (Table 2.1 entries 6, 11-13) and low TONs were still observed. We performed ³¹P NMR spectroscopy of complex (*t*-Bu⁴PCP)IrHCl **c3** to investigate the reasons behind the observed low catalytic activity. The diagnostic phosphine shift of complex **c3** is 67.02 ppm in the ³¹P NMR spectrum and we found that the complex had become significantly oxidized while being exposed to the glovebox atmosphere (Figure 2.2a). Hence, we investigated the transfer dehydrogenation of **COA/TBE** system with the same complex in a J. Young NMR tube (set up d) (Table 2.1 entry 7). After heating the reaction mixture to the required temperature for dehydrogenation, ³¹P NMR revealed that the all of the complex had oxidized product (Figure 2.2b).

It was concluded that rigorous air-free conditions were needed for the catalytic activity for dehydrogenation type reactions and even low ppm oxygen levels from the glovebox resulted in inhibition of catalytic activity. This conclusion is in agreement with

previous reports by Jensen and Yamashita that reported (PCP)-Ir type pincer catalysts can be inhibited by small amounts of impurities.²⁵⁻²⁶

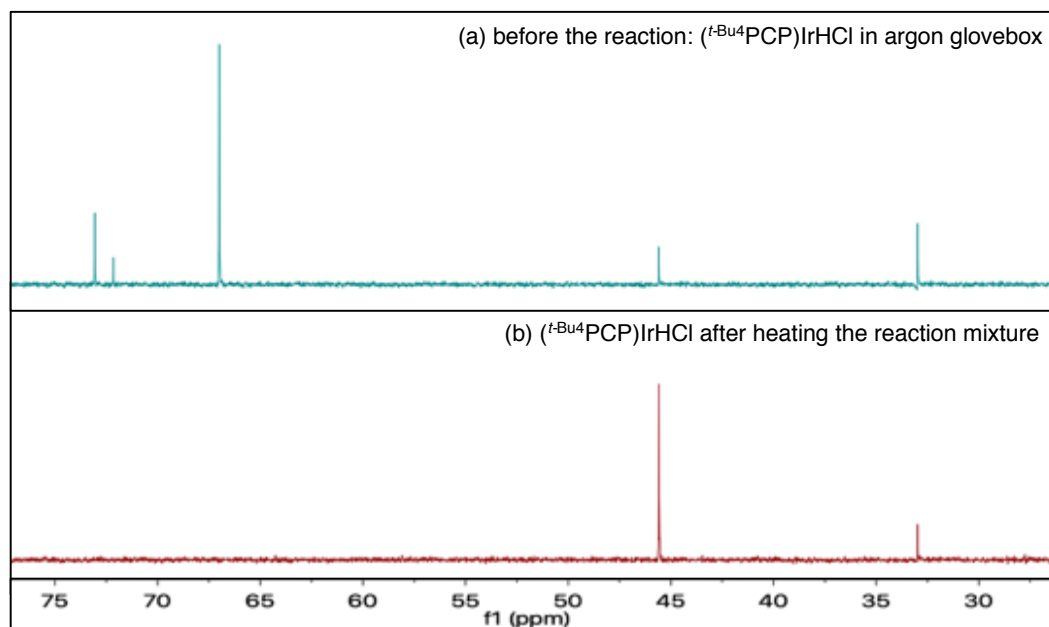


Figure 2.2 (a) ^{31}P NMR of $(t\text{-Bu}_4\text{PCP})\text{IrHCl}$ **c3** Before the Reaction (b) ^{31}P NMR of $(t\text{-Bu}_4\text{PCP})\text{IrHCl}$ **c3** After Heating the Reaction Mixture in Table 2.1 Entry 7

Hence, all dehydrogenation reactions must be performed in a flame-dried sealed Schlenk pressure flask with rigorously distilled, degassed *via* performing freeze-pump-thaw x5 cycles, and dried solvents with molecular sieves, NaH, or Na-K alloy. We have observed improved catalytic activity of the Ir pincer ligated complexes when these preparations were made.

2.4 TRANSFER DEHYDROGENATION OF HETEROCYCLIC ALKANES CATALYZED BY IRIIDIUM Pincer LIGATED COMPLEXES

2.4.1 6-Methoxy-1,2,3,4-Tetrahydronaphthalene Transfer Dehydrogenation

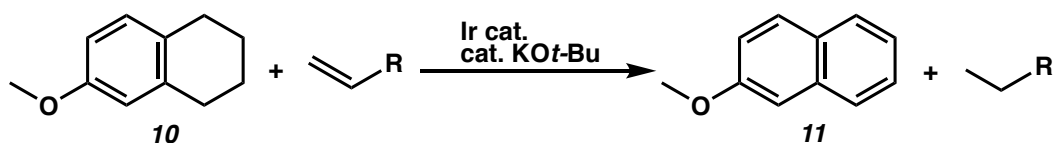
A. Introduction

Substituted naphthalene derivatives are important building blocks in pharmaceuticals and in many biologically active compounds that possess antibiotic and anticancer activities.²⁷⁻³¹ In addition, substituted naphthalene derivatives have found applications due to their desired optical and electronic characteristics.³²⁻³⁴ There have been great efforts in developing new methods for the synthesis of naphthalene skeletons in the recent years. However, the synthesis of substituted naphthalenes can be cumbersome and is difficult *via* conventional electrophilic aromatic substitution owing to the poor regioselectivity.³⁵ Hence, it is of interest to develop new facile regioselective methods towards the synthesis of such molecules without lengthy synthetic sequences. For example, constructing substituted naphthalenes from corresponding cyclohexanes *via* C(sp³)-H dehydrogenation by Ir pincer ligated complexes can be an attractive method to access such compounds.

Once we had established a successful rigorous air-free reaction set up and conditions for dehydrogenation systems by Ir pincer ligated complexes, the next part of our study focused on investigating the catalytic activity of synthesized Ir pincer ligated complexes towards transfer dehydrogenative aromatization by using

6-methoxy-1,2,3,4-tetrahydronaphthalaene (**10**) to 2-methoxynaphthalene (**11**) as a model substrate (Scheme 2.10).

Scheme 2.10 Transfer Dehydrogenation of 6-Methoxy-1,2,3,4-Tetrahydronaphthalene Catalyzed by Ir Pincer Ligated Complexes

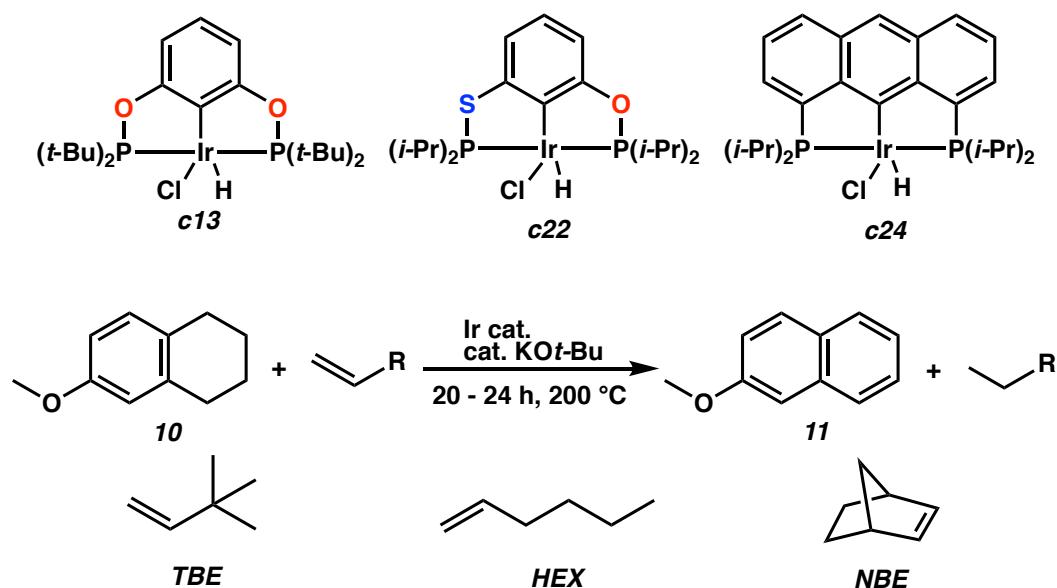


B. Catalyst Screening and Reaction Optimization

We began reaction optimization on 6-methoxy-1,2,3,4-tetrahydronaphthalene (**10**) using complexes ($i\text{-Bu}^4\text{POCOP}$)–Ir **c13**, ($i\text{-Pr}^4\text{PSCOP}$)–Ir **c22**, and ($i\text{-Pr}^4\text{anthrphos}$)–Ir **c24** and 3,3-dimethyl-1-butene (**TBE**) as an H_2 acceptor (Table 2.2). The reactions were carried out neat under an argon atmosphere at 200 °C. We first conducted a control experiment where only $\text{KO}t\text{-Bu}$ was added without the Ir pincer ligated complex to ensure desired product is not generated from this mild base alone (Table 2.2 entry 1); product was not observed in the absence of Ir.

We found that complexes **c13** and **c24** were the most active in dehydrogenating **10** and up to 52.5% of 2-methoxynaphthol (**11**) was generated and up to 96.5% of TBE was hydrogenated (Table 2.2 entry 2 and 4), while complex **c22** showed modest activity even when running the reaction for longer times (Table 2.2 entry 3).

Table 2.2 Catalyst and Acceptor Screening of 6-Methoxy-1,2,3,4-Tetrahydronaphthalene Transfer Dehydrogenation



entry	cat.	loading (mol.%)	H ₂ acceptor	equiv. of acceptor	acceptor conv.	11 yield ^b	TON ^c
1	-	-	TBE	1.0	-	0.2%	-
2	c13	0.13	TBE	1.0	96.5%	52.5%	404
3	c22	0.36	TBE	1.0	37.9%	33.2% ^d	92
4	c24	0.24	TBE	1.0	90.5%	49.8%	207
5	c13	0.12	NBE	1.0	98.3%	44.0%	293
6	c13	0.15	NBE	2.5	87.5%	63.9%	426
7	c13	0.25	HEX	1.0	82.9%	48.6%	194
8	c13	0.63	HEX	2.5	94.5%	67.1%	106

[a] Conditions: 3.2 mmol of **10**, Ir cat. with at least 1.2 equiv. KO t -Bu. [b] Conversion determined by GC. [c] TON per dehydrogenation. [d] reaction carried for 48 h.

In all cases, only the fully dehydroaromatized product 2-methoxynaphthalene (**11**) was observed and no olefinic product was observed corresponding to one dehydrogenation

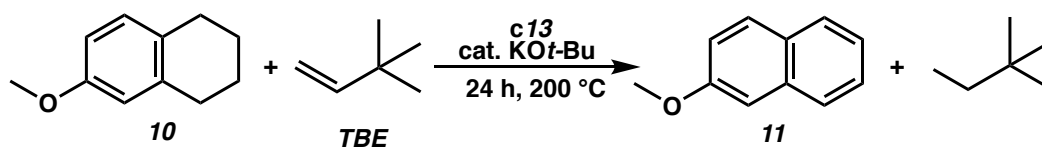
cycle. Compared to the other complexes, (*t*-Bu⁴POCOP)-Ir **c13** affords better access to the metal site attributed to the more open geometry of P-Ir-P acute angle and the shorter C-O and P-O bond lengths of the POCOP ligand.³⁶⁻³⁷ For instance, (*t*-Bu⁴POCOP)-Ir **c13** has bite angle of 157.55(3)° and complex (*t*-Bu⁴PCP)-Ir **c3** has bite angle of 164.510(8)°.

In addition, complex **c13** is air-stable which is advantageous relative to the other complexes. Thus, we selected it to further optimize the reaction conditions for dehydroaromatizing **10**.

We next examined 1-hexene (**HEX**) and norbornene (**NBE**) as alternative H₂ acceptors due to their economic advantage compared to **TBE**. However, **TBE** ultimately proved to be the best H₂ acceptor as determined by yield of **11** under similar conditions for **10** (Table 2.2 entries 5-8). In addition, when higher catalyst loading and equivalence of acceptor was used, only a modest increase of Ir catalytic activity was observed (Table 2.2 entry 6 and 8). Hence, we decided to further optimize the dehydrogenation of **10** using **TBE** only as an acceptor (Table 2.3). While increasing either the equivalence of **TBE** or the catalyst loading alone had minimal effect on increasing the yield (Table 2.3 entry 1 and 2), higher conversions were achieved when both parameters are increased simultaneously (Table 2.3 entry 3 and 4). However, excessively high **TBE** to catalyst ratio deteriorated the catalytic activity (Table 2.3 entry 5). A likely explanation is that the **TBE** inhibits the catalyst by binding to it and favoring the resting state vinyl complex **H** shown in Scheme 1.6 in Chapter 1. Further optimization resulted in 99% yield of 2-methoxynaphthalene (**11**) (Table 2.3 entry 6).

Next the effect of temperature on the catalytic activity of (t -Bu⁴POCOP)-Ir **c13** was studied (Figure 2.3). The transfer dehydrogenation of **10** using **TBE** was run at 150 °C and 120 °C for longer times, while keeping all other conditions constant (Table 2.3 entries 7-9). It was observed that lowering the temperature decreased catalytic activity.

Table 2.3 Reaction Optimization of 6-Methoxy-1,2,3,4-Tetrahydronaphthalene Transfer Dehydrogenation Using Complex (t -Bu⁴POCOP)-Ir **c13**



entry	cat. loading (mol.%)	equiv. of TBE	TBE conv.	11 yield ^b	TON ^c
1	0.15	1.5	73.0%	41.6%	277
2	0.15	2.0	51.1%	53.2%	341
3	0.26	2.0	51.4%	56.3%	198
4	0.40	2.0	97.9%	72.9%	182
5	0.41	3.0	44.9%	54.7%	133
6	0.59 ^d	3.0	75.8%	99.0%	169
7*	0.16	1.0	78.6%	39.2%	245
8*	0.16	1.0	100.0%	38.2%	242
9**	0.16	1.0	60.5%	17.1%	107

[a] Conditions: 3.2 mmol of **10**, precatalyst with at least 1.2 equiv. KO t -Bu. [b] Conversion determined by GC ¹H NMR using cis-1,4-diacetoxy-2-butene as an internal standard. [c] TON per dehydrogenation. [d] **c13** (t -Bu⁴POCOP)-Ir-C₂H₄ ethylene version was used. *entries 10 and 11 were run at 150 °C for 22 h and 48 h. ** entry 12 was run at 120 °C for 72 h.

When the reaction was run at 150 °C and reaction time was increased from 22 h to 48 h, the maximum TONs achieved was 245. Similarly, when the reaction was run at 120

°C for 72 h, complex **c13** exhibited low catalytic activity, achieving a maximum of 107 TONs. Hence, we conclude that carrying the reaction at 200 °C is necessary for achieving optimal conversions. In all cases, only the fully dehydroaromatized product **11** was observed and we do not observe an olefinic intermediate, hence we conclude that the direct dehydroaromatization of **10** is selective to the desired product.

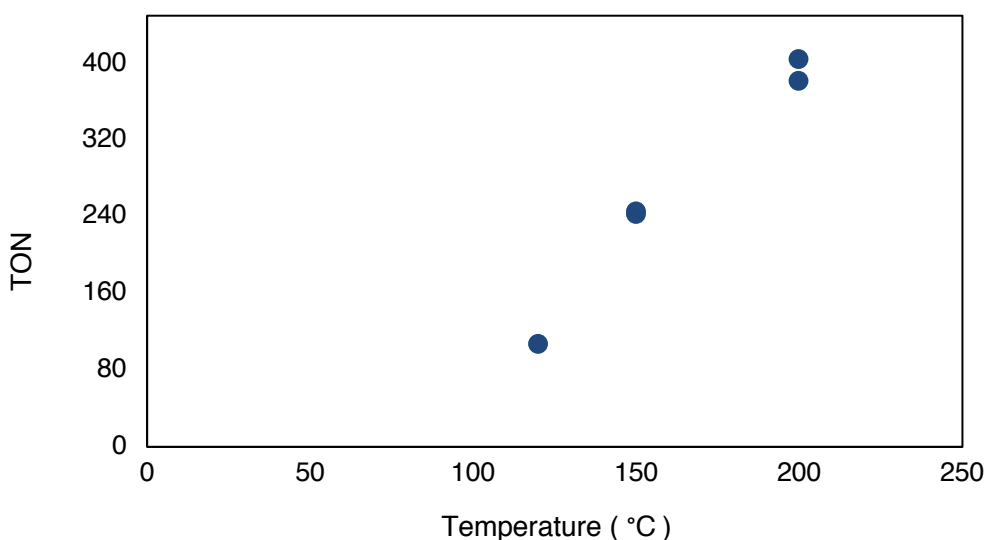


Figure 2.3 Temperature Effect on (*t*-Bu⁴POCOP)-Ir **c13** Catalytic Activity as Dehydrogenation Catalyst of 6-Methoxy-1,2,3,4-Tetrahydronaphthalene **10**

2.4.2 Indane Transfer Dehydrogenation

A. Introduction

Many indene derivatives have interesting biological activity and have applications in material science.³⁸⁻⁴² The traditional approaches of indene syntheses include intramolecular electrophilic substitution reaction or cyclization induced by a nucleophilic attack to a suitable

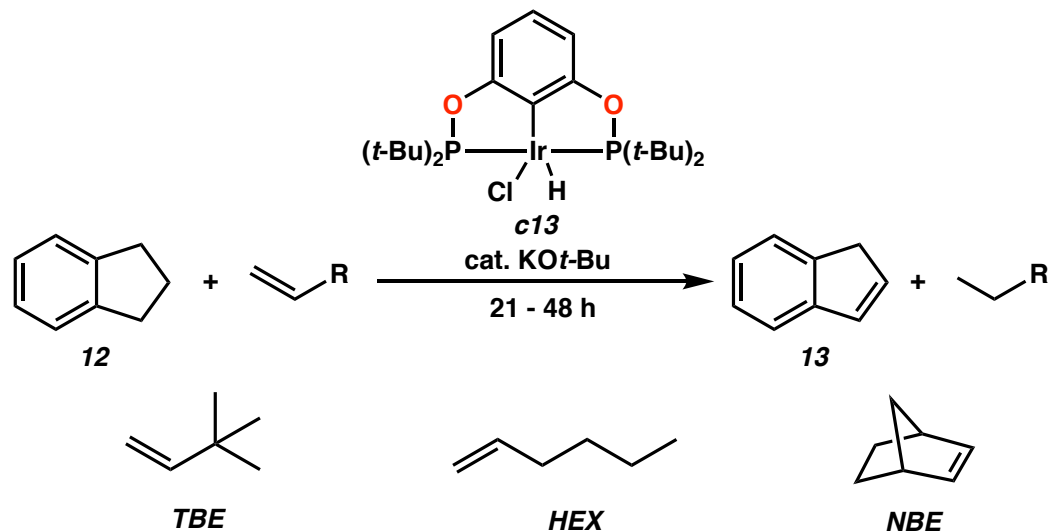
functional group.⁴³⁻⁴⁵ These synthetic methods require highly functionalized arenes, which can be cumbersome to prepare industrially. Here, we present an alternative and complementary approach to prepare indene *via* the direct dehydroaromatization of indane using complex (*t*-Bu⁴POCOP)-Ir **c13** (Table 2.4).

B. Reaction Optimization

Having established optimized reaction conditions in the previous section 2.4.1, we used similar condition and carried out the reactions neat under an argon atmosphere after drying and distilling all reagents. The transfer dehydrogenation of indane (**12**) was investigated using **TBE** as the H₂ acceptor at 200 °C (Table 2.4 entry 1). The reaction successfully generated indene (**13**) with a yield of 42.3% and TONs of 184. Replications of the reactions with **TBE** or **HEX** as H₂ acceptors generated no product and formed black carbonaceous deposits in the flask (Table 2.4 entry 2 and 3). It is not fully understood why the results could not be replicated. One possibility is that both **12** and **13** are acidic, and at high temperatures other side reactions such as polymerization may occur.

Alternatively, the reaction was investigated at lower temperatures 180 °C and 150 °C, while carrying out the reactions for longer times (48 h) (Table 2.4 entries 4-7). In contrary to the transfer dehydrogenation of **10** to **11** results observed in the previous section 2.4.1, we found that complex (*t*-Bu⁴POCOP)-Ir **c13** catalytic activity increased when decreasing the temperature. When the transfer dehydrogenation of indane (**12**) was investigated at 180 °C, the obtained yield of indene (**13**) was 47.5% (Table 2.4 entry 4).

Table 2.4 Transfer Dehydrogenation of Indane to Indene by Complex $(t\text{-Bu}_4\text{POCOP})\text{-Ir}$ **c13**



entry	cat. loading (mol.%)	H ₂ acceptor	equiv. of acceptor	temperature (°C)	conv of acceptor	13 yield ^b	TON ^c
1	0.23	TBE	1	200	42.0%	42.3%	184
2	0.24	TBE	1	200	96.5%	-	-
3	0.23	HEX	1	200	24.6%	-	-
4	0.26	TBE	1	180	95.5%	47.5%	182
5	0.24	TBE	1	150	98.3%	60.8%	253
6	0.26	HEX	1	150	73.0%	27.1%	104
7	0.26	NBE	1	150	51.1%	58.1%	224
8	0.59	TBE	2.5	150	45.4%	95.8%	162

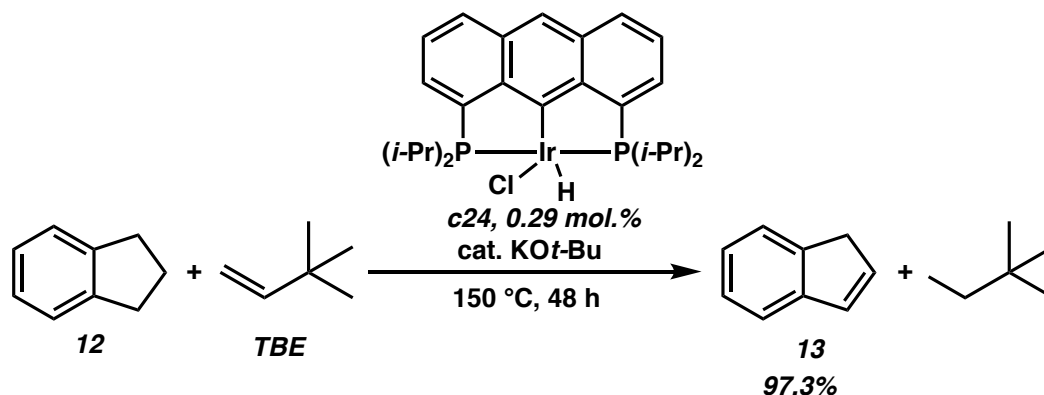
[a] Conditions: 3.2 mmol of **12**, precatalyst with at least 1.2 equiv. KOt-Bu. [b] Yield determined by GC and ¹H NMR using cis-1,4-diacetoxy-2-butene as an internal standard. [c] TON per dehydrogenation.

However, when the reaction was carried under similar conditions at 150 °C, 60.8% of indene (**13**) was generated (Table 2.4 entry 5). It is worth noting that using **HEX** as an H₂ acceptor was worse than **TBE** or **NBE** in this dehydrogenation system (Table 2.4 entry 6 and

7). After reaction optimization using complex **c13**, **13** was generated in excellent yields showing that this catalytic system is highly effective (Table 2.4 entry 8). In all cases, only indene (**13**) and the hydrogenated olefin was observed and no side products were generated.

Given that (*i*-Pr⁴anthrphos)-Ir **c24** exhibited high catalytic activity when used as a catalyst for transfer dehydrogenating **10** to **11** in the previous section 2.4.1, we employed it to transfer dehydrogenate **12** to **13** with TBE as the H₂ acceptor (Scheme 2.11). As we expected, complex **c24** achieved excellent yields generating 97.3% of **13** and 335 TONs. In summary, both complexes **c13** and **c24** exhibited high catalytic activity when dehydrogenating **12** to **13** and in all cases, the catalytic systems was selective to indene (**13**).

Scheme 2.11 Transfer Dehydrogenation of Indane Catalyzed by Complex (*i*-Pr⁴Anthrphos)-Ir **c24**



2.4.3 6-Methoxy-1,2,3,4-Tetrahydroquinoline Transfer Dehydrogenation

A. Introduction

Substituted quinoline scaffolds are important compounds that have been shown to possess a critical and a diverse range of biological activities such as antimalarial, antimicrobial, anti-inflammatory, and many other characteristics.⁴⁶⁻⁵⁰ In addition, some of these scaffolds have found applications as functional materials for organic light-emitting diodes.⁵¹⁻⁵³

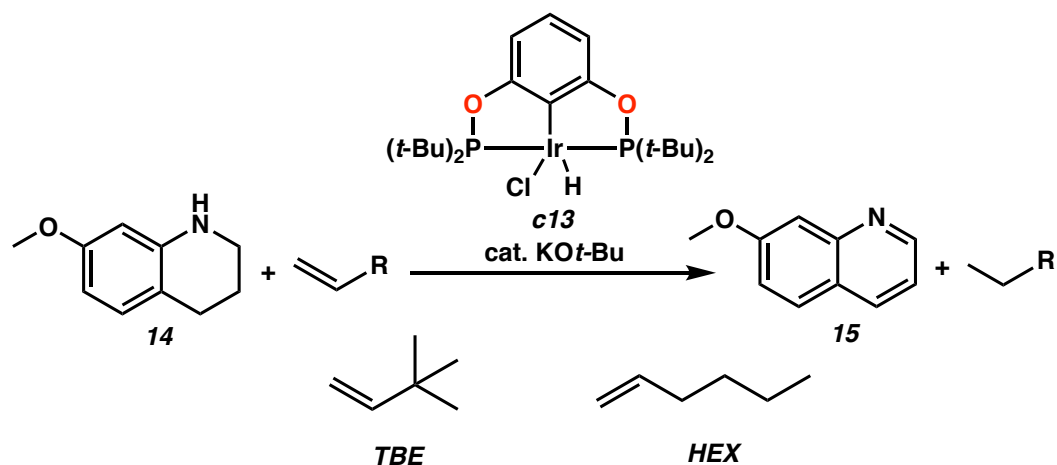
Owing to their great synthetic utility and useful properties, there has been great interest in finding new methods for the synthesis of quinoline scaffolds in the recent years. However, most of the current methods that synthesize substituted quinolines suffer from harsh and toxic conditions, requiring an oxygen atmosphere, and complex raw reagents.⁵⁰ The direct dehydroaromatization from alkane precursors can be an alternative and a complementary method to the current approaches. Here we present the synthesis of 6-methoxyquinoline and *via* C(sp³)–H dehydrogenation of 6-methoxy-1,2,3,4-tetrahydroquinoline by Ir pincer ligated complexes.

B. Catalyst Screening and Reaction Optimization

We commenced investigating the transfer dehydrogenation of 6-methoxy-1,2,3,4-tetrahydroquinoline (**14**) using complex (*t*-Bu⁴POCOP)–Ir **c13** and **TBE** as the H₂ acceptor at 200 °C (Table 2.5, entry 1). The reactions were carried out neat under an argon atmosphere after drying and distilling all reagents. Surprisingly, the complex

exhibited modest catalytic activity at the investigated initial conditions (cat. loading 1.38 mol.%) and reaction time (19 h) and only 29.9% of 6-methoxyquinoline (**15**) was generated.

Table 2.5. Transfer Dehydrogenation of 6-Methoxy-1,2,3,4-Tetrahydroquinoline by Complex (t-Bu₄POCOP)-Ir **c13**



entry	cat. loading (mol.%)	H ₂ acceptor	equiv. of acceptor	temperature (°C)	reaction time	15 yield ^b	TON ^c
1	1.38	TBE	3.0	200	19 h	29.9%	21
2	1.62	TBE	5.0	200	43 h	50.9%	31
3	1.98	TBE	5.0	150	48 h	16.7%	9
4	1.80	HEX	5.0	200	22 h	70.2%	39
5	4.09	HEX	6.0	200	22 h	93.5%	22
6	4.06	HEX	6.0	160	96 h	68.1%	17

[a] Conditions: 3.2 mmol of **14**, precatalyst with at least 1.2 equiv. KO^tBu. [b] Yield determined by GC and ¹H NMR using cis-1,4-diacetoxy-2-butene as an internal standard. [c] TON per dehydrogenation.

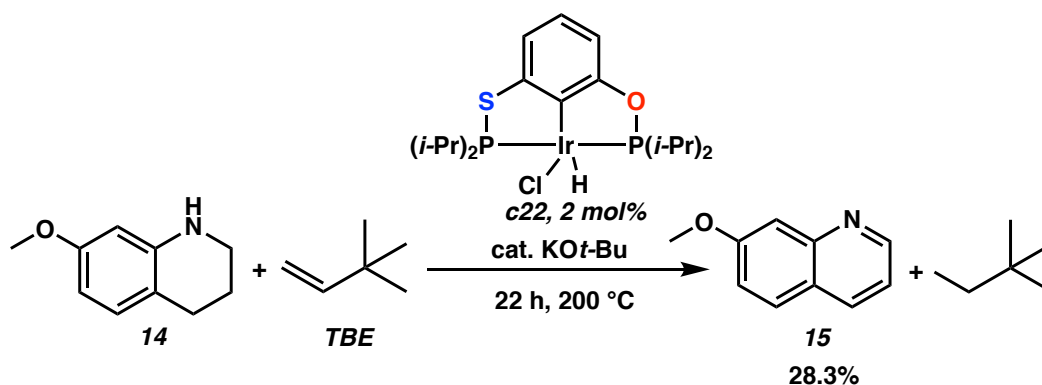
Hence, we carried out the reaction for longer time (43 h) and slightly increasing the cat. loading to 1.62 mol.%, and we observed increased yield of **15** to 50.9% (Table 2.5 entry 2). It is evident that the transfer dehydrogenation of **14** with **TBE** as an H₂ acceptor is slower

compared to previously discussed substrates 6-methoxy-1,2,3,4-tetrahydronaphthalene (**10**) (section 2.4.1) and indane (**12**) (section 2.4.2). Since we obtained better results when lowering the temperature for the transfer dehydrogenation of **12**, we also lowered the temperature to 150 °C when investigating the transfer dehydrogenation of **14** and increasing the catalyst loading to 1.98 mol.% (Table 2.5 entry 3). However, the yield of **15** was significantly deteriorated and only 16.7% was obtained.

Alternatively, the dehydrogenation reaction of **14** was investigated using **HEX** as the H₂ acceptor instead of **TBE**. We were delighted to find that the catalytic activity of **c13** was higher and 70% of **15** was generated when the reaction was carried out under similar conditions at 200 °C (Table 2.5 entry 4). Increasing the catalyst loading while maintaining all the other parameters similar generated optimized reaction conditions and excellent yields up to 93.5% of **15** (Table 2.5 entry 5). We then investigated lowering the temperature to 160 °C when using **HEX** as the H₂ acceptor but we found that the catalytic activity was poor even when carrying out the reaction for 96 h (Table 2.5 entry 6). It is not fully understood why using **HEX** was a better H₂ acceptor compared to **TBE** and generated better yields of **15**. This finding is contrary to literature reports where (PCP)-Ir pincer type complexes have been shown to have greater binding affinity to terminal and linear olefins relative to **TBE**. The greater steric hinderance of **TBE** is known to mitigate the binding of dehydrogenated products to the Ir metal center, thereby increasing (PCP)-Ir pincer complexes' catalytic activity.^{1, 54}

Given that Huang and co-workers reported good catalytic activity of $(i\text{-Pr}^4\text{PSCOP})\text{-Ir}$ **c22** when dehydrogenating *N*-heterocyclic alkanes,⁵ we investigated dehydrogenating **14** to **15** using complex **c22** (Scheme 2.12). However, we observed lower catalytic activity comparable to complex **c13** when the reaction was run under similar conditions with **TBE** as the H_2 acceptor and only 28.3% of **15** was generated. Hence, further optimization with complex **c22** was not performed. In all cases, the investigated transfer dehydrogenation reactions of **14** generated the fully dehydroaromatized substrate **15** as the only product and no side reactions were observed.

Scheme 2.12 Transfer Dehydrogenation of 6-Methoxy-1,2,3,4-Tetrahydroquinoline **14** by Complex $(i\text{-Pr}^4\text{PSCOP})\text{-Ir}$ **c22**



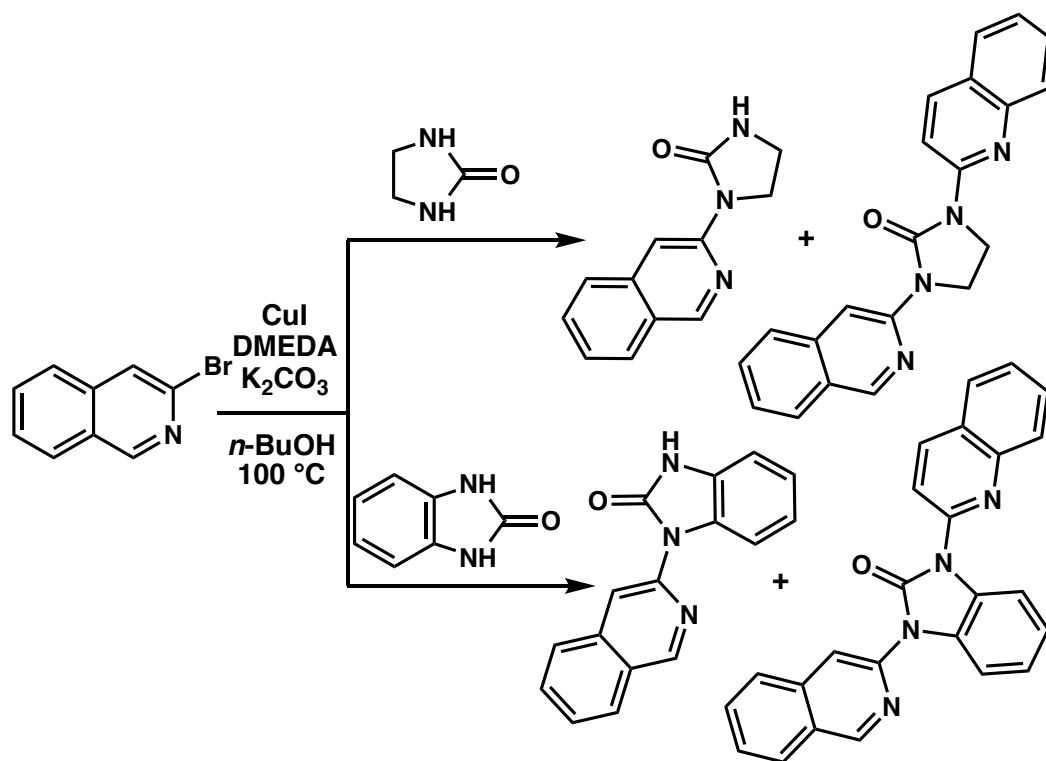
2.4.4 7-Bromo-1,2,3,4-Tetrahydroisoquinoline Transfer Dehydrogenation

A. Introduction

Isoquinoline skeletons constitute important structural framework in natural products, pharmaceuticals, and functional materials.⁵⁵⁻⁵⁹ In addition, brominated isoquinoline derivatives are extremely useful synthetic blocks that are used to synthesize

novel isoquinoline derivatives with fluorescence properties (Scheme 2.13).⁶⁰⁻⁶³ Hence, there has been significant interest in constructing isoquinoline scaffolds. Classical methods involve Bischler-Napieralski and Pictet-Spengler reactions which require harsh acidic conditions limiting their practical usage.⁶⁴⁻⁶⁵ In addition, selective bromination of quinolines is cumbersome and require lengthy reaction periods and difficult work up.⁶⁶⁻⁶⁸

Scheme 2.13 Selected Examples of Brominated Isoquinoline Synthetic Utility

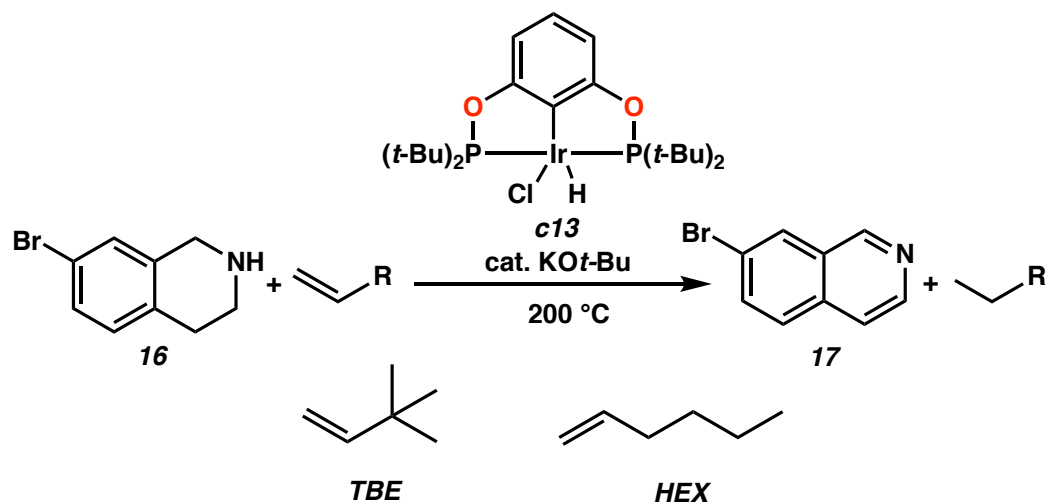


Herein, we present an alternative and complementary facile method of the synthesis of 7-bromoisoquinoline *via* the direct $C(sp^3)$ -H dehydrogenation of 7-bromo-1,2,3,4-tetrahydroisoquinoline by Ir pincer ligated complexes.

B. Reaction Optimization

We began investigating the transfer dehydrogenation of 7-bromo-1,2,3,4-tetrahydroisoquinoline (**16**) using complex (*t*-Bu⁴POCOP)-Ir **c13** and **TBE** as the H₂ acceptor at 200 °C (Table 2.6, entry 1). The reactions were carried out neat under an argon atmosphere after drying and distilling all reagents. The complex exhibited good catalytic activity at the investigated conditions and 66.7% of 7-bromoisoquinoline (**17**) was generated. In an attempt to optimize the product yield, we carried out the reaction with excess **TBE** and longer reaction times up to 144h, we only observed 50.1% and 49.1% of **17** however (Table 2.6 entry 2 and 3). Similar to what we observed in the previous section 2.4.3 when investigating the transfer dehydrogenation of **14**, we found that high concentrations of **TBE** limited the catalytic activity of complex **c13** due to the possibility of shifting the binding equilibrium at higher concentrations. Hence, alternatively we investigated the transfer dehydrogenation of **16** with **HEX** as the H₂ acceptor (Table 2.6 entry 4). We optimized reaction conditions with **HEX** and we achieved excellent yields up to 91.4% of **17** was generated. In all cases, only the fully dehydroaromatized product **17** was observed and no side reactions were detected, thus providing a new complementary and an alternative selective method toward the synthesis of brominated isoquinoline skeletons.

Table 2.6 Transfer Dehydrogenation of 7-Bromo-1,2,3,4-Tetrahydroisoquinoline by Complex (t-Bu₄POCOP)-Ir **c13**



entry	cat. loading (mol.%)	H ₂ acceptor	equiv. of acceptor	reaction time	17 yield ^b	TON ^c
1	3.42	TBE	1.0	24 h	66.7%	20
2	8.27	TBE	10.0	45 h	50.1%	6
3	8.75	TBE	exs	144 h	49.1%	6
4	6.24	HEX	exs	24 h	91.4%	15

[a] Conditions: 3.2 mmol of **16**, precatalyst with at least 1.2 equiv. KOt-Bu. [b] Yield determined by GC and ¹H NMR using cis-1,4-diacetoxy-2-butene as an internal standard. [c] TON per dehydrogenation.

2.4.5 Tetralone Derivatives Transfer Dehydrogenation

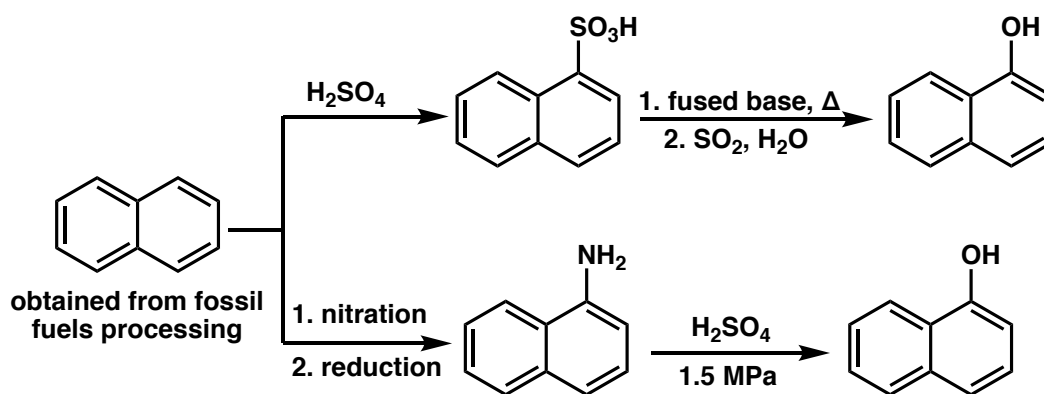
A. Introduction

Naphthol derivatives serve as important building blocks in pharmaceuticals, agrochemicals, polymers, and natural products.⁶⁹⁻⁷¹ Classical industrial methods to make naphthol compounds rely on the alkali fusion of naphthalene sulfuric acid or

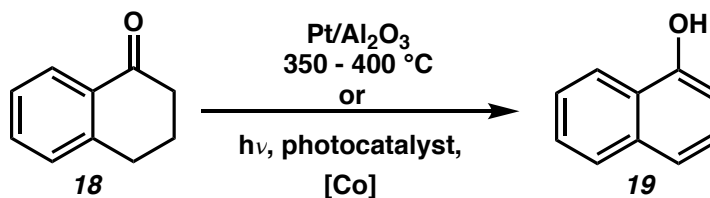
α -naphthylamine hydrolysis at elevated temperatures and high pressures (Scheme 2.14).⁷²

Due to their synthetic utility, alternative approaches have been reported utilizing the direct dehydrogenation of 1-tetralone to 1-naphthol *via* heterogeneous catalysis at high temperatures or *via* photocatalytic continuous flow technology (Scheme 2.15).⁷³⁻⁷⁶

Scheme 2.14 Industrial Methods for the Synthesis of α -Naphthol



Scheme 2.15 Selected Examples of 1-Tetralone Dehydrogenation



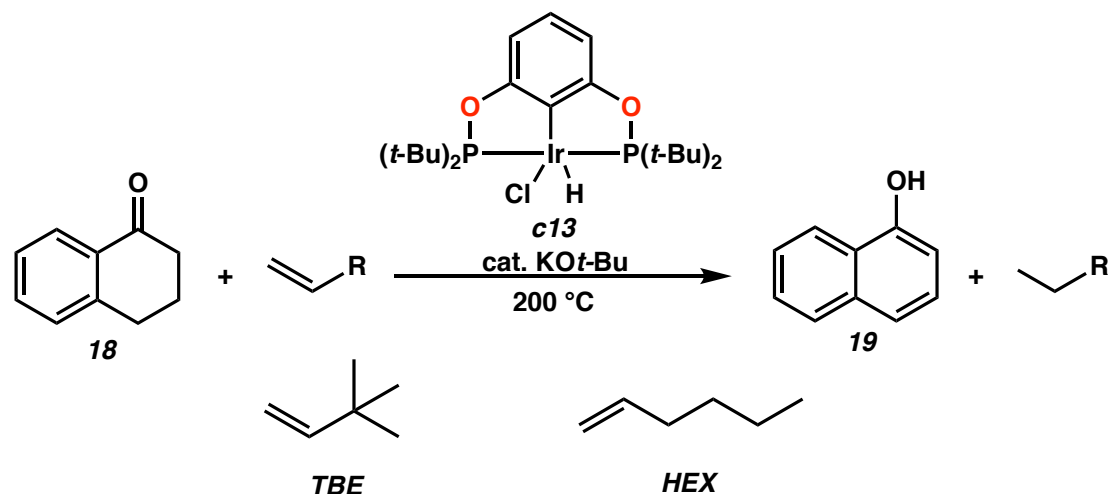
While these methods are promising, they suffer from the requirement of high temperatures and aerobic conditions. In addition, the requirement of a photocatalyst system lacks industrial practicality and would be difficult to translate to large scale. As shown in the introduction, Goldman and Nozaki reported the dehydrogenation of oxygenated heterocycles and ketones using Ir pincer ligated complexes, albeit with very limited

applicability. Here we present an alternative and complementary method of 1-tetralone (**18**) transfer dehydrogenation to 1-naphthol (**19**) using Ir pincer ligated complexes. In addition, fluorinated phenol skeletons are synthetically useful and often encountered in biologically active molecules and in pharmaceuticals.⁷⁷⁻⁸⁰ Thus, we also present the transfer dehydrogenation of 7-fluoro-1-tetralone (**20**) to 7-fluoro-1-naphthalenol (**21**).

B. Reaction Optimization of 1-Tetralone Transfer Dehydrogenation

We began investigating the transfer dehydrogenation of 1-tetralone (**18**) using complex (*t*-Bu⁴POCOP)-Ir **c13** and **TBE** as the H₂ acceptor at 200 °C (Table 2.7, entry 1 and 2). The reactions were carried out neat under an argon atmosphere after drying and distilling all reagents. The complex exhibited good catalytic activity at the investigated conditions and 47.6% of 1-naphthol (**19**) was generated. In an attempt to optimize the product yield, we carried out the reaction with higher equivalence of **TBE** and found that the yield of **19** was increased to 62.3% (Table 2.7 entry 4). We also investigated using **HEX** as an alternative acceptor under similar conditions to entry 2 and observed similar yields and up to 46.9% was generated (Table 2.7 entry 3). Overall, the catalytic activity of complex **c13** did not change when changing the H₂ acceptor in this system. That being said, we found that annulene and tetralin were generated as by-products in both cases.

Table 2.7 Transfer Dehydrogenation of 1-Tetralone by Complex (*t*-Bu⁴POCOP)-Ir **c13**



entry	cat. loading (mol.%)	H ₂ acceptor	equiv. of acceptor	reaction time	19 yield ^b	TON ^c
1	-	TBE	1.4	24 h	-	-
2	1.59	TBE	1.8	24 h	47.6%	30
3	1.00	HEX	1.8	45 h	46.9%	47
4	1.60	TBE	3.1	24 h	62.3%	39

[a] Conditions: 3.2-4.0 mmol of **18**, precatalyst with at least 1.2 equiv. KO^tBu. [b] Yield determined by GC and ¹H NMR using cis-1,4-diacetoxy-2-butene as an internal standard. [c] TON per dehydrogenation.

C. Reaction Optimization of 7-Fluoro-1-Tetralone Transfer Dehydrogenation

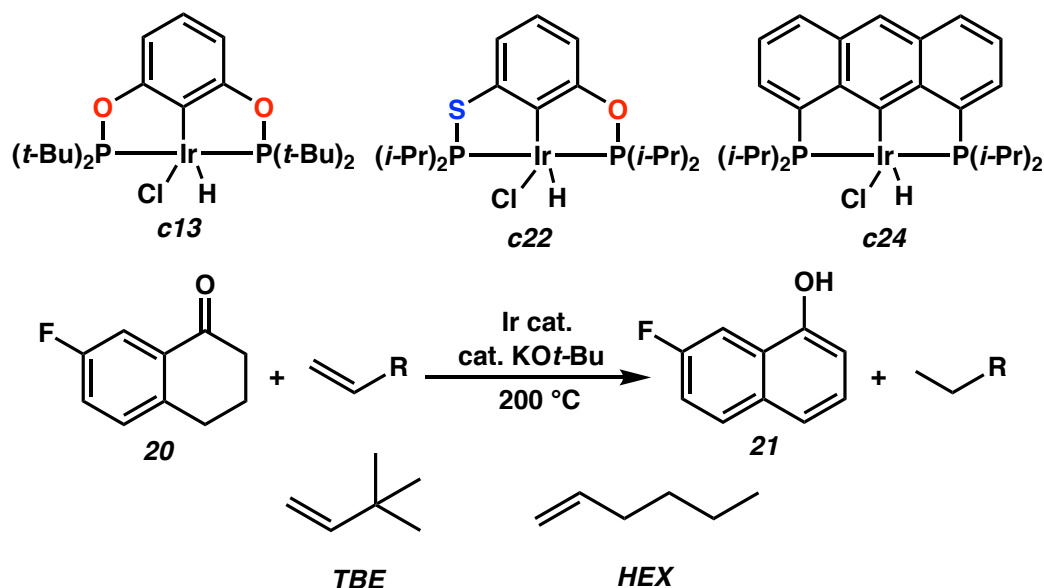
Similarly, we began investigating the transfer dehydrogenation of 7-fluoro-1-tetralone (**20**) using TBE as the H₂ and complex (*t*-Bu⁴POCOP)-Ir **c13** given its superior performance relative to the other investigated complexes shown in the previous sections. The reactions were carried out neat at 200 °C under an argon atmosphere after drying and distilling all reagents (Table 2.8). We found that the complex exhibited low catalytic activity even when carrying the reaction for 48 h and up to 17.9 % of

7-fluoronaphthalen-1-ol (**21**) was generated (Table 2.8 entries 1-3). Increasing the catalyst loading 4.61 mol.% increased the yield of **21** up to 20.6% (Tables 2.8 entry 4 and 5). It is evident that complex **c13** exhibits very low TOF in this system and a substantial increase of catalyst loading and reaction time is required to generate reasonable yields of **21**.

Therefore, we then investigated **HEX** as the H₂ acceptor and found that **c13** catalytic activity was higher and up to 36.6% of **21** was generated (Tables 2.8 entry 6 and 7). We do not fully understand why the catalytic activity increased with **HEX**, and one possible explanation is that **HEX** binding affinity to the complex may be higher than the product itself, leading to releasing it faster from the metal complex.

Alternatively, we investigated the transfer dehydrogenation of **20** to **21** using complexes (*i*-Pr⁴PSCOP)-Ir **c22** and (*i*-Pr⁴anthrphos)-Ir **c24** given that reported studies with these complexes exhibited high catalytic activity when employed on dehydrogenating heteroatomic systems. Complex **c22** exhibited similar low catalytic activity to **c13** under the same conditions and only up to 12.2% of **21** was generated (Table 2.8 entry 8). In contrary, complex **c24** exhibited excellent catalytic activity and up to 80.6% of **21** was generated (Table 2.8 entry 9).

Table 2.8 Transfer Dehydrogenation of 7-Fluoro-1-Tetralone Transfer Dehydrogenation by Ir Pincer Ligated Complexes



entry	cat. / loading (mol.%)	H ₂ acceptor	equiv. of acceptor	reaction time	19 yield ^b	TON ^c
1	c13 ^d /1.07	TBE	4.2	20 h	14.5%	13
2	c13/1.67	TBE	3.7	15 h	12.6%	7
3	c13/1.78	TBE	4.0	48 h	17.9%	10
4	c13/3.47	TBE	4.8	24 h	12.3%	3
5	c13 ^d /4.61	TBE	4.0	24 h	20.6%	4
6	c13/1.99	HEX	5.1	24 h	23.4%	12
7	c13/4.04	HEX	6.8	24 h	36.6%	9
8	c22/1.33	TBE	3.6	24 h	12.2%	9
9	c24/1.14	TBE	4.9	24 h	80.6%	71

[a] Conditions: 3.2 mmol of **20**, precatalyst with at least 1.2 equiv. KO^tBu. [b] Yield determined by GC and ¹H NMR using cis-1,4-diacetoxy-2-butene as an internal standard. [c] TON per dehydrogenation. [d] **c13** (^tBu₄POCOP)-Ir-C₂H₄ ethylene version was used.

Despite the similarity of the tridentate pincer structure of complexes **c13**, **c22**, and **c24**, the transfer dehydrogenation of **20** to **21** epitomizes how these complexes offer unexpected reactivities in different systems. We suspect that **c13** may form a more stable adduct with the naphthol product than the more sterically hindered **c24** given the more open geometry of P–Ir–P and shorter C–O and P–O bond lengths. Similarly, we believe the geometry of **c22** may account for its low catalytic activity. In all cases, we observed unidentified aromatic and olefinic side products and some decomposed starting material in reactions subjected to **c22**.

2.4.6 Acenaphthene Transfer Dehydrogenation

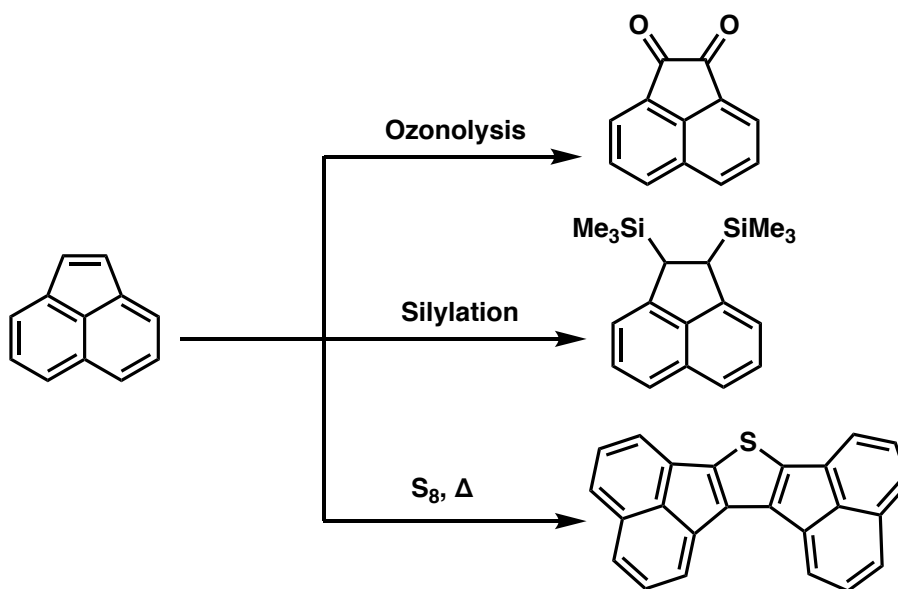
A. Introduction

Polycyclic aromatic hydrocarbons (PAHs) generally exhibit attractive electron-donating properties or electron-accepting properties making them useful in various applications. Such applications include functional dyes, semiconductors, and fluorescent materials.⁸¹⁻⁸⁶ Specifically, acenaphthylene is considered a versatile building block for constructing PAHs owing to its highly reactive C–C double bond ascribed to the ring strain of the fused cyclopentane ring.⁸⁷

Acenaphthylene is more expensive than acenaphthene and its derivatives are synthetically useful and serve as a versatile building block in organic reactions and materials applications owing to their capability to undergo ozonolysis or silylation reactions or to perform Diels-Alder reactions (Scheme 2.16).⁸⁷⁻⁹³ Hence, there has been a great interest in

finding and developing methods for the preparation of acenaphthylene and its derivatives (Scheme 2.17).

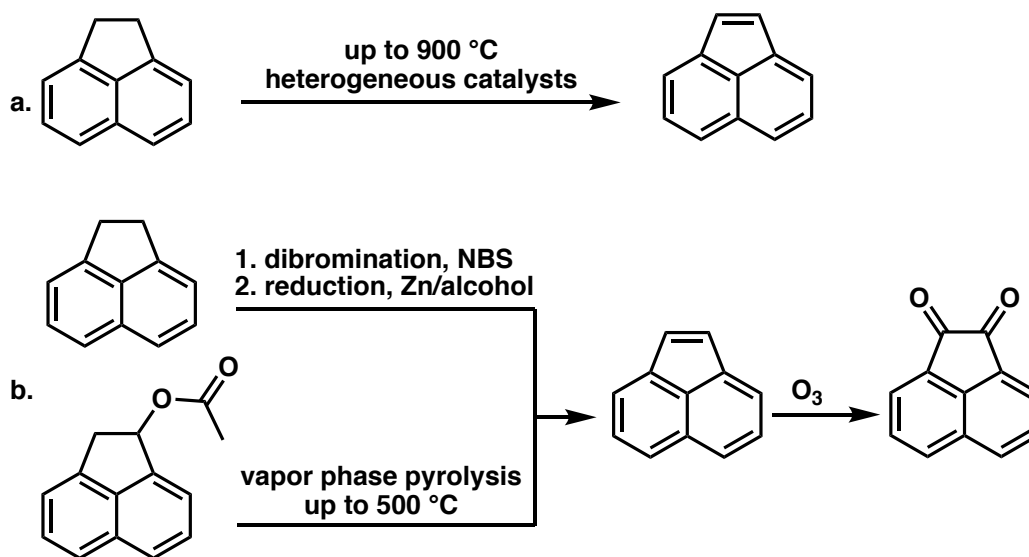
Scheme 2.16 Selected Examples Manifesting Acenaphthylene Synthetic Utility



Industrially, the only method of producing acenaphthylene is from dehydrogenating acenaphthene using heterogeneous catalysts at elevated temperatures up to 900 °C (Scheme 2.17a).⁹⁴⁻⁹⁵ Alternatively, there has been reports of synthetic approaches to acenaphthylene *via* dibromination of acenaphthene using two equivalents of *N*-bromosuccinimide (**NBS**) followed by debromination using zinc and an alcohol, or *via* vapor phase pyrolysis (Scheme 2.17b).⁹⁶ These approaches suffer from the use of stoichiometric toxic reagents or from highly energy intensive pyrolysis at up to 500 °C. We present the direct dehydroaromatization of acenaphthene to acenaphthylene without the need of stoichiometric

reagents or oxidants, and with milder conditions relative to industry practice by using Ir pincer ligated complexes.

Scheme 2.17 Selected Methods of Acenaphthylene Synthesis

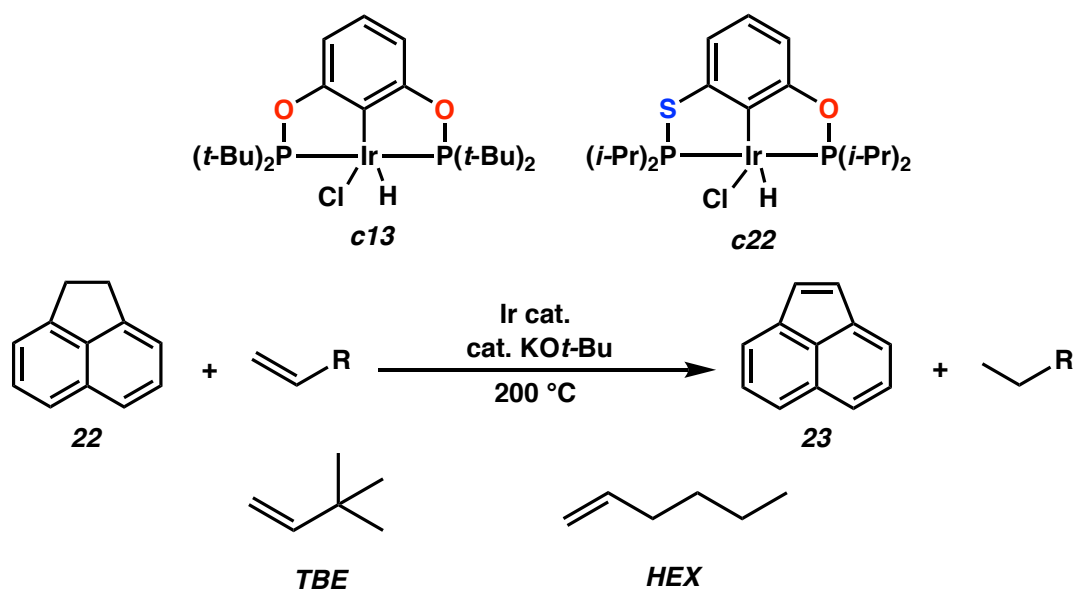


B. Reaction Optimization

We began investigating the transfer dehydrogenation of acenaphthene (**22**) using complex (*t*-Bu⁴POCOP)–Ir **c13** and TBE as the H₂ acceptor at 200 °C (Table 2.9, entry 1). The reactions were carried out neat at 200 °C under an argon atmosphere after drying and distilling all reagents. The complex exhibited low catalytic activity at the investigated conditions and only 20.3% of acenaphthylene (**23**) was generated. Alternatively, we performed the reaction using HEX as the H₂ acceptor and observed an increase in yield of **23** and up to 49.2% was generated (Table 2.9 entry 2 and 3). Steric hindrance of **22** is suspected to be responsible for the moderate catalytic activity in this system. We then investigated the catalytic activity of (*i*-Pr⁴PSCOP)–Ir **c22** in transfer dehydrogenating **22** to

23 using **TBE** as the H_2 acceptor (Table 2.9 entry 4). We observed poor catalytic activity of **c22** and only trace amounts of product were observed. In all cases only the desired product **23** was observed along with remaining unreacted starting material.

Table 2.9 Transfer Dehydrogenation of Acenaphthene using (*t*-Bu⁴POCOP)-Ir **c13** and (*i*-Pr⁴PSCOP)-Ir **c122**



entry	cat./loading (mol.%)	H ₂ acceptor	equiv. of acceptor	reaction time	19 yield ^b	TON ^c
1	c13/1.78	TBE	3.5	24 h	20.3%	11
2	c13/3.22	HEX	4.2	20 h	41.5%	13
3	c13/4.21	HEX	6.2	24 h	49.1%	13
4	c22/1.07	TBE	4.0	48 h	2.6%	2

[a] Conditions: 3.2 mmol **22**, precatalyst with at least 1.2 equiv. KO t -Bu. [b] Yield determined by GC and ^1H NMR using cis-1,4-diacetoxy-2-butene as an internal standard. [c] TON per dehydrogenation.

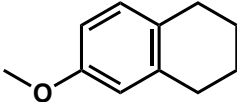
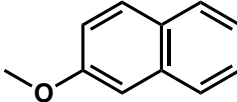
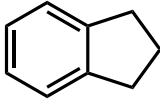
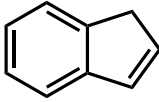
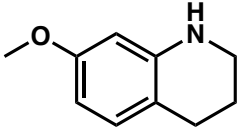
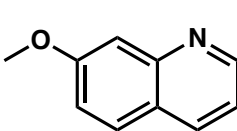
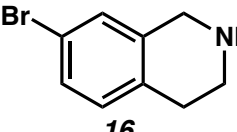
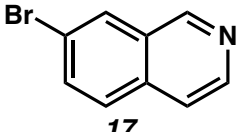
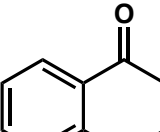
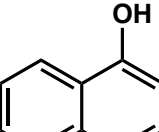
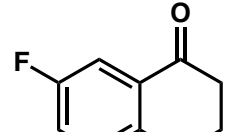
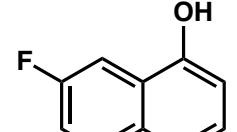
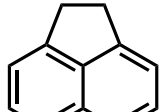
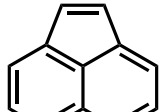
2.5 SUMMARY AND CONCLUSIONS

Aromatic frameworks are a core building block in organic chemistry and have been found in diverse applications such as pharmaceuticals and materials due to their synthetic utility. The direct dehydroaromatization of C(sp³)-H alkanes may seem conceptually simple but in fact is a challenging transformation. Industrially practiced methods utilize energy-intensive processes operating at high pressures and temperatures to overcome the endergonic and unreactive nature of alkanes. While there has been great advancement in the dehydrogenation transformation recently, the direct dehydroaromatization of substituted substrates generating functionalized aromatics is significantly underdeveloped. Hence, there is a great interest in developing methods for the synthesis of functionalized aromatics under milder conditions.

We have successfully extended the applicability of Ir-catalyzed dehydrogenation systems using pincer ligated complexes on substituted heterocyclic alkanes with functionalities known to be strongly coordinating and poorly compatible with (PCP)-Ir type catalysts (Table 2.10). For example, synthetically useful compounds such as fluorinated naphthol and brominated hydroisoquinoline were obtained in excellent yields up to 91%. Functional groups tolerated by our conditions include ketones, ethers, and fused arenes. We found that in most cases, **c13** and **c24** had higher catalytic activity relative to **c22**. In addition, in some cases using **HEX** as the H₂ acceptor instead of **TBE** generated higher yields, which is considerably more economical.

In all cases except with **20**, the fully dehydroaromatized substrate was the only observed product. Hence, our method provides a new selective and complementary route to these important and synthetically useful building blocks.

Table 2.10 Successfully Optimized Studied Dehydroaromatized Substrates by Ir Pincer Ligated Complexes

Substrate	Product	yield	cat./mol.%	H ₂ acceptor	temp (C°)	TON ^c
 10	 11	99.0%	c13 ^d /0.59	TBE	200	169
 12	 13	95.8%	c13/0.59	TBE	150	162
 14	 15	93.5%	c13/4.09	HEX	200	22
 16	 17	91.4%	c13/6.24	HEX	200	15
 18	 19	62.3%	c13/1.60	TBE	200	39
 20	 21	80.6%	c24/4.09	TBE	200	71
 22	 23	49.1%	c13/4.21	HEX	200	13

[a] Conditions: 3.2 – 4.0 mmol, precatalyst with at least 1.2 equiv. KO^tBu. [b] Yield determined by GC and ¹H NMR using cis-1,4-diacetoxy-2-butene as an internal standard. [c] TON per dehydrogenation. [d] ^tBu⁴POCOP)Ir(C₂H₄) ethylene version of **c13**.

2.6 NOTES AND REFERENCES

1. Kumar, A.; Bhatti, T. M.; Goldman, A. S., *Chemical Reviews* **2017**, 117 (19), 12357-12384.
2. Gupta, M.; Hagen, C.; Kaska, W. C.; Cramer, R. E.; Jensen, C. M., *Journal of the American Chemical Society* **1997**, 119 (4), 840-841.
3. Gupta, M.; Hagen, C.; Flesher, R. J.; Kaska, W. C.; Jensen, C. M., *Chem. Commun.* **1996**, (17), 2083-2084.
4. Yao, W.; Jia, X.; Leng, X.; Goldman, A. S.; Brookhart, M.; Huang, Z., *Polyhedron* **2016**, 116, 12-19.
5. Yao, W.; Zhang, Y.; Jia, X.; Huang, Z., *Angewandte Chemie International Edition* **2014**, 53 (5), 1390-1394.
6. Punji, B.; Emge, T. J.; Goldman, A. S., *Organometallics* **2010**, 29 (12), 2702-2709.
7. Huang, Z.; Brookhart, M.; Goldman, A. S.; Kundu, S.; Ray, A.; Scott, S. L.; Vicente, B. C., *Adv. Synth. Catal.* **2009**, 351 (1-2), 188-206.
8. Gupta, M.; C. Kaska, W.; M. Jensen, C., *Chem. Commun.* **1997**, (5), 461-462.
9. Lyons, T. W.; Bézier, D.; Brookhart, M., *Organometallics* **2015**, 34 (16), 4058-4062.
10. Ando, H.; Kusumoto, S.; Wu, W.; Nozaki, K., *Organometallics* **2017**, 36 (12), 2317-2322.
11. Zhang, X.; Wang, D. Y.; Emge, T. J.; Goldman, A. S., *Inorg. Chim. Acta* **2011**, 369 (1), 253-259.

12. Renkema, K. B.; Kissin, Y. V.; Goldman, A. S., *Journal of the American Chemical Society* **2003**, 125 (26), 7770-7771.
13. Zhang, X.; Fried, A.; Knapp, S.; Goldman, A. S., *Chem. Commun.* **2003**, (16), 2060-2061.
14. Brayton, D. F.; Jensen, C. M., *Chem. Commun.* **2014**, 50 (45), 5987-5989.
15. Akshai Kumar, A. S. G. In *The Privileged Pincer-Metal Platform: Coordination Chemistry & Applications*, Gerard Van Koten, R. A. G., Ed. Springer, Cham: Cham, 2015; Vol. 54, pp 307-334.
16. Moulton, C. J.; Shaw, B. L., *J. Chem. Soc., Dalton Trans.* **1976**, (11), 1020-1024.
17. Hebden, T. J.; Goldberg, K. I.; Heinekey, D. M.; Zhang, X.; Emge, T. J.; Goldman, A. S.; Krogh-Jespersen, K., *Inorg. Chem.* **2010**, 49 (4), 1733-1742.
18. Göttker-Schnetmann, I.; White, P. S.; Brookhart, M., *Organometallics* **2004**, 23 (8), 1766-1776.
19. Göttker-Schnetmann, I.; White, P.; Brookhart, M., *Journal of the American Chemical Society* **2004**, 126 (6), 1804-1811.
20. Göttker-Schnetmann, I.; Brookhart, M., *Journal of the American Chemical Society* **2004**, 126 (30), 9330-9338.
21. Bézier, D.; Brookhart, M., *ACS Catalysis* **2014**, 4 (10), 3411-3420.
22. Haelnel, M. W.; Oevers, S.; Angermund, K.; Kaska, W. C.; Fan, H.-J.; Hall, M. B., *Angewandte Chemie International Edition* **2001**, 40 (19), 3596-3600.
23. Romero, P. E.; Whited, M. T.; Grubbs, R. H., *Organometallics* **2008**, 27 (14), 3422-3429.

24. Ozerov, O. V.; Guo, C.; Papkov, V. A.; Foxman, B. M., *Journal of the American Chemical Society* **2004**, 126 (15), 4792-4793.
25. Kwan, E. H.; Kawai, Y. J.; Kamakura, S.; Yamashita, M., *Dalton Trans.* **2016**, 45 (40), 15931-15941.
26. M. Jensen, C., *Chem. Commun.* **1999**, (24), 2443-2449.
27. Ponra, S.; Vitale, M.; Michelet, V.; Ratovelomanana-Vidal, V., *Arkivoc* **2015**, 2016.
28. Wang, Y.; Zhang, X.; Zhao, J.; Xie, S.; Wang, C., *J. Med. Chem.* **2012**, 55 (7), 3502-3512.
29. Humljan, J.; Kotnik, M.; Contreras-Martel, C.; Blanot, D.; Urleb, U.; Dessen, A.; Šolmajer, T.; Gobec, S., *J. Med. Chem.* **2008**, 51 (23), 7486-7494.
30. Krohn, K.; Kouam, S. F.; Cludius-Brandt, S.; Draeger, S.; Schulz, B., *Eur. J. Org. Chem.* **2008**, 2008 (21), 3615-3618.
31. Lowell, A. N.; Fennie, M. W.; Kozlowski, M. C., *The Journal of Organic Chemistry* **2008**, 73 (5), 1911-1918.
32. Pan, M.; Lin, X.-M.; Li, G.-B.; Su, C.-Y., *Coord. Chem. Rev.* **2011**, 255 (15), 1921-1936.
33. Anthony, J. E., *Angewandte Chemie International Edition* **2008**, 47 (3), 452-483.
34. Watson, M. D.; Fechtenkötter, A.; Müllen, K., *Chemical Reviews* **2001**, 101 (5), 1267-1300.
35. de Koning, C. B.; Rousseau, A. L.; van Otterlo, W. A. L., *Tetrahedron* **2003**, 59 (1), 7-36.

36. Kuklin, S. A.; Sheloumov, A. M.; Dolgushin, F. M.; Ezernitskaya, M. G.; Peregudov, A. S.; Petrovskii, P. V.; Koridze, A. A., *Organometallics* **2006**, 25 (22), 5466-5476.
37. Choi, J.; MacArthur, A. H. R.; Brookhart, M.; Goldman, A. S., *Chemical Reviews* **2011**, 111 (3), 1761-1779.
38. Banothu, J.; Basavoju, S.; Bavantula, R., *J. Heterocycl. Chem.* **2015**, 52 (3), 853-860.
39. El-Sheshtawy, H. S.; Abou Baker, A. M., *J. Mol. Struct.* **2014**, 1067, 225-232.
40. Dang, J.-S.; Wang, W.-W.; Zhao, X.; Nagase, S., *Org. Lett.* **2014**, 16 (1), 170-173.
41. Ouros, A.; Oberson de Souza, M.; Pastore, H., *Journal of the Brazilian Chemical Society* **2014**, 25.
42. Matano, Y.; Saito, A.; Suzuki, Y.; Miyajima, T.; Akiyama, S.; Otsubo, S.; Nakamoto, E.; Aramaki, S.; Imahori, H., *Chemistry – An Asian Journal* **2012**, 7 (10), 2305-2312.
43. Buechi, G.; Wuest, H., *The Journal of Organic Chemistry* **1971**, 36 (4), 609-610.
44. Jana, A.; Misztal, K.; Żak, A.; Grela, K., *The Journal of Organic Chemistry* **2017**, 82 (8), 4226-4234.
45. Jayaram, V.; Sridhar, T.; Sharma, G. V. M.; Berrée, F.; Carboni, B., *The Journal of Organic Chemistry* **2017**, 82 (3), 1803-1811.
46. Foley, M.; Tilley, L., *Pharmacol. Ther.* **1998**, 79 (1), 55-87.
47. Kaminsky, D.; Meltzer, R. I., *J. Med. Chem.* **1968**, 11 (1), 160-163.
48. Rossiter, S.; Péron, J.-M.; Whitfield, P. J.; Jones, K., *Bioorg. Med. Chem. Lett.* **2005**, 15 (21), 4806-4808.
49. Stork, G.; Niu, D.; Fujimoto, A.; Koft, E. R.; Balkovec, J. M.; Tata, J. R.; Dake, G. R., *Journal of the American Chemical Society* **2001**, 123 (14), 3239-3242.

50. Mahato, S.; Mukherjee, A.; Santra, S.; Zyryanov, G. V.; Majee, A., *Org. Biomol. Chem.* **2019**, 17 (34), 7907-7917.
51. Bizzarri, C.; Spuling, E.; Knoll, D. M.; Volz, D.; Bräse, S., *Coord. Chem. Rev.* **2018**, 373, 49-82.
52. Kim, J. I.; Shin, I.-S.; Kim, H.; Lee, J.-K., *Journal of the American Chemical Society* **2005**, 127 (6), 1614-1615.
53. Bangcuyo, C. G.; Rampey-Vaughn, M. E.; Quan, L. T.; Angel, S. M.; Smith, M. D.; Bunz, U. H. F., *Macromolecules* **2002**, 35 (5), 1563-1568.
54. Biswas, S.; Huang, Z.; Choliy, Y.; Wang, D. Y.; Brookhart, M.; Krogh-Jespersen, K.; Goldman, A. S., *Journal of the American Chemical Society* **2012**, 134 (32), 13276-13295.
55. Costa, E. V.; Pinheiro, M. L. B.; Maia, B. H. L. N. S.; Marques, F. A.; Ruiz, A. L. T. G.; Marchetti, G. M.; Carvalho, J. E. d.; Soares, M. B. P.; Costa, C. O. S.; Galvão, A. F. C.; Lopes, N. P.; Koolen, H. H. F.; Bezerra, D. P.; Barison, A., *J. Nat. Prod.* **2016**, 79 (6), 1524-1531.
56. Zhang, Z.-H.; Zhang, H.-J.; Deng, A.-J.; Wang, B.; Li, Z.-H.; Liu, Y.; Wu, L.-Q.; Wang, W.-J.; Qin, H.-L., *J. Med. Chem.* **2015**, 58 (18), 7557-7571.
57. DeBono, A.; Capuano, B.; Scammells, P. J., *J. Med. Chem.* **2015**, 58 (15), 5699-5727.
58. Bentley, K. W., *Nat. Prod. Rep.* **2006**, 23 (3), 444-463.
59. Wen, L.-R.; Dou, Q.; Wang, Y.-C.; Zhang, J.-W.; Guo, W.-S.; Li, M., *The Journal of Organic Chemistry* **2017**, 82 (3), 1428-1436.

60. Stabile, P.; Lamonica, A.; Ribecai, A.; Castoldi, D.; Guercio, G.; Curcuruto, O., *Tetrahedron Letters* **2010**, 51 (24), 3232-3235.
61. Klapars, A.; Huang, X.; Buchwald, S. L., *Journal of the American Chemical Society* **2002**, 124 (25), 7421-7428.
62. Balewski, Ł.; Sączewski, F.; Gdaniec, M.; Kornicka, A.; Cicha, K.; Jalińska, A., *Molecules (Basel, Switzerland)* **2019**, 24 (22), 4070.
63. Shiraiwa, M.; Sakamoto, T.; Yamanaka, H., *Chem. Pharm. Bull. (Tokyo)* **1983**, 31 (7), 2275-2280.
64. Bischler, A.; Napieralski, B., *Berichte der deutschen chemischen Gesellschaft* **1893**, 26 (2), 1903-1908.
65. Pictet, A.; Spengler, T., *Berichte der deutschen chemischen Gesellschaft* **1911**, 44 (3), 2030-2036.
66. Zhang, H.-P.; Li, H.-Y.; Xiao, H.-F., *Journal of Chemical Research* **2013**, 37 (9), 556-558.
67. Eisch, J. J. In *Adv. Heterocycl. Chem.*, Katritzky, A. R., Boulton, A. J., Eds. Academic Press: 1967; Vol. 7, pp 1-37.
68. Kress, T. J.; Costantino, S. M., *J. Heterocycl. Chem.* **1973**, 10 (3), 409-410.
69. Tyman, J. H. P. In *Studies in Organic Chemistry*, Elsevier: New York, 1996; Vol. 52, pp 558-661.
70. Chien, R.-H.; Lai, C.-T.; Hong, J.-L., *The Journal of Physical Chemistry C* **2011**, 115 (13), 5958-5965.

71. Deria, P.; Von Bargen, C. D.; Olivier, J.-H.; Kumbhar, A. S.; Saven, J. G.; Therien, M. J., *Journal of the American Chemical Society* **2013**, 135 (43), 16220-16234.
72. For industrial naphthol synthesis: (a) E.W. Schoeffel, D. M. B. Naphthalene. August 28, **1956**. (b) Stevens, D., Harris, G.H., Pearlman, M.B. Phenols From Aromatic Sulfonic, Sulfamic, and Sulfone Compounds. December 2, **1955**.
73. He, X.; Zheng, Y.-W.; Lei, T.; Liu, W.-Q.; Chen, B.; Feng, K.; Tung, C.-H.; Wu, L.-Z., *Catalysis Science & Technology* **2019**, 9 (13), 3337-3341.
74. Izawa, Y.; Pun, D.; Stahl, S. S., *Science* **2011**, 333 (6039), 209.
75. Girard, S. A.; Huang, H.; Zhou, F.; Deng, G.-J.; Li, C.-J., *Organic Chemistry Frontiers* **2015**, 2 (3), 279-287.
76. Franzen, H.; Kempf, H., *Berichte der deutschen chemischen Gesellschaft* **1917**, 50 (1), 101-104.
77. Chang, J.; Song, X.; Huang, W.; Zhu, D.; Wang, M., *Chem. Commun.* **2015**, 51 (84), 15362-15365.
78. Fancelli, D.; Abate, A.; Amici, R.; Bernardi, P.; Ballarini, M.; Cappa, A.; Carenzi, G.; Colombo, A.; Contursi, C.; Di Lisa, F.; Dondio, G.; Gagliardi, S.; Milanesi, E.; Minucci, S.; Pain, G.; Pelicci, P. G.; Saccani, A.; Storto, M.; Thaler, F.; Varasi, M.; Villa, M.; Plyte, S., *J. Med. Chem.* **2014**, 57 (12), 5333-5347.
79. Spadaro, A.; Frotscher, M.; Hartmann, R. W., *J. Med. Chem.* **2012**, 55 (5), 2469-2473.
80. Liu, X.; Jiang, L.; Li, J.; Wang, L.; Yu, Y.; Zhou, Q.; Lv, X.; Gong, W.; Lu, Y.; Wang, J., *Journal of the American Chemical Society* **2014**, 136 (38), 13094-13097.

81. Li, Y.; Clevenger, R. G.; Jin, L.; Kilway, K. V.; Peng, Z., *The Journal of Physical Chemistry C* **2016**, 120 (2), 841-852.
82. Yuan, B.; Zhuang, J.; Kirmess, K. M.; Bridgmohan, C. N.; Whalley, A. C.; Wang, L.; Plunkett, K. N., *The Journal of Organic Chemistry* **2016**, 81 (18), 8312-8318.
83. Pho, T. V.; Toma, F. M.; Chabinye, M. L.; Wudl, F., *Angewandte Chemie International Edition* **2013**, 52 (5), 1446-1451.
84. Nishida, J.-i.; Tsukaguchi, S.; Yamashita, Y., *Chemistry – A European Journal* **2012**, 18 (29), 8964-8970.
85. Wood, J. D.; Jellison, J. L.; Finke, A. D.; Wang, L.; Plunkett, K. N., *Journal of the American Chemical Society* **2012**, 134 (38), 15783-15789.
86. Brunetti, F. G.; Gong, X.; Tong, M.; Heeger, A. J.; Wudl, F., *Angewandte Chemie International Edition* **2010**, 49 (3), 532-536.
87. Matsuura, K.; Nishida, J.-i.; Ito, T.; Yokota, R.; Kitamura, C.; Kawase, T., *Tetrahedron* **2019**, 75 (2), 278-285.
88. Laguerre, M.; Felix, G.; Dunogues, J.; Calas, R., *The Journal of Organic Chemistry* **1979**, 44 (24), 4275-4278.
89. Nakayama, J. In *Comprehensive Heterocyclic Chemistry II*, Katritzky, A. R., Rees, C. W., Scriven, E. F. V., Eds. Pergamon: Oxford, 1996; pp 607-677.
90. Ding, L.; Yang, C.; Su, Z.; Pei, J., *Science China Chemistry* **2015**, 58 (2), 364-369.
91. Cantrell, T. S.; Shechter, H., *The Journal of Organic Chemistry* **1968**, 33 (1), 114-118.

92. Abe, M.; Eto, M.; Yamaguchi, K.; Yamasaki, M.; Misaka, J.; Yoshitake, Y.; Otsuka, M.; Harano, K., *Tetrahedron* **2012**, 68 (18), 3566-3576.
93. Yavari, I.; Khajeh-Khezri, A., *Synthesis* **2018**, 50 (20), 3947-3973.
94. Schmidt, R.; Griesbaum, K.; Behr, A.; Biedenkapp, D.; Voges, H.-W.; Garbe, D.; Paetz, C.; Collin, G.; Mayer, D.; Höke, H., *Ullmann's Encyclopedia of Industrial Chemistry* **2014**, 1-74.
95. Griesbaum, K.; Behr, A.; Biedenkapp, D.; Voges, H.-W.; Garbe, D.; Paetz, C.; Collin, G.; Mayer, D.; Höke, H., *Ullmann's Encyclopedia of Industrial Chemistry* **2000**.
96. Anderson, A. G.; Anderson, R. G., *Journal of the American Chemical Society* **1955**, 77 (24), 6610-6611.

APPENDIX 1

EXPERIMENTAL SECTION AND SPECTRA RELEVANT TO CHAPTER 2

A1.1 MATERIALS AND METHODS

Unless noted in the specific procedure, reactions were performed in oven-dried glassware. All dehydrogenation reactions were degassed by freeze-pump-thaw x 5 cycles and were carried out under air-free conditions in an oven-dried glassware. All liquid reagents were purified by distillation and dried using molecular sieves, NaH, or Na-K alloy. For all the investigated dehydrogenation systems, the substrate was mixed with the H₂ acceptor in a 4 mL sealed Schlenk pressure flask under an argon atmosphere. Then synthesized Ir pincer complexes were added to the reaction mixture with at least 1.2 equivalents of the Ir pincer complexes of KO*t*-Bu when the Ir-HCl version of precatalyst is used.

¹H and ³¹P NMR spectra were recorded on a Varian spectrometer 400 MHz with broadband auto-tune OneProbeor or on a Bruker AV III HD 400 MHz spectrometer equipped with a Prodigy liquid nitrogen temperature cryoprobe, and are

reported in terms of chemical shift relative to residual CHCl_3 (δ 7.26). ^{19}F NMR spectra were recorded on Varian 400 MHz spectrometer. Dehydrogenation conversions were determined using ^1H NMR with cis-1,4-diacetoxy-2-butene standard.

In addition, the conversions were determined using an Agilent 6850 GC-FID equipped with a Supelco column (SPBTM-1, fused silica capillary column, 30 m x 0.25 μm film thickness) and using methods with temperature programs shown in Tables A1.1 and A1.2 and inlet program showed in Table A1.3. The obtained products were also confirmed by spiking the reaction with a commercial sample of the product.

Table A1.1 ZAS2 General Method Temperature Ramping Program for **10**, **14**, **16**, **18**, **20**, and **22** Transfer Dehydrogenation

Oven Ramp	°C/min	Next °C	Hold min
Initial	-	38	1.50
Ramp 1	10.00	150	0.00
Ramp 2	20.00	250	5.00

Table A1.2 ZAS_INDANE Method GC Temperature Ramping Program for Indane **12** to Indene **13** Transfer Dehydrogenation

Oven Ramp	°C/min	Next °C	Hold min
Initial	-	38	1.50
Ramp 1	5.00	50	5.00
Ramp 2	10.00	100	0.00
Ramp 3	5.00	170	5.00
Ramp 4	20.00	250	0.00

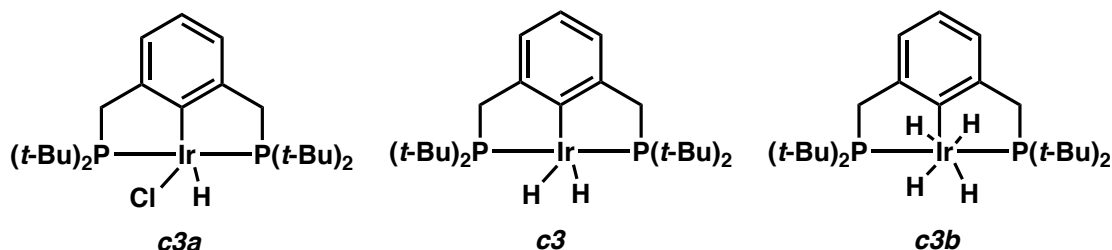
Table A1.3 Inlet Parameters used in All Methods

Inlet	Setting
Mode	Split
Gas	He
Heater	250 °C
Pressure	9.52 psi
Total Flow	82.2
Split Ratio	100:1
Split Flow	78.5 mL/min

A1.2 KNOWN IRIDIUM PINCER LIGATED COMPLEXES

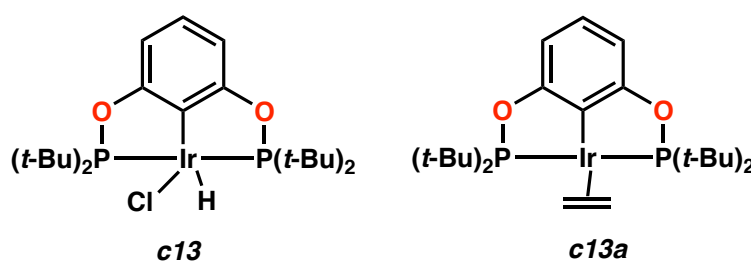
GENERAL SYNTHESIS PROCEDURE

A1.2.1 Synthesis of (*t*-Bu⁴PCP)IrHCl **c3a** and (*t*-Bu⁴PCP)IrH₄ **c3b** Complexes



0.240 g of the commercially available *t*-Bu⁴PCP ligand **1** and 0.5 equivalent of [Ir(COD)Cl]₂, 0.224 g, were added in 10 mL toluene and heated to reflux for 72 h under argon atmosphere. After cooling the reaction mixture to room temperature, the mother liquor was evaporated under vacuum. Complex (*t*-Bu⁴PCP)IrHCl **c3a** was extracted with pentane (60 mL x 3) *via* a cannula and the combined pentane solutions were evaporated to obtain the red-orange crystalline product. Then complex **c3a** (0.150 g) was dissolved in pentane (100 mL), and a 1.0 M solution (in THF) of LiBEt₃H (0.29 mL) was added dropwise *via* syringe under H₂ atmosphere, causing the red solution to turn a pale orange brownish. The reaction mixture was stirred for 2 h and then dried over vacuum and then dissolved in pentane and filtered in a syringe obtaining the (*t*-Bu⁴PCP)IrH₄ complex **c3b**. Complex **c3b** is air and nitrogen sensitive so it should only be kept in an argon glovebox.¹ (*t*-Bu⁴PCP)IrHCl **c3a**: ¹H NMR (400 MHz, Benzene-*d*₆) δ 7.03 (d, 2H, Ar-H), 7.96 (m, 1H, Ar-H), 3.25 – 3.06 (m, 4H, CH₂), 1.36 (dt, *J* = 6.7 Hz, 36H, 2x P(*t*-Bu)₂), -42.50 (t, *J* = 12.6 Hz, 1H, Ir-H). ³¹P NMR (162 MHz, Benzene-*d*₆) δ 67.09 (s). ¹³C NMR (101 MHz, Benzene-*d*₆) δ 151.48 (t, Ar-C), 122.58, 121.07 (t, 4 Ar-C), 33.59 (m, 2 x CH₂), 29.65 (t, 4x *t*-Bu₄), 28.06 (t, 4x CH₃). (*t*-Bu⁴PCP)IrH₄ **c3b**: ¹H NMR (400 MHz, Benzene-*d*₆) δ 7.09 (s,

A1.2.2 Synthesis of (*t*-Bu⁴POCOP)IrHCl c13 and (*t*-Bu⁴POCOP)IrC₂H₄ c13a Complexes



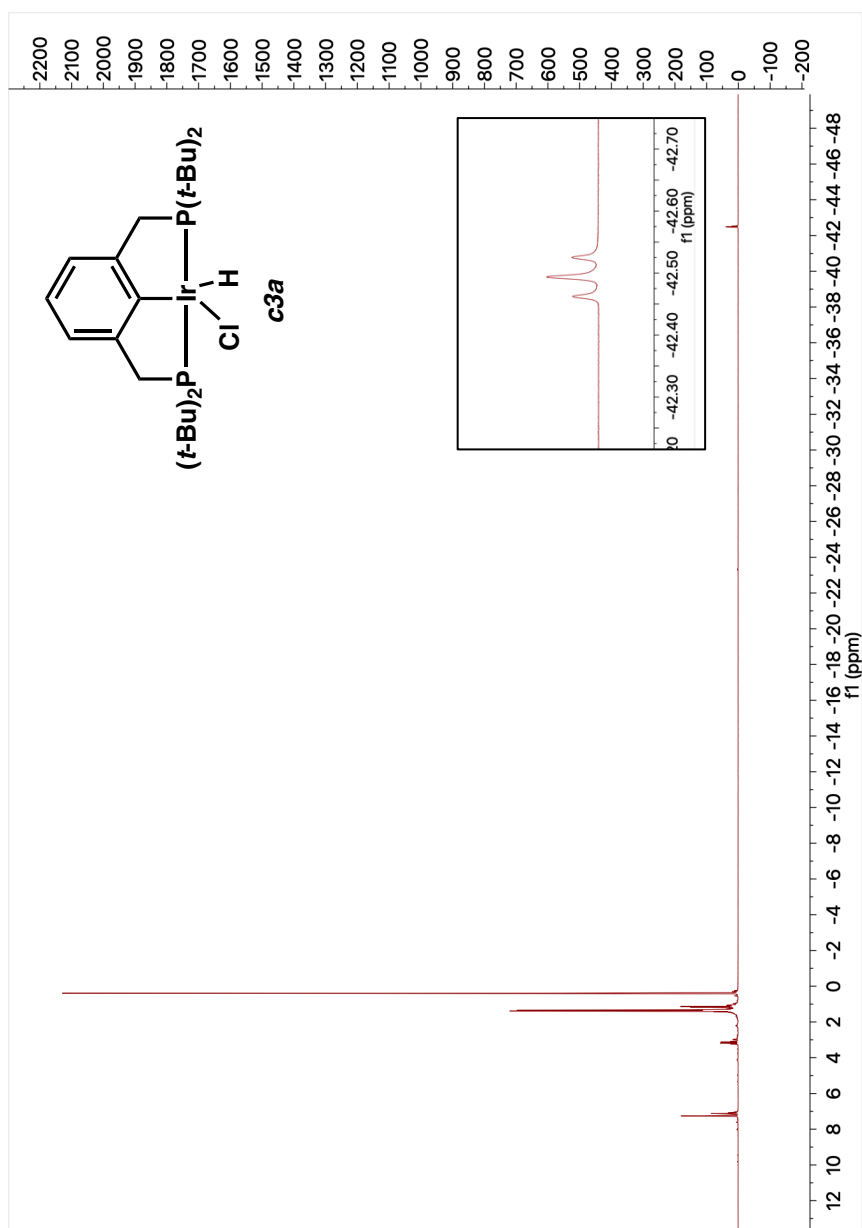
0.500 g of resorcinol **2** was dissolved in 45 mL THF. Then two equivalents of DBU and (*t*-Bu)₂PCl were added slowly. The reaction mixture was run at room temperature stirring overnight. After cooling the reaction mixture to room temperature, the mother liquor was evaporated under vacuum. The ligand (*t*-Bu⁴POCOP) **3** was extracted with pentane *via* a cannula and filtered over a pad of Celite under vacuum. The pentane solution was dried over vacuum and the **3** was obtained.² ¹H NMR (400 MHz, Chloroform-*d*) δ 7.10 (td, *J* = 8.4, 2.8 Hz, 1H, Ar-H), 6.96 (p, *J* = 2.1 Hz, 1H, Ar-H), 6.77 (dp, *J* = 8.4, 2.1 Hz, 2H, Ar-H), 1.66 – 0.75 (m, 36H, 2x P(*t*-Bu)₂). ³¹P NMR (162 MHz, Chloroform-*d*) δ 153.22. (s). ¹³C NMR (101 MHz, Chloroform-*d*) δ 161.23 (d, *J* = 9.7 Hz, 2C, Ar-C), 129.85, 111.61 (d, *J* = 10.9 Hz, 3C, Ar-C), 108.82 (t, *J* = 11.5 Hz, 1C, Ar-C), 35.39 (d, *J* = 26.7 Hz, 4C, P-C), 27.22 (d, *J* = 15.7 Hz, 12C, C-C)

Synthesis of (*t*-Bu⁴POCOP)IrHCl **13a and (*t*-Bu⁴POCOP)Ir(C₂H₄) **13** Complexes**

1.0143 g of the of the (*t*-Bu⁴POCOP) ligand and 0.5 equivalents [Ir(COD)Cl]₂, 0.8505 g, were added in 30 mL toluene and heated to reflux for 72 h under argon atmosphere. After cooling the reaction mixture to room temperature, the mother liquor was evaporated under vacuum. The obtained crystalline powder was filtered in air and washed with pentane. (*t*-Bu⁴POCOP)IrHCl **13a** is air stable and can be stored in vial on the shelf. Then for (*t*-Bu⁴POCOP)IrH(C₂H₄) **13** synthesis, 0.260 g of **13a** and 1.2 equivalents of NaO*t*-Bu were dissolved in 40 mL degassed toluene. It's important to ensure that the solvent is nitrogen free as the complex is air and nitrogen sensitive. The resulting suspension was stirred for 10 min at room temperature. Ethylene was bubbled through the solution overnight. Then, solution was cannula-filtered through a pad of Celite, volatiles were evaporated under vacuum, and the resulting red solid was dried under vacuum and kept in argon glovebox.²). (*t*-Bu⁴POCOP)IrHCl **13a**: ¹H NMR (400 MHz, Benzene-*d*₆) δ 6.81 – 6.68 (m, 3H, Ar-H), 1.24 (dt, *J* = 7.3 Hz, 36H, 2x P(*t*-Bu)₂), -40.69 (t, *J* = 13.1 Hz, 1H, Ir-H). ³¹P NMR (162 MHz, Benzene-*d*₆) δ 175.34 (d, *J* = 6.0 Hz). (*t*-Bu⁴POCOP)IrH(C₂H₄) **13**: ¹H NMR (400 MHz, Benzene-*d*₆) δ 7.04 – 6.98 (m, 1H, Ar-H), 6.91 (s, 1H, Ar-H), 6.89 (d, *J* = 0.9 Hz, 1H, Ar-H), 3.07 (t, *J* = 2.6 Hz, 4H, C₂H₄), 1.21 (m, 36H, 2x P(*t*-Bu)₂). ³¹P NMR (162 MHz, Benzene-*d*₆) δ 181.13 (s).

A1.3 NOTES AND REFERENCES

1. For complex **1** a) Gupta, M.; Hagen, C.; Kaska, W. C.; Cramer, R.E.; Jensen, C. M. *Chem. Commun.* **1996**, 2083–2084. b) Gupta, M.; Hagen, C.; Kaska, W. C.; Cramer, R. E.; Jensen, C. M. *J Am Chem Soc* **1997**, *119*, 840–841. (c) Moulton, C. J.; Shaw, B. L. *J. Chem. Soc., Dalton Trans.* **1976**, *11*, 1020–1024.
2. For complex **2** (a) Bézier, D.; Brookhart, M. *ACS Catalysis* **2014**, *4*, 3411–3420. (b) Göttker-Schnetmann, I.; Brookhart, M. *J. Am. Chem. Soc.* **2004**, *126*, 9330–9338. (c) Göttker-Schnetmann, I.; White, P. S.; (d) Brookhart, M. *J. Am. Chem. Soc.* **2004**, *126*, 1804–1811. (d) Göttker-Schnetmann, I.; White, P. S.; (e) Brookhart, M. *Organometallics* **2004**, *23*, 1766–1776. (f) Ahuja, R.; Punji, B.; Findlater, M.; Supplee, C.; Schinski, W.; Brookhart, M.; Goldman, A. S. *Nature Chemistry* **2010**, *3*, 167–171.
3. For complex **3**: Haenel, M. W.; Oevers, S.; Angermund, K.; Kaska, W. C.; Fan, H.-J.; Hall, M. B. *Angew. Chem., Int. Ed.* **2001**, *40*, 3596–3600.
4. For complex **4**: Yao, W.; Zhang, Y.; Jia, X.; Huang, Z. *Angew. Chem., Int. Ed.* **2014**, *53*, 1390–1394.

A1.4 RELEVANT SPECTRA**Figure A1.1** ^1H NMR (400 MHz, CDCl_3) of Complex **c3a**

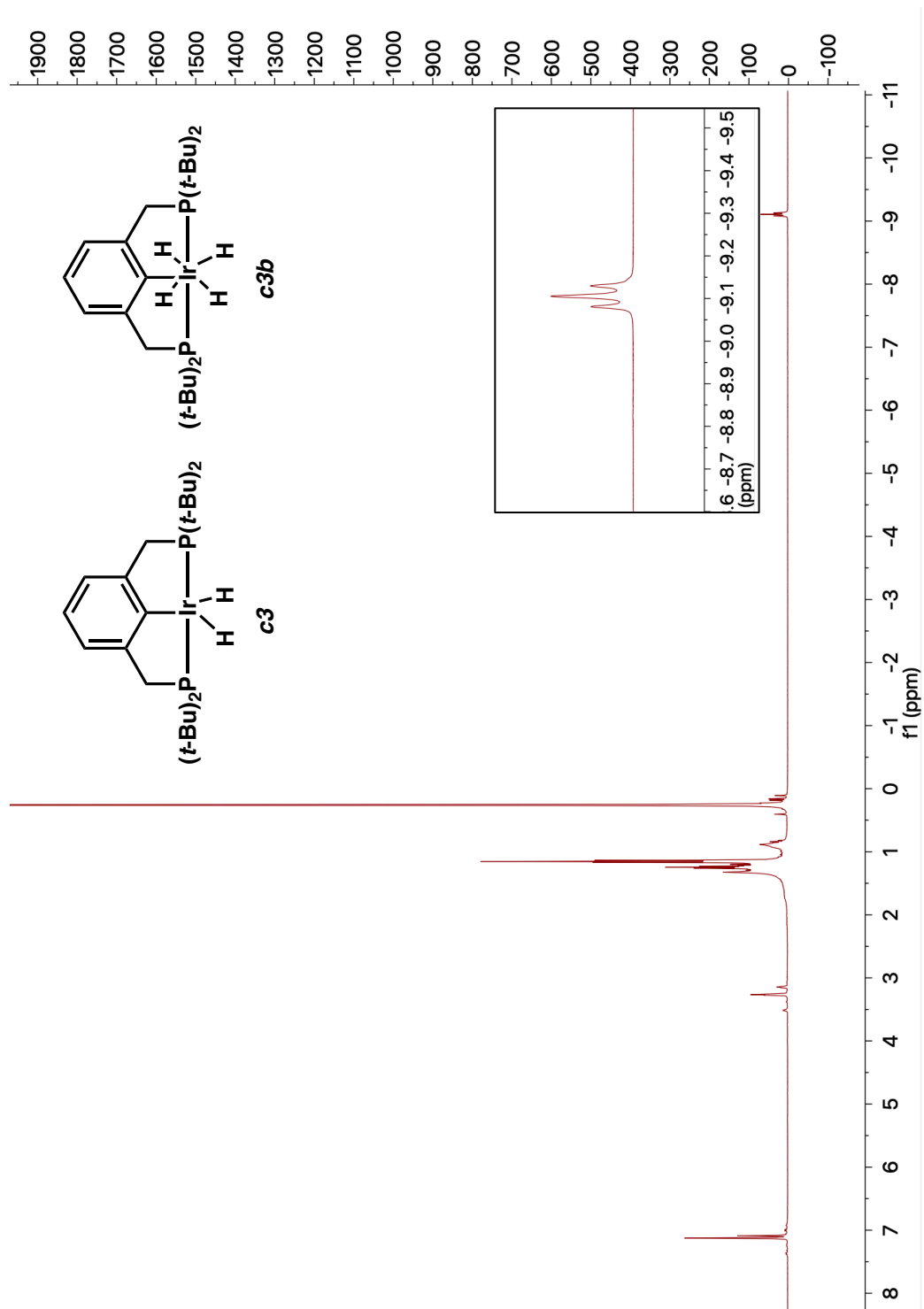


Figure A1.2 ^1H NMR (400 MHz, CD_6D_6) of Complexes **c3/c3b**

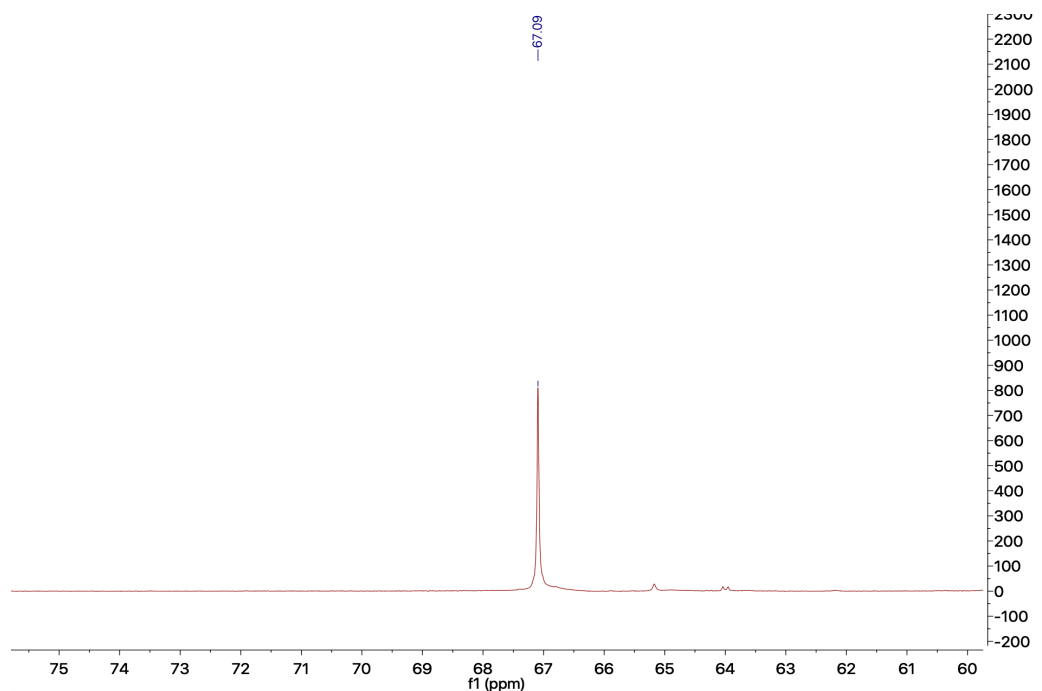


Figure A1.3 ^{31}P NMR (400 MHz, C_6D_6) of Complex **c3a**

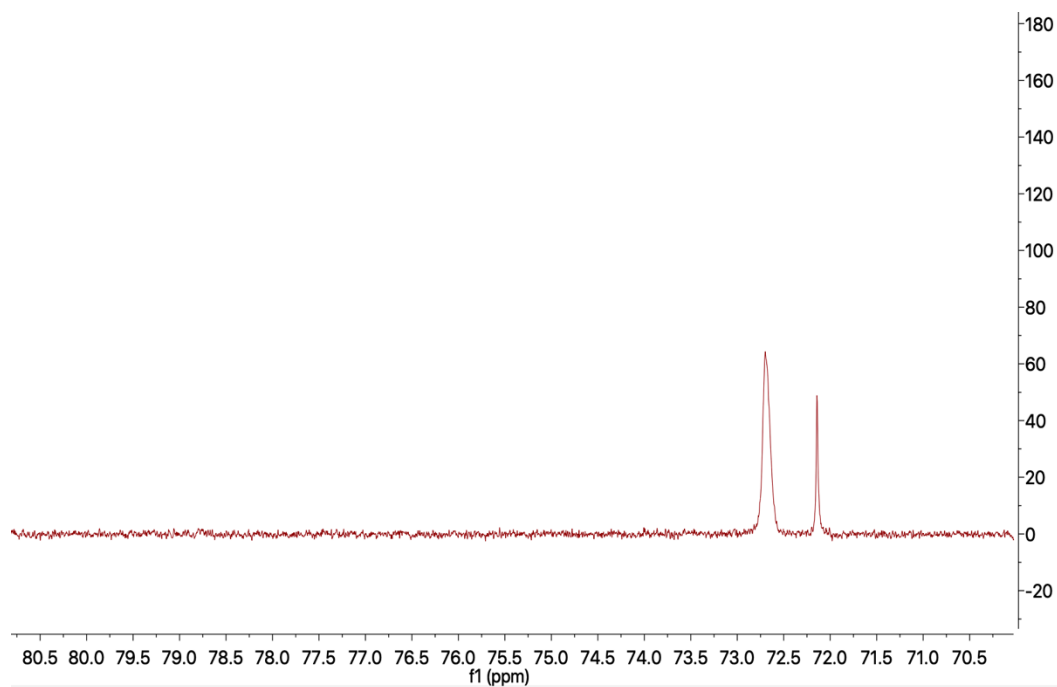


Figure A1.4 ^{31}P NMR (400 MHz, C_6D_6) of Mixture of Complexes **c3/c3b**

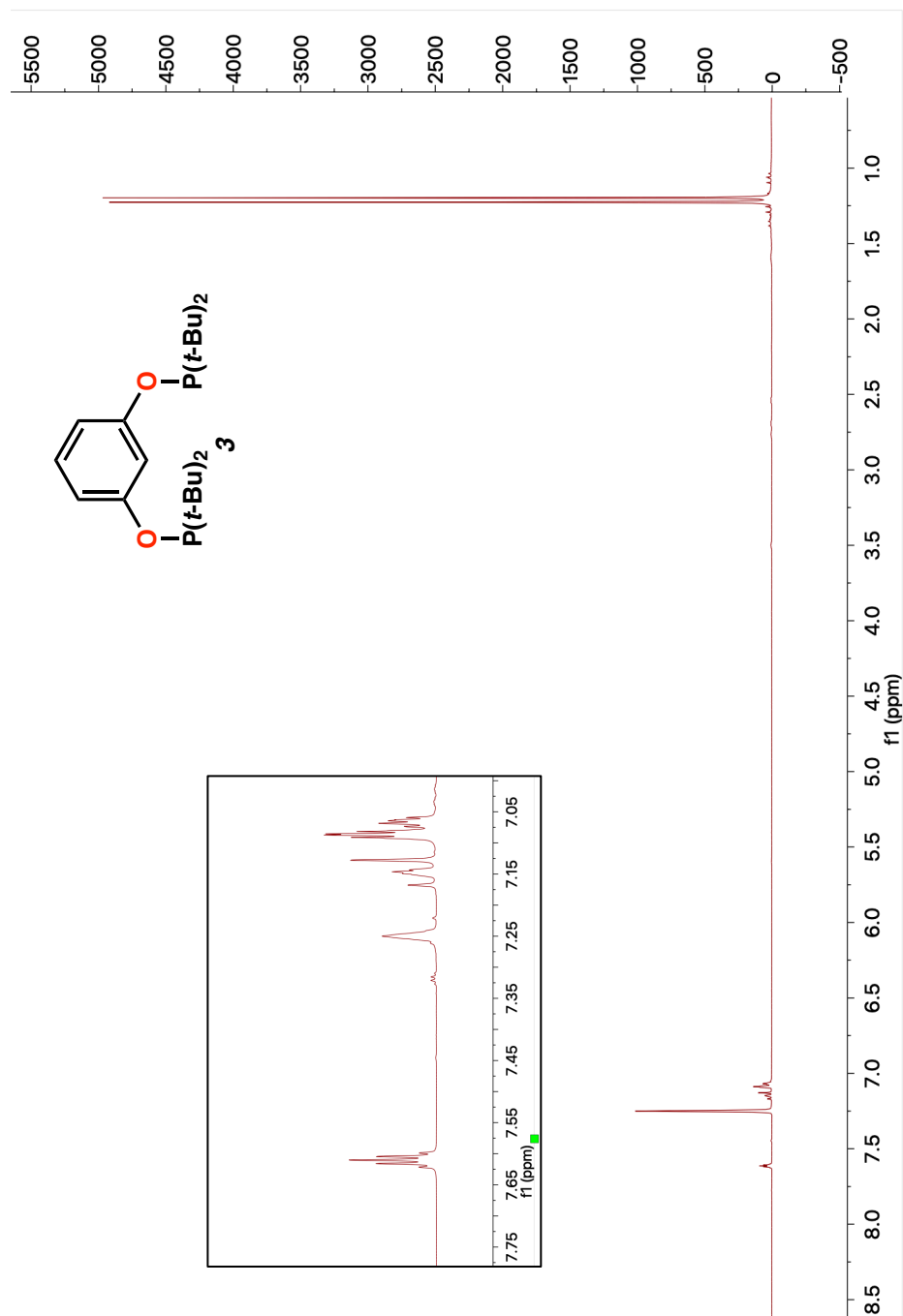


Figure A1.5 ^1H NMR (400 MHz, C6D6) of Ligand **3**.

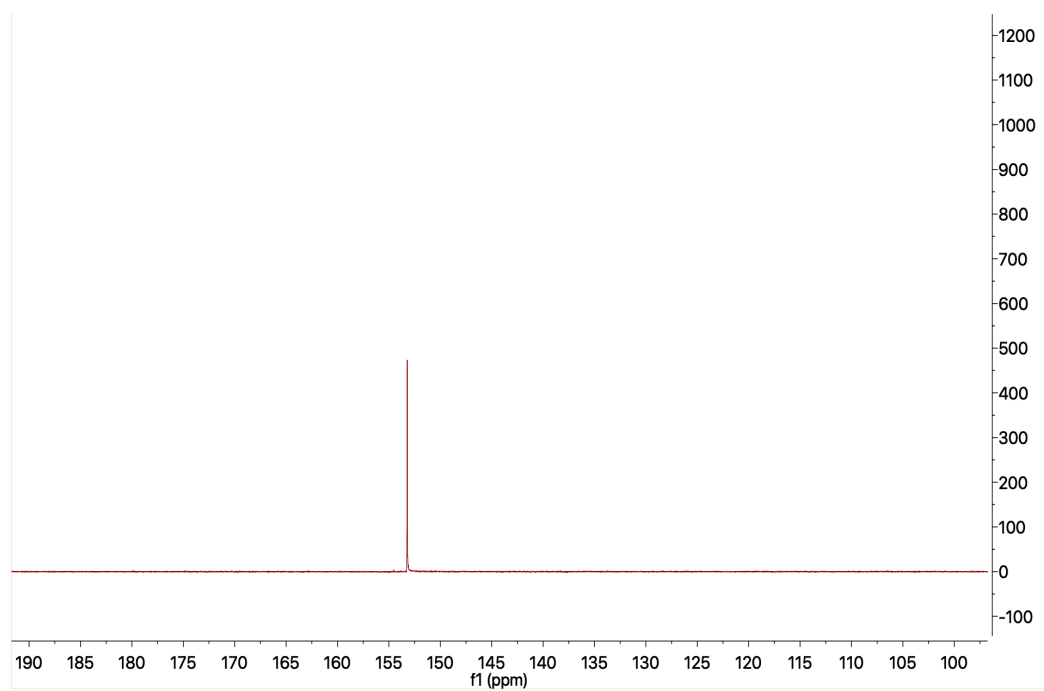


Figure A1.6 ^{31}P NMR (400 MHz, C_6D_6) of Ligand **3**

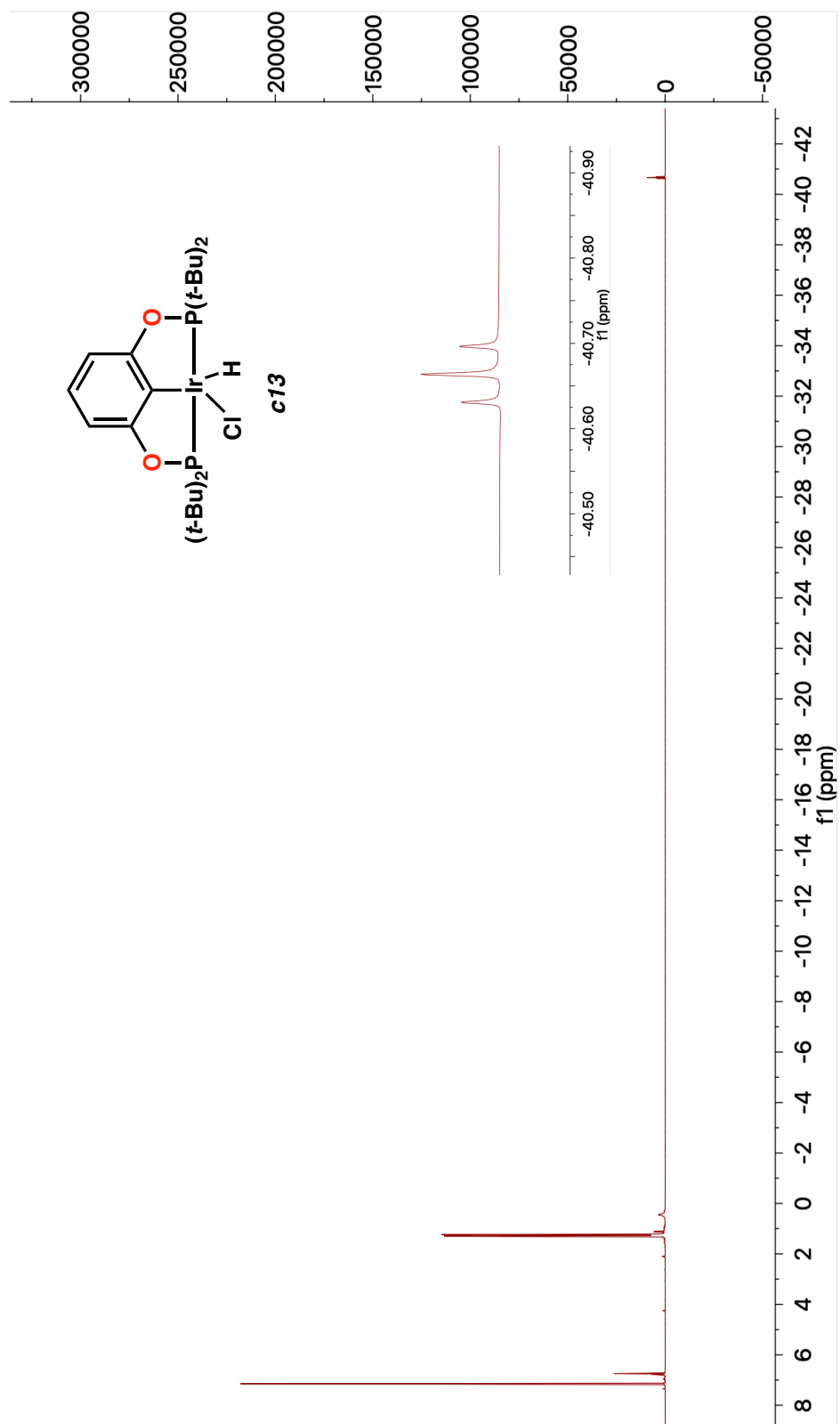


Figure A1.7 ^1H NMR (400 MHz, CDCl_3) of Ligand **c13**

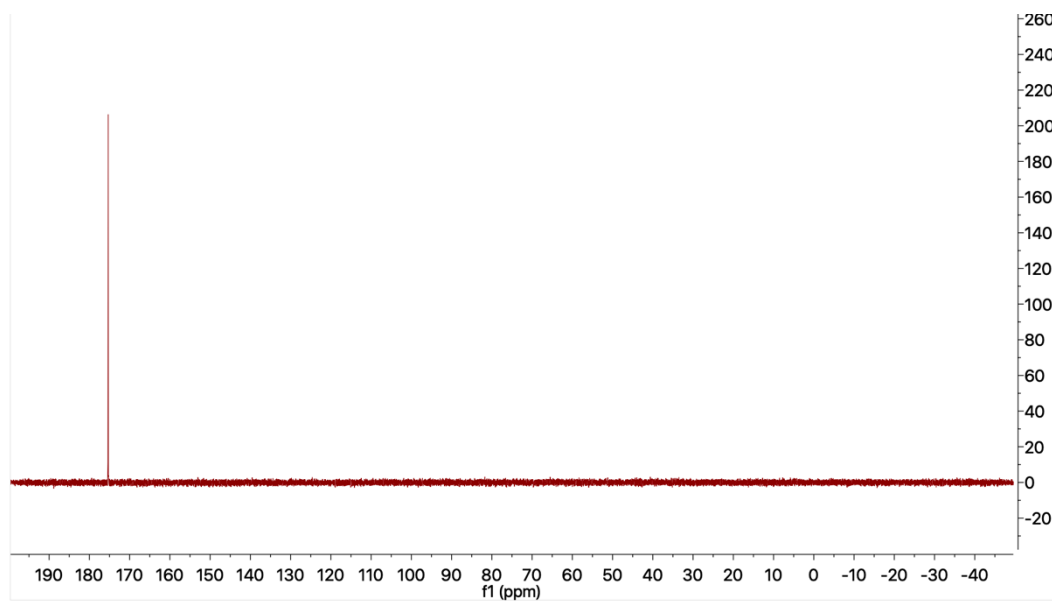


Figure A1.8 ^{31}P NMR (400 MHz, C_6D_6) of Complex **c13**

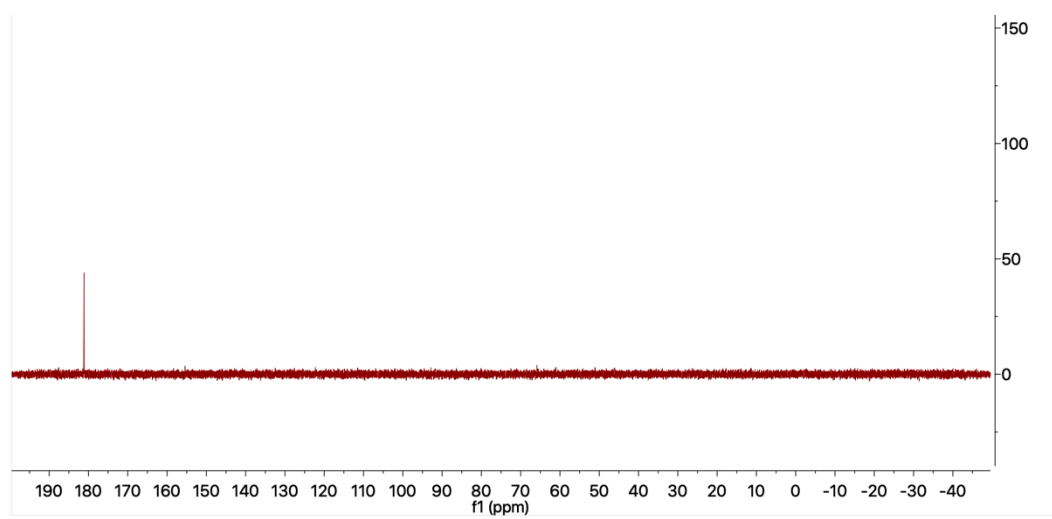


Figure A1.9 ^{31}P NMR (400 MHz, C_6D_6) of Complex **c13a**

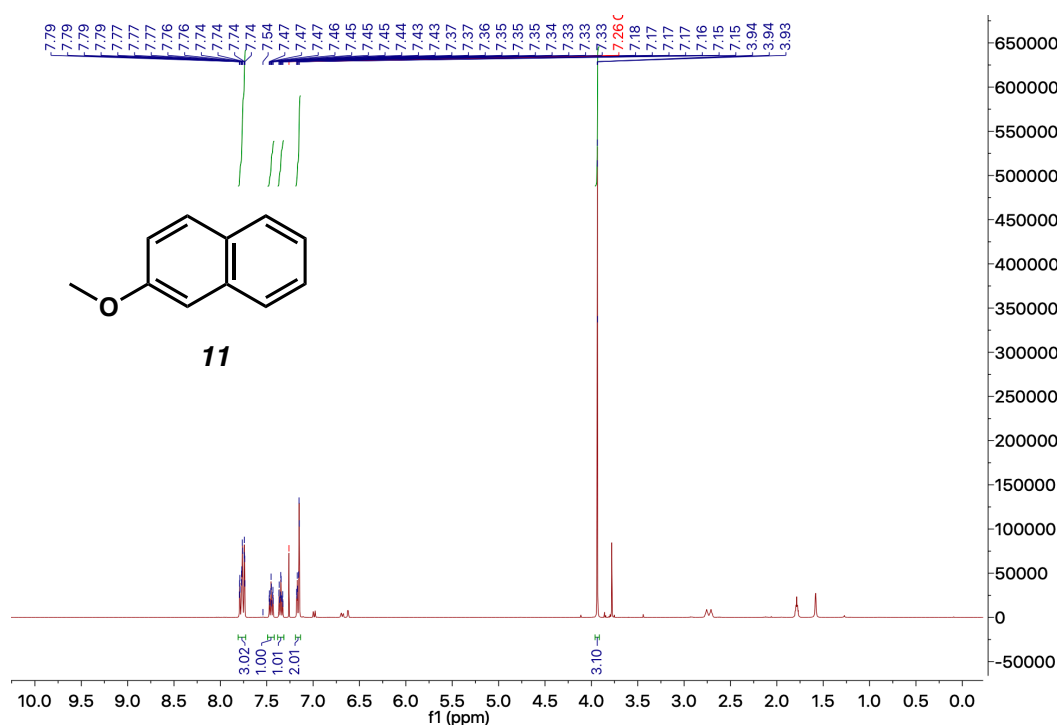


Figure A1.10 Table 2.3 Entry 6 ^1H NMR (400 MHz, Chloroform-d) of **11** (Isolated with **10**), Yield Calculated with *Cis*-1,4-Diacetoxy-2-Butene Standard

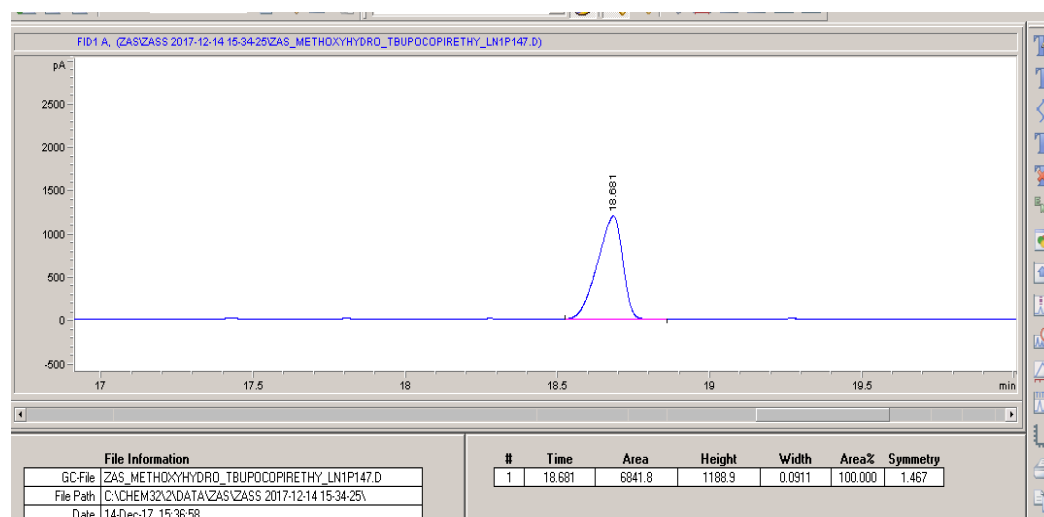


Figure A1.11 GC Spectra of **10** Crude Reaction: Showing Full Conversion to **11**@18.68 Using ZAS2 Method in Table A1.1, **10** rt is Typically@18.25

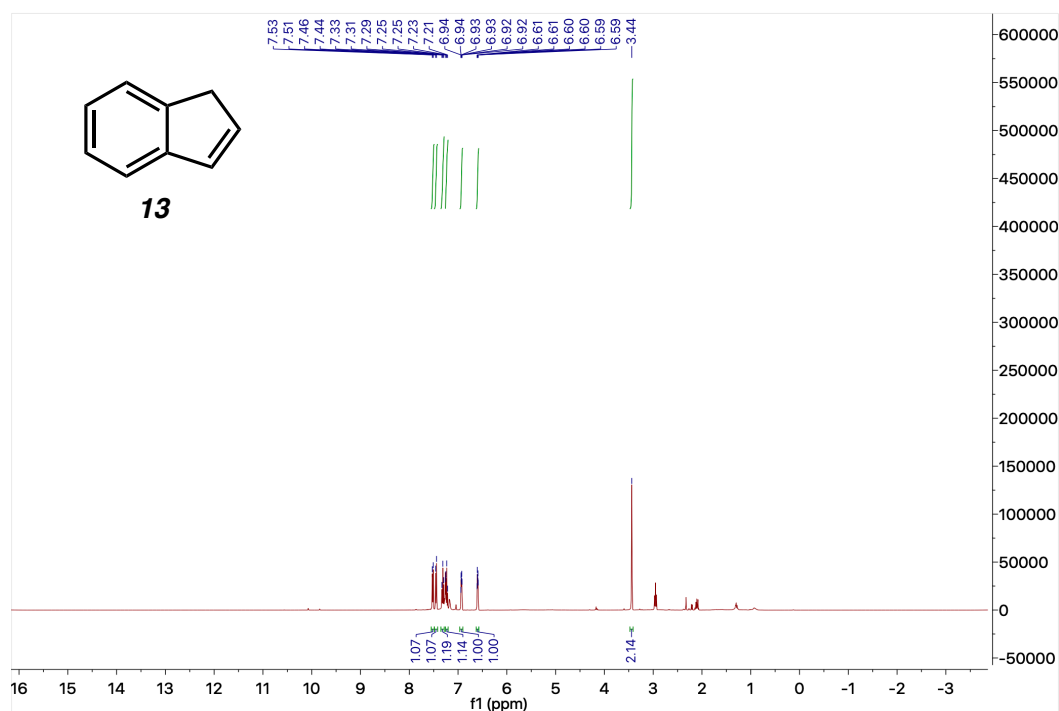


Figure A1.12 Table 2.4 Entry 8 ¹H NMR (400 MHz, Chloroform-d) of Indene (**13**) (Isolated with Indane (**12**)), Yield Calculated with Cis-1,4-Diacetoxy-2-Butene Standard

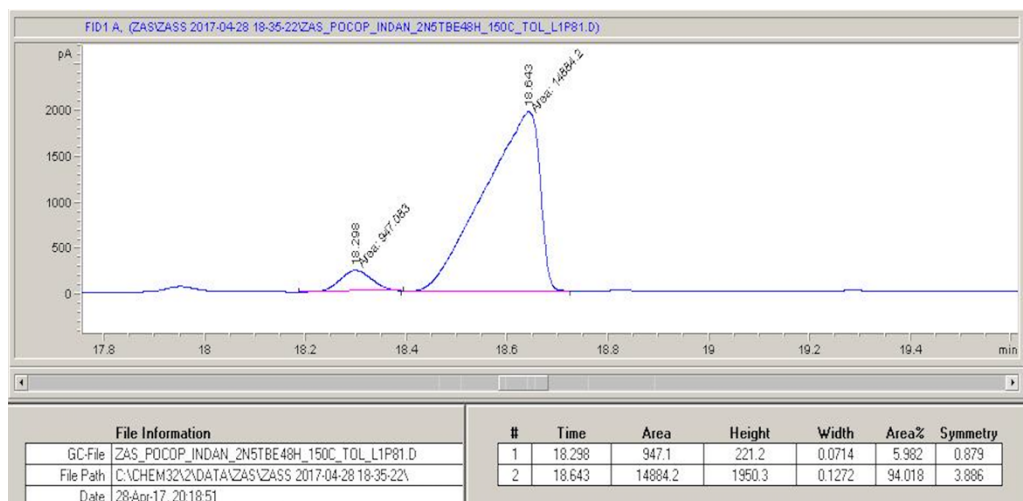


Figure A1.13 GC Spectra of **12** Crude Reaction: **12**@18.29 and **13**@18.64 Using ZAS_Indane Method in Table A1.2

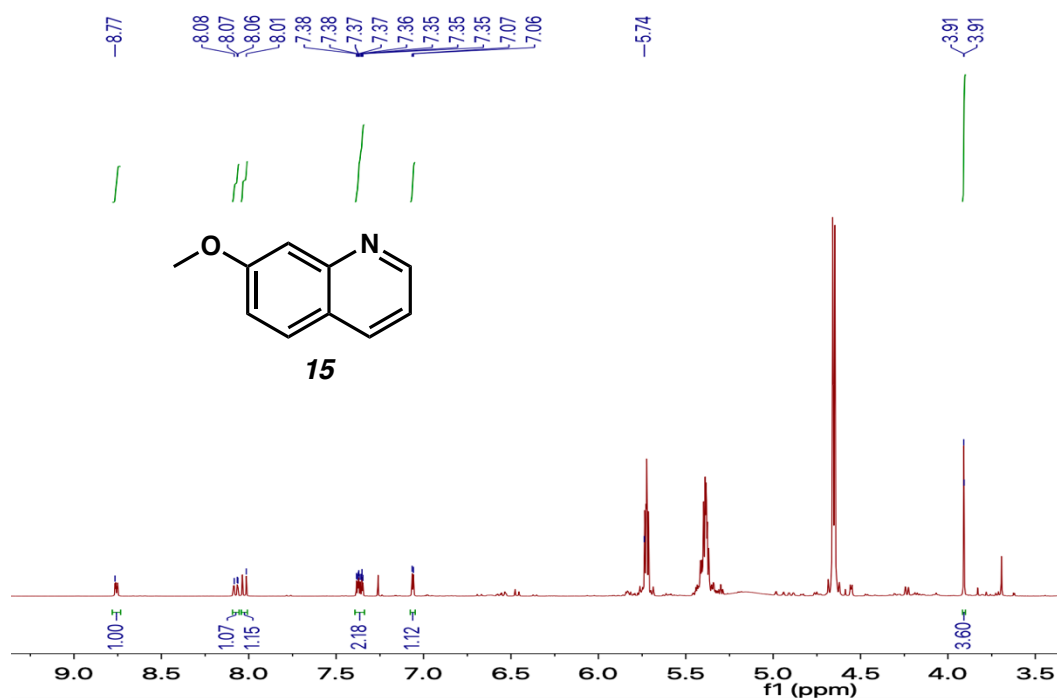


Figure A1.14 Table 2.5 Entry 5 ¹H NMR (400 MHz, Chloroform-d) of Crude Reaction, Yield Calculated with *Cis*-1,4-Diacetoxy-2-Butene Standard

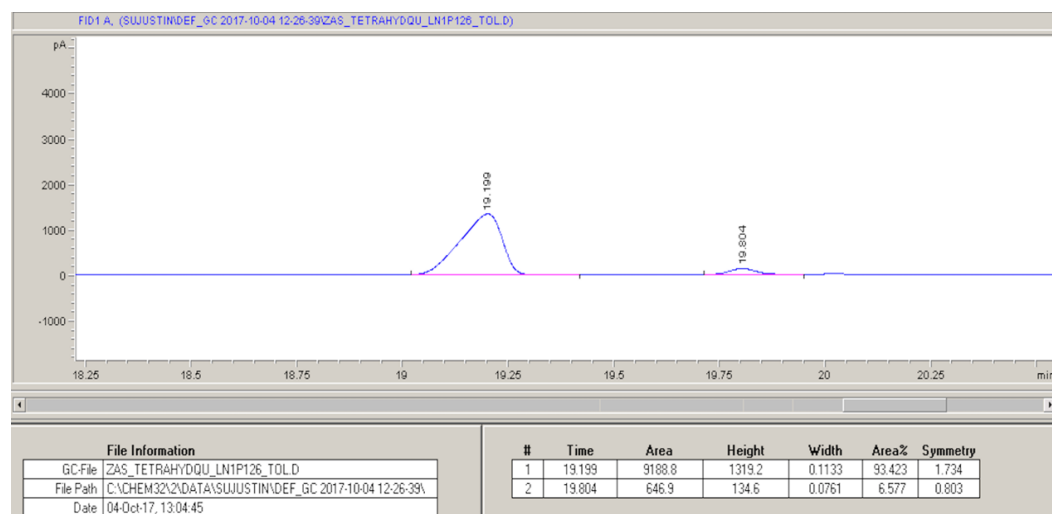


Figure A1.15 GC Spectra of **14** Crude Reaction: **15**@19.80 and **14**@19.20 Using ZAS2 Method in Table A1.1

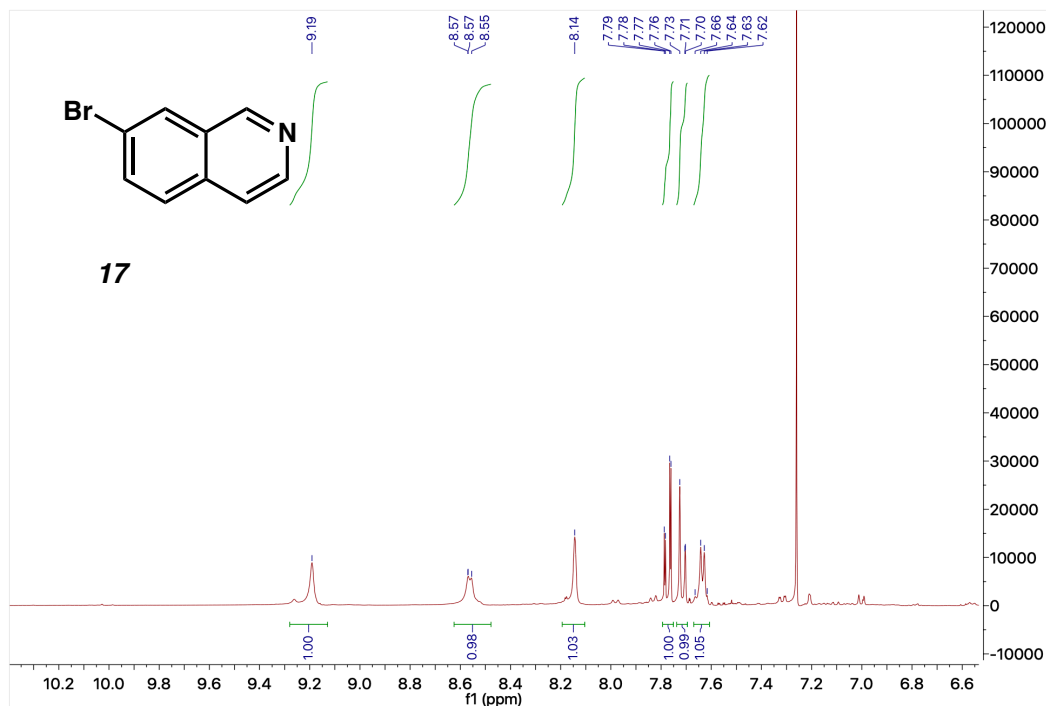


Figure A1.16 Table 2.6 Entry 4 ¹H NMR (400 MHz, Chloroform-d) of Crude Reaction, Yield Calculated with *Cis*-1,4-Diacetoxy-2-Butene Standard

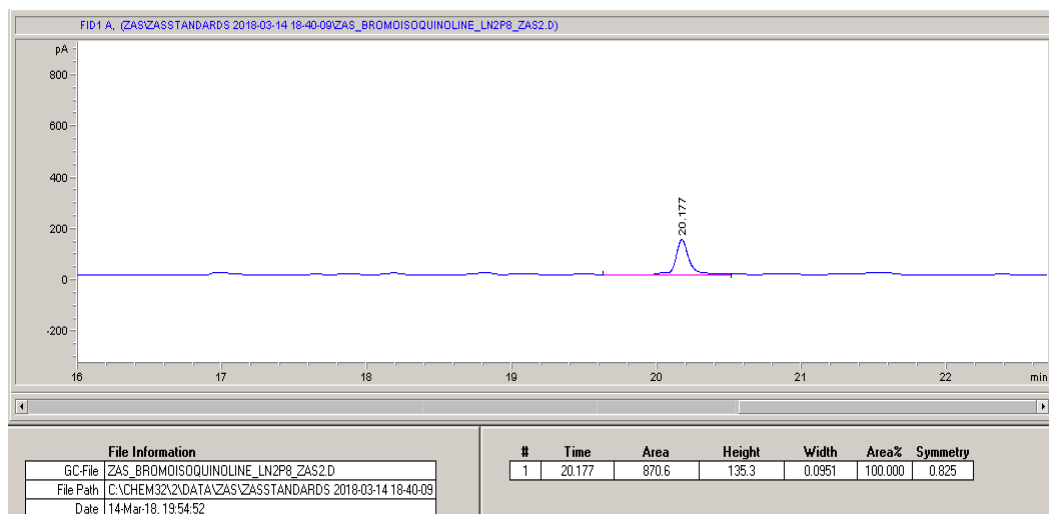


Figure A1.17 GC Spectra of 16 Crude Reaction: Showing Full Conversion: 17@20.18, 16 rt is Typically@19.51 Using ZAS2 Method in Table A1.1

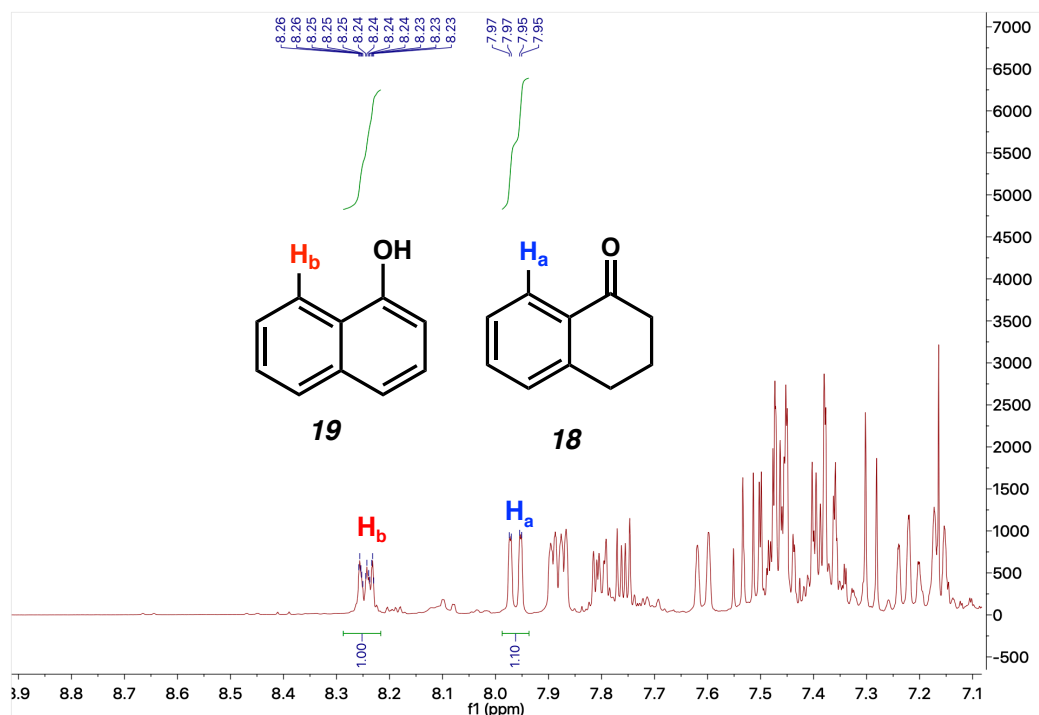


Figure A1.18 Table 2.7 Entry 4 ^1H NMR (400 MHz, Chloroform- d) of Crude Reaction

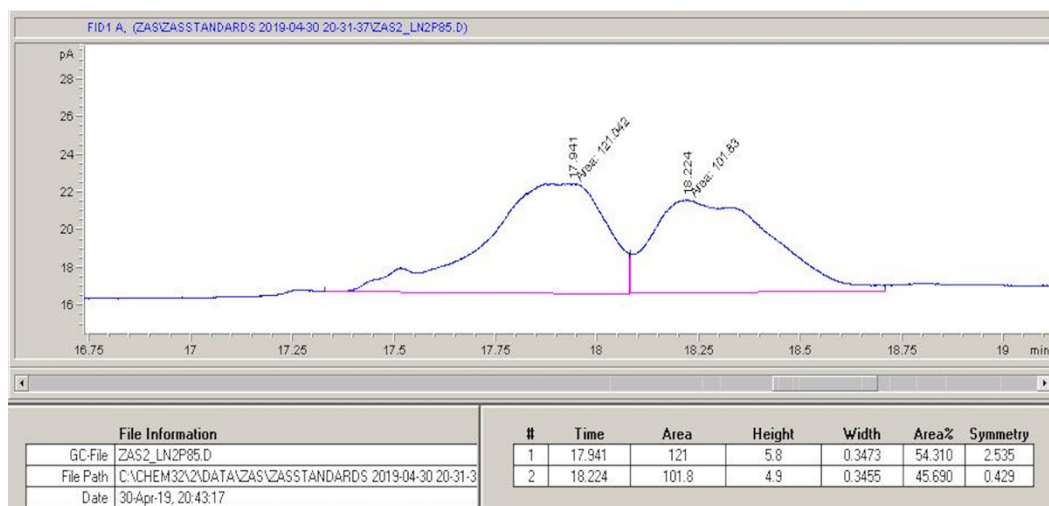


Figure A1.19 GC Spectra of **18** Crude Reaction: **18**@17.94 and **19**@18.22 Using ZAS2 Method in Table A1.1

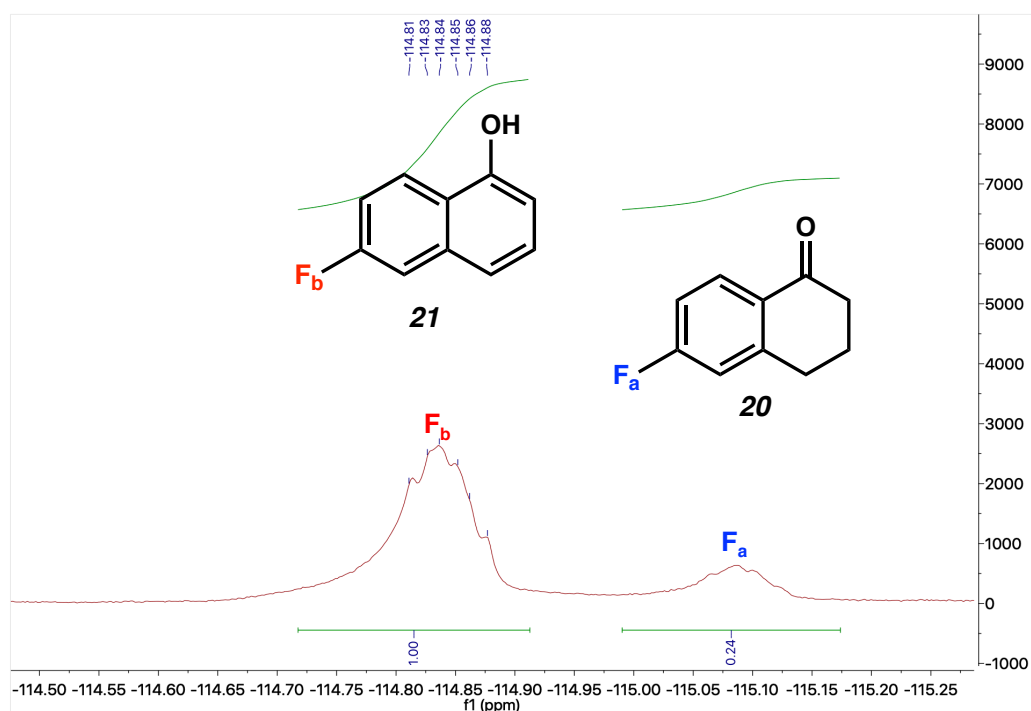


Figure A1.20 Table 2.8 Entry 9 ^{19}F NMR (376 MHz, neat reaction) of Crude Reaction, Yield Calculated with α,α,α -Trifluorotoluene as in Internal Standard

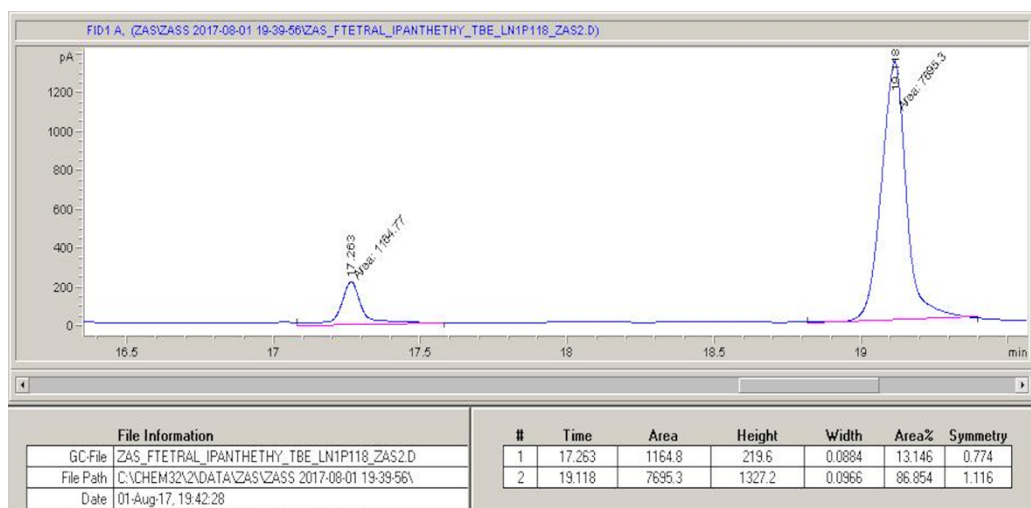


Figure A1.21 GC Spectra of **20** Crude Reaction: **20**@17.26 and **21**@19.12 Using ZAS2 Method in Table A1.1

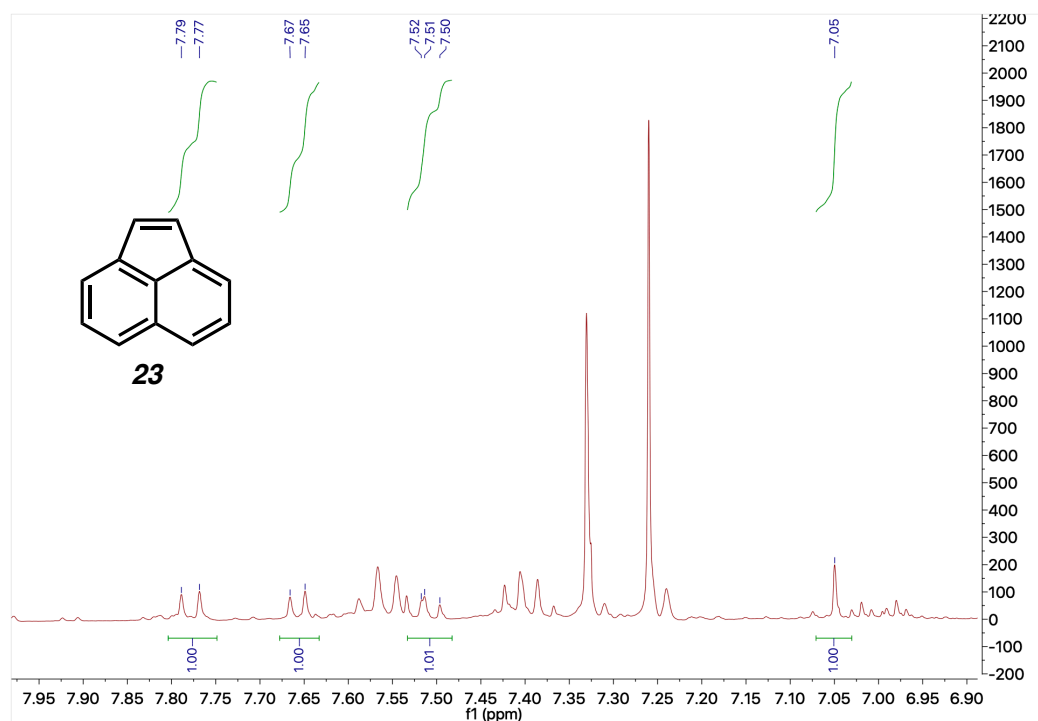


Figure A1.22 Table 2.9 Entry 3 ^1H NMR (400 MHz, Chloroform- d) of Crude Reaction, Yield Calculated with *Cis*-1,4-Diacetoxy-2-Butene Standard

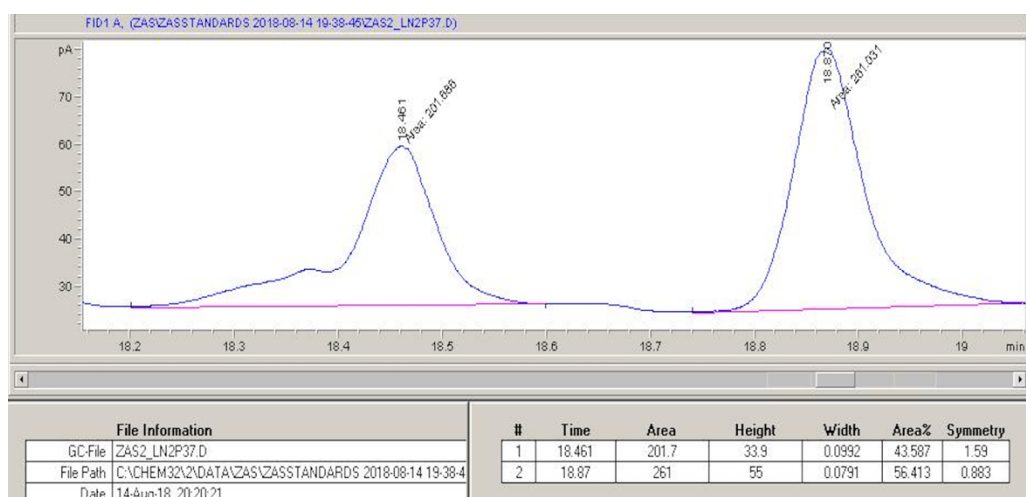


Figure A1.23 GC Spectra of **22** Crude Reaction: **23**@18.46 and **22**@18.87 Using ZAS2 Method Table A1.1

APPENDIX 2

C(SP³)-H DEHYDROGENATION ATTEMPTS OF CHALLENGING HETEROCYCLIC ALKANES BY IRIDIUM PINCER LIGATED COMPLEXES

A2.1 INTRODUCTION

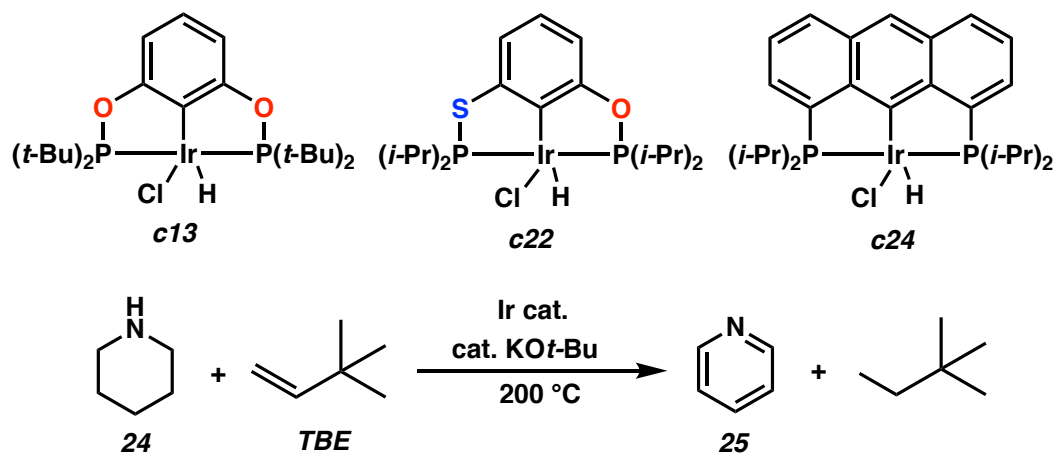
In Chapter 2, we successfully demonstrated Ir pincer-catalyzed C(sp³)-H transfer dehydrogenation of a diverse collection of substrates bearing functional groups that are typically known to strongly coordinate to transition-metal centers and inhibit catalysis. In efforts to expand the application of Ir pincer ligated complexes as transfer dehydrogenation catalysts and explore their reactivity, we extended the investigated heterocyclic substrate scope to additional functionalities containing sulfur and chlorine heteroatoms, and silane and cyano groups. That being said, the dehydrogenative transformation of these substrates proved to be challenging. In this appendix, we present our attempts in dehydrogenating these

additional heterocyclic substrates by Ir pincer ligated complexes and provide insights to the substrates with functionalities that could be promising in optimizing this transformation.

A2.2 ATTEMPTS TO TRANSFER DEHYDROGENATE PIPERIDINE AND N-METHYLPYRROLIDINE

Pyridine and its derivatives are of great synthetic interest owing to their properties and applications in organometallic chemistry, biologically active systems, and materials.¹ Goldman in 2003 and Huang in 2014 reported the transfer dehydrogenation of secondary and tertiary amines using Ir pincer ligated complexes (*t*-Bu⁴POCOP)-Ir **c13** and (*i*-Pr⁴PSCOP)-Ir **c22** in moderate to excellent yields (Scheme 2.3 in Chapter 2).^{2,3} Given the importance of pyridine and the promising relevant reported examples, we were interested in investigating the application of Ir pincer ligated complexes as potential catalysts for the direct transfer dehydroaromatization of piperidine (**24**) to pyridine (**25**). We commenced the investigation using complex (*t*-Bu⁴POCOP)-Ir **c13** and **TBE** as the H₂ acceptor (Table A2.1, entries 1-4). The reactions were carried out neat at 200 °C under an argon atmosphere after drying and distilling all reagents. We observed that **c13** was not catalytically active and only trace amounts were generated even when increasing the catalyst loading from 0.21 to 0.63 mol.% and reaction time from 21 h to 48 h. Alternatively, we investigated the dehydrogenation of **24** using complexes (*i*-Pr⁴PSCOP)-Ir **c22** and (*i*-Pr⁴anthrphos)-Ir **c24** with **TBE** as the H₂ acceptor (Table A2.1 entry 5 and 6). However, we observed that complexes **c22** and **c24** were also not catalytically active in transfer dehydrogenating **24** to **25**.

Table A2.1 Investigated Conditions of Piperidine Transfer Dehydrogenation Attempts by Ir Pincer Ligated Complexes

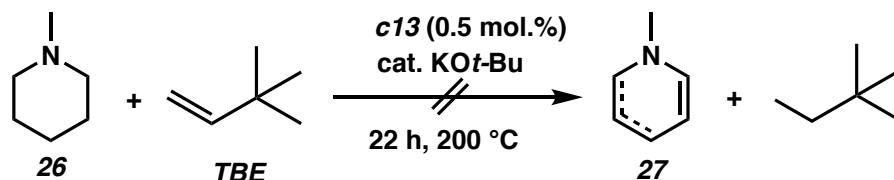


entry	cat./(mol.%)	equiv. acceptor	of	reaction time	25 yield ^b	TON ^c
1	c13/0.22	1.0		21 h	-	-
2	c13/0.21	1.0		48 h	1.2%	6
3	c13 ^d /0.42	1.0		25 h	0.5%	1
4	c13 ^d /0.63	2.5		24 h	-	-
5	c22/0.16	1.8		48 h	-	-
6	c24/0.16	1.5		42 h	0.7%	4

[a] Conditions: 3.2-4.0 mmol of **24**, precatalyst with at least 1.2 equiv. KO^{*t*}-Bu. [b] Yield determined by GC and ¹H NMR using cis-1,4-diacetoxy-2-butene as an internal standard. [c] TON per dehydrogenation.

We believe **24** likely inhibits catalysis due to its Lewis basic nature in the form of an unprotected secondary amine. Hence, we then investigated the transfer dehydrogenation of *N*-methylpiperidine (**26**) to methylpyridine (**27**) using complex **c13** and **TBE** as the H₂ acceptor (Scheme A2.1).

Scheme A2.1 Attempts to Transfer Dehydrogenate N-Methylpiperidine by Complex (t-Bu⁴POCOP)-Ir **c13**



Unfortunately, we found that **c13** was not catalytically active and did not observe any activation of **26**. This result is in agreement with previous reports by Goldman where no catalytic activity was observed when attempting the dehydrogenation of **26** by complex (t-Bu⁴PCP)-Ir **c3** (Figure A2.1).³

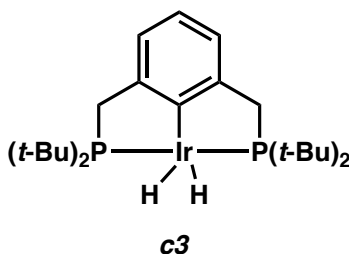


Figure A2.1 Complex (t-Bu⁴PCP)-Ir **c3** Chemical Structure

A2.3 ATTEMPTS TO TRANSFER DEHYDROGENATE FIVE-MEMBERED RING DERIVATIVES

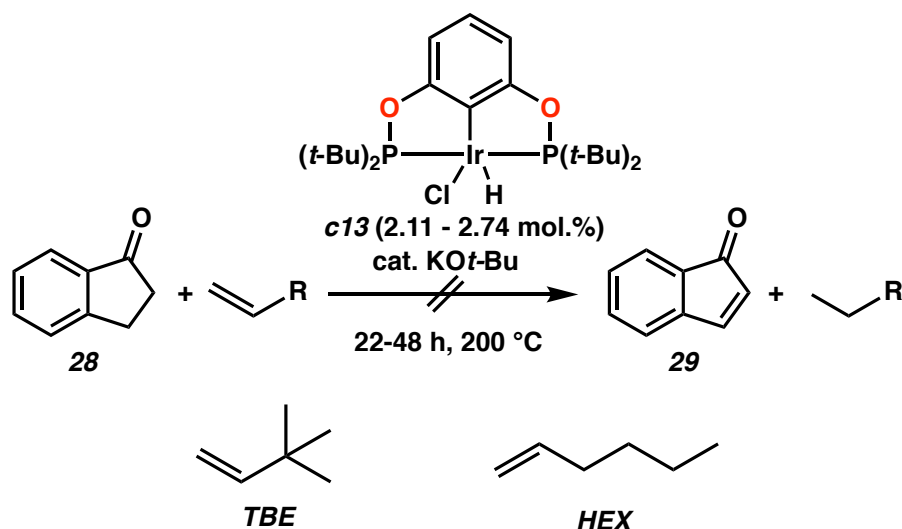
Pentene and five-membered ring skeletons are found especially in organometallic applications.^{4,5} Owing to their importance, we were interested to investigate the dehydrogenation of a diverse collection of five-membered ring derivatives using Ir pincer ligated complexes to provide facile and complimentary

methods to the current approaches. In this section we discuss our attempts in dehydrogenating 5-methoxy-1-indanone, 1-chlorocyclopentene, 5-iodo-2,3,-dihydrobenzofuran, and 4-aminoindan.

A2.3.1 Investigations of 5-Methoxy-1-Indanone Transfer Dehydrogenation

We began our investigation of the transfer dehydrogenation of 5-methoxy-1-indanone (**28**) using complex $(t\text{-Bu}^4\text{POCOP})\text{-Ir}$ **c13** and **TBE** as the H_2 acceptor (Scheme A2.2). The reactions were carried out neat at 200 °C under an argon atmosphere after drying and distilling all reagents. We did not observe any product and we believe **28** was decomposing since we did not observe any indicative aromatic peaks in the ^1H NMR spectrum. We also investigated using **HEX** as an alternative acceptor but observed similar findings and no dehydrogenated product was generated.

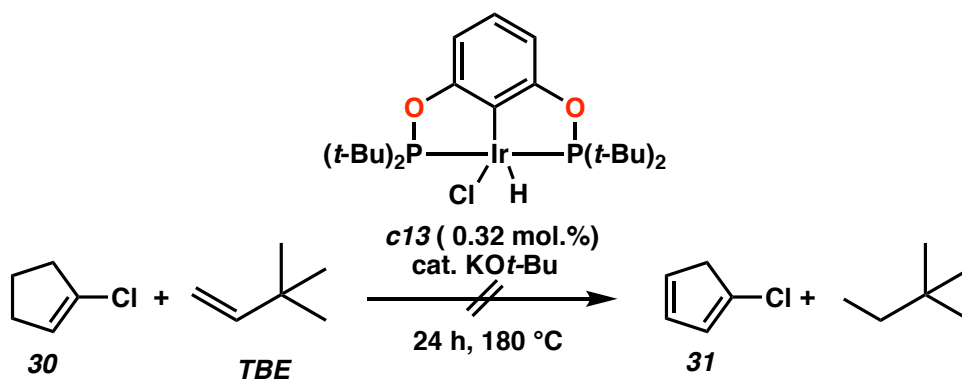
Scheme A2.2 Attempts to Transfer Dehydrogenate 5-Methoxy-1-Indanone by Complex $(t\text{-Bu}^4\text{POCOP})\text{-Ir}$ **c13**



A2.3.2 Investigations of 1-Chlorocyclopentene Transfer Dehydrogenation

We began our investigation of the transfer dehydrogenation of 1-chlorocyclopentene (**30**) using complex (*t*-Bu⁴POCOP)-Ir **c13** and TBE as the H₂ acceptor (Scheme A2.3). The reactions were carried out neat at 180 °C under an argon atmosphere after drying and distilling all reagents. We did not observe the desired product 1-chlorocyclopentadiene (**31**). The substrate **30** was unreactive and may have inhibited catalysis by coordinating to the Ir metal center. We also investigated the disproportionation of **30** to **31** and 1-chlorocyclopentane without using an H₂ acceptor but we did not observe any conversion.

Scheme A2.3 Attempts to Transfer Dehydrogenate 1-Chlorocyclopentene by Complex (*t*-Bu⁴POCOP)-Ir **c13**

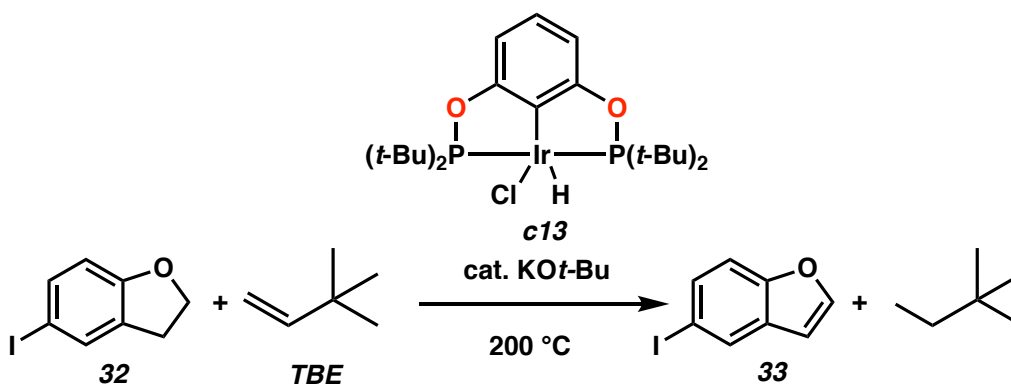


A2.3.3 Investigations of 5-Iodo-2,3-Dihydrobenzofuran Transfer Dehydrogenation

We began our investigation of the transfer dehydrogenation of 5-iodo-2,3-dihydrobenzofuran (**32**) using complex (*t*-Bu⁴POCOP)-Ir **c13** and TBE as the H₂ acceptor (Table A2.2). The reactions were carried out neat at 200 °C under an argon atmosphere after drying and distilling all reagents. We believe the reaction

generated 5-iodobenzofuran (**33**) in modest yield (30%). We observed other unidentified products in the aromatic region in the ¹H NMR spectrum. Although this transformation seems promising, further investigations are required to validate the observed findings and optimize reaction conditions upon successful confirmation.

Table A2.2 Investigated Conditions of 5-Iodo-2,3-Dihydrobenzofuran Transfer Dehydrogenation by Ir Pincer Ligated Complexes



entry	cat./(mol.%)	equiv. acceptor	of	reaction time	33 yield ^b	TON ^c
1	c13/5.50%	exs		21 h	25.9%	5
2	c13/7.26%	exs		24 h	30.0%	4

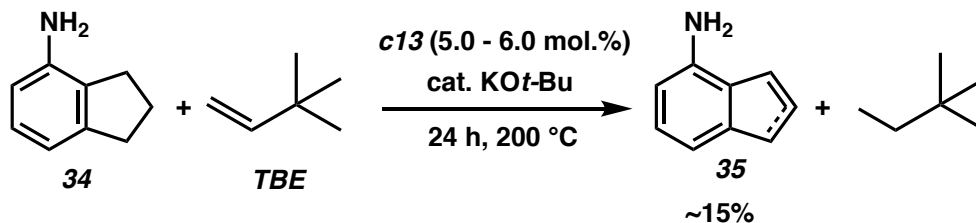
[a] Conditions: 3.2-4.0 mmol of **32**, precatalyst with at least 1.2 equiv. KO^t-Bu. [b] Yield determined by GC and ¹H NMR using cis-1,4-diacetoxy-2-butene as an internal standard. [c] TON per dehydrogenation.

A2.3.4 Investigations of 4-Aminoindan Transfer Dehydrogenation

We investigated the transfer dehydrogenation of 4-aminoindan (**34**) using complex (^t-Bu⁴POCOP)-Ir **c13** and TBE as the H₂ acceptor (Scheme A2.4). The reactions were carried out neat at 200 °C under an argon atmosphere after drying and distilling all reagents. We believe the dehydrogenated substrate **35** was generated in yields up to 15%. However, we observed other unidentified products in the aromatic

region in the ¹H NMR spectrum and we could not identify which isomer was generated. Further investigations are necessary to confirm the obtained isomer of the product and optimize reaction conditions upon successful confirmation.

Scheme A2.4. Attempts to Transfer Dehydrogenate 4-Aminoindan by Complex (t-Bu⁴POCOP)-Ir **c13**



A2.4 ATTEMPTS TO TRANSFER DEHYDROGENATE CARBONYL CONTAINING CYCLIC ALKANE DERIVATIVES

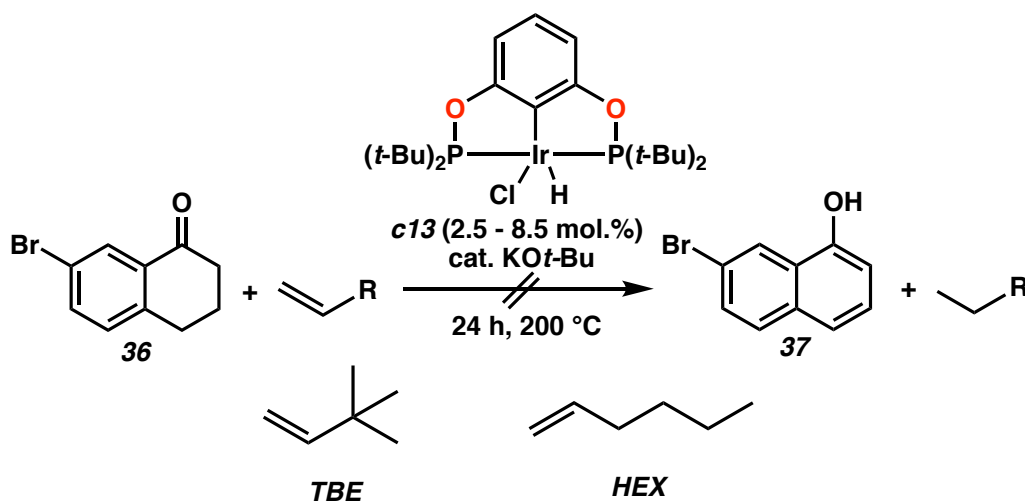
Aromatic and olefinic carbonyl skeletons constitute a common substructure of a large variety of biologically active substances and materials with unique properties.⁶⁻⁹ In addition, carbonyl derivatives can participate in nucleophilic addition reactions, the Wittig reaction, condensation reactions, and silylation reactions, and hence are a useful functional handle for a variety of organic reactions.¹⁰⁻¹³ Owing to their properties and synthetic utility, it is of interest to dehydrogenate cyclic carbonyl derivatives using Ir pincer ligated complexes as dehydrogenation catalysts, in attempt to provide an alternative and complementary method to the current approaches. In this section we discuss our attempts at dehydrogenating 7-bromo-1-tetralone, tetrahydrothiopyran-4-one,

4-methoxy-5,6,7,8-tetrahydronaphthalene-1-carbaldehyde, 8-fluoro-1-benzosuberone, 5,6,7,8-tetrahydro-2-naphthoic acid, 1-acetylcyclohexene, 3-(4-bromo-2-fluorophenyl)cyclohexan-1-one, and 6-methoxy-3,4-dihydronaphthalen-1(2H)-one.

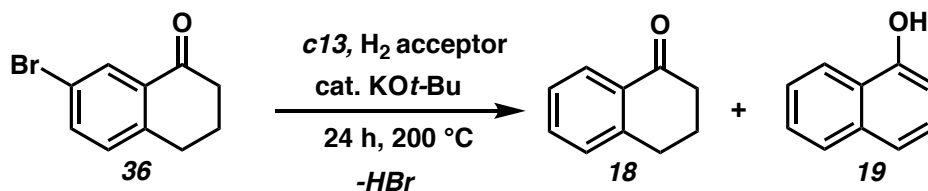
A2.4.1 Investigations of 7-Bromo-1-Tetralone Transfer Dehydrogenation

We began our investigation of the transfer dehydrogenation of 7-bromo-1-tetralone (**36**) using complex $(t\text{-Bu}^4\text{POCOP})\text{-Ir}$ **c13** and using both **TBE** and **HEX** as H_2 acceptors (Scheme A2.5). The reactions were carried out neat at 200 °C under an argon atmosphere after drying and distilling all reagents. We found that an aromatic product was generated based on the ^1H NMR spectrum observed ppm shifts, however it was not the desired 7-bromo-1-naphthol (**37**) dehydrogenated product. After further investigation, we found that a debrominated naphthol **19** is generated instead, along with the decomposed **36** to 1-tetralone (**18**) (Scheme A2.6).

Scheme A2.5 Attempts to Transfer Dehydrogenate 7-Bromo-1-Tetralone by Complex $(t\text{-Bu}^4\text{POCOP})\text{-Ir}$ **c13**



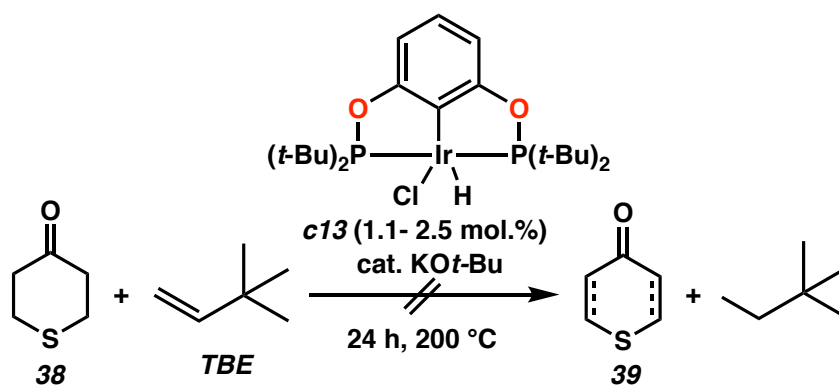
Scheme A2.6 Debromination of 7-Bromo-1-Tetralone and Transfer Dehydrogenation by Complex (*t*-Bu⁴POCOP)-Ir **c13**



A2.4.2 Investigations of Tetrahydrothiopyran-4-one Transfer Dehydrogenation

We investigated the transfer dehydrogenation of tetrahydrothiopyran-4-one (**38**) using complex (*t*-Bu⁴POCOP)-Ir **c13** and **TBE** as the H₂ acceptor (Scheme A2.7). The reactions were carried out neat at 200 °C under an argon atmosphere after drying and distilling all reagents. We did not observe the desired product **39** and we believe **38** likely inhibited catalysis by coordinating to the Ir metal center via the thioether.

Scheme A2.7 Attempts to Transfer Dehydrogenate Tetrahydrothiopyran-4-one by Complex (*t*-Bu⁴POCOP)-Ir **c13**



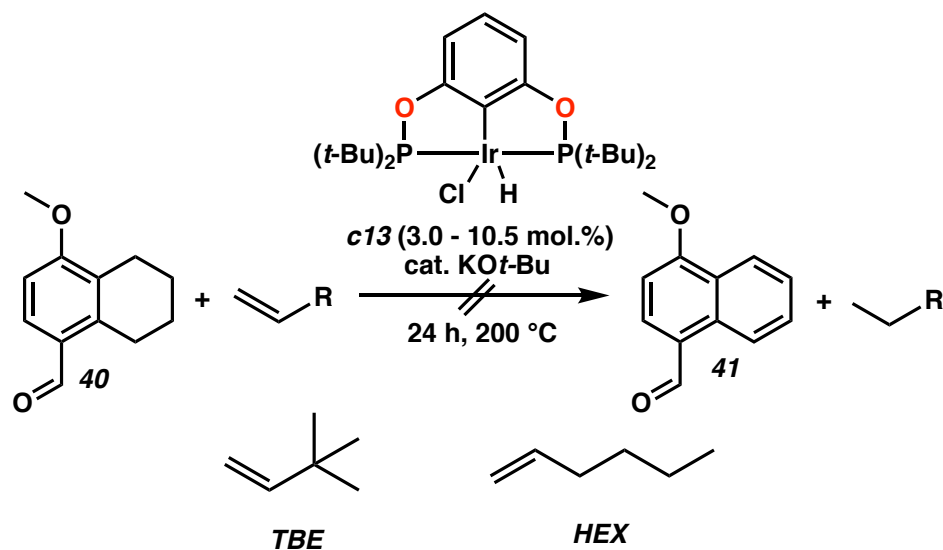
A2.4.3 Investigations of 4-Methoxy-5,6,7,8-Tetrahydronaphthalene-1-Carbaldehyde Transfer Dehydrogenation

We investigated the transfer dehydrogenation of 4-methoxy-5,6,7,8-tetrahydronaphthalene-1-carbaldehyde (**40**) using complex (*t*-Bu⁴POCOP)-Ir **c13** and both **TBE** and **HEX** as H₂ acceptors (Scheme A2.8). The reactions were carried out neat at 200 °C under an argon atmosphere after drying and distilling all reagents. We did not observe the desired product **41** and we believe **40** likely inhibited catalysis by coordinating to the Ir metal center.

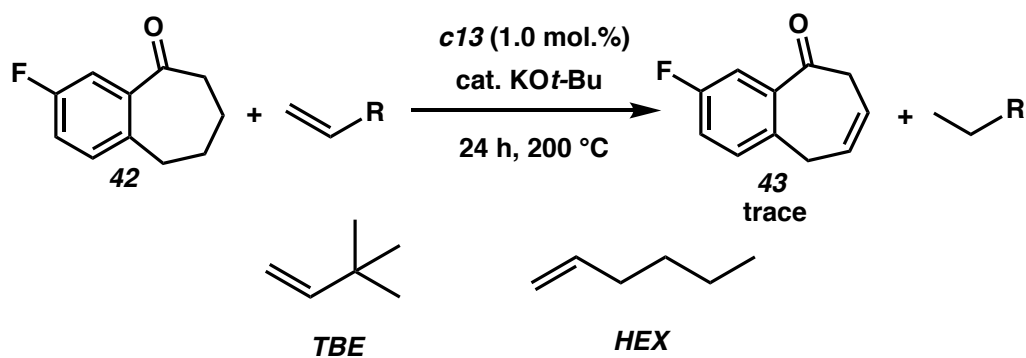
A2.4.4 Investigations of 8-Fluoro-1-Benzosuberone Transfer Dehydrogenation

We investigated the transfer dehydrogenation of 8-fluoro-1-benzosuberone (**42**) using complex (*t*-Bu⁴POCOP)-Ir **c13** and both **TBE** and **HEX** as H₂ acceptors (Scheme A2.9). The reactions were carried out neat at 200 °C under an argon atmosphere after drying and distilling all reagents. We believe we observed trace amounts of **43**, however further investigations are required to validate our findings and confirm that the desired product was obtained. Upon successful confirmation, reaction conditions will be optimized to achieve higher yields of **43**.

Scheme A2.8 Attempts to Transfer Dehydrogenate 4-Methoxy-5,6,7,8-Tetrahydronaphthalene-1-Carbaldehyde by Complex $(t\text{-Bu}_4\text{POCOP})\text{-Ir } \mathbf{c13}$



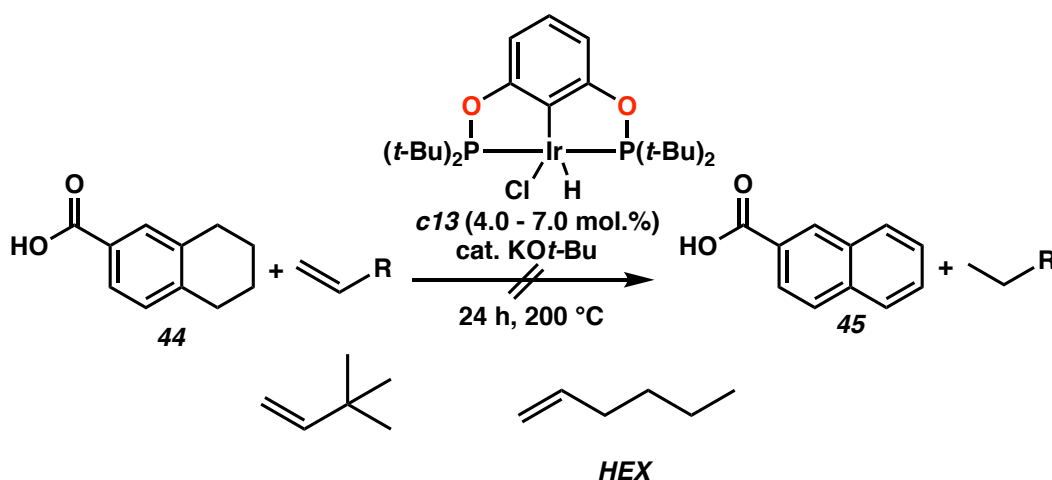
Scheme A2.9 Attempts to Transfer Dehydrogenate 8-Fluoro-1-Benzosuberone by Complex $(t\text{-Bu}_4\text{POCOP})\text{-Ir } \mathbf{c13}$



A2.4.5 Investigations of 5,6,7,8-Tetrahydro-2-Naphthoic Acid Transfer Dehydrogenation

We investigated the transfer dehydrogenation of 5,6,7,8-tetrahydro-2-naphthoic acid (**44**) using complex $(t\text{-Bu}_4\text{POCOP})\text{-Ir}$ **c13** and both **TBE** and **HEX** as H_2 acceptors (Scheme A2.10). The reactions were carried out neat at 200 °C under an argon atmosphere after drying and distilling all reagents. We did not observe the desired dehydrogenated product **45**. We are not surprised by this result as this substrate contains a carboxylic acid moiety; however, we wanted to explore complex **c13** catalytic activity in harsh environments given that we successfully transfer dehydrogenated substrates containing acidic functionalities in excellent yields, as presented in Chapter 2.

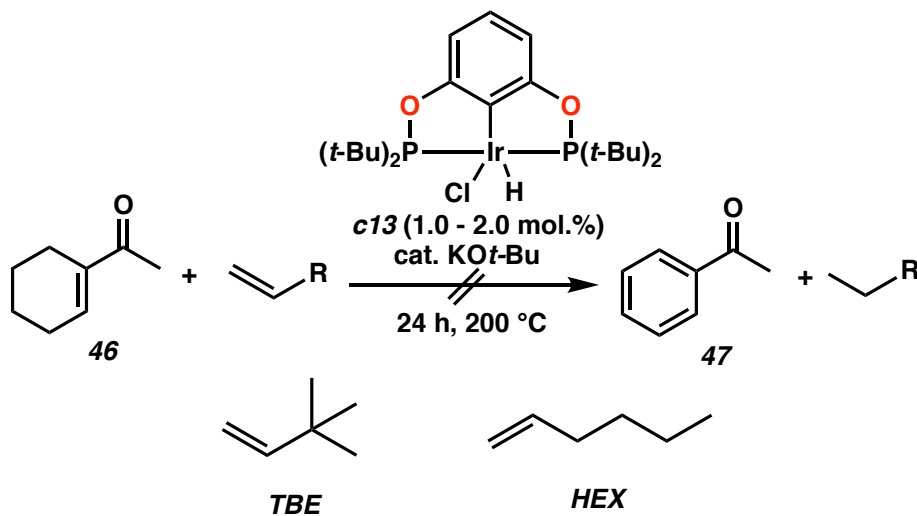
Scheme A2.10 Attempts to Transfer Dehydrogenate 5,6,7,8-Tetrahydro-2-Naphthoic Acid by Complex $(t\text{-Bu}_4\text{POCOP})\text{-Ir}$ **c13**



A2.4.6 Investigations of 1-Acetylcyclohexene Transfer Dehydrogenation

We investigated the transfer dehydrogenation of 1-acetylcyclohexene (**46**) using complex $(t\text{-Bu}^4\text{POCOP})\text{-Ir}$ **c13** and both **TBE** and **HEX** as H_2 acceptors (Scheme A2.11). The reactions were carried out neat at 200 °C under an argon atmosphere after drying and distilling all reagents. We varied the catalyst loading between 1.0 to 2.0 mol.% but we did not observe the desired dehydrogenated product methylbenzoate (**47**). We also investigated the disproportionation of **46** to **47** without using an olefinic acceptor but did not observe any conversion. It is likely that **46** inhibit catalysis by coordinating to the Ir metal center.

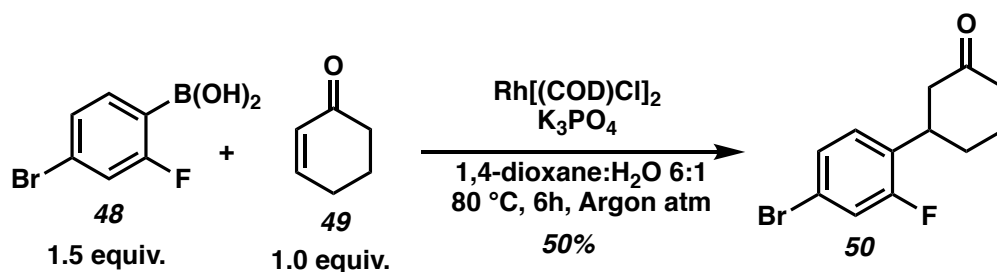
Scheme A2.11 Attempts to Transfer Dehydrogenate 1-Acetylcyclohexene by Complex $(t\text{-Bu}^4\text{POCOP})\text{-Ir}$ **c13**



A2.4.7 Synthesis of 3-(4-Bromo-2-Fluorophenyl)Cyclohexan-1-one and Transfer Dehydrogenation Attempts

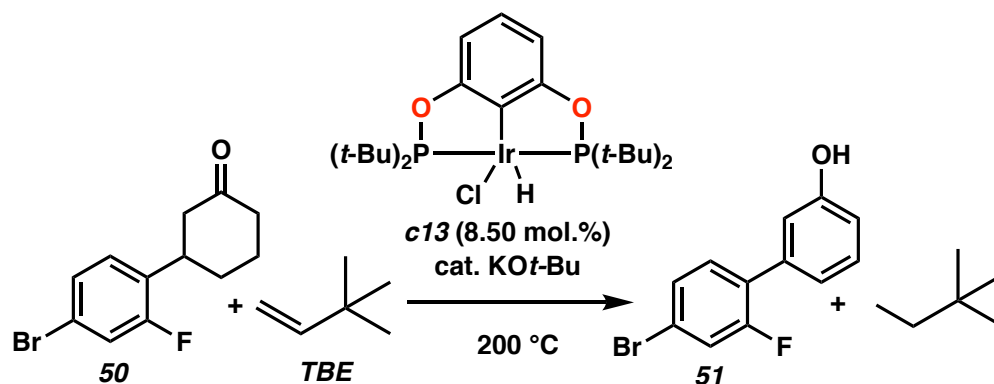
We were interested in transfer dehydrogenating a substrate with multiple functionalities to investigate the tolerance of Ir pincer ligated complexes in such systems. Hence, we synthesized 3-(4-bromo-2-fluorophenyl)cyclohexan-1-one (**50**) from 4-bromo-2-fluorobenzeneboronic acid (**48**) and 2-cyclohexenone (**49**) utilizing rhodium catalyzed 1,4-conjugate addition following literature procedures.^{14,15}

Scheme A2.12 3-(4-Bromo-2-Fluorophenyl)Cyclohexan-1-one Synthesis via Rhodium Catalyzed 1,4-Conjugate Addition



After successfully synthesizing **50** we investigated its transfer dehydrogenation using complex (*t*-Bu⁴POCOP)-Ir **c13** and TBE as the H₂ acceptor to 4'-bromo-2'-fluoro-[1,1'-biphenyl]-3-ol (**51**) (Scheme A2.13). The reactions were carried out neat at 200 °C under an argon atmosphere after drying and distilling all reagents. We could not identify the product as there were several peaks observed in the aromatic region in the ¹H NMR spectrum. However, the diagnostic peak of **50** at 3.20 ppm was no longer observed, indicating full conversion of the starting material. Further investigations are necessary to identify the products and optimize reaction conditions upon successful confirmation.

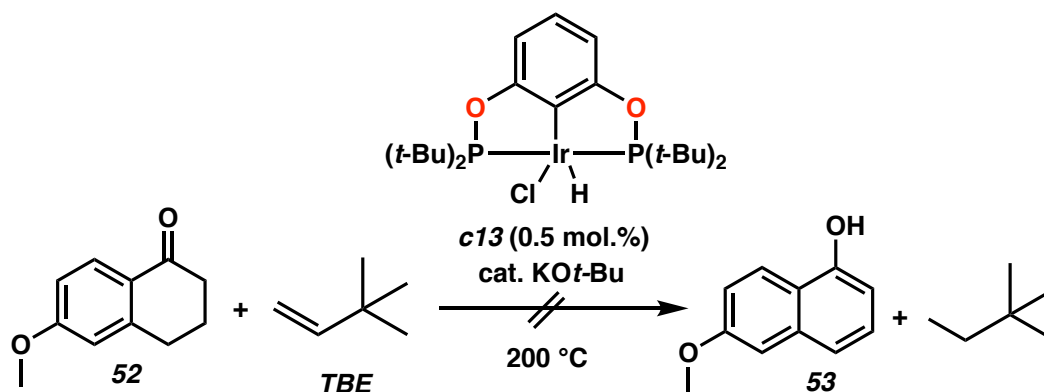
Scheme A2.13 3-(4-Bromo-2-Fluorophenyl)Cyclohexan-1-one Transfer Dehydrogenation Attempts by Complex (*t*-Bu⁴POCOP)-Ir **c13**



A2.4.8 Investigations of 6-Methoxy-3,4-Dihydronaphthalen-1(2H)-one Transfer Dehydrogenation

We investigated the transfer dehydrogenation of 6-methoxy-3,4-dihydronaphthalen-1(2H)-one (**52**) using complex (*t*-Bu⁴POCOP)-Ir **c13** and TBE as the H₂ acceptor (Scheme A2.14). The reactions were carried out neat at 200 °C under an argon atmosphere after drying and distilling all reagents. We did not observe the desired dehydrogenated product **53**. That being said, we believe this reaction is promising and increasing the catalyst loading and or experimenting with other Ir pincer ligated complexes may generate conversion given that we've seen high catalytic activity of investigated Ir pincer ligated complexes when dehydrogenating tetralone derivatives in Chapter 2. Hence, further investigations are required to study this system.

Scheme A2.14 6-Methoxy-3,4-Dihydronaphthalen-1(2H)-one Transfer Dehydrogenation Attempts by Complex $(t\text{-Bu}_4\text{POCOP})\text{-Ir}$ **c13**



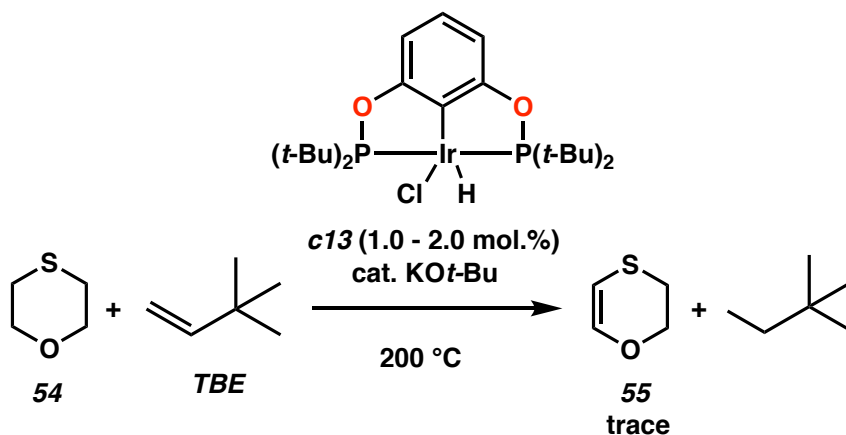
A2.5 ATTEMPTS TO TRANSFER DEHYDROGENATE CYCLOHEXYL DERIVATIVES

Functionalized arenes and olefins are found as substructures in many organic compounds that are synthetically useful and have biological and physical properties.¹⁶⁻²¹ Hence it is of interest to use Ir pincer ligated complexes as dehydrogenation catalysts to dehydrogenate cyclohexyl derivatives to functionalized arenes and olefins as a new and complementary method to the current approaches. In this section, we present our attempts in transfer dehydrogenating 1,4-thioxane, 2-cyclohexene-1-acetonitrile, phenylcyclohexane, 1-bromo-4-cyclohexylbenzene, 3-bromocyclohexene, chlorocyclohexane, 1-(trimethylsiloxy)cyclohexene, julolidine, and paroxetine by Ir pincer ligated complexes.

A2.5.1 Investigations of 1,4-Thioxane Transfer Dehydrogenation

We investigated the transfer dehydrogenation of 1,4-thioxane (**54**) using complex $(t\text{-Bu}^4\text{POCOP})\text{-Ir}$ **c13** and TBE as the H_2 acceptor (Scheme A2.15). The reactions were carried out neat at 200 °C under an argon atmosphere after drying and distilling all reagents. We observed trace amounts of the olefinic product **55**, however further investigations are required to validate our findings and optimize reaction conditions upon successful confirmation of the desired product. In all cases, we did not observe what would be the fully dehydrogenated product 1,4-oxathiline.

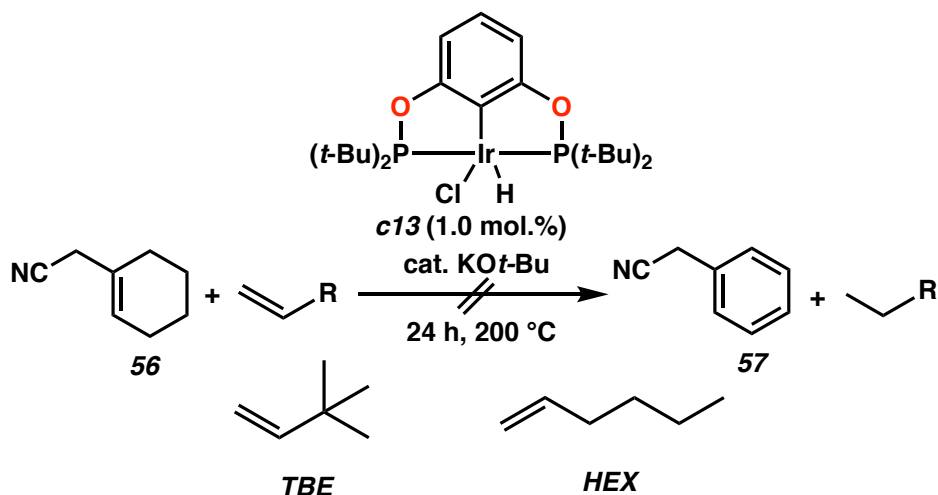
Scheme A2.15 1,4-Thioxane Transfer Dehydrogenation Attempts by Complex $(t\text{-Bu}^4\text{POCOP})\text{-Ir}$ **c13**



A2.5.2 Investigations of 2-Cyclohexene-1-Acetonitrile Transfer Dehydrogenation

We investigated the transfer dehydrogenation of 2-cyclohexene-1-acetonitrile (**56**) using complex $(t\text{-Bu}^4\text{POCOP})\text{-Ir}$ **c13** and using both **TBE** and **HEX** as H_2 acceptors (Scheme A2.16). The reactions were carried out neat at 200 °C under an argon atmosphere after drying and distilling all reagents. In all cases, we did not observe the desired dehydrogenated product **57**. Instead, we observed isomerization of **56**. We also investigated the disproportionation of **56** to **57** and similarly observed isomerization of **56**. It is likely that operating the reaction at the required high temperatures for dehydrogenation is causing isomerization, and hence this substrate is not ideal for such transformation.

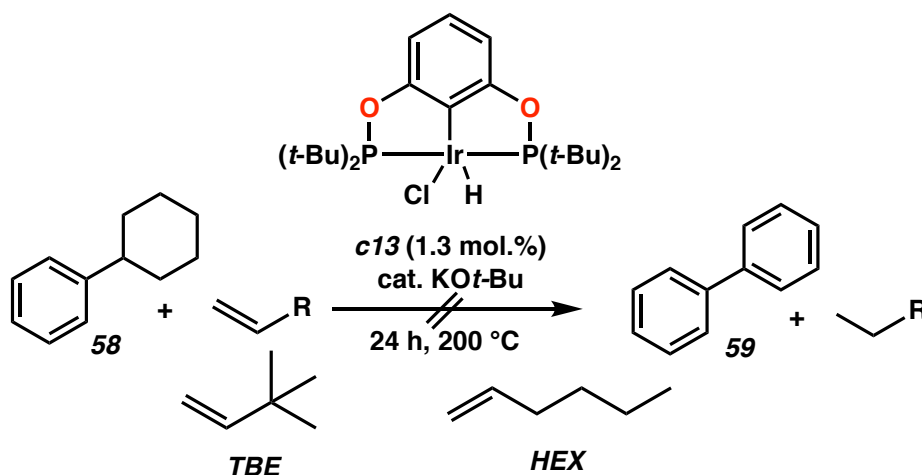
Scheme A2.16 2-Cyclohexene-1-Acetonitrile Transfer Dehydrogenation Attempts by Complex $(t\text{-Bu}^4\text{POCOP})\text{-Ir}$ **c13**



A2.5.3 Investigations of Phenylcyclohexane Transfer Dehydrogenation

We investigated the transfer dehydrogenating of phenylcyclohexane (**58**) to biphenyl (**59**) using complex (*t*-Bu⁴POCOP)-Ir **c13** and using both **TBE** and **HEX** as H₂ acceptors (Scheme A2.17). The reactions were carried out neat at 200 °C under an argon atmosphere after drying and distilling all reagents. In all cases, we did not observe the desired biphenyl (**59**) product and **58** was unreactive.

Scheme A2.17 Phenylcyclohexane Transfer Dehydrogenation Attempts by Complex (*t*-Bu⁴POCOP)-Ir **c13**

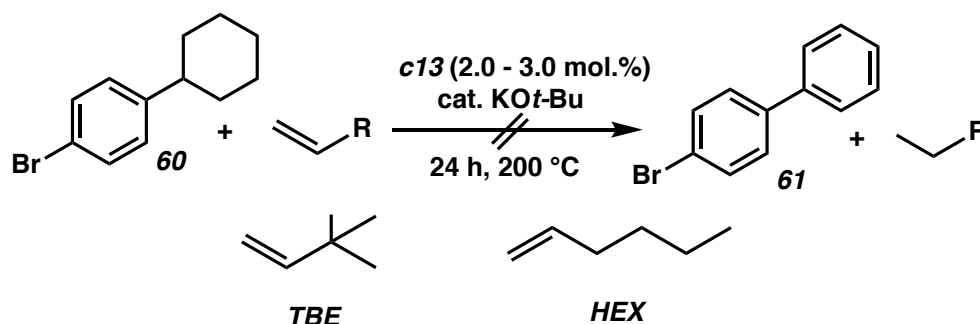


A2.5.4 Investigations of 1-Bromo-4-Cyclohexylbenzene Transfer Dehydrogenation

We investigated the transfer dehydrogenation of 1-bromo-4-cyclohexylbenzene (**60**) to 4-bromo-biphenyl (**61**) using complex (*t*-Bu⁴POCOP)-Ir **c13** and using both **TBE** and **HEX** as H₂ acceptors (Scheme A2.18).

The reactions were carried out neat at 200 °C under an argon atmosphere after drying and distilling all reagents. We did not observe the desired dehydrogenated product **61**, and **60** was unreactive.

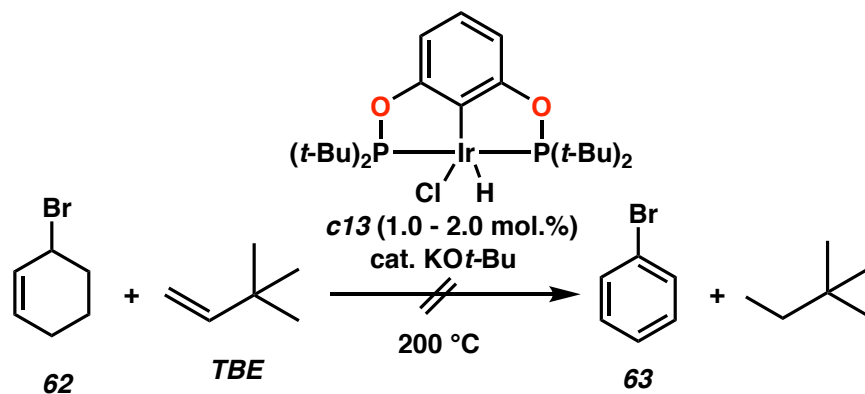
Scheme A2.18 1-Bromo-4-Cyclohexylbenzene Transfer Dehydrogenation Attempts by Complex (*t*-Bu⁴POCOP)-Ir **c13**



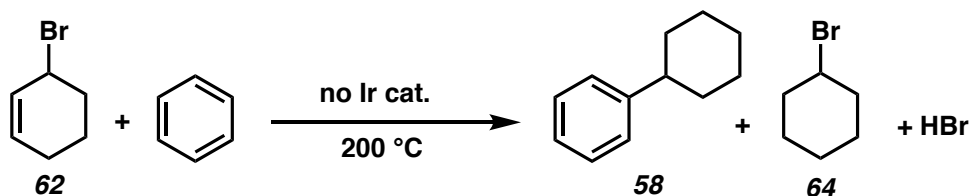
A2.5.5 Investigations of 3-Bromo-Cyclohexene Transfer Dehydrogenation

We investigated the transfer dehydrogenation of 3-bromocyclohexene (**62**) to 1-bromobenzene (**63**) using complex (*t*-Bu⁴POCOP)-Ir **c13** and using **TBE** as the H₂ acceptor (Scheme A2.19). The reactions were carried out neat at 200 °C under an argon atmosphere after drying and distilling all reagents. We did not observe **63** and instead we observed phenylcyclohexane (**58**), benzene, and 1-bromocyclohexane (**64**). We investigated the disproportionation of **62** using complex (*t*-Bu⁴POCOP)-Ir **c13** and observed similar results. In addition, we carried out a 1:1 reaction mixture of **62** and benzene at 200 °C without the addition of an Ir complex or KO*t*-Bu and observed similar results (Scheme A2.20). Hence, the generated phenylcyclohexane (**58**) is likely not catalyzed by complex **c13** and possibly occurred *via* a Friedel-Craft type alkylation *via* electrophilic aromatic substitution followed by H atom transfer.

Scheme A2.19 3-Bromocyclohexene Transfer Dehydrogenation Attempts by Complex (*t*-Bu₄POCOP)-Ir **c13**



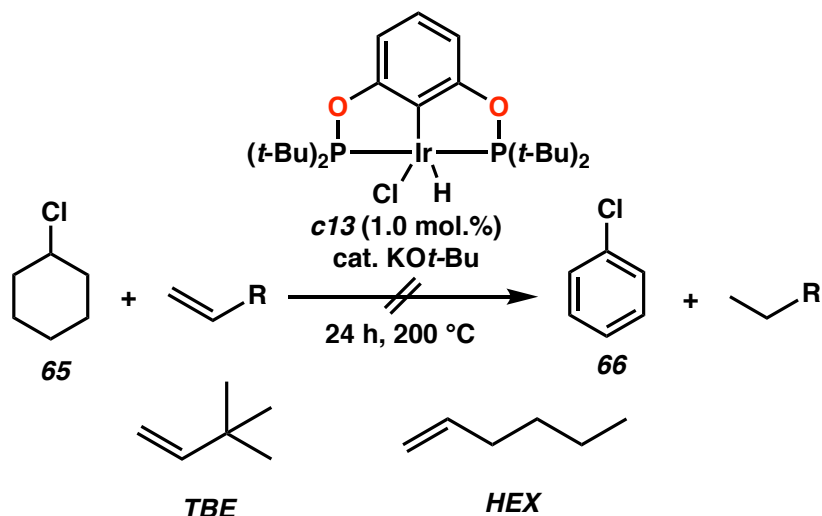
Scheme A2.20 3-Bromocyclohexene Reaction with Benzene without an Ir Complex



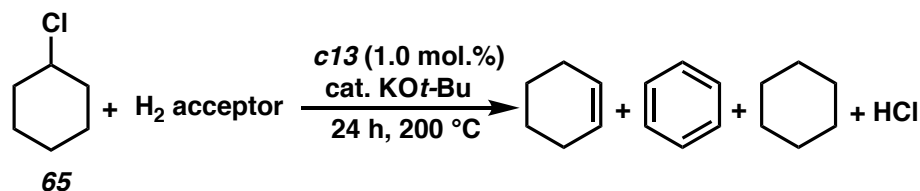
A2.5.6 Investigations of Chlorocyclohexane Transfer Dehydrogenation

We investigated the transfer dehydrogenation of chlorocyclohexane (**65**) to chlorobenzene (**66**) using complex (*t*-Bu₄POCOP)-Ir **c13** and using both **TBE** and **HEX** as H₂ acceptors (Scheme A2.21). The reactions were carried out neat at 200 °C under an argon atmosphere after drying and distilling all reagents. In all cases we did not observe the desired dehydrogenated product **66**. Instead we observed 1-cyclohexene, cyclohexane, and benzene (Scheme 2.22). 1-Cyclohexene is likely generated from elimination of the chloride, and cyclohexane and benzene are likely generated from 1-cyclohexene disproportionation as we will demonstrate in Chapter 3.

Scheme A2.21 Chlorocyclohexane Transfer Dehydrogenation Attempts by Complex $(t\text{-Bu}^4\text{POCOP})\text{--Ir } \mathbf{c13}$



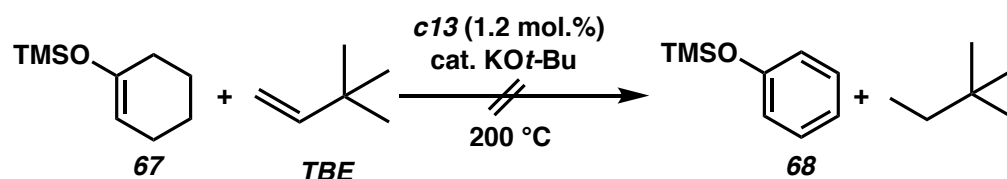
Scheme A2.22 Chlorocyclohexane Decomposition to 1-Cyclohexene During Transfer Dehydrogenation Attempts



A2.5.7 Investigations of 1-(Trimethylsiloxy)Cyclohexene Transfer Dehydrogenation

We investigated the transfer dehydrogenation of 1-(trimethylsiloxy)cyclohexene (**67**) to trimethyl(phenoxy)silane (**68**) using complex $(t\text{-Bu}^4\text{POCOP})\text{--Ir } \mathbf{c13}$ and using **TBE** as the H_2 acceptor (Scheme A2.23). The reactions were carried out neat at $200\text{ }^\circ\text{C}$ under an argon atmosphere after drying and distilling all reagents. We did not observe **68** and **67** was not activated and unreactive toward complex **c13**.

Scheme A2.23 1-(Trimethylsiloxy)Cyclohexene Transfer Dehydrogenation Attempts by Complex (*t*-Bu₄POCOP)-Ir **c13**



A2.5.8 Investigations of Julolidine Transfer Dehydrogenation

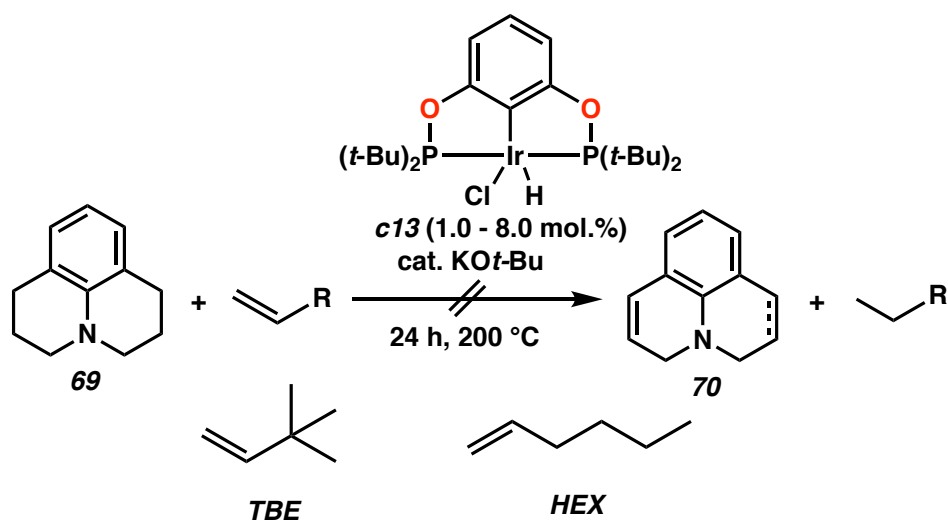
Julolidine (**69**) is a natural product that has been shown to have photoconductive and other useful properties along with its derivatives.^{22,23} We wanted to extend the application of Ir pincer ligated complexes as dehydrogenation catalysts on a natural product to demonstrate late stage dehydrogenation ability. We investigated the transfer dehydrogenating of **69** using complex (*t*-Bu₄POCOP)-Ir **c13** and using both **TBE** and **HEX** as H₂ acceptors (Scheme A2.24). However, we did not observe any olefinic product possibly due to steric hinderance of the investigated substrate and its unreactive nature toward complex **c13**.

A2.5.9 Investigations of Paroxetine Transfer Dehydrogenation

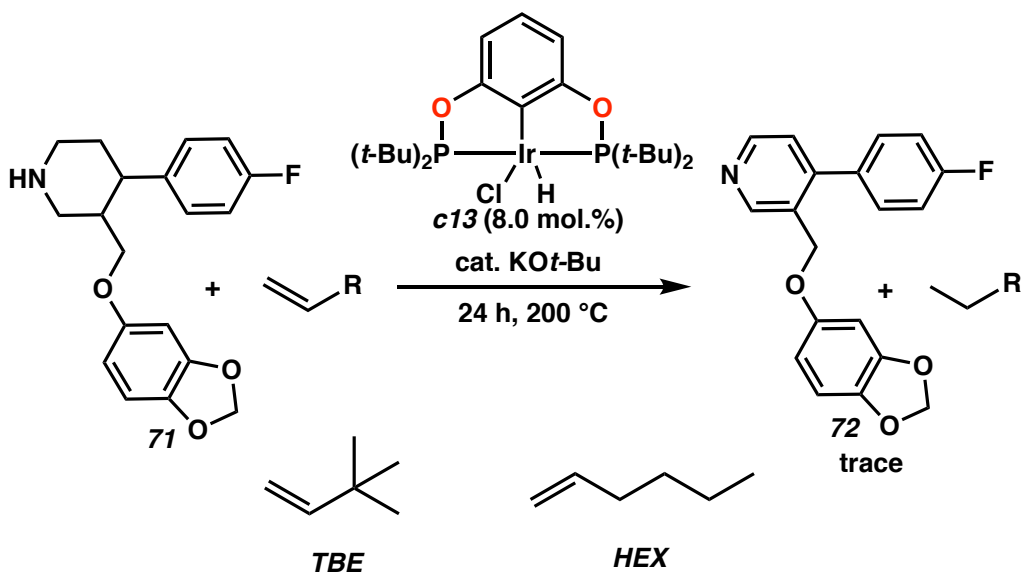
Paroxetine (**71**) is a widely used drug to treat depression and other medical conditions.^{24,25} We wanted to extend the application of Ir pincer ligated complexes as dehydrogenation catalysts on drug-like molecules to demonstrate the efficacy of late stage dehydrogenation. We investigated the transfer dehydrogenating of **71** using complex (*t*-Bu₄POCOP)-Ir **c13** and using both **TBE** and **HEX** as H₂ acceptors (Scheme A2.25). We believe we observed trace amounts of the dehydrogenated product **72**, further investigations are required to validate our findings. Upon

successful confirmation, optimization conditions will be carried out to achieve higher yields of **72**.

Scheme A2.24 Julolidine Transfer Dehydrogenation Attempts by Complex $(t\text{-Bu}_4\text{POCOP})\text{-Ir } \mathbf{c13}$



Scheme A2.25 Paroxetine Transfer Dehydrogenation Attempts by Complex $(t\text{-Bu}_4\text{POCOP})\text{-Ir } \mathbf{c13}$



A2.6 SUMMARY AND CONCLUSIONS

Functional aromatics and olefins constitute common substructures in a large variety of complex molecules, materials, and polymers. Hence, there is a great interest in developing methods for the synthesis of substituted and unsubstituted aromatics. Utilizing Ir pincer ligated complexes to dehydrogenate functional cycloalkanes is attractive and can be a complementary method toward current approaches. In Chapter 2, we demonstrated the successful transfer dehydrogenation of a diverse collection of heterocyclic alkanes containing functionalities known to strongly coordinate to metal centers and inhibit catalysis. In efforts to expand our scope of work we extended our studies to investigate heterocyclic substrates containing functionalities with halides, carbonyls, five- and six- membered heterocyclic rings, and thiols (Figure A2.2). However, the direct dehydrogenation of C(sp³)-H alkanes may seem conceptually simple but in fact is a challenging transformation and in some cases not feasible, especially when dehydrogenating heteroatomic substrates. In the case of **26**, **28**, **30**, **36**, **38**, **40**, **44**, **46**, **52**, **56**, **58**, **60**, **62**, **65**, **67** and **69**, it was not possible to generate a dehydrogenated product due to binding to the Ir metal center, steric hindrance, the basic or acidic nature of the substrate, decomposition of the substrate, isomerization of the substrate, and or unreactivity toward the investigated Ir pincer ligated complexes.

On the other hand, transfer dehydrogenating **24**, **32**, **34**, **42**, **50**, **54**, and **71**, is potentially promising and further investigations are required to validate the obtained product. Upon successful confirmation of the desired product, reaction

conditions will be optimized to achieve higher yields. All in all, the obtained results showcased the limited capability of Ir pincer ligated complexes as dehydrogenation catalysts for functionalized heterocyclic substrates.

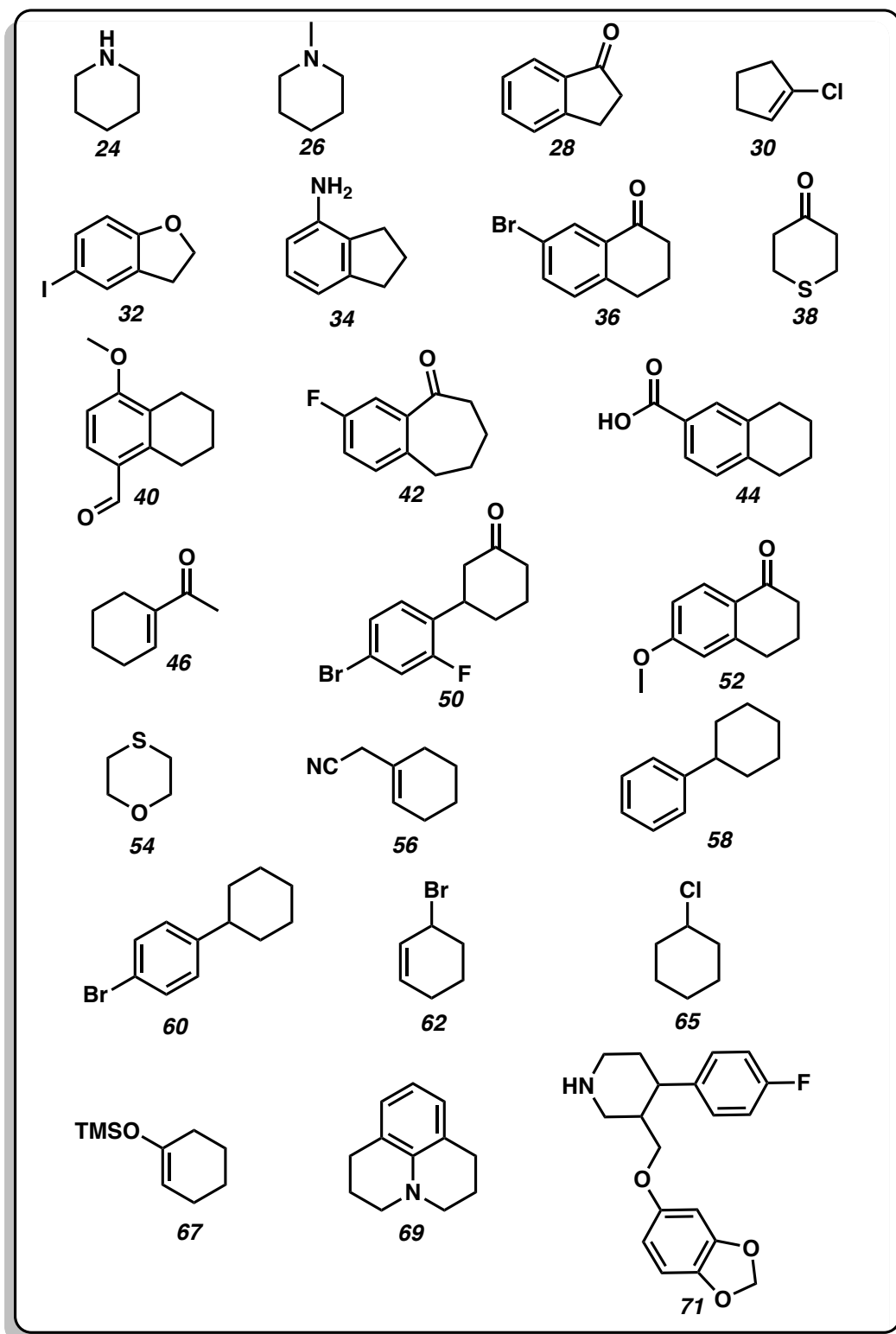


Figure A2.2 Summary of Investigated Substrate Scope in Appendix 2

A2.7 NOTES AND REFERENCES

1. Fraser, H. L.; Floyd, M. B.; Barrios Sosa, A. C. In *Prog. Heterocycl. Chem.*; Gribble, G. W., Joule, J. A., Eds.; Elsevier: 2005; Vol. 17, p 261.
2. Yao, W.; Zhang, Y.; Jia, X.; Huang, Z. *Angewandte Chemie International Edition* **2014**, 53, 1390.
3. Zhang, X.; Fried, A.; Knapp, S.; Goldman, A. S. *Chem. Commun.* **2003**, 2060.
4. Ke, Z.; Tsui, G. C.; Peng, X.-S.; Yeung, Y.-Y. In *Prog. Heterocycl. Chem.*; Gribble, G. W., Joule, J. A., Eds.; Elsevier: 2016; Vol. 28, p 219.
5. Omae, I. *Coord. Chem. Rev.* **2004**, 248, 995.
6. Fan, Z.; Nakayama, K.; Sawanobori, T.; Hiraoka, M. *Pflügers Archiv* **1992**, 421, 409.
7. Zhang, X.; Xie, T.; Cui, M.; Yang, L.; Sun, X.; Jiang, J.; Zhang, G. *ACS Appl. Mater. Interfaces* **2014**, 6, 2279.
8. Somersall, A. C.; Guillet, J. E. *Macromolecules* **1972**, 5, 410.
9. Denmark, S. E.; Fu, J. *Chemical Reviews* **2003**, 103, 2763.
10. Kidonakis, M.; Mullaj, A.; Stratakis, M. *The Journal of Organic Chemistry* **2018**, 83, 15553.
11. Jayaram, V.; Sridhar, T.; Sharma, G. V. M.; Berrée, F.; Carboni, B. *The Journal of Organic Chemistry* **2018**, 83, 843.
12. Carey, F. A.; Sundberg, R. J. In *Advanced Organic Chemistry: Part A: Structure and Mechanisms*; Carey, F. A., Sundberg, R. J., Eds.; Springer US: Boston, MA, 1977, p 325.

13. Ranu, B. C.; Jana, R. *Eur. J. Org. Chem.* **2006**, 2006, 3767.
14. Edwards, H. J.; Hargrave, J. D.; Penrose, S. D.; Frost, C. G. *Chemical Society Reviews* **2010**, 39, 2093.
15. Hayashi, T.; Yamasaki, K. *Chemical Reviews* **2003**, 103, 2829.
16. Pahlavan, F.; Hosseinneshad, S.; Samieadel, A.; Hung, A.; Fini, E. *Industrial & Engineering Chemistry Research* **2019**, 58, 11939.
17. Liu, J.; Zheng, H.-X.; Yao, C.-Z.; Sun, B.-F.; Kang, Y.-B. *Journal of the American Chemical Society* **2016**, 138, 3294.
18. Cui, L.; Matusaki, Y.; Tada, N.; Miura, T.; Uno, B.; Itoh, A. *Adv. Synth. Catal.* **2013**, 355, 2203.
19. Rossi, R.; Lessi, M.; Manzini, C.; Marianetti, G.; Bellina, F. *Synthesis* **2016**, 48, 3821.
20. Zhan, Z.-P.; Yang, R.-F.; Lang, K. *Tetrahedron Letters* **2005**, 46, 3859.
21. Binder, J. B.; Raines, R. T. *Curr. Opin. Chem. Biol.* **2008**, 12, 767.
22. Varejão, J. O. S.; Varejão, E. V. V.; Fernandes, S. A. *Eur. J. Org. Chem.* **2019**, 2019, 4273.
23. Enoki, T.; Matsuo, K.; Ohshita, J.; Ooyama, Y. *Phys. Chem. Chem. Phys.* **2017**, 19, 3565.
24. Despia, C. F.; Dominey, A. P.; Harrowven, D. C.; Linciau, B. *Eur. J. Org. Chem.* **2014**, 2014, 4335.
25. Vardanyan, R. In *Piperidine-Based Drug Discovery*; Vardanyan, R., Ed.; Elsevier: 2017, p 299.

APPENDIX 3

EXPERIMENTAL SECTION AND SPECTRA RELEVANT TO APPENDIX 2

A3.1 MATERIALS AND METHODS

Unless noted in the specific procedure, reactions were performed in oven-dried glassware. All dehydrogenation reactions were degassed by freeze-pump-thaw x 5 cycles and were carried out under air-free conditions in dry glassware. All liquid reagents were purified by distillation and dried using molecular sieves, NaH, or Na-K alloy. For all the investigated dehydrogenation systems, the substrate was mixed with the H₂ acceptor in a 4 mL sealed Schlenk pressure flask under an argon atmosphere. Then synthesized Ir pincer complexes were added to the reaction mixture with at least 1.2 equivalents of the Ir pincer complexes of KO^{*t*}-Bu when the Ir-HCl version of catalyst is used.

¹H NMR spectra were recorded on Bruker AV III HD 400 MHz spectrometer equipped with a Prodigy liquid nitrogen temperature cryoprobe, and are reported in

terms of chemical shift relative to residual CHCl_3 (δ 7.26). Dehydrogenation conversions were determined using ^1H NMR with cis-1,4-diacetoxy-2-butene standard.

In addition, the conversions were determined using an Agilent 6850 GC-FID equipped with a Supelco column (SPBTM-1, fused silica capillary column, 30 m x 0.25 μm film thickness) and using methods with temperature programs shown in Table A3.1 and inlet program shown in Table A3.2.

Table A3.1 ZAS2 General Method Temperature Ramping Program for The Investigated Substrates in Appendix 2

Oven Ramp	°C/min	Next °C	Hold min
Initial	-	38	1.50
Ramp 1	10.00	150	0.00
Ramp 2	20.00	250	5.00

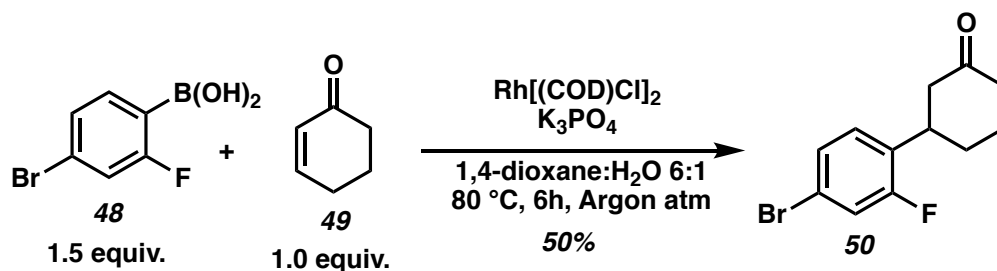
Table A3.2 Inlet Parameters used in All Methods

Inlet	Setting
Mode	Split
Gas	He
Heater	250 °C
Pressure	9.52 psi
Total Flow	82.2
Split Ratio	100:1
Split Flow	78.5 mL/min

A3.2 GENERAL PROCEDURE FOR DEHYDROGENATION REACTIONS

For all the investigated dehydrogenation systems, 3.2 to 4.0 mmol of the substrate was mixed with the state equivalence of the H₂ acceptor in a 4 mL sealed Schlenk pressure flask under an argon atmosphere. Then the synthesized Ir pincer ligated complex was added to the reaction mixture with at least 1.2 catalytic equivalents of KO^tBu under an argon atmosphere. The reaction mixture was then dried by freeze-pump-thaw method x five cycles and then backfilled with argon gas. Lastly, the Schlenk flask was placed in heated silicone oil stirring for the duration of reaction and specified temperature.

A3.3 SYNTHESIS PROCEDURE OF 3-(4-BROMO-2-FLUOROPHENYL)CYCLOHEXAN-1-ONE



An 8 mL vial was charged with 0.40 g (1.8 mmol) of 4-bromo-2-fluorobenzeneboronic acid (**48**), 0.14 mL (1.2 mmol) of 2-cyclohexenone (**49**), 50 mg of $[\text{Rh}(\text{COD})\text{Cl}]_2$, 0.66 g (3 mmol, 3 Molar) of K_3PO_4 in 1 mL DI H_2O , and 5 mL dioxane and an argon atmosphere. Then the reaction mixture was heated at 80 °C for 6 h. After cooling the reaction mixture, the generated product **50** was extracted *via* a silica column using a 1:4 mixture of diethyl ether and pentane and then dried under vacuum. The obtained product was a colorless viscous liquid.

4'-bromo-2'-fluoro-[1,1'-biphenyl]-3-ol (**51**): ^1H NMR (400 MHz, Chloroform-*d*) δ 7.22 – 7.18 (m, 1H), 7.16 (dd, J = 9.9, 2.0 Hz, 1H), 7.06 – 7.00 (m, 1H), 3.20 (tdd, J = 11.0, 5.8, 3.5 Hz, 1H), 2.50 – 2.23 (m, 4H), 2.14 – 1.88 (m, 2H), 1.89 – 1.62 (m, 2H).

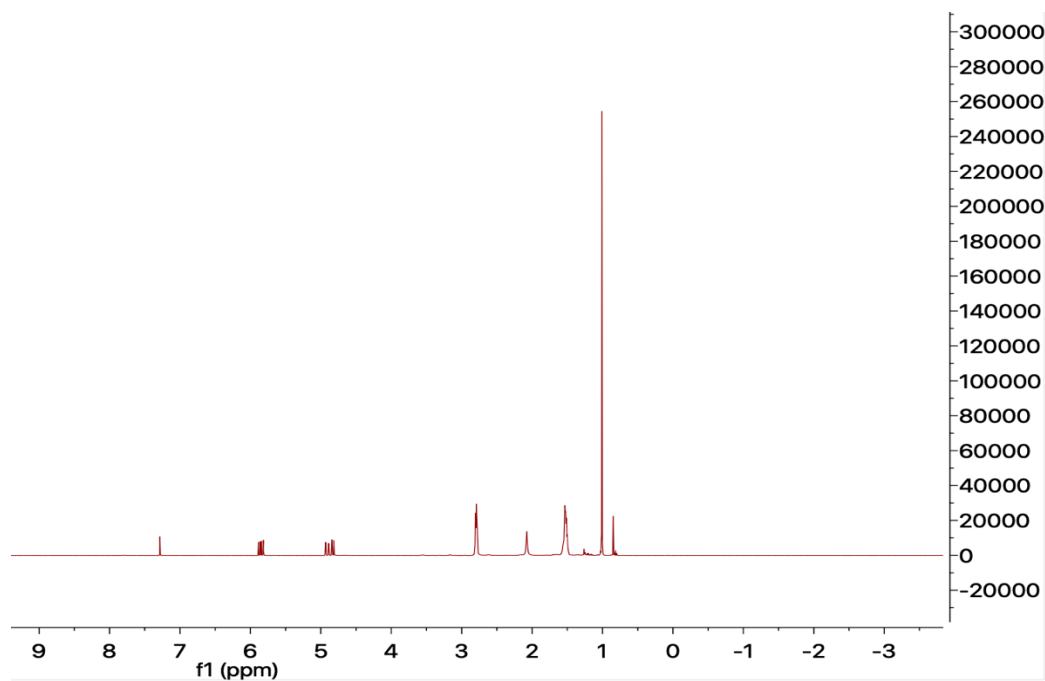
A3.4 ^1H NMR SPECTRA OF REACTIONS

Figure A3.1 Table A2.1 Entry 1: Crude Reaction of Piperidine (**24**) Showing No Conversion

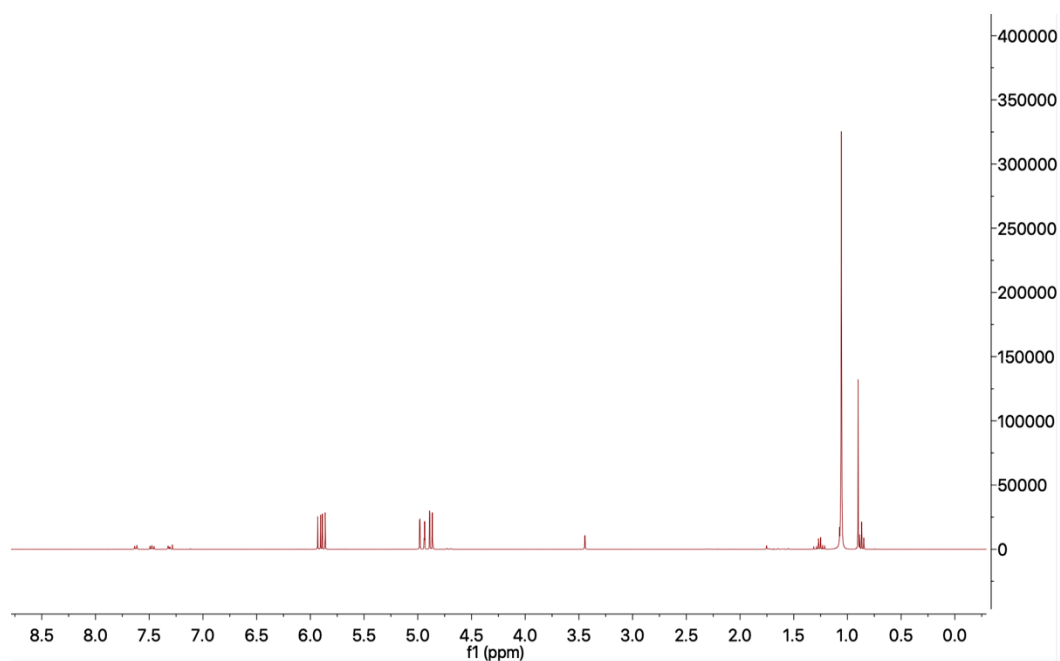


Figure A3.2 Table A2.1 Entry 5: Crude Reaction of Piperidine (**24**) Showing No Conversion

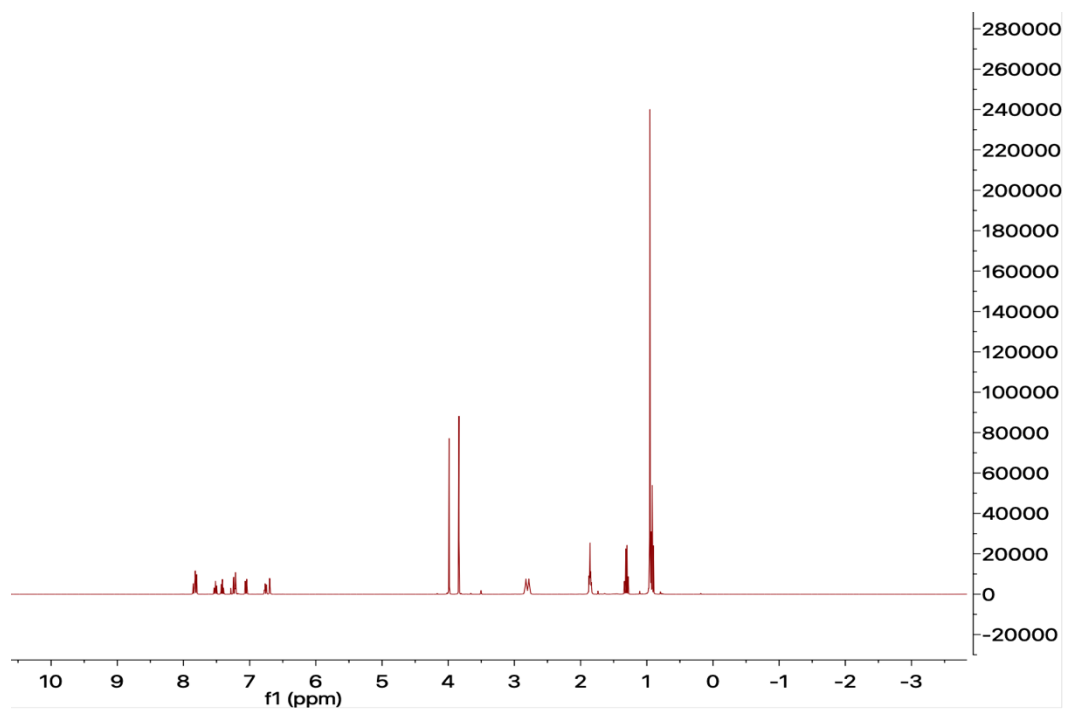


Figure A3.3 Table A2.1 Entry 6: Crude Reaction of Piperidine (**24**) Showing Low Conversion

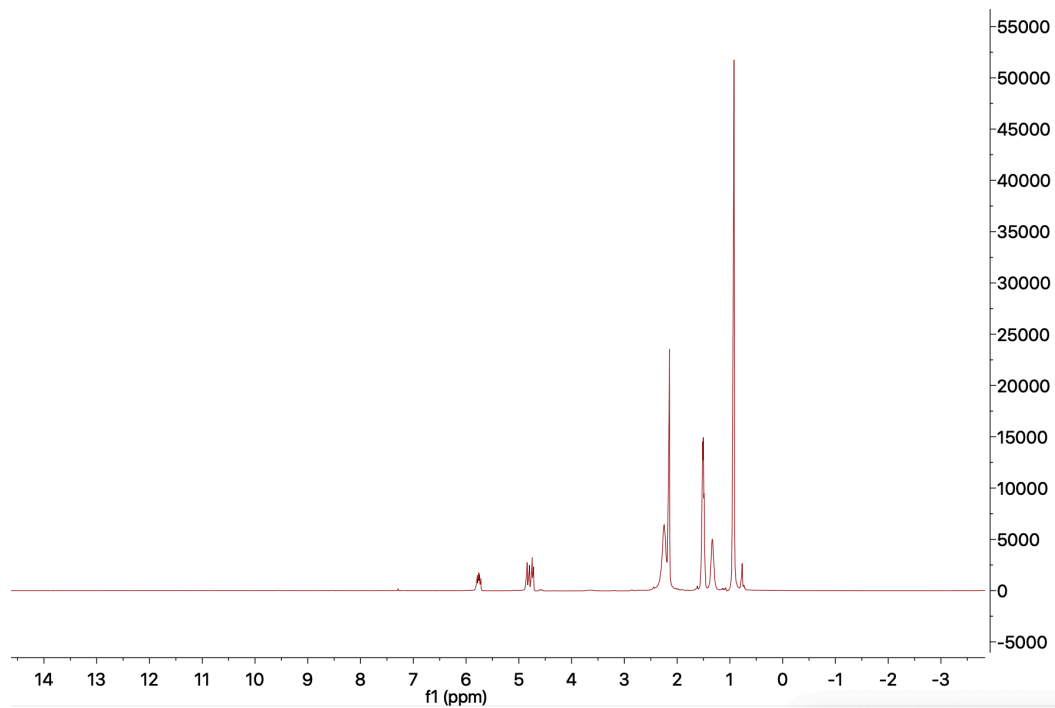


Figure A3.4 Scheme A2.1: Crude Reaction of N-Methylpiperidine (**26**) Showing No Conversion

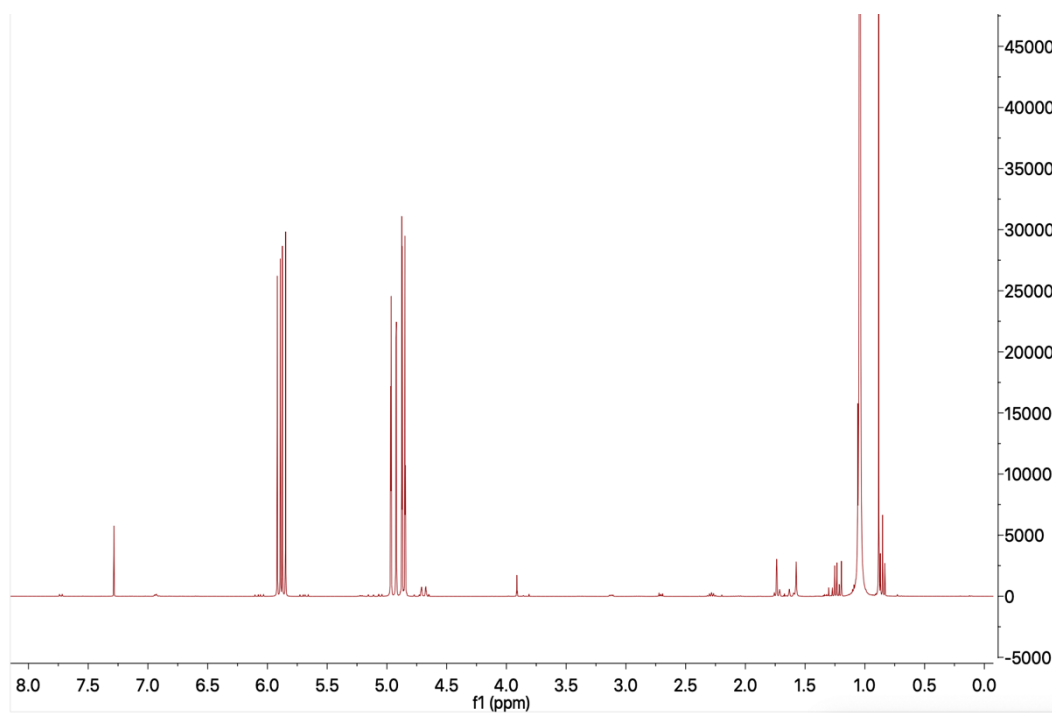


Figure A3.5 Scheme A2.2: Crude Reaction of 5-Methoxy-1-Indanone (**28**) Showing Decomposition

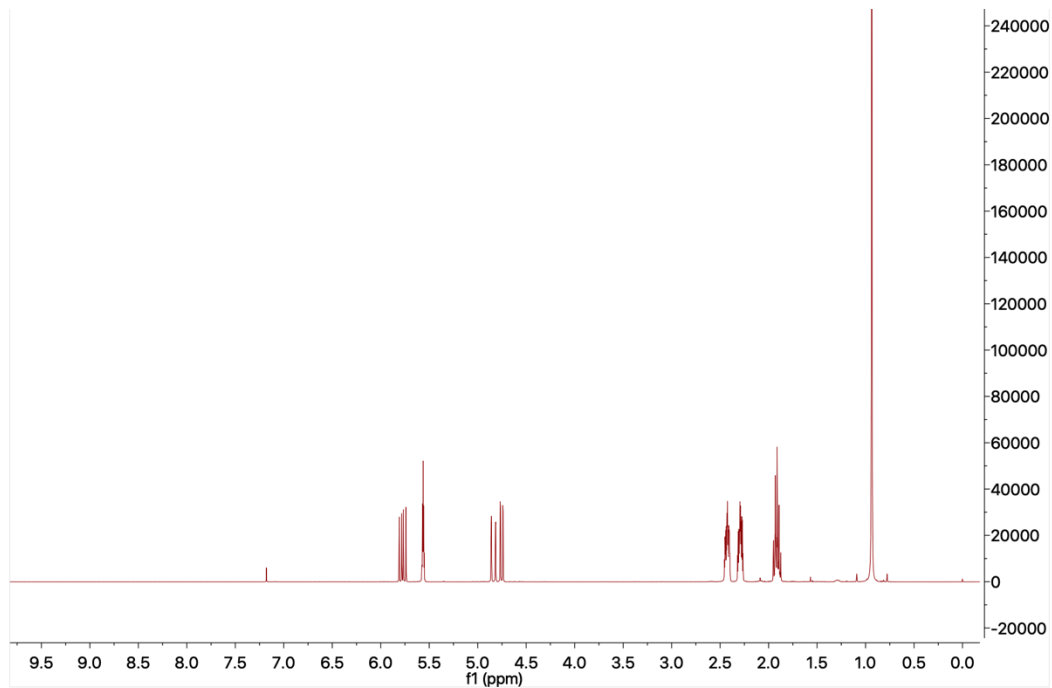


Figure A3.6 Scheme A2.3: Crude Reaction of 1-Chlorocyclopentene (**30**) Showing No Conversion

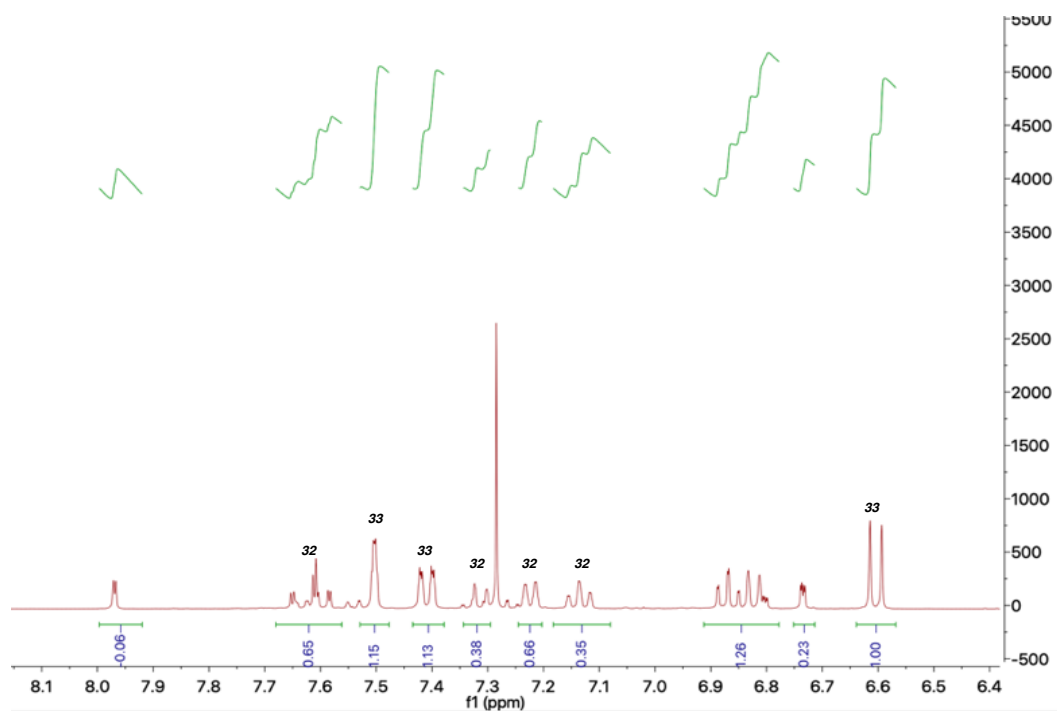


Figure A3.7 Table A2.2 Entry 1: Crude Reaction of 5-iodo-2,3-Dihydrobenzofuran (**32**)

Showing Conversion to 5-Iodobenzofuran (**33**)

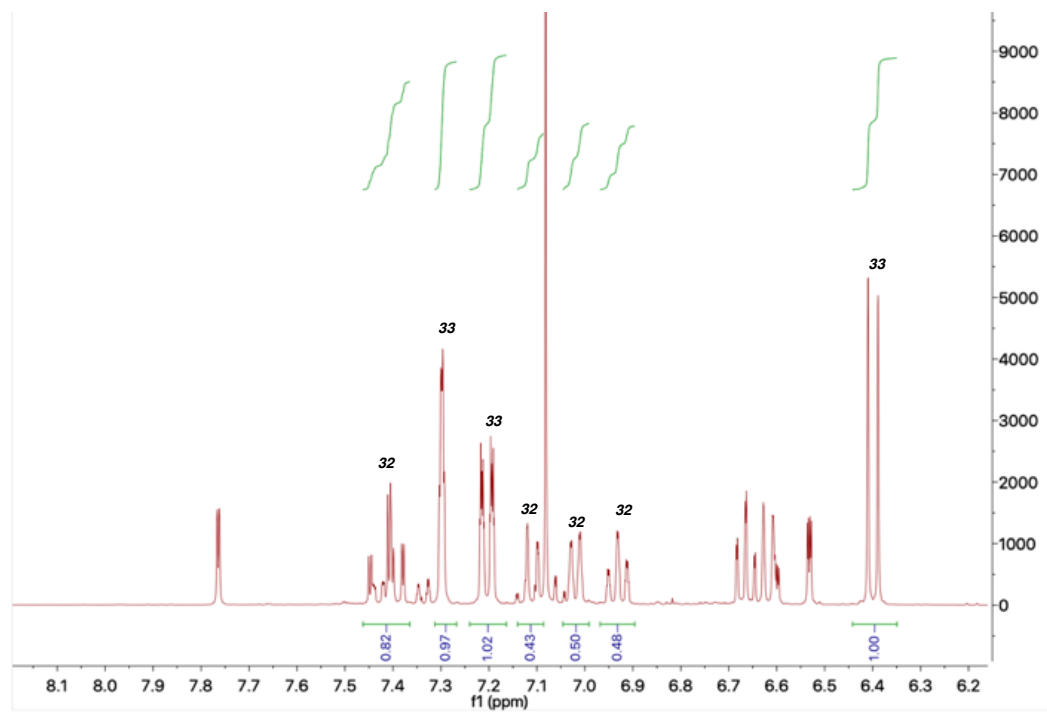


Figure A3.8 Table A2.2 Entry 2: Crude Reaction of 5-iodo-2,3-Dihydrobenzofuran (**32**)

Showing Conversion to 5-Iodobenzofuran (**33**)

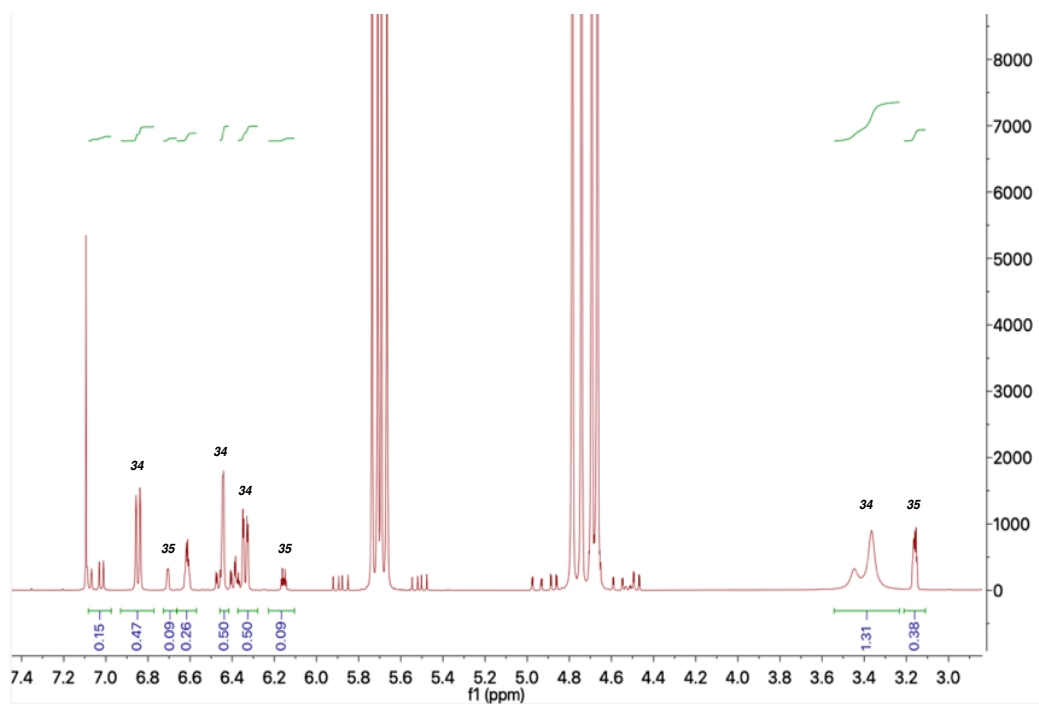


Figure A3.9 Scheme A2.4: Crude Reaction of 4-Aminoindan (**34**) Showing Low conversion to **35**

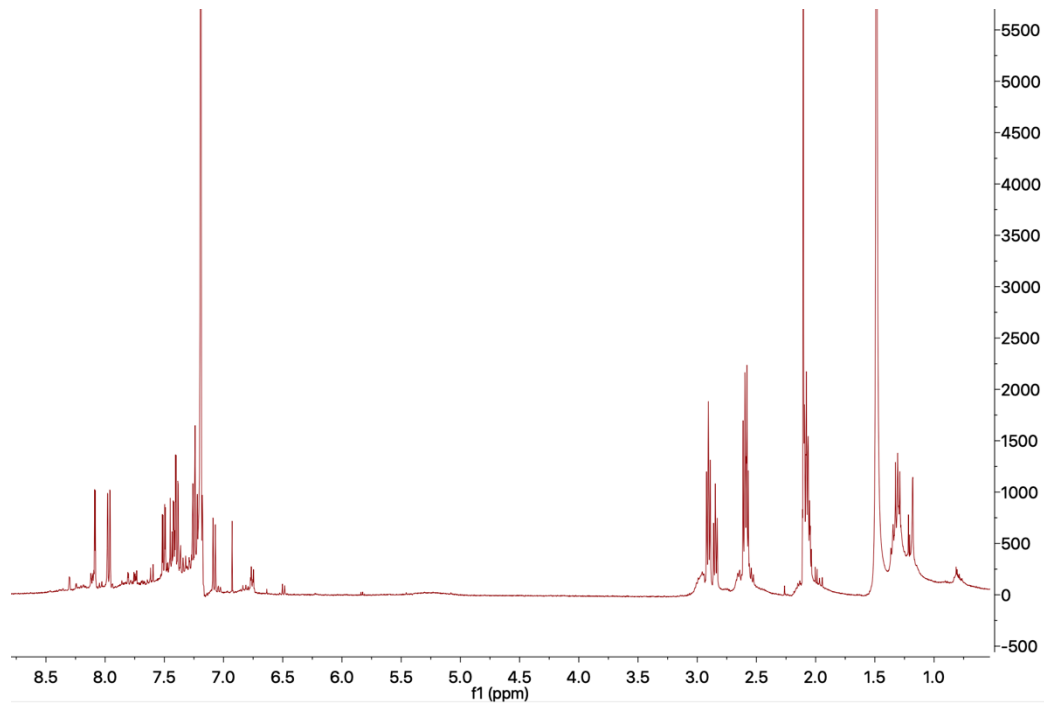


Figure A3.10 Scheme A2.5: Crude Reaction of 7-Bromo-1-Tetralone (**36**) Showing Debromination to 1-Tetralone (**18**) and Some Conversion to Naphthol (**19**)

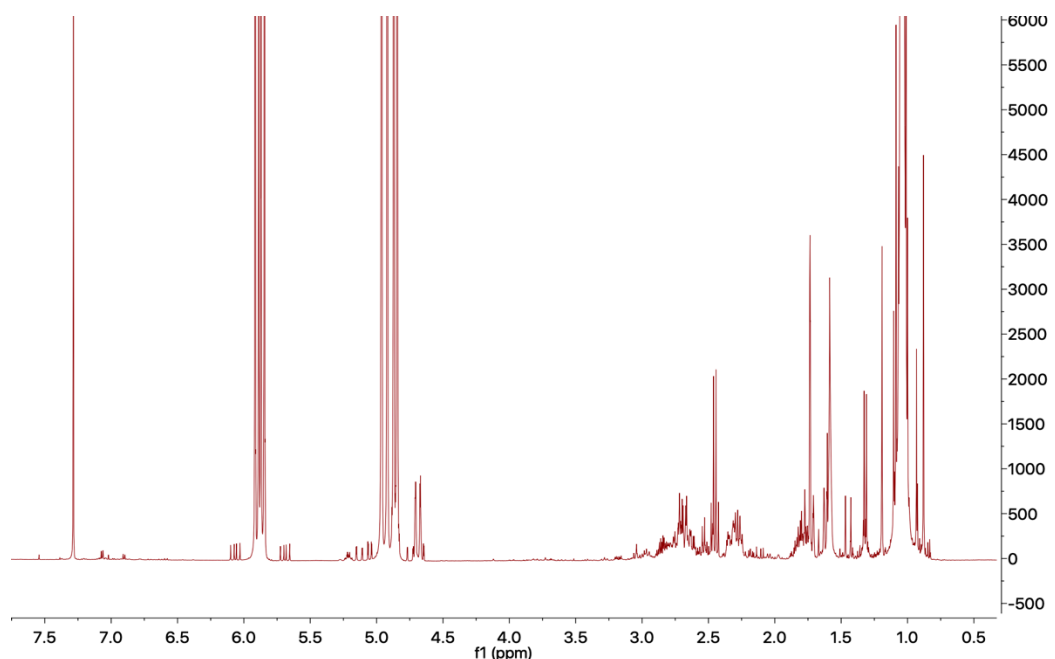


Figure A3.11 Scheme A2.7: Crude Reaction of Tetrahydrothiopyran-4-one (**38**) Showing No Conversion

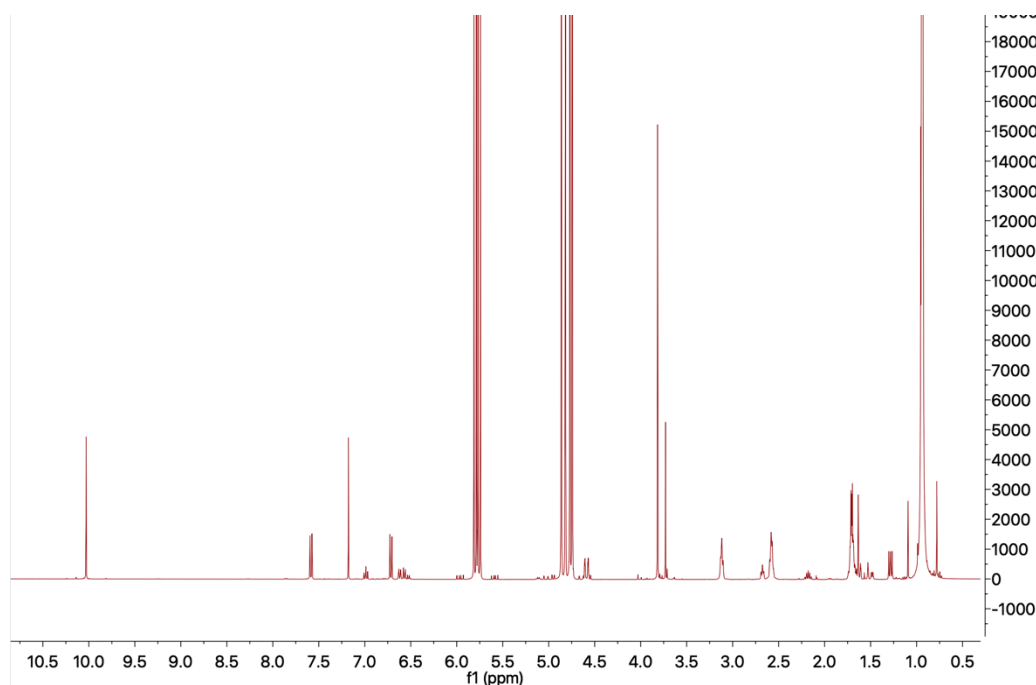


Figure A3.12 Scheme A2.8: Crude Reaction of 4-Methoxy-5,6,7,8-Tetrahydronaphthalene-1-Carbaldehyde (**40**) Showing No Conversion

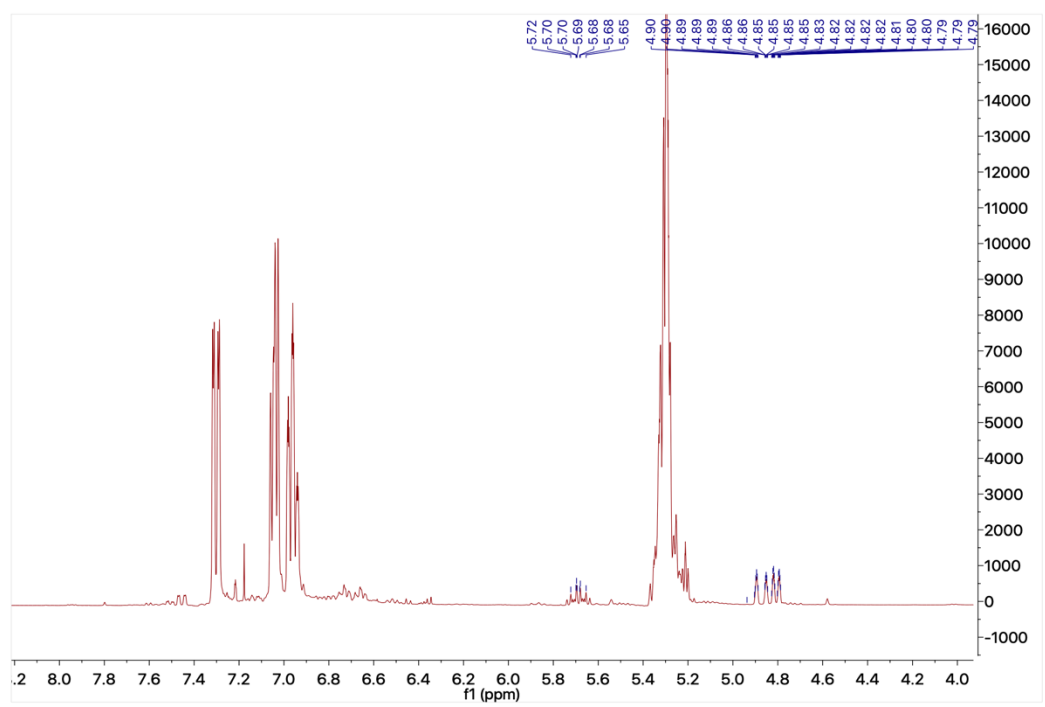


Figure A3.13 Scheme A2.9: Crude Reaction of 8-Fluoro-1-Benzosuberone (**42**)

Showing Possible Trace of **43** with Olefinic Peaks at 5.69 ppm and 4.83 ppm

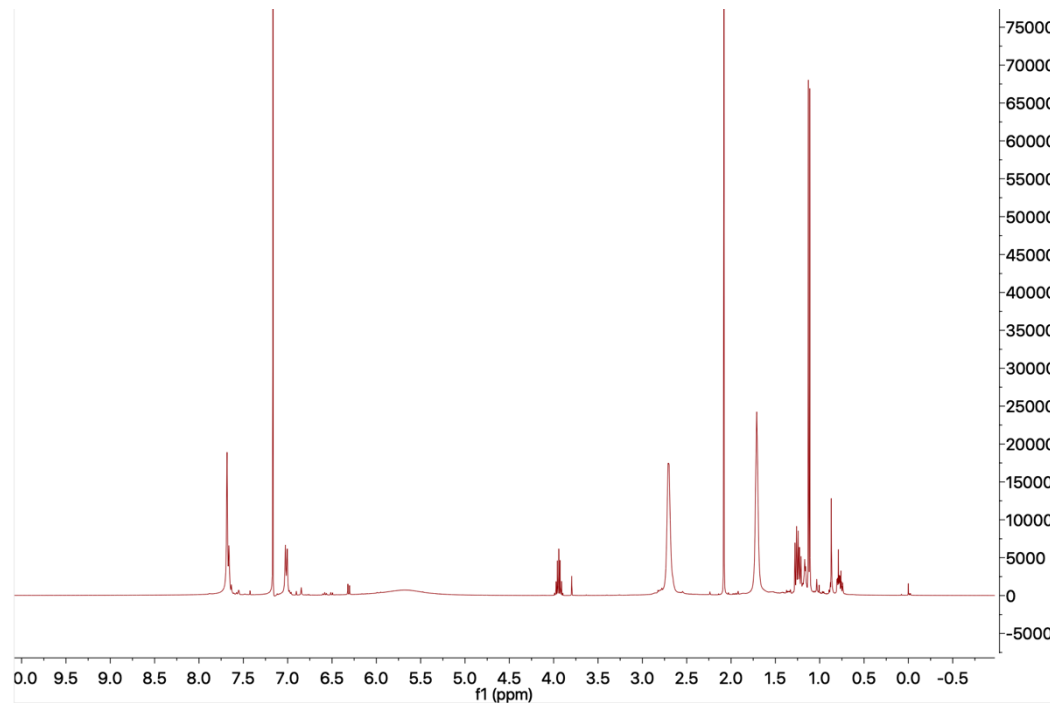


Figure A3.14 Scheme A2.10: Crude Reaction of 5,6,7,8-Tetrahydro-2-Naphthoic Acid

(**44**) Showing No Conversion

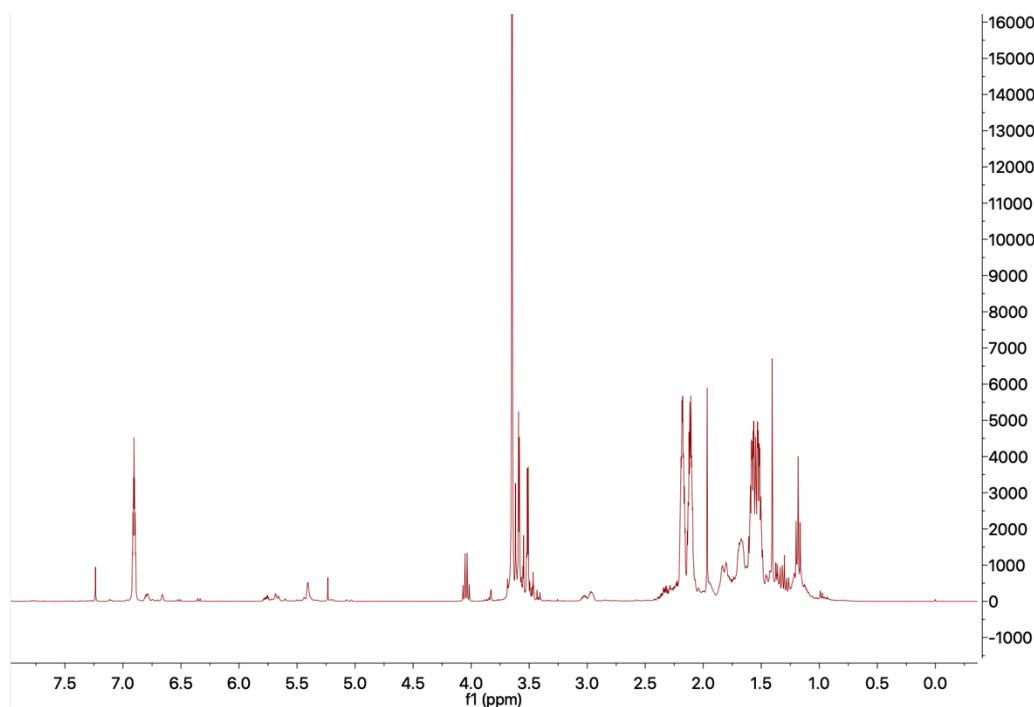


Figure A3.15 Scheme A2.11: Crude Reaction of 1-Acetylcyclohexene (**46**) Showing No Conversion

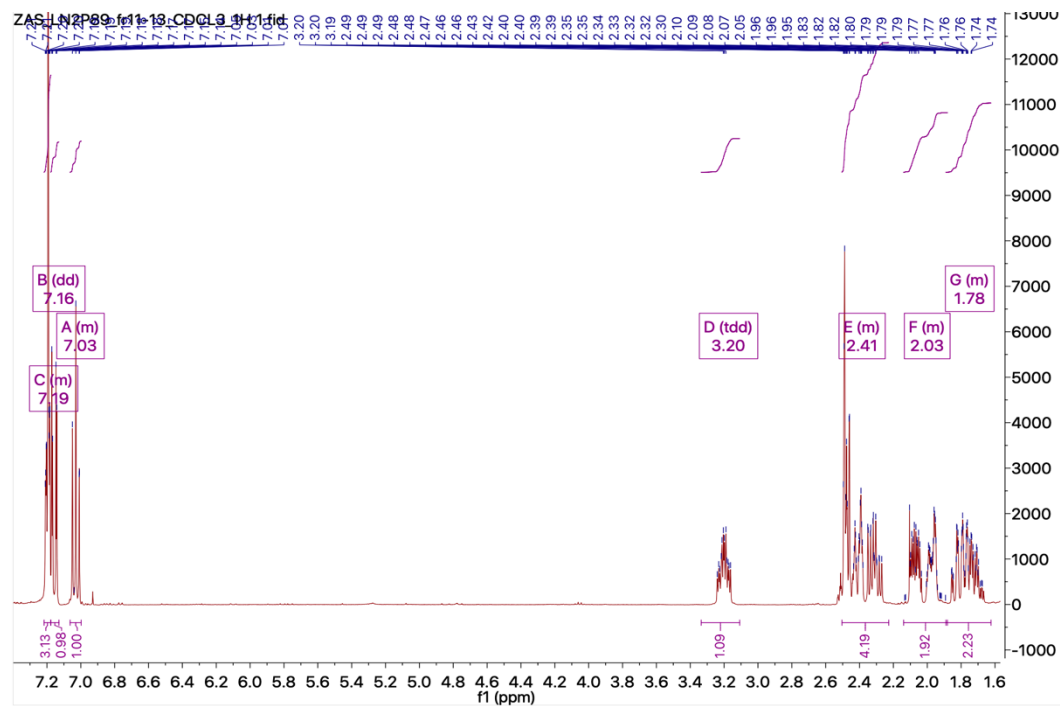


Figure A3.16 Scheme A2.12: ^1H NMR of Synthesized 3-(4-Bromo-2-Fluorophenyl)Cyclohexan-1-one (**50**)

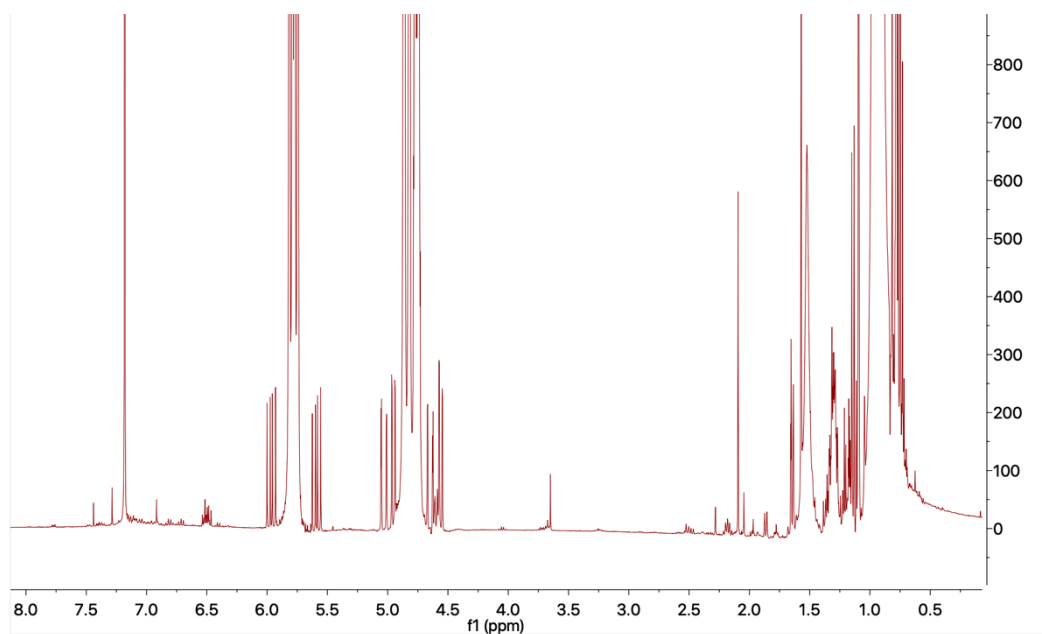


Figure A3.17 Scheme A2.13: Crude Reaction of 3-(4-Bromo-2-Fluorophenyl)Cyclohexan-1-one (**50**) Showing Disappearance of Diagnostic ¹H NMR Shift at 3.20 ppm

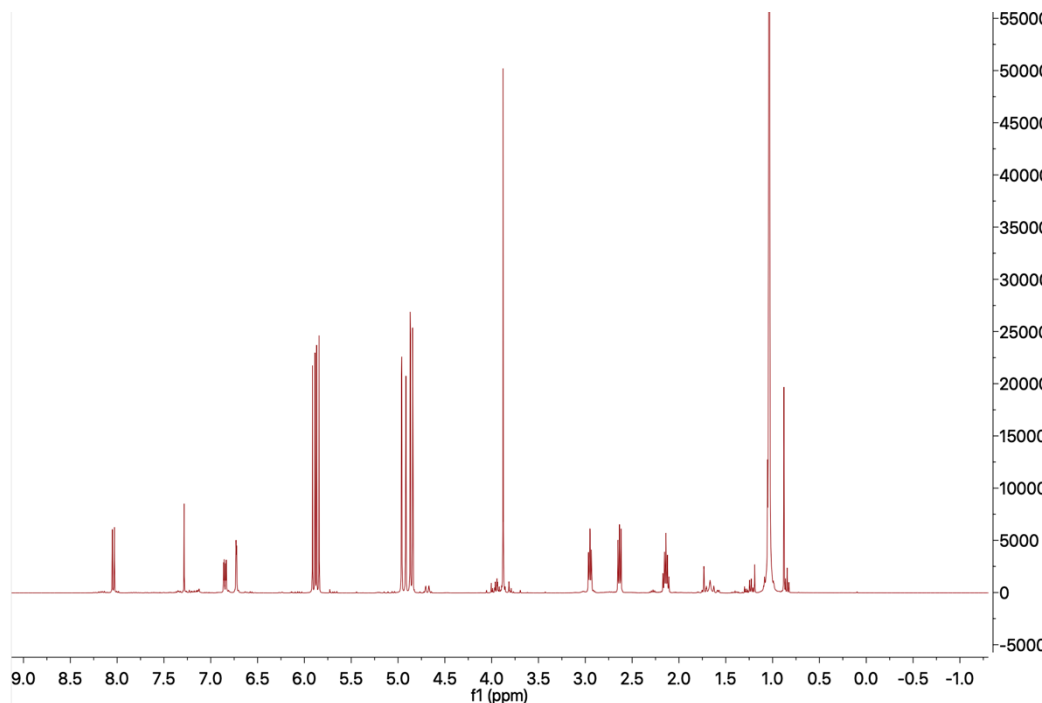


Figure A3.18 Scheme A2.14: Crude Reaction of 6-Methoxy-3,4-Dihydronaphthalen-1(2H)-one (**52**) Showing No Conversion

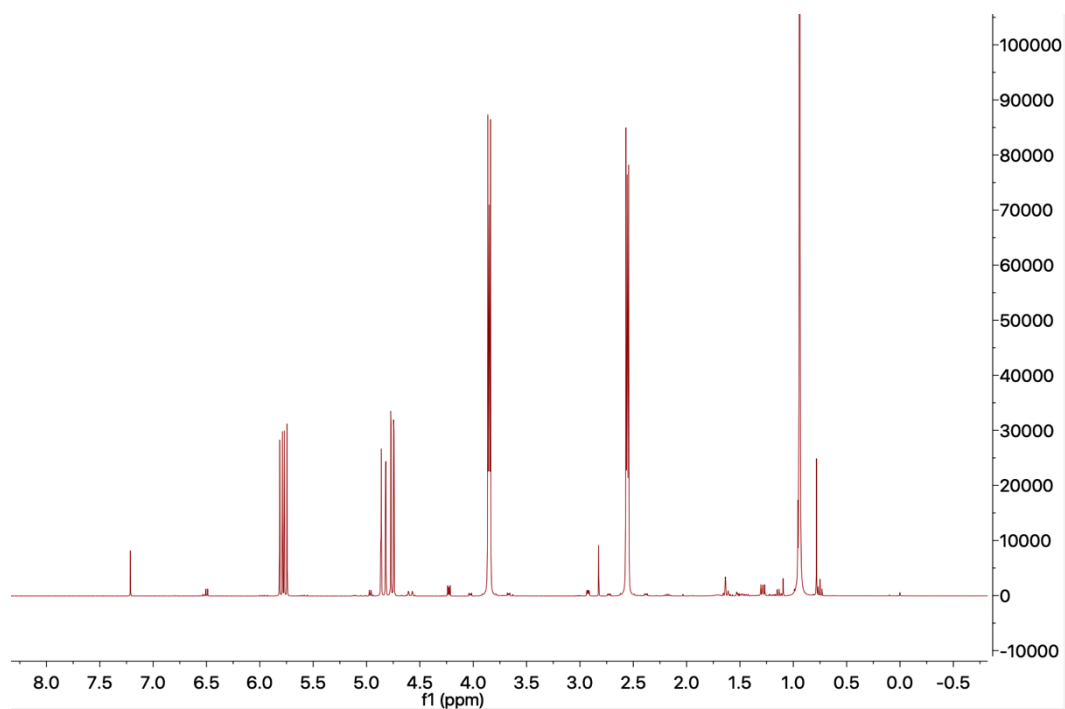


Figure A3.19 Scheme A2.15: Crude Reaction of 1,4-Thioxane (**54**) Showing Trace Conversion to **55**

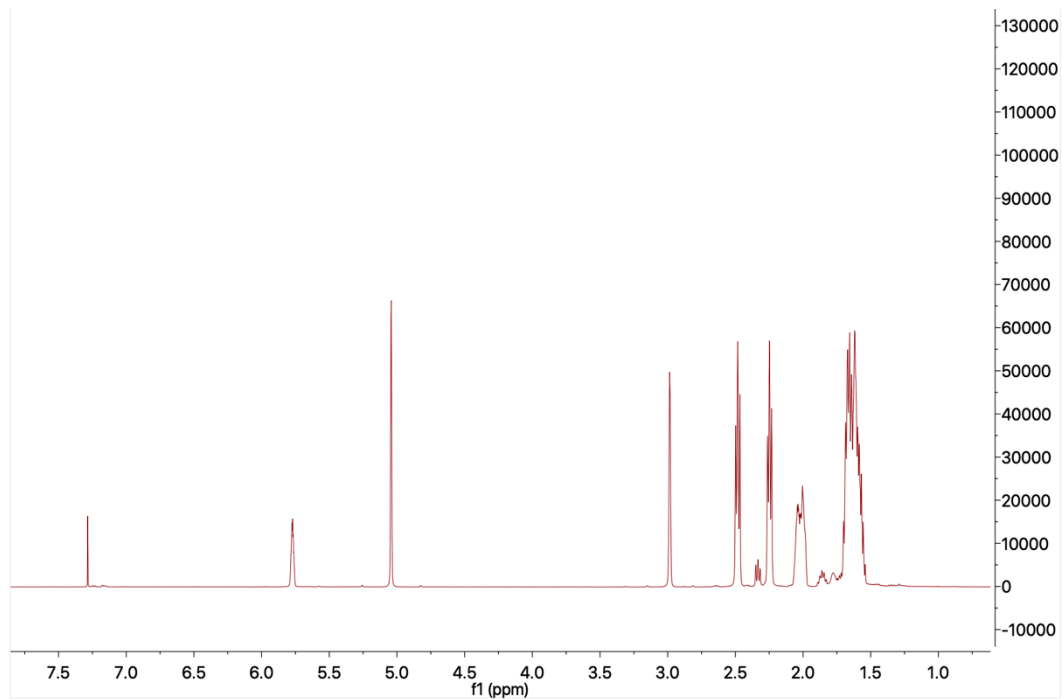


Figure A3.20 Scheme A2.16: Crude Reaction of 2-Cyclohexene-1-Acetonitrile (**56**) Showing Isomerization of **56**

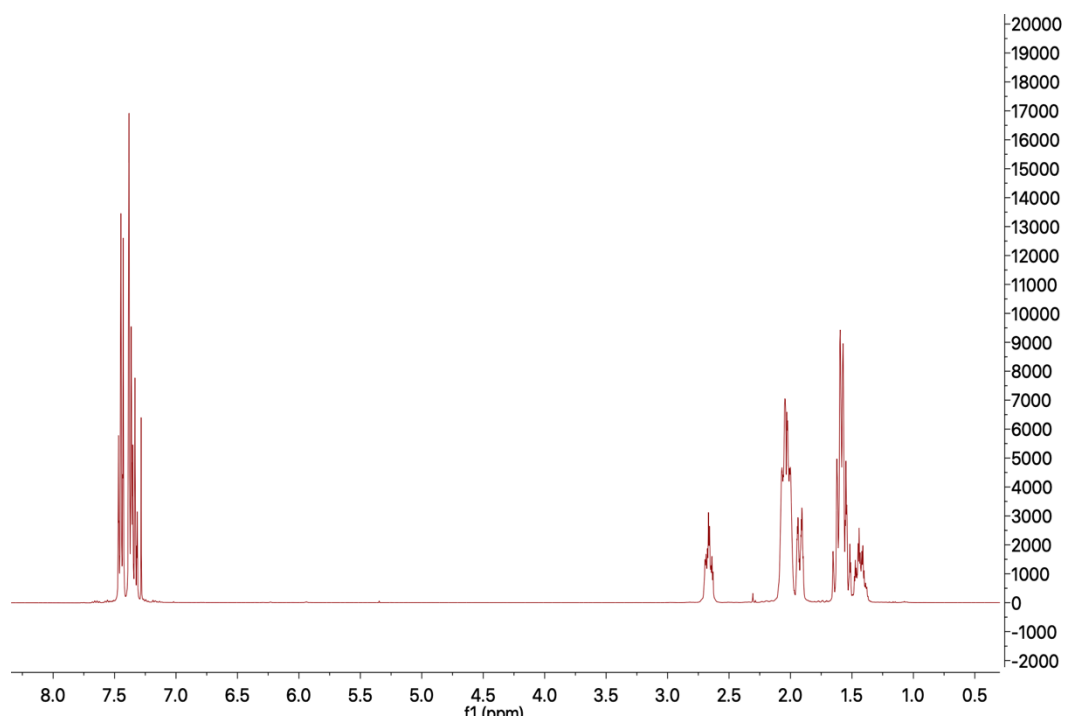


Figure A3.21 Scheme A2.17: Crude Reaction of Phenylcyclohexane (**58**) Showing No Conversion

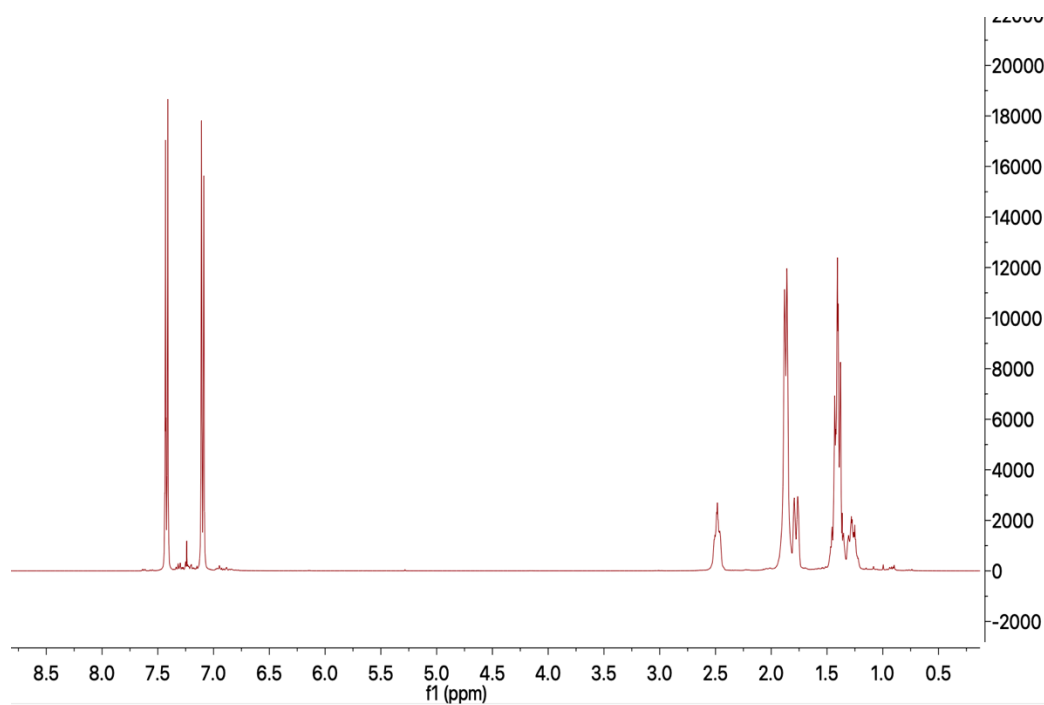


Figure A3.22 Scheme A2.18: Crude Reaction of 1-Bromo-4-Cyclohexylbenzene (**60**) Showing No Conversion

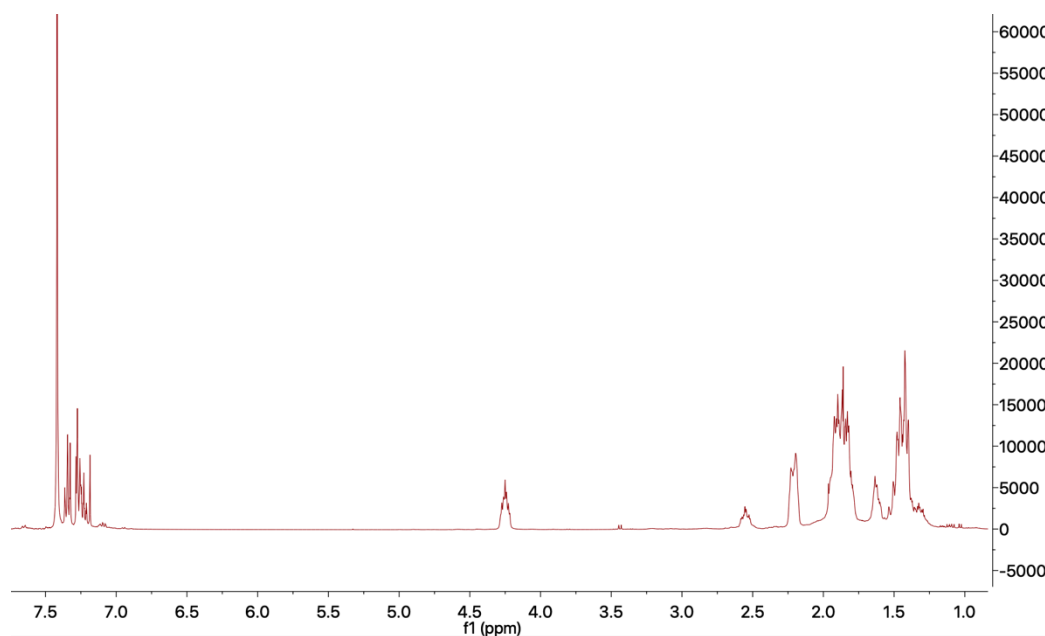


Figure A3.23 Scheme A2.19: Crude Reaction of 3-Bromocyclohexene (**62**) Showing Conversion to **64** and **58**

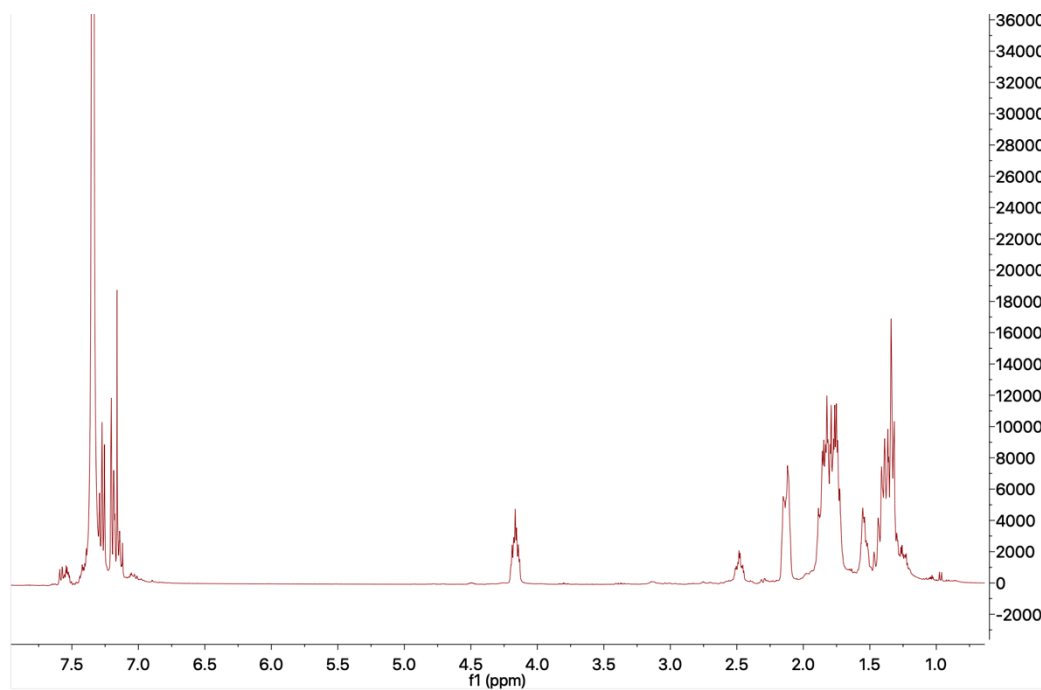


Figure A3.24 Scheme A2.20: Crude Reaction of 3-Bromocyclohexene (**62**) Showing Conversion to **64** and **58**

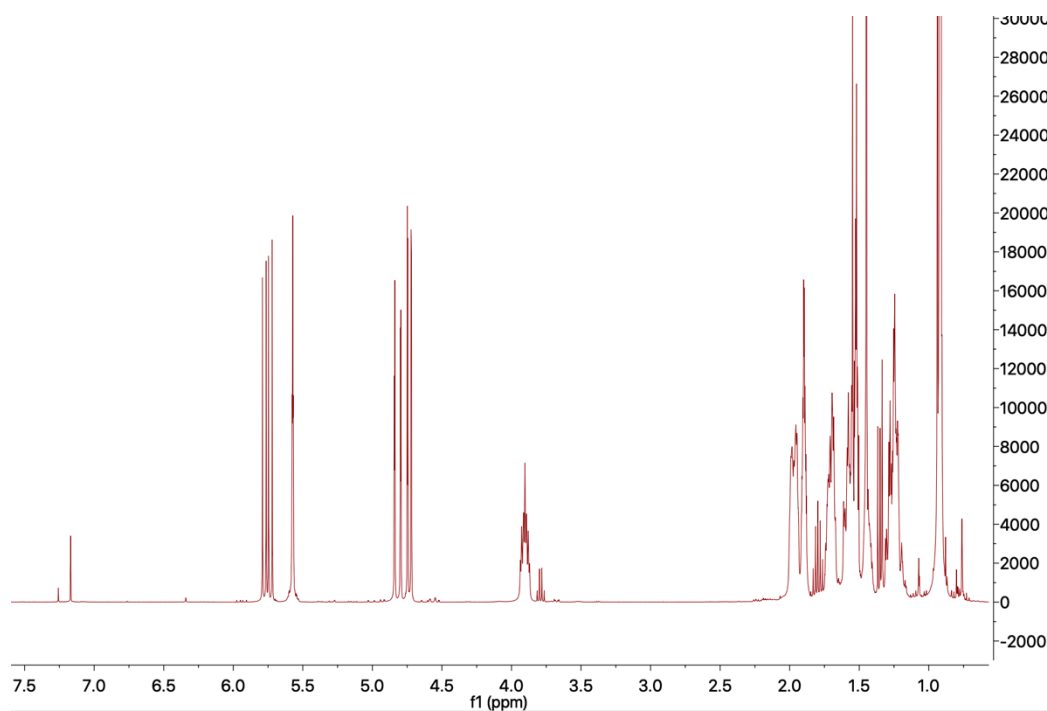


Figure A3.25 Schemes A2.21 and A2.22: Crude Reaction of Chlorocyclohexane (**65**)
Decomposition to 1-Cyclohexene, Cyclohexane, and Benzene

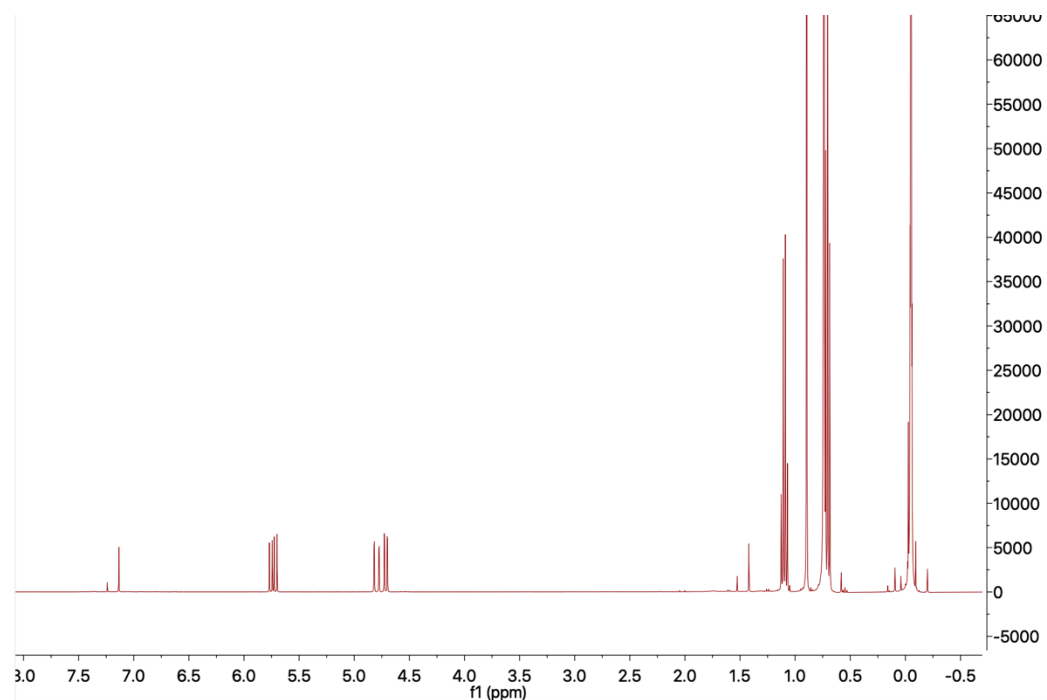


Figure A3.26 Schemes A2.23: 1-(Trimethylsiloxy)cyclohexene (**67**) Showing No
Conversion

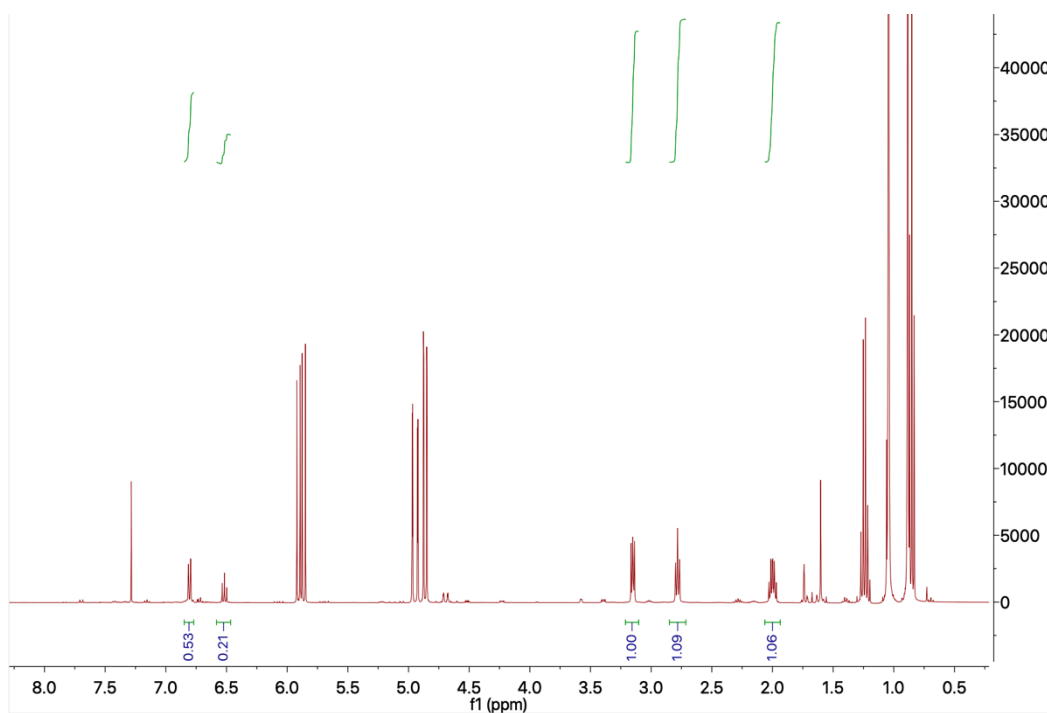


Figure A3.27 Scheme A2.24: Crude Reaction of Unreacted Julolidine (**69**) and No Conversion

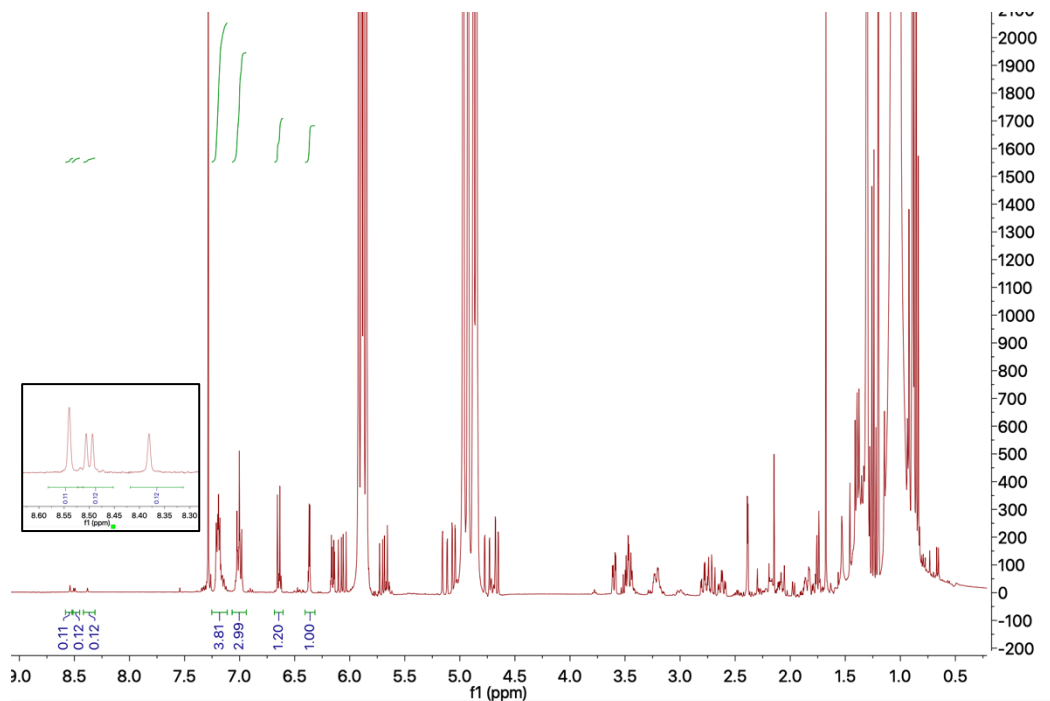


Figure A3.28 Scheme A2.25: Crude Reaction of Paroxetine (**71**) Showing Trace Conversion to **72**

APPENDIX 4

PROGRESS TOWARD THE SYNTHESIS OF A NOVEL ASYMMETRIC NHC-PHOSPHONITE HYBRID PINCER LIGAND

A4.1 INTRODUCTION

Most of the early examples of studied complexes showed poor thermal stability at the temperatures needed to achieve reasonable reaction rates. Pincer ligated complexes, however, were found to be thermally stable at these elevated temperatures, making them useful for this transformation.¹ These complexes are stable due to the tridentate coordination of ligands with the metal center. In 1996, Jensen and co-workers reported the first thermally stable pincer ligated complex, (*t*-Bu⁴PCP)-Ir **c3**.²⁻⁴ Since then, variations of complex **c3** have been reported with different aryl backbones, various linkers, and ligating groups (Figure A4.1).⁵⁻⁶

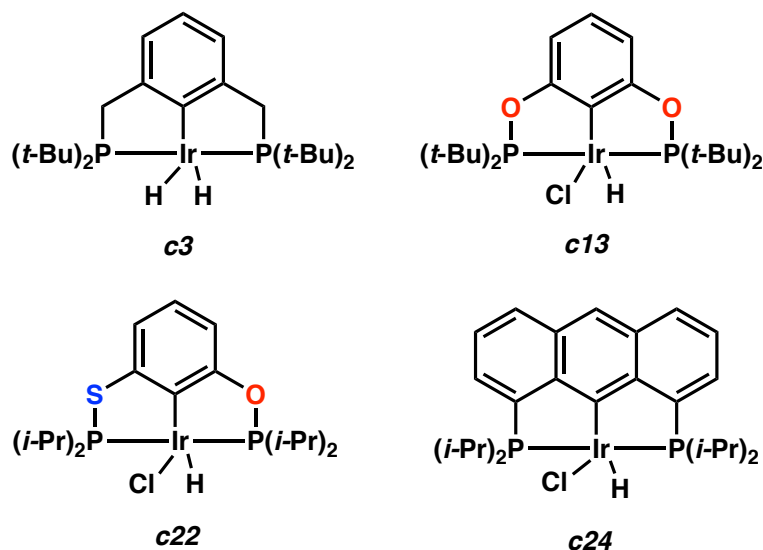
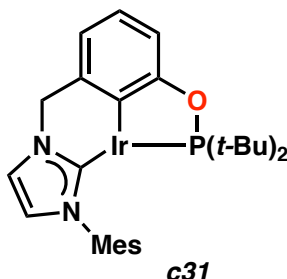


Figure A4.1 Various Reported Ir Pincer Ligated Complexes

That being said, it was found that varying the electronics around the Ir metal center is not as effective as varying the geometry and steric effects in improving catalytic activity.⁷ We have also demonstrated the different reactivities of $(t\text{-Bu}^4\text{POCOP})\text{-Ir}$ **c13**, $(i\text{-Pr}^4\text{PSCOP})\text{-Ir}$ **c22**, and $(i\text{-Pr}^4\text{anthraphos})\text{-Ir}$ **c24** when dehydrogenating heterocyclic substrates and the varying tolerance to different functionalities. The results we obtained indicated varying steric hinderance around the Ir metal center contributed a major role in the observed variant reactivities.

Hence, we were interested to synthesize a novel asymmetric NHC-phosphinite ligand and metalate it generating complex $(t\text{-Bu}^2\text{Mes-NHCCOP})\text{-Ir}$ **c31** (Figure A4.2). We hypothesize this complex could potentially increase Ir catalytic activity in dehydrogenating heterocyclic substrates to functionalized arenes

and unsubstituted cyclic alkanes to aromatics due to the increased steric effects and the geometry around the metal center from the NHC.



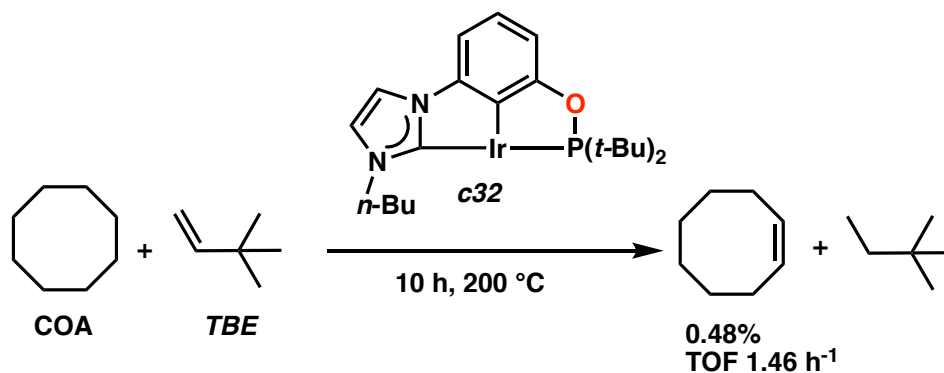
proposed novel hybrid NHC-phosphonite complex

Figure A4.2 Proposed Novel Asymmetric NHC-Phosphonite Complex
(*t*-Bu₂Mes-NHCCOP)-Ir **c31**

A4.2 RELATED LITERATURE

Braunstein and co-workers reported the first hybrid imidazolium-phosphinite (*t*-Bu₂*n*-Bu-NHCCOP)-Ir **c32** complex in 2013 and employed it as a dehydrogenation catalyst when transfer dehydrogenating the **COA/TBE** system in a preliminary investigation (Scheme A4.1).⁸ They found that complex **c32** exhibited low catalytic activity and only 0.48% of cyclooctene was obtained.

Scheme A4.1 Reported NHC-Phosphonite Complex (*t*-Bu₂*n*-Bu-NHCCOP)-Ir **c32** by Braunstein



Braunstein 2013

Although Braunstein and co-workers reported low catalytic activity for their catalyst, they explained that the low insolubility of complex **c32** in neat alkanes may be a factor contributing to its poor performance in dehydrogenating COA. However, we believe our proposed complex **c31** could be promising in this context for three reasons. First, Braunstein noted that switching the NHC side group from a methyl to an *n*-Bu increased catalytic activity. In our proposed complex **c31**, we propose to use a mesityl (Mes) NHC which would enhance solubility in neat alkanes. Second, it was noted that the stronger σ -donor properties of the NHC ligands should facilitate the C-H oxidative addition step of the alkane while disfavoring the reductive elimination of the product. We anticipate that changing the geometry around the Ir metal center and increasing the bulk on the NHC ligand from the Mes group could potentially enhance its catalytic activity by making the reductive elimination of the product more favorable relatively. Third, NHC ligands generally exhibit higher thermal stability than their phosphine analogues, hence higher temperatures could be investigated in transfer dehydrogenation systems using our proposed complex **c31**.⁹

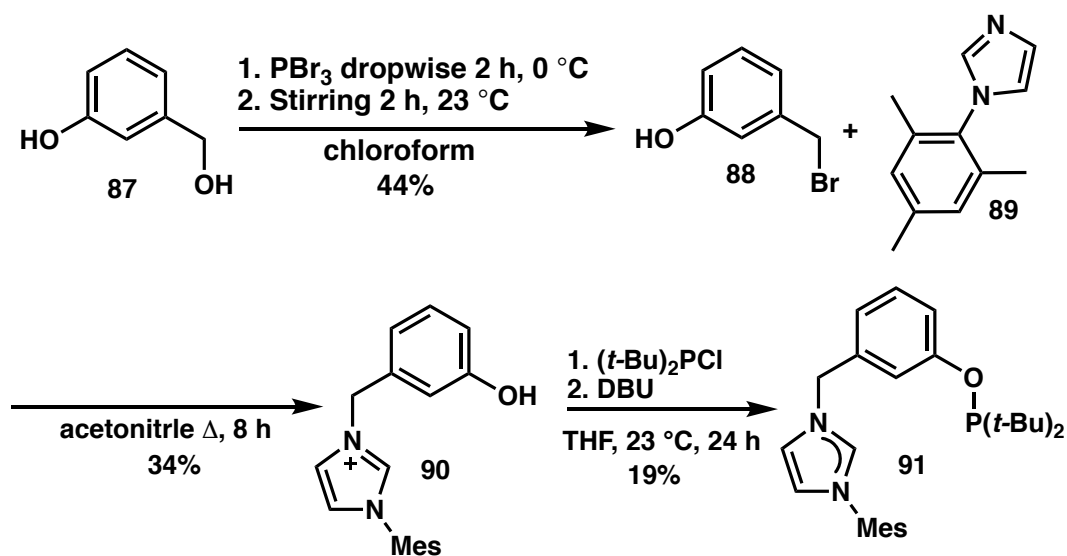
For these reasons we believe our proposed complex **c31** could be a good candidate for catalyzing dehydrogenation reactions

A4.3 Synthesis of *t*-Bu²Mes-NHCCOP Ligand **91**

Modifying the Braunstein and Heinekey published procedures, we first synthesized 3-hydroxybenzylbromide (**88**) by treating 3-hydroxybenzenealcohol (**87**) with PBr₃ according to Voegtle and co-workers procedure (Scheme A4.2).^{8, 10-11} Then we treated **88** with an equivalent of 1-mesitylimidazole (**89**) affording 1-mesityl-3-(3-hydroxybenzyl) imidazole salt (**90**). The diagnostic ¹H NMR shift is the NCHN observed at 9.60 ppm with purity above 98%. The purified product was also analyzed by LC/MS and the exact mass (293.1 g/mol) was observed. The molecular weight was also confirmed with HRMS. We then treated **90** with (*t*-Bu)₂PCl and DBU which successfully afforded the desired novel imidazolium-phosphinite hybrid ligand **91**. However, attempts to isolate **91** and purify it were challenging due to the nature of insolubility of the ligand in organic solvents and lack of crystallinity of the ligand. The diagnostic phosphinite peak was observed at 155.24 ppm in the ³¹P NMR spectrum.

Scheme A4.2 Synthesis of Novel Asymmetric NHC-Phosphonite Complex

(*t*-Bu₂Mes-NHCCOP)-Ir **c32**

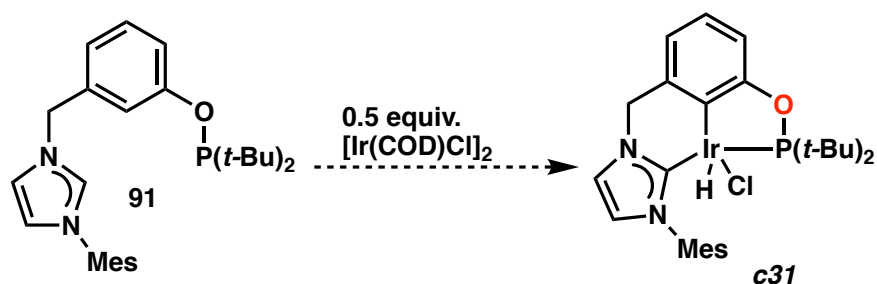


We will investigate several methods for isolating **91** including column chromatography by varying polar organic solvents ratios and we will investigate recrystallizing the ligand to purify it by the solvent diffusion method.

A4.4 SUMMARY AND FUTURE WORK

Varying the steric effects around Ir pincer ligated complexes have been shown to be effective in changing its catalytic activity when employed as dehydrogenation catalysts. NHC ligands have strong σ -donor properties and could facilitate the C–H oxidative addition step, which is typically rate determining in dehydrogenation mechanisms catalyzed by Ir pincer ligated complexes. We proposed a novel asymmetric NHC-phosphonite ligand that could be a good candidate for catalyzing dehydrogenation reactions. We successfully synthesized the

novel ligand; however, isolation and purification were challenging. Once the ligand is purified and isolated, we envision metalation with half an equivalent $[\text{Ir}(\text{COD})\text{Cl}]_2$ generating complex **c31** (Scheme A4.3). Upon successful synthesis of the desired Ir complex, we will then investigate its dehydrogenation catalytic activity on the **COA/TBE** system to evaluate its performance. Then, we will expand the scope to include a wide array of substrates.



A4.5 NOTES AND REFERENCES

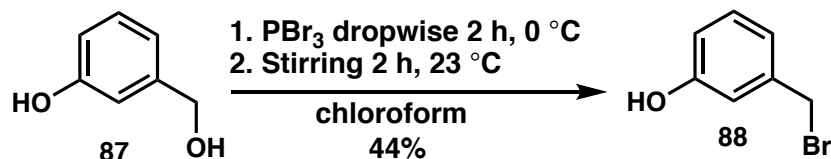
1. M. Jensen, C., *Chem. Commun.* **1999**, (24), 2443-2449.
2. Gupta, M.; C. Kaska, W.; M. Jensen, C., *Chem. Commun.* **1997**, (5), 461-462.
3. Gupta, M.; Hagen, C.; Kaska, W. C.; Cramer, R. E.; Jensen, C. M., *Journal of the American Chemical Society* **1997**, 119 (4), 840-841.
4. Gupta, M.; Hagen, C.; Flesher, R. J.; Kaska, W. C.; Jensen, C. M., *Chem. Commun.* **1996**, (17), 2083-2084.
5. Akshai Kumar, A. S. G. In *The Privileged Pincer-Metal Platform: Coordination Chemistry & Applications*, Gerard Van Koten, R. A. G., Ed. Springer, Cham: Cham, 2015; Vol. 54, pp 307-334.
6. Kumar, A.; Bhatti, T. M.; Goldman, A. S., *Chemical Reviews* **2017**, 117 (19), 12357-12384.
7. Kundu, S.; Choliy, Y.; Zhuo, G.; Ahuja, R.; Emge, T. J.; Warmuth, R.; Brookhart, M.; Krogh-Jespersen, K.; Goldman, A. S., *Organometallics* **2009**, 28 (18), 5432-5444.
8. Liu, X.; Braunstein, P., *Inorg. Chem.* **2013**, 52 (13), 7367-7379.
9. Jacobsen, H.; Correa, A.; Poater, A.; Costabile, C.; Cavallo, L., *Coord. Chem. Rev.* **2009**, 253 (5), 687-703.
10. Przybilla, K. J.; Vögtle, F., *Chem. Ber.* **1989**, 122 (2), 347-355.
11. Schultz, K. M.; Goldberg, K. I.; Gusev, D. G.; Heinekey, D. M., *Organometallics* **2011**, 30 (6), 1429-1437.

A4.6 EXPERIMENTAL SECTION AND SPECTRA

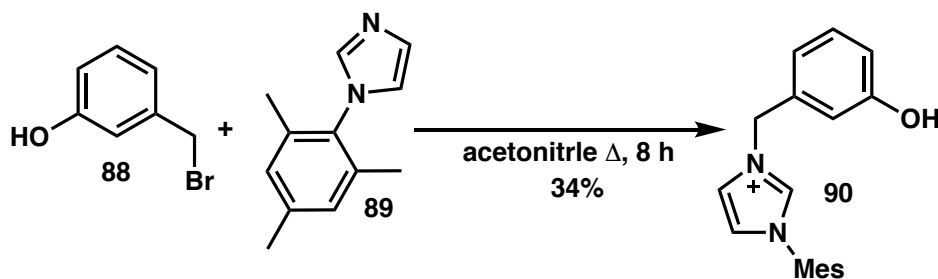
A4.6.1 Materials and Methods

Unless noted in the specific procedure, all liquid reagents were distilled and reactions were performed in an oven-dried glassware under an argon atmosphere . All dehydrogenation reactions were degassed by freeze-pump-thaw x 5 cycles and were carried out under air-free conditions in dry glassware. ^1H NMR and ^{31}P NMR spectra were recorded on Bruker AV III HD 400 MHz spectrometer equipped with a Prodigy liquid nitrogen temperature cryoprobe, and are reported in terms of chemical shift relative to residual CHCl_3 (δ 7.26). LC/MS was acquired with an Agilent 6140 quadrupole LC/MS with an Agilent Eclipse Plus C_{18} RHHD 1.8 μm column (2.1x 50, 11,072 plates). The method used was a standard 10-minute gradient with 5% to 95% acetonitrile to water (0.1% acetic acid) ratio. HRMS were acquired using an Agilent 6200 Series TOF with a JEOL JMS-600H in fast atom bombardment (FAB+).

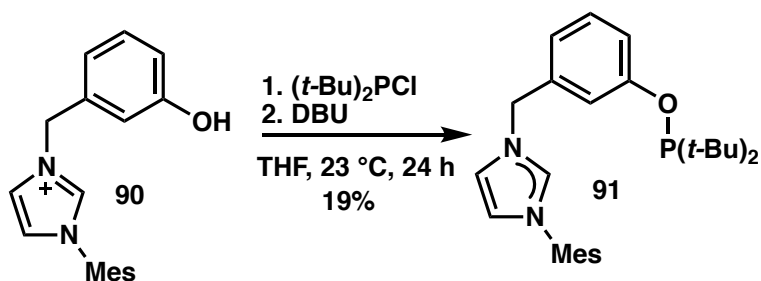
A4.6.2 General Procedure of *t*-Bu²Mes-NHCCOP Ligand 91 Synthesis



Synthesis of 3-(bromomethyl)phenol (88). 10.172 g of 3-hydroxybenzyl alcohol was suspended in 50 mL absolute chloroform. The suspension was cooled to 0 °C and then 4.0 mL of PBr₃ was added dropwise over a period of 2 h while stirring under argon. The reaction was subsequently stirred for another 2 h and then poured onto ice. The phases were separated and the organic phase was extracted twice with chloroform. The extract was dried in a rotavap obtaining a yellow oil similar to literature reports. However, upon ³¹P NMR it was discovered that phosphine impurities existed. Further purification with silica gel column chromatography using 25% Et₂O in hexanes was required to obtain a white product with a cotton-like texture. The product is stable and can be refrigerated for a long time.³ R_f = 0.4 (25% Et₂O in hexanes). ¹H NMR (400 MHz, Chloroform-*d*) δ 7.24 (t, *J* = 7.9 Hz, 1H, Ar-H), 6.99 (dd, *J* = 7.7, 1.2 Hz, 1H, Ar-H), 6.90 (dd, *J* = 2.6, 1.7 Hz, 1H, Ar-H), 6.79 (ddd, *J* = 8.1, 2.6, 0.9 Hz, 1H, Ar-H), 4.75 (s, br., 1H, OH), 4.46 (s, 2H, CH₂). ¹³C NMR (101 MHz, Chloroform-*d*) δ 155.62 (s, 1C, Ar-C-O), 139.44 (s, 1C, Ar-C-C), 130.08 (s, 1C, Ar-C), 121.51 (s, 1C, Ar-C), 115.91 (s, 1C, Ar-C), 115.53 (s, 1C, Ar-C), 33.12 (s, 1C, CH₂).



Synthesis of 3-(3-hydroxybenzyl)-1-mesityl-1H-imidazol-3-ium Salt 90. This ligand precursor was prepared by a modification of the procedure reported by Braunstein and Heinekey.^{5,6} 1.041 g of 3-(bromomethyl)phenol and 1.036 g of 1-mesitylimidazole were refluxed in 45 mL acetonitrile overnight. The solution was then dried under vacuum. The product was then purified in a silica gel column plug with 10% MeOH in DCM yielding the pure product as white solid. R_f = 0.6 (10% MeOH in DCM). ^1H NMR (400 MHz, $\text{DMSO}-d_6$) δ 9.69 (s, 1H, OH), 9.60 (t, J = 1.6 Hz, 1H, im-H), 8.07 (t, J = 1.8 Hz, 1H, im-H), 7.97 (t, J = 1.8 Hz, 1H, im-H), 7.29 – 7.22 (m, 1H, Ar-H), 7.16 (s, 2H, Mes-H), 6.85 – 6.76 (m, 3H, Ar-H), 5.45 (s, 2H, CH_2), 2.34 (s, 3H, p -Me-Mes), 2.02 (s, 6H, 2x o -Me-Mes). ^{13}C NMR (101 MHz, $\text{DMSO}-d_6$) δ 158.32 (1C, C-OH), 140.76 (1C, Mes-C), 138.12 (1C, NCN), 136.54 (1C, Ar-C), 134.69 (2C, Mes), 131.60 (1C, Ar-H), 130.65 (1C, Ar-H), 129.73 (2C, Mes-C), 124.75 (1C, Mes-C-N), 123.83 (1C, im-C), 118.67 (1C, im-C), 116.11 (1C, Ar-C), 115.11 (1C, Ar-C), 52.77 (1C, CH_2), 21.07 (1C, p -Me-Mes), 17.38 (2C, o -Me-Mes). LC/MS MW = 293.1 g/mol. HRMS (FAB+) m/z calc'd for $\text{C}_{19}\text{H}_{21}\text{N}_2\text{O}$ $[\text{M}+\text{H}]^+$: 293.1654, found 293.1655.



Synthesis of 3-(3-((di-tert-butylphosphanyl)oxy)benzyl)-1-mesityl-1H-imidazol-3-ium Ligand 91. 0.075 g of 3-(3-hydroxybenzyl)-1-mesityl-1H-imidazol-3-ium **23a** was dissolved in 15 mL THF. 51 mL $(t\text{-Bu})_2\text{PCl}$ was then added *via* a syringe slowly to the THF solution. 0.5 mL DBU (excess) was then added to the reaction mixture and it was stirred at room temperature for 21 h. The solution was dried under vacuum and then washed with Et_2O x 2. The desired phosphonite peak was observed at 155.24 ppm, however the product shows that it is 70% pure based on ^1H NMR. Purification of the product is still under progress. ^{31}P NMR (162 MHz, Benzene- d_6) δ 155.24.

A4.6.3 NMR Spectra

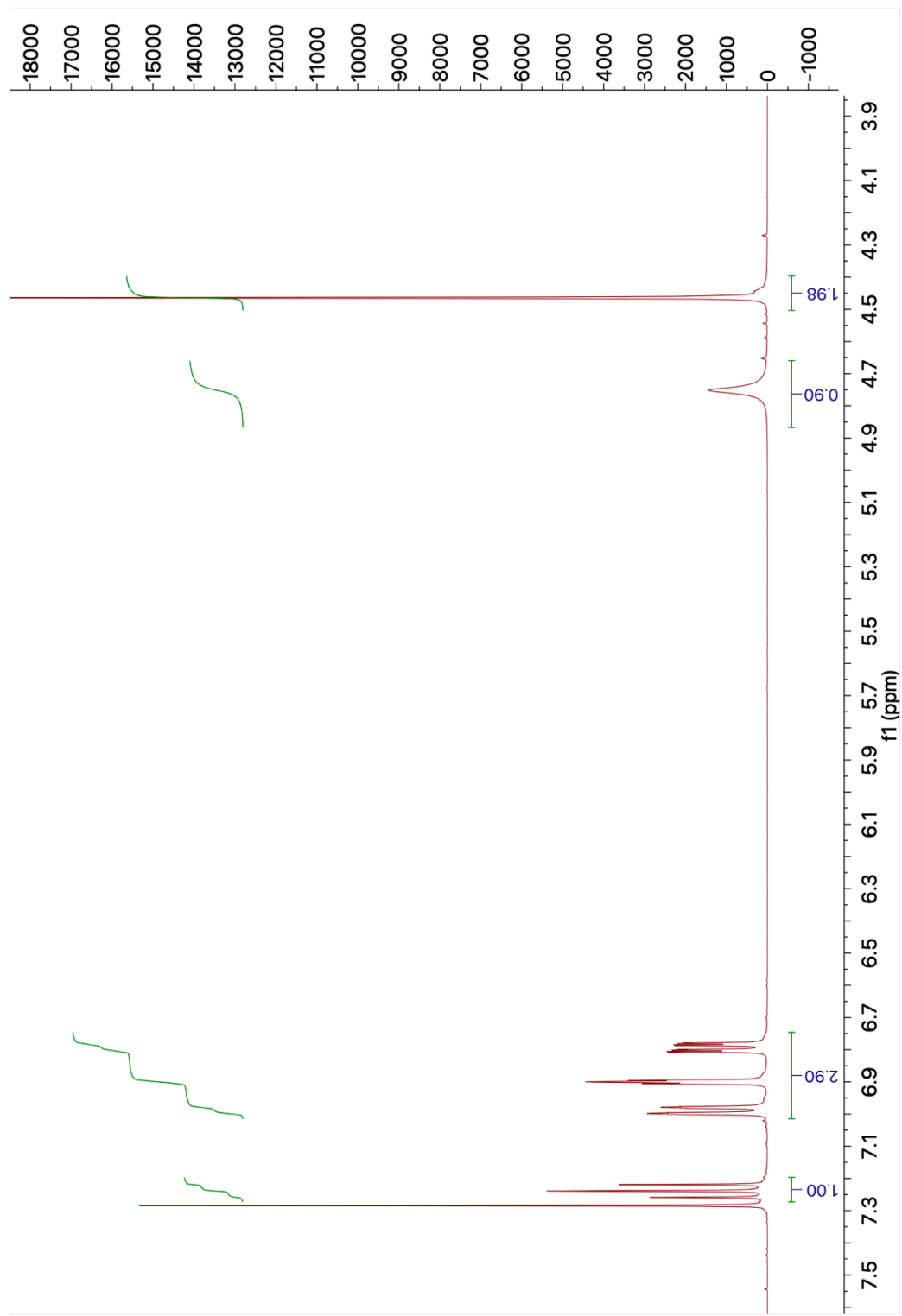


Figure A4.3 ^1H NMR (400 MHz, CDCl_3) of **88**

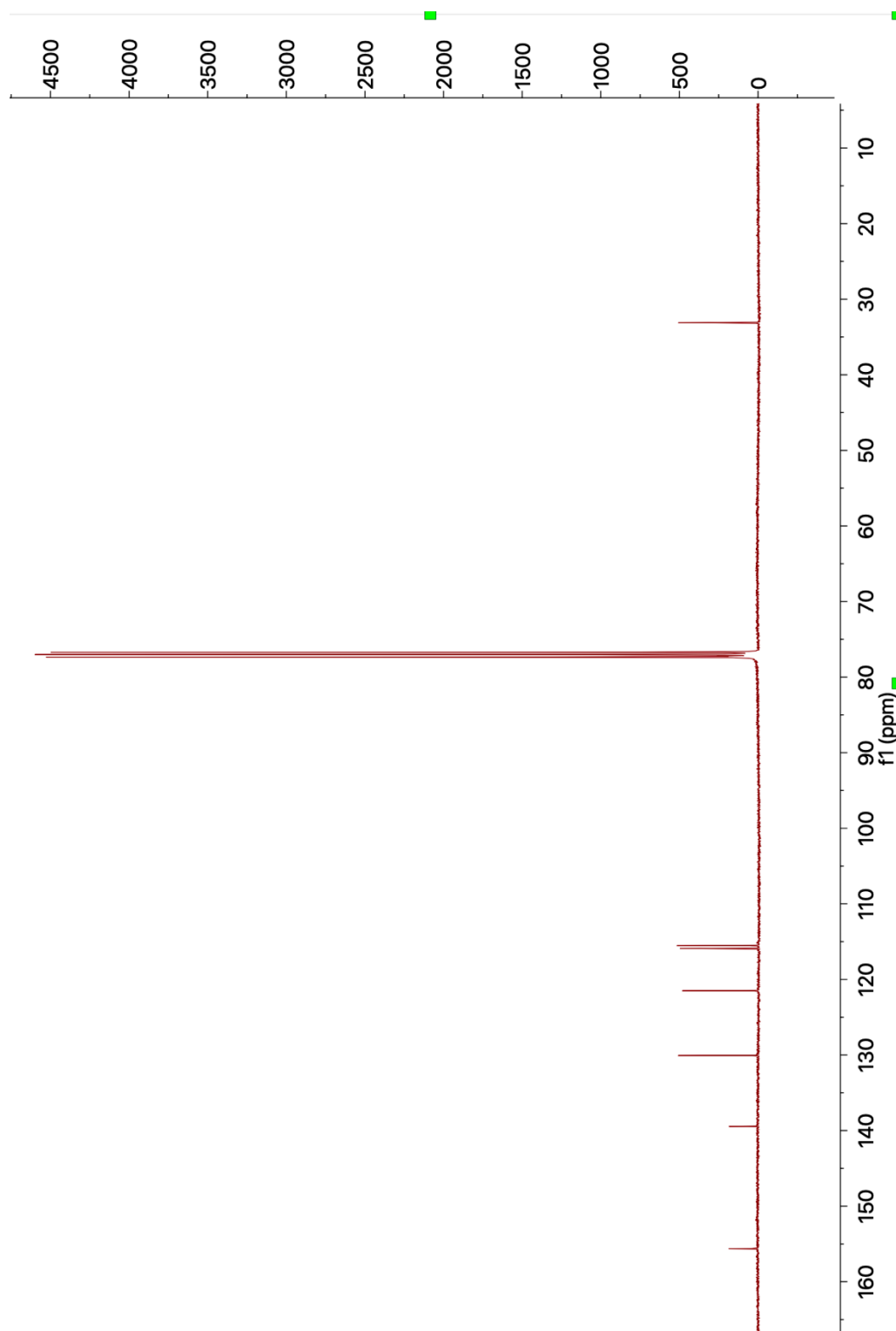


Figure A4.4 ^{13}C NMR (101 MHz, CDCl_3) of **88**

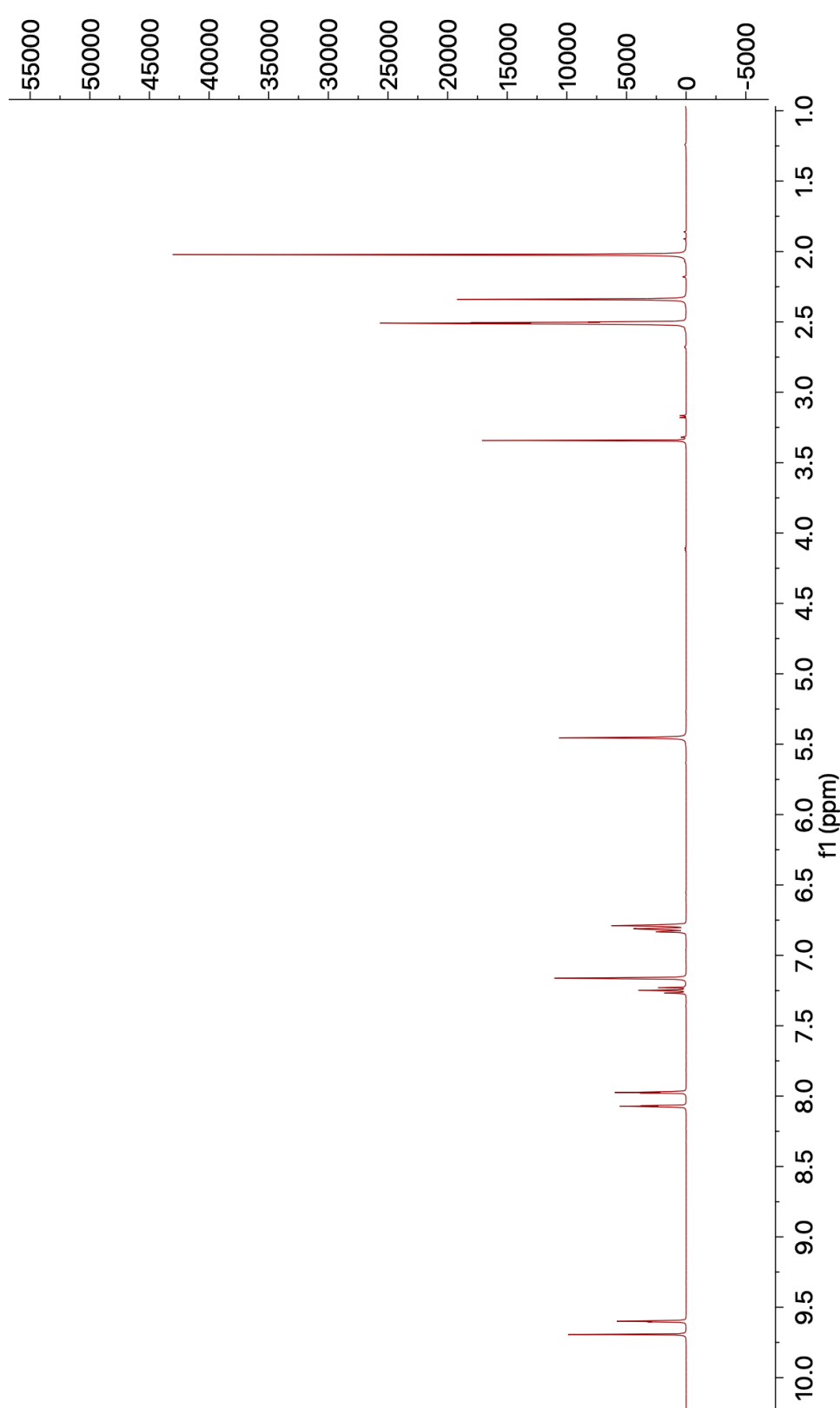


Figure A4.5 ^1H NMR (400 MHz, $\text{DMSO}-d_6$) of **90**

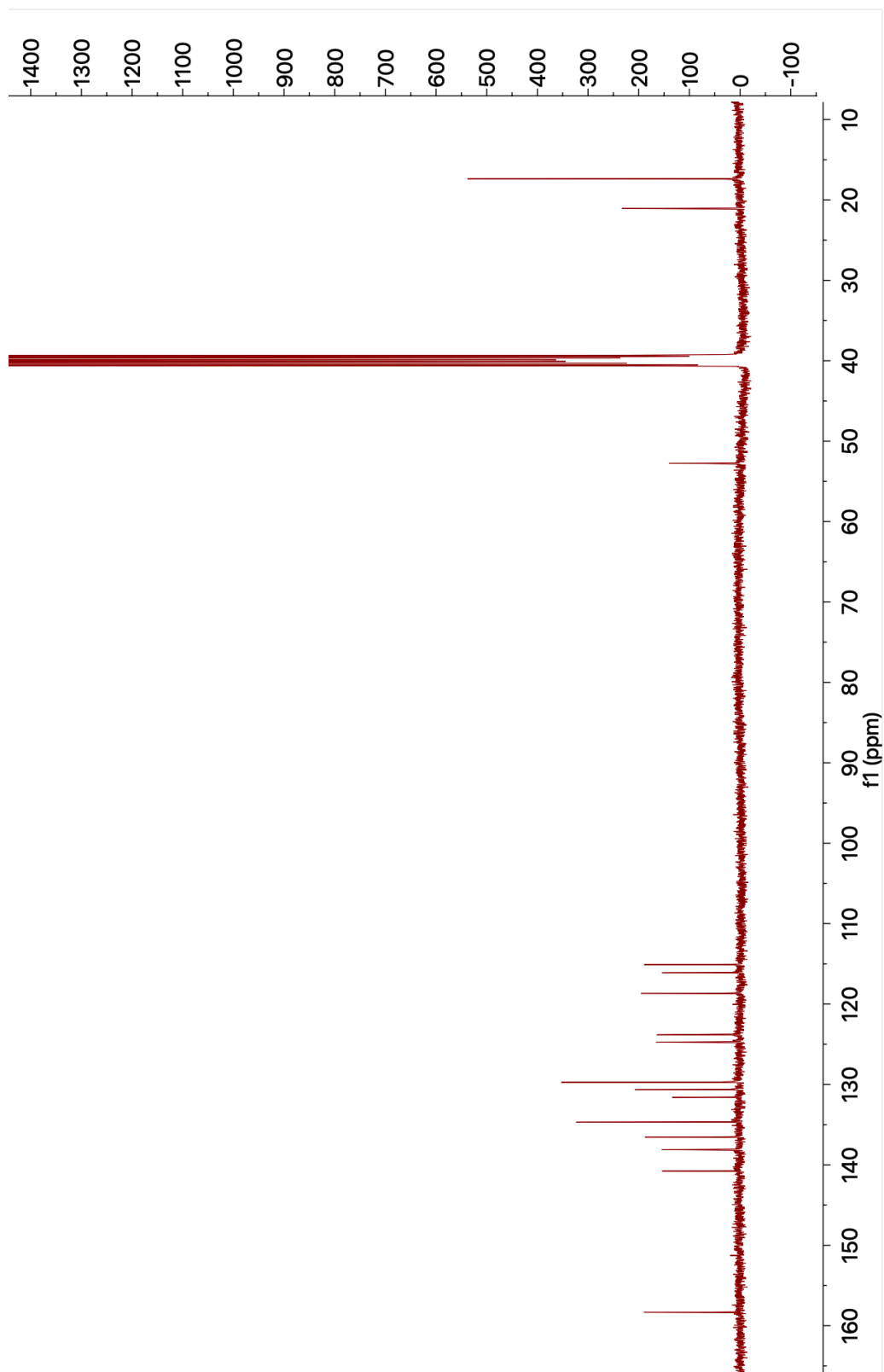


Figure A4.6 ^{13}C NMR (101 MHz, DMSO-d_6) of **90**

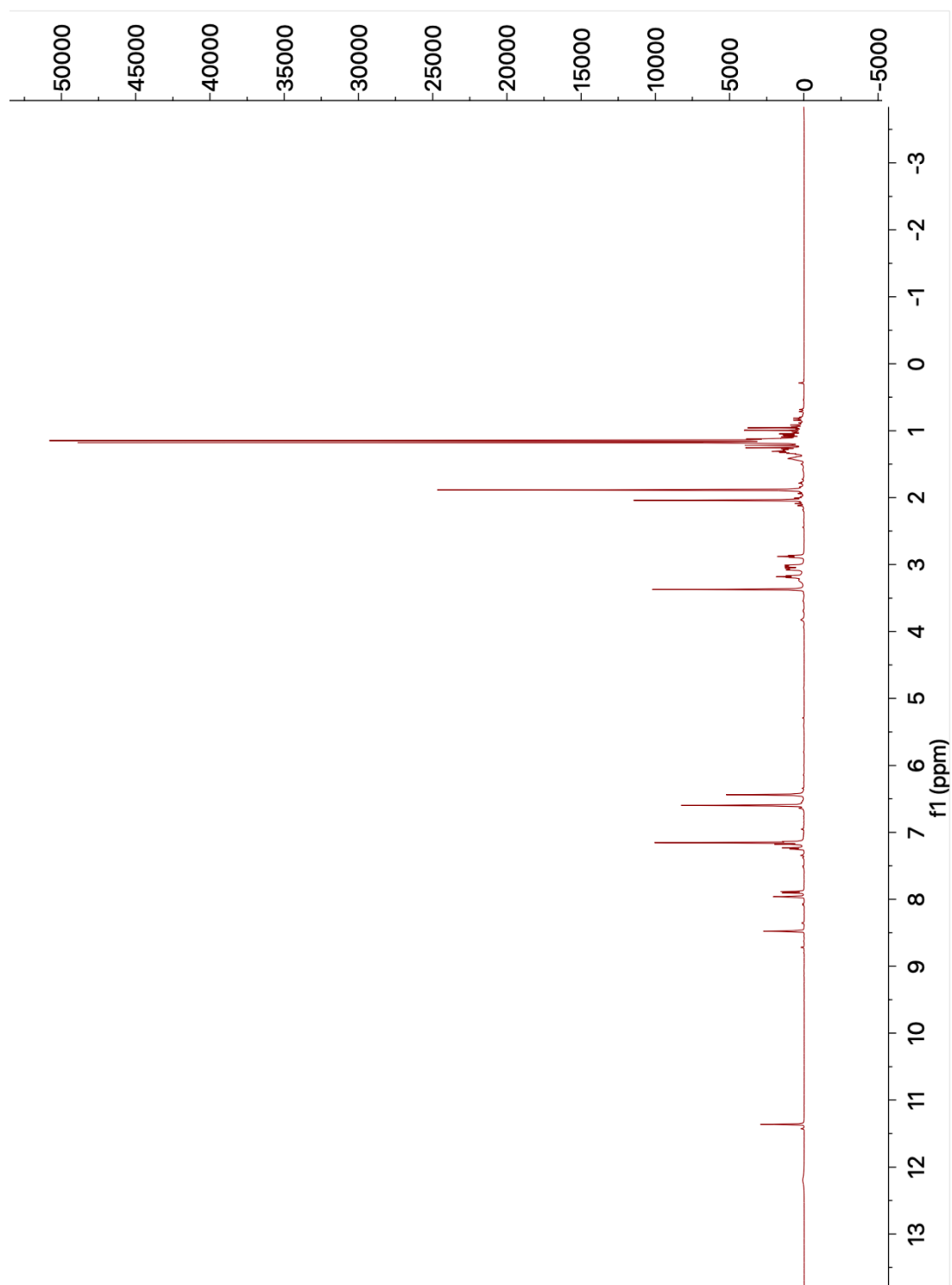


Figure A4.7 ^1H NMR (400 MHz, CDCl_3) of **91**

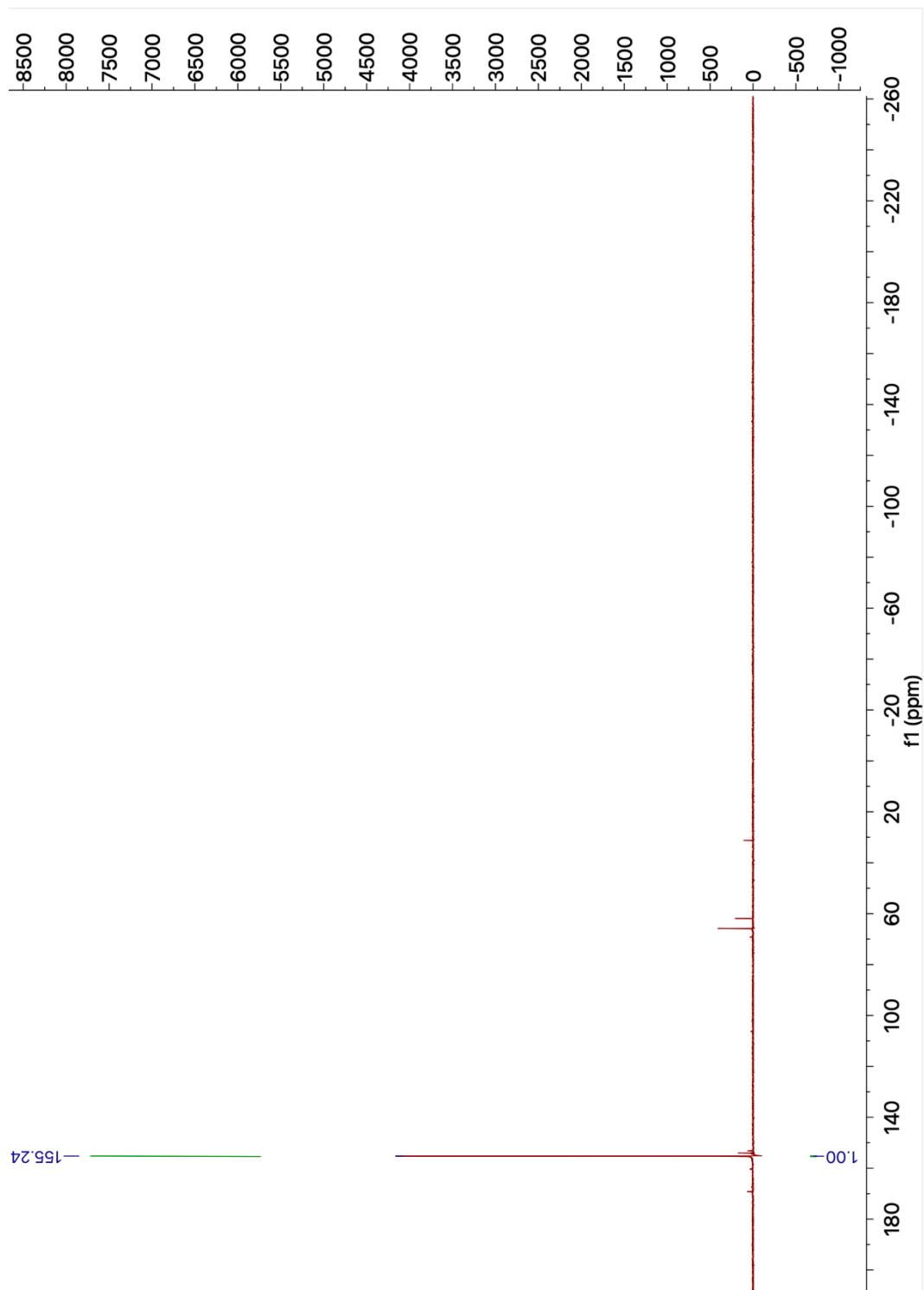


Figure A4.8 ^{31}P NMR (162 MHz, Benzene- d_6) of **91**

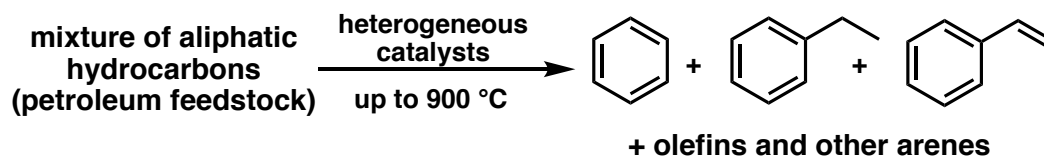
CHAPTER 3

C(SP³)-H DEHYDROAROMATIZATION OF 1-CYCLOHEXENE AND 4-VINYL-1-CYCLOHEXENE VIA DISPROPORTIONATION CATALYZED BY Iridium Pincer Ligated Complexes

3.1 INTRODUCTION

Alkanes are a ubiquitous class of chemicals that are extracted from crude oils *via* distillation and refining processes. They are typically considered to be inert, and as a result they find limited synthetic use. Small olefins and aromatics however, are more reactive and allow easier functionalization to serve as building blocks in various applications in the preparation of complex molecules, pharmaceuticals, and materials.¹⁻³ Amongst the most important industrial building blocks are benzene, ethylbenzene, and styrene. However, these do not naturally exist and the current industrial production of small aromatics is through dehydrogenating aliphatic hydrocarbons from crude oil using heterogeneous catalysts, which is a highly energy-intensive process operating at high pressures up to 60 bar and temperatures up to 900 °C (Scheme 3.1).⁴

Scheme 3.1 Important Aromatics Industrial Production



As shown in the previous chapters, the direct dehydrogenation of C(sp³)-H alkanes may seem conceptually simple but in fact it is a challenging transformation and is in some cases not feasible. This transformation is difficult due to the distinct inert nature of alkanes and the endergonic nature of dehydrogenation, making it necessary to employ energy-intensive processes with high temperatures in order to amplify the entropic contributions to the equilibrium. With the diminishing oil supply, there is a commercial need to find new routes to convert less valuable materials into more useful building blocks. We were interested to investigate the catalytic activity of the Ir pincer complexes (*t*-Bu⁴POCOP)-Ir **c13**, (*i*-Pr⁴PSCOP)-Ir **c22**, and (*i*-Pr⁴anthrphos)-Ir **c24** in disproportionating cyclohexenyl derivatives. The advantage of our proposed system is that we do not employ a sacrificial olefin as an H₂ acceptor, and the investigated substrates in this chapter act as both the H₂ donor and acceptor simultaneously.

3.2 RELATED LITERATURE

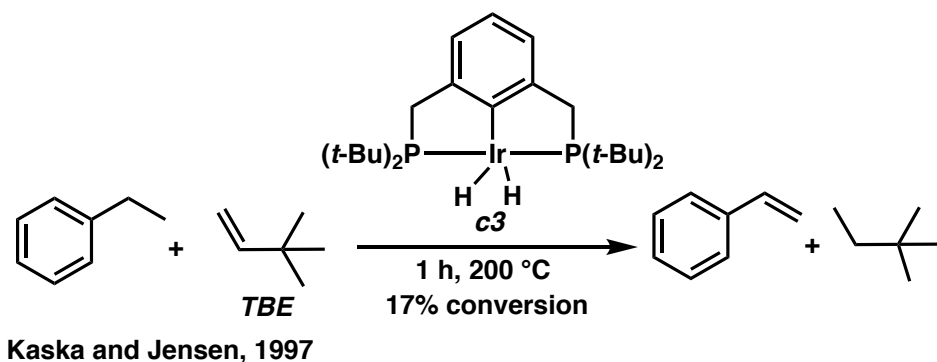
There is a great interest in developing and identifying methods for the synthesis of unsubstituted aromatics under milder conditions. Since the first reports of homogeneous transition metals as catalysts for alkane dehydrogenation by Crabtree and Felkin, substantial progress has been achieved in the field of

homogeneous catalytic alkane dehydrogenation using Ir pincer ligated complexes.⁴⁻

¹⁰ That being said, the direct dehydroaromatization of alkane precursors using Ir pincer ligated complexes remains limited due to the believed nature of arenes coordination to metal centers.¹¹⁻¹²

For example, in 1997 Kaska and Jensen reported the transfer dehydrogenation of ethylbenzene to styrene using complex $(t\text{-Bu}^4\text{PCP})\text{-Ir}$ **c3** and TBE as the H_2 acceptor reporting only up to 17% conversion (Scheme 3.2).¹³

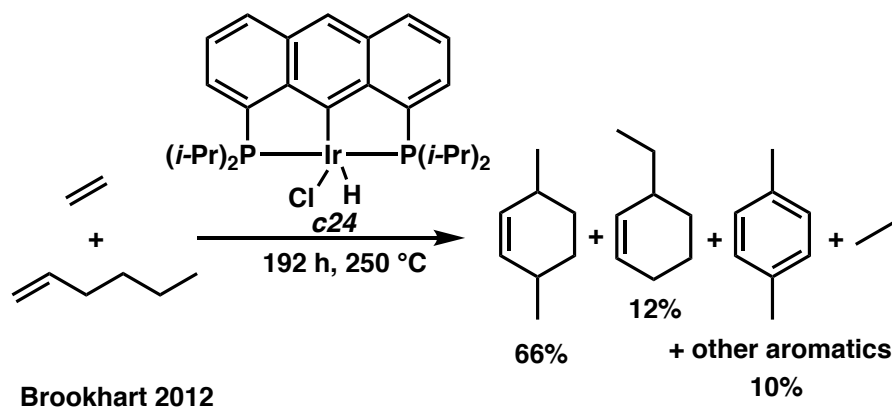
Scheme 3.2 Styrene Formation via Ethylbenzene Transfer Dehydrogenation by Complex $(t\text{-Bu}^4\text{PCP})\text{-Ir}$ **c3**



Brookhart and co-workers reported a one pot method to synthesize *p*-xylene from ethylene and 1-hexene transfer dehydrogenation followed by Diels Alder reactions using complex $(i\text{-Pr}^4\text{anthrphos})\text{-Ir}$ **c24** (Scheme 3.3). However, *p*-xylene was a minor product and its yield was reported as a mixture of aromatics up to 10.3% after 192 h of reaction time.

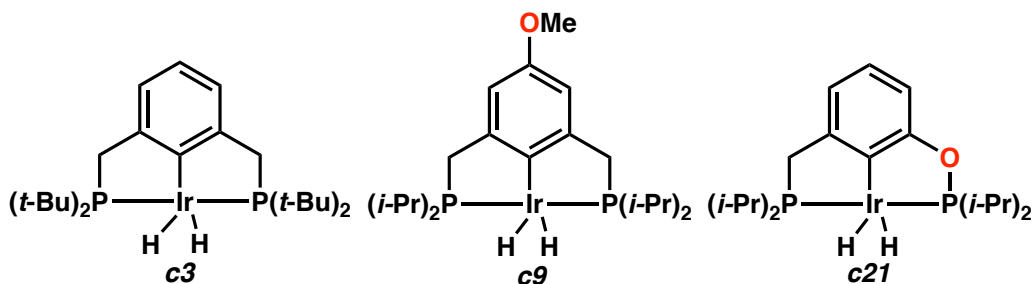
Scheme 3.3 *p*-Xylene Formation as a Minor Product via Dehydrogenation by Complex

(*i*-Pr⁴Anthraphos)-Ir **c24**

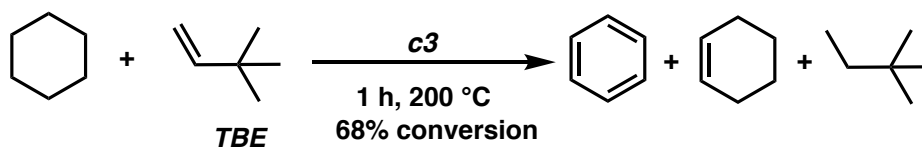


To date only four previous studies reported benzene formation *via* dehydrogenation catalyzed by Ir pincer ligated complexes (Scheme 3.4). Jensen and Kaska first reported the dehydrogenation of cyclohexane to benzene using **TBE** as the H₂ acceptor catalyzed by complex (*t*-Bu⁴PCP)-Ir **c3** (Scheme 3.4a).^{12, 14} **TBE** was partially hydrogenation and found to inhibit catalysis at high concentrations. Later in 2004, Goldman observed the formation of small amounts of benzene when transfer dehydrogenating *n*-hexane using complex (*i*-Pr⁴OMe-PCP)-Ir **c9** and **NBE** as the H₂ acceptor (Scheme 3.4b).¹⁵ More recently in 2011, Brookhart and Goldman reported the dehydroaromatization of *n*-hexane and *n*-dodecane using complex (*i*-Pr⁴PCOP)-Ir **c21** and **TBE** as the H₂ acceptor (Scheme 3.4c). In the latter example, at least 4 equivalents of **TBE** were required to render the reaction's thermodynamics favorable.¹⁶ In addition, these reactions are not selective for benzene and a complex mixture of several products consisting of dienes, trienes, monenes, and aromatics was generated.

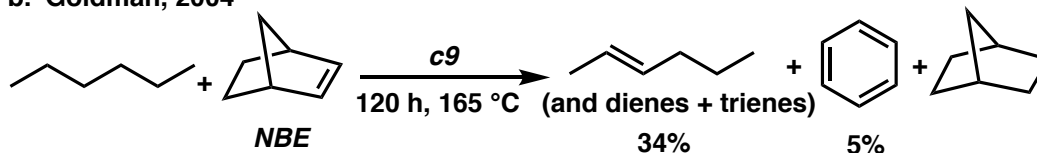
Scheme 3.4 Reported Studies of Benzene Formation via Dehydrogenation by Ir Pincer
Ligated Complexes



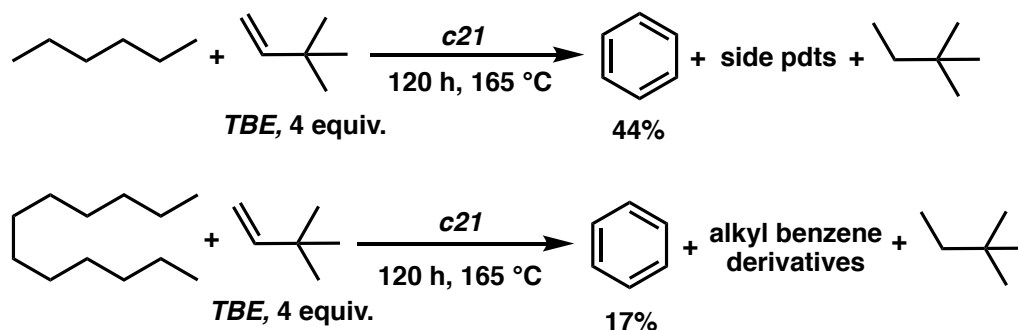
a. Kaska and Jensen, 1997



b. Goldman, 2004



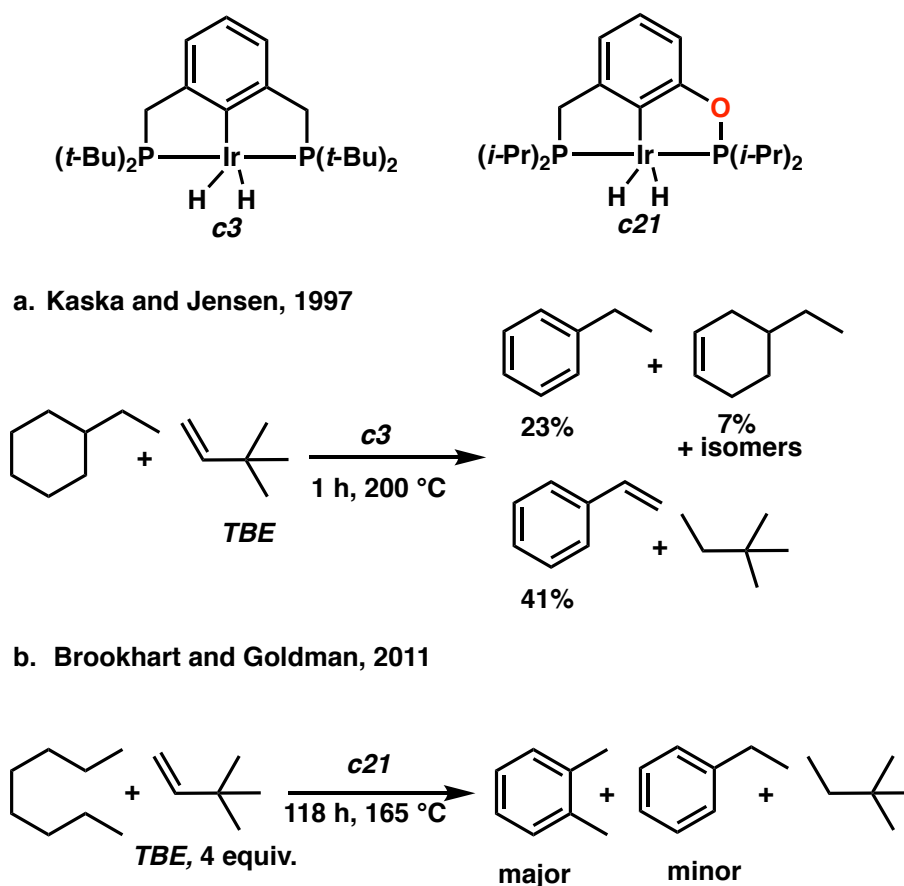
c. Brookhart and Goldman, 2011



Ethylbenzene formation *via* Ir pincer ligated catalysts has also been limited and only two studies were previously reported. Kaska and Jensen reported the synthesis of ethylbenzene from cyclohexane transfer dehydrogenation using

complex $(t\text{-Bu}^4\text{PCP})\text{-Ir}$ **c3** and **TBE** as the H_2 acceptor (Scheme 3.5a).¹³ Goldman also reported the formation of ethylbenzene when studying *n*-octane transfer dehydrogenation using complex $(i\text{-Pr}^4\text{PCOP})\text{-Ir}$ **c21** and **TBE** as the H_2 acceptor as the minor product (Scheme 3.5b).

Scheme 3.5 Only Reported Studies of Ethylbenzene Formation via Dehydrogenation by Ir Pincer Ligated Complexes

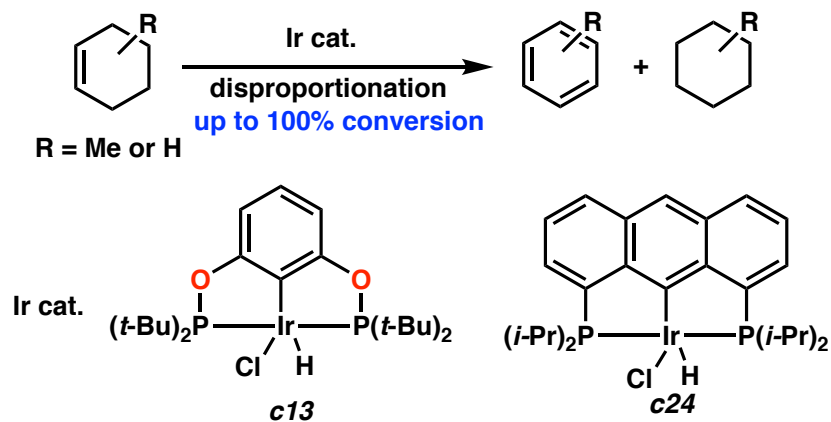


While the previous examples show tremendous achievements in the field, these methods suffer from requiring several equivalents of **TBE** and harsh reaction conditions (high temperatures, extended reaction times), making them uneconomical. In addition, these methods are non-selective toward dehydroaromatization and

generate a complex mixture of side products, imposing separation challenges and thus lack of industrial practicality especially at large scales. There is a need to find and develop alternative methods that are more economical, selective toward dehydroaromatization, industrially scalable, and which operate at milder conditions

Herein, we present a facile method of benzene and ethylbenzene formation via the disproportionation of 1-cyclohexene and 4-vinyl-1-cyclohexene and without the need of an exogenous H_2 acceptor, at temperatures as low as 120 °C (Scheme 3.6).

Scheme 3.6 Our Work in Cyclohexenyl Derivatives Dehydrogenation by Ir Pincer Ligated Complexes

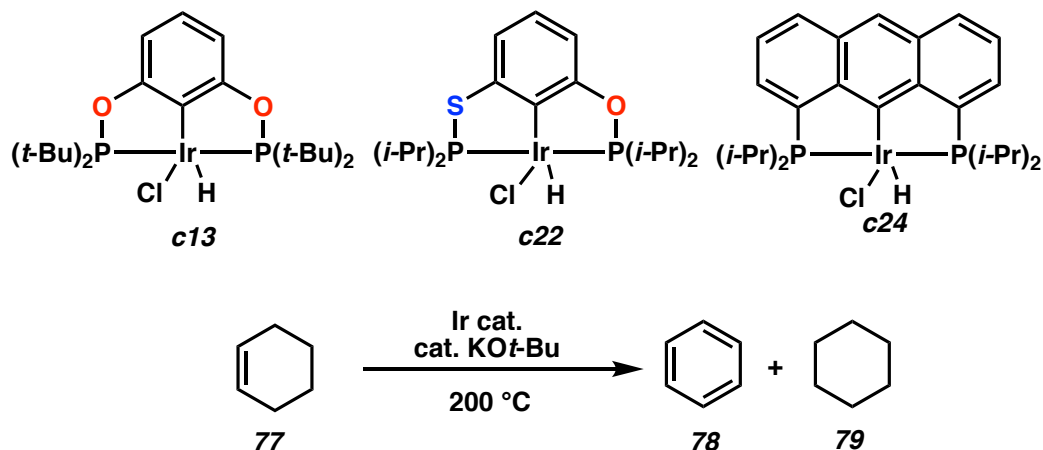


3.3 1-CYCLOHEXENE DISPROPORTIONATION BY Iridium Pincer Ligated Complexes

We were interested to explore the reactivities and catalytic activity of complexes $(t-Bu_4POCOP)Ir$ **c13**, $(i-Pr_4PSCOP)Ir$ **c22**, and $(i-Pr_4anthraphos)Ir$ **c24** in

disproportionating 1-cyclohexene (**77**) to benzene (**78**) and cyclohexane (**79**) and understand how geometry may affect arenes inhibition (Table 3.1).

Table 3.1 1-Cyclohexene Disproportionation Investigated by Ir Pincer Ligated Complexes



entry	cat.	loading (mol.%)	time (h)	conversion	78 yield ^b	TON ^c
1	c13	0.14	22 h	100.0%	33.0%	714
2	c13	0.13	11 h	100.0%	33.0%	769
3	c22	0.29	22 h	71.3%	23.1%	246
4	c22	0.33	22 h	56.7%	13.4%	180
5	c24	0.27	23 h	100.0%	33.0%	370

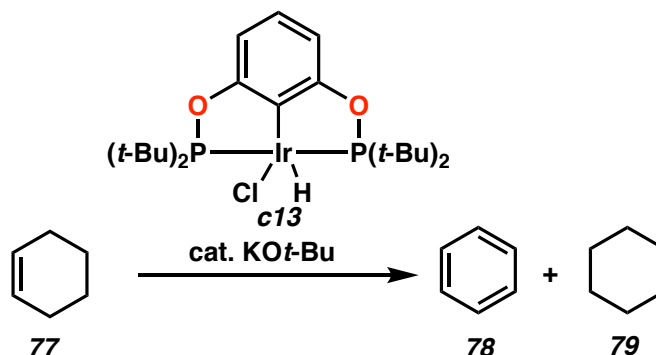
[a] Conditions: 3.5 - 5 mmol of **78**, precatalyst with at least 1.2 equiv. KO^{*t*}-Bu. [b] Yield determined by GC and ¹H NMR using hexamethylbenzene as an internal standard. [c] TON per conversion.

We commenced the investigations with complex **c13** and found that it was catalytically active and achieved 100% conversion of **77** and 33% of **78** and 66% of **79** was generated when the reaction was carried at 200 °C for 22 h (Table 3.1 entry 1). We carried the reaction again with a shorter reaction period, 11 h, and observed similar results (Table 3.1 entry 2). We then investigated the reactivity of complex

c22 under similar conditions and found that it was not as catalytically active as complex **c13** in disproportionating **77** to **78** and **79**, even when increasing the catalyst loading compared to **c13** from 0.14 mol.% to 0.33 mol.%, and only up to 71.3% conversion was achieved (Table 3.1 entry 3 and 4). We also investigated the catalytic activity of complex **c24** and found that it was very active in disproportionating **77** to **78** and **79** and 100% conversion was achieved and up to 33.0% of benzene (**78**) was generated (Table 3.1 entry 5).

Given complex (t -Bu⁴POCOP)-Ir **c13** has exhibited superior catalytic activity when dehydrogenating **77** and various substrate systems in Chapter 2, we decided to optimize reaction conditions using it as a catalyst as the next step (Table 3.2). We wanted to investigate the effect of lowering the temperature on complex **c13** catalytic activity. We investigated the disproportionation of **77** to **78** and **79** at 100 °C while extending the reaction time to 28 h, and observed 100.0% conversion of **77** (Table 3.2 entry 1). We also carried the reaction again under similar conditions but for a shorter period of time, 6 h, and observed slightly lower conversion of **77** up to 92.6% (Table 3.2 entry 2). We found optimal conditions were achieved when carrying the reaction at 120 °C for 4 h and adding 0.52 mol.% of complex **c13** (Table 3.2 entry 3). In all cases, we only observed **78** and **78** and we did not observe any cyclohexadiene intermediates even when we did not obtain full conversion of **77**.

Table 3.2 Optimizing 1-Cyclohexene Disproportionation by Complex $(t\text{-Bu}_4\text{POCOP})\text{-Ir}$
c13

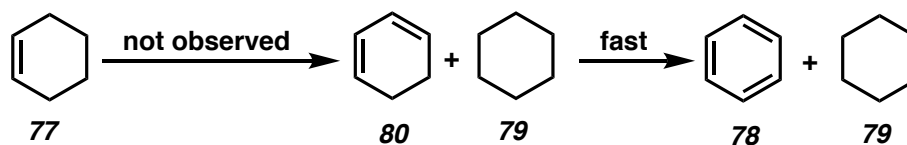


entry	loading (mol.%)	time (h)	temperature (°C)	conversion	78 yield ^b	TON ^c
1	0.20	28 h	100	100.0%	33.0%	278
2	0.36	6 h	100	92.6%	30.5%	463
3	0.52	4 h	120	100.0%	33.0%	192

[a] Conditions: 3.5 mmol of **78**, precatalyst with at least 1.2 equiv. KO t -Bu. [b] Yield determined by GC and ^1H NMR using hexamethylbenzene as an internal standard. [c] TON per conversion.

The inhibition of $(t\text{-Bu}_4\text{PCP})\text{-Ir}$ **c3** by benzene and other arenes was noted by Kaska and Jensen, and formation of a C-H addition complex to (PCP)-Ir type catalysts has been described by Goldman.^{12, 14, 17} We thus investigated the time course of the reaction and catalytic activity over time to gain an insight of the mechanism of **77** disproportionation by complex **c13**. We looked at the reaction products over a period of 6 hours every 10 minutes for the first 30 minutes and then every 30 minutes for the remaining 5.5 hours (Table 3.3). In all cases, we only observed **78** and **79** and remaining unreacted **77**. It's evident that the second dehydrogenation of **77** is very fast because we did not observe any hexadiene intermediates even within the first 10 minutes of reaction time (Scheme 3.7).

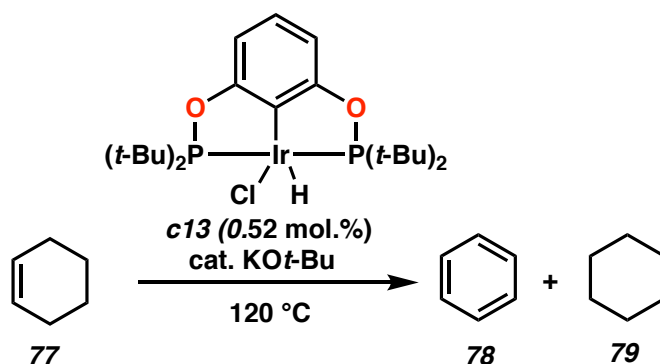
Scheme 3.7 1-Cyclohexene Disproportionation Pathway



We also observed that around 60% conversion of **77** was achieved within the first hour of reaction time. These data show that the initial dehydrogenation of 1-cyclohexene is faster than the subsequent dehydrogenations which is in agreement with previous reports by Jensen, and was explained by catalyst inhibition by the arene products.¹⁴

Hence, we then investigated the disproportionation of **77** with spiking the reaction initially with 20 mol.% and 50 mol.% benzene (Table 3.3). Surprisingly, we did not observe significant catalyst inhibition of (*t*-Bu⁴POCOP)-Ir **c13** (Figure 3.1). It appears that the high activity for the disproportionation of 1-cyclohexene (**77**) catalyzed by **c13** may be enabled by its ability to operate in the presence of arene products. These results indicate that a key mechanistic feature of our system is a lack of catalyst inhibition by arenes.

Table 3.3 Kinetics Investigation of 1-Cyclohexene Disproportionation by Complex
(*t*-Bu₄POCOP)-Ir **c13**



entry	time	AVG 77 conversion	spiked with 20% benzene	spiked with 50% benzene
1	10 min	18.2%	10.71%	16.67%
2	20 min	31.4%	21.67%	27.53%
3	30 min	41.4%	30.07%	40.83%
4	1.0 h	63.7%	51.06%	64.49%
5	1.5 h	79.1%	65.20%	74.57%
6	2.0 h	88.1%	75.23%	80.70%
7	2.5 h	93.3%	-	85.50%
8	3.0 h	96.5%	86.18%	88.95%
9	3.5 h	98.2%	89.98%	91.85%
10	4.0 h	100.0%	92.44%	94.07%
11	4.5 h	-	94.08%	95.34%
12	5.0 h	-	95.74%	96.28%
13	6.0 h	-	96.85%	97.95%

[a] Conditions: 3.5 mmol of **78**, precatalyst with at least 1.2 equiv. KOt-Bu. [b] Yield determined by GC and ¹H NMR using hexamethylbenzene as an internal standard.

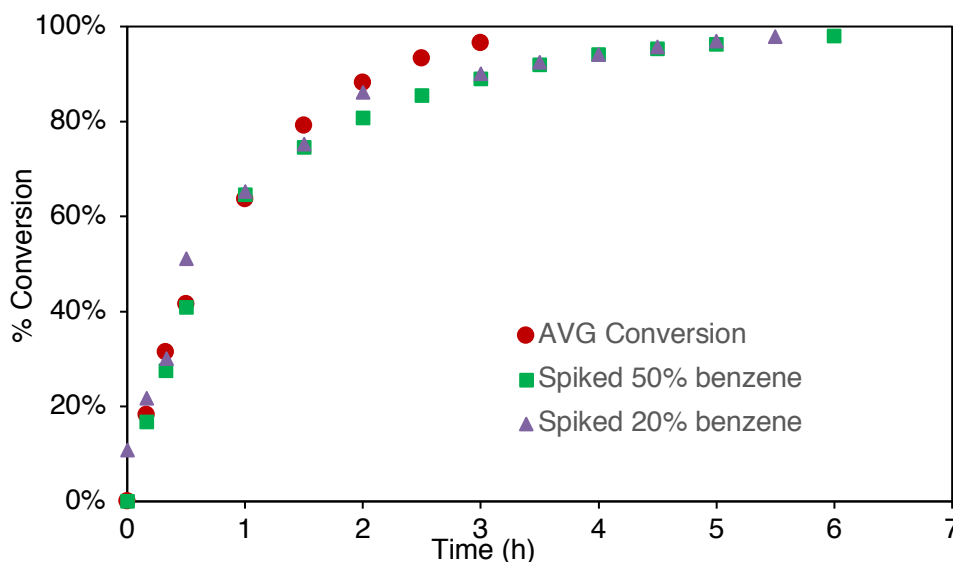
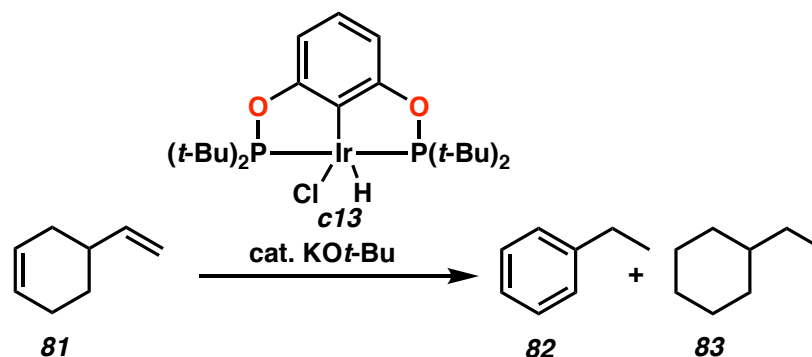


Figure 3.1 1-Cyclohexene Disproportionation Conversion by Complex (t -Bu⁴POCOP)-Ir **c13**

3.4 4-VINYL-1-CYCLOHEXENE DISPROPORTIONATION TO BY COMPLEX (t -Bu⁴POCOP)-Ir **c13**

Following the same approach, we were interested in disproportionating 4-vinyl-1-cyclohexene (**81**). We subjected **81** to the disproportionation conditions using complex (t -Bu⁴POCOP)-Ir **c13** (Table 3.4). We expected that we would make styrene, however after optimizing reaction conditions, we observed 100% conversion and only ethylbenzene (**82**) and ethylcyclohexane (**83**) was observed with a statistical distribution of 2:1 respectively (Table 3.4 entry 3).¹⁸ In all cases, no styrene product was generated.

Table 3.4 Optimizing 4-Vinyl-1-Cyclohexene Disproportionation by Complex
(*t*-Bu₄POCOP)-Ir **c13**



entry	loading (mol.%)	time (h)	temperature (°C)	conversion	78 yield ^b	TON ^c
1	0.47	28 h	200	98.2%	61.8%	209
2	0.52	4 h	120	92.6%	62.7%	178
3	0.52	6 h	120	100.0%	63.8%	192

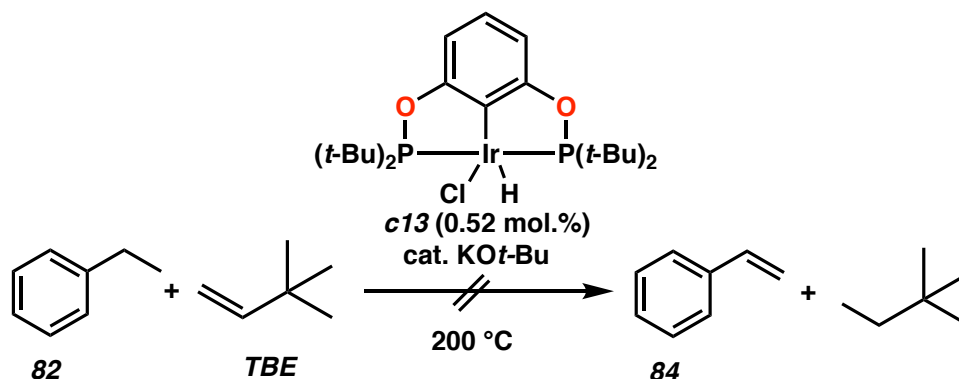
[a] Conditions: 3.0 mmol of **78**, precatalyst with at least 1.2 equiv. KOt-Bu. [b] Yield determined by GC and ¹H NMR using hexamethylbenzene as an internal standard. [c] TON per conversion.

We investigated ethylbenzene (**82**) transfer dehydrogenation by complex **c13** and using **TBE** as the H₂ acceptor (Scheme 3.8). We did not observe styrene and complex **c13** was not catalytically active in this system; perhaps styrene is not thermodynamically favored.

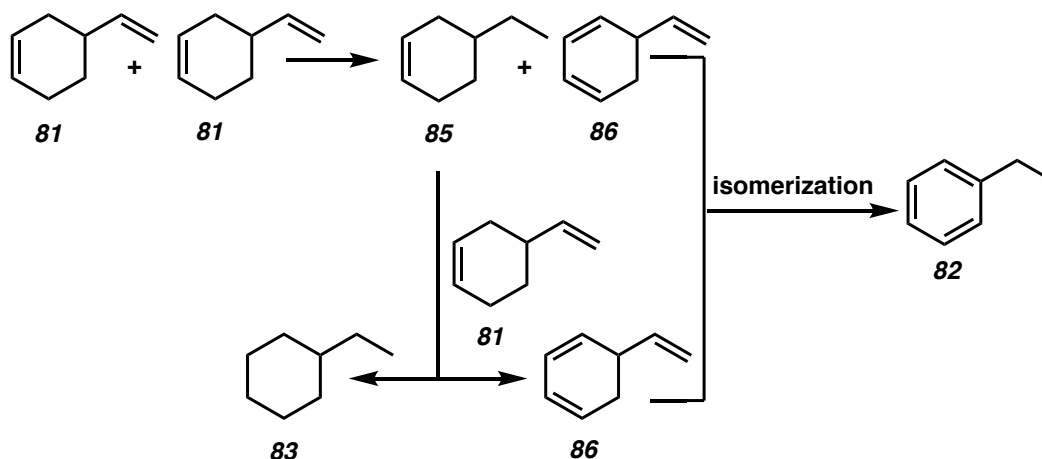
A plausible reaction pathway for the disproportionation of 4-vinyl-1-cyclohexene (**81**) disproportionation starts with the transfer hydrogenation between 2 equivalents of **81** to provide **85** and **86** (Scheme 3.9). The transfer of one equivalent of H₂ between **85** and **81** generates **86** and **83**. The isomerization of **86** to

82 completes the transformation. This reaction pathway explains the observed 2:1 ratio of **82** to **83**.

Scheme 3.8 Attempts to Transfer Dehydrogenate Ethylbenzene to Styrene



Scheme 3.9 Plausible Reaction Pathway of 4-Vinyl-1-Cyclohexene Disproportionation



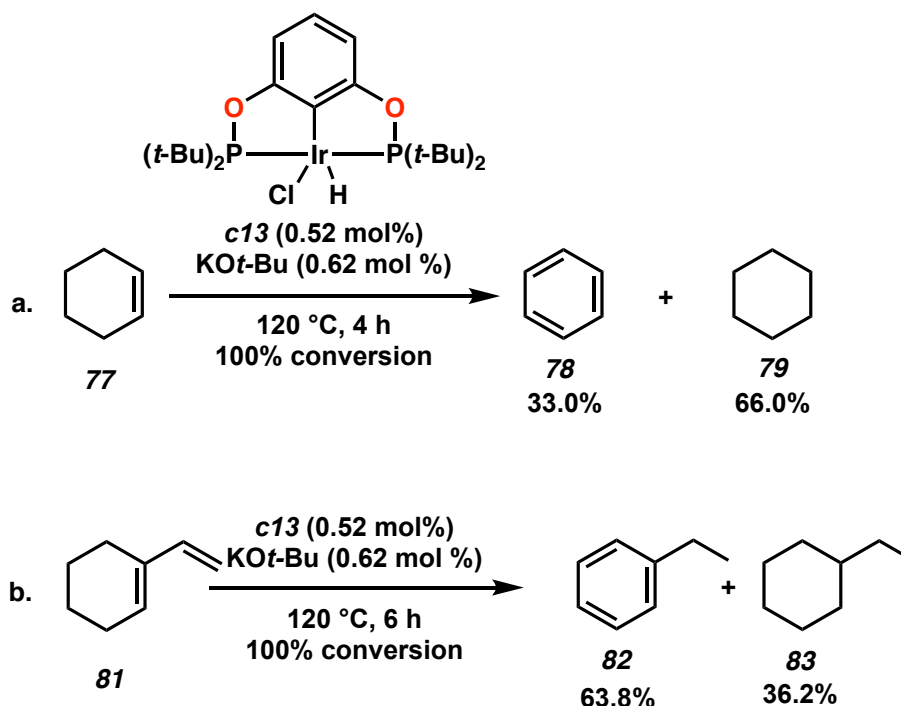
3.5 SUMMARY AND CONCLUSIONS

Benzene and ethylbenzene are among the most important industrial building blocks. The direct dehydroaromatization of $C(sp^3)$ -H alkanes and alkenes to aromatics may seem conceptually simple but in fact is a challenging transformation. The current industry practice utilizes energy-intensive processes operating at high

pressures and temperatures due to the requirement of such conditions to overcome the endergonic and unreactive nature of alkanes. Previous reports utilizing Ir pincer ligated complexes in the context of dehydrogenating alkanes to benzene and other aromatics have been limited. Our study provides a novel pathway to access important aromatic building blocks like benzene and ethylbenzene without the need of a sacrificial olefin.

We demonstrated the disproportionation of 1-cyclohexene to benzene and cyclohexane, and the disproportionation of 4-vinyl-1-cyclohexene to ethylbenzene and ethylcyclohexane with complex $(t\text{-Bu}^4\text{POCOP})\text{-Ir}$ **c13** (Scheme 3.10). In both cases we obtained 100.0% conversion at significantly lower temperatures relative to previous reports. We observed lower catalytic activity when complex $(i\text{-Pr}^4\text{PSCOP})\text{-Ir}$ **c22** was employed as a dehydrogenation catalyst when disproportionating 1-cyclohexene. The lower catalytic activity is indicative that steric hinderance around the Ir metal center likely mitigates arene inhibition. We further investigated this hypothesis by spiking the reaction initially with benzene and did not observe significant catalyst inhibition of $(t\text{-Bu}^4\text{POCOP})\text{-Ir}$ **c13**. These results indicate that a key mechanistic feature of our system is a lack of catalyst inhibition by arenes.

Scheme 3.10 Industrially Relevant Disproportionation via Dehydrogenation Forming
Benzene and Ethylbenzene by Complex $(t\text{-Bu}_4\text{POCOP})\text{-Ir}$ **c13**



Overall, we provided a new route to access important building blocks like benzene and ethylbenzene. 85% of styrene commercial production comes from the direct dehydrogenation of ethylbenzene, and hence our method has promising commercial applications and could be supported with heterogeneous catalysis as a second step to make styrene, providing a new method to its synthesis.¹⁹

3.6 NOTES AND REFERENCES

1. Michael Findlater, J. C., Alan S. Goldman, Maurice Brookhart. In *Alkane C-H Activation Activation By Single-Site Metal Catalysis*, 1 ed.; Perez, P. J., Ed. Springer Netherlands: Dordrecht, 2012; pp 113-141.
2. Gunnoe, B. T. In *Alkane C-H Activation Activation By Single-Site Metal Catalysis*, 1 ed.; Perez, P. J., Ed. Springer Netherlands: Dordrecht, 2012; pp 1-15.
3. Schulze, M., *Chem. Ing. Tech.* **2014**, 86 (8), 1304-1304.
4. Chenier, P. J., *Survey of Industrial Chemistry*. 3 ed.; Springer US: New York, 2002; p XV, 515.
5. Crabtree, R. H.; Mihelcic, J. M.; Quirk, J. M., *Journal of the American Chemical Society* **1979**, 101 (26), 7738-7740.
6. Baudry, D.; Ephritikhine, M.; Felkin, H., *J. Chem. Soc., Chem. Commun.* **1980**, (24), 1243-1244.
7. Crabtree, R. H.; Demou, P. C.; Eden, D.; Mihelcic, J. M.; Parnell, C. A.; Quirk, J. M.; Morris, G. E., *Journal of the American Chemical Society* **1982**, 104 (25), 6994-7001.
8. Crabtree, R. H.; Mellea, M. F.; Mihelcic, J. M.; Quirk, J. M., *Journal of the American Chemical Society* **1982**, 104 (1), 107-113.
9. Akshai Kumar, A. S. G. In *The Privileged Pincer-Metal Platform: Coordination Chemistry & Applications*, Gerard Van Koten, R. A. G., Ed. Springer, Cham: Cham, 2015; Vol. 54, pp 307-334.

10. Kumar, A.; Bhatti, T. M.; Goldman, A. S., *Chemical Reviews* **2017**, 117 (19), 12357-12384.
11. Gupta, M.; Hagen, C.; Flesher, R. J.; Kaska, W. C.; Jensen, C. M., *Chem. Commun.* **1996**, (17), 2083-2084.
12. Gupta, M.; Hagen, C.; Kaska, W. C.; Cramer, R. E.; Jensen, C. M., *Journal of the American Chemical Society* **1997**, 119 (4), 840-841.
13. Gupta, M.; C. Kaska, W.; M. Jensen, C., *Chem. Commun.* **1997**, (5), 461-462.
14. M. Jensen, C., *Chem. Commun.* **1999**, (24), 2443-2449.
15. Zhu, K.; Achord, P. D.; Zhang, X.; Krogh-Jespersen, K.; Goldman, A. S., *Journal of the American Chemical Society* **2004**, 126 (40), 13044-13053.
16. Ahuja, R.; Punji, B.; Findlater, M.; Supplee, C.; Schinski, W.; Brookhart, M.; Goldman, A. S., *Nat. Chem.* **2010**, 3, 167.
17. Kanzelberger, M.; Singh, B.; Czerw, M.; Krogh-Jespersen, K.; Goldman, A. S., *Journal of the American Chemical Society* **2000**, 122 (44), 11017-11018.
18. The proton NMR of the reaction was 97% pure and the impurities were mostly in the aliphatic region.
19. W. M. Castor, D. H. J., *Ullmann's Encyclopedia of Industrial Chemistry*. 5th ed.; Wiley-VCH: Weinheim, 1994; p 332.

APPENDIX 5

EXPERIMENTAL SECTION AND SPECTRA RELATED TO CHAPTER 3

A5.1 MATERIALS AND METHODS

Unless noted in the specific procedure, reactions were performed in oven-dried glassware. All dehydrogenation reactions were degassed by freeze-pump-thaw x 5 cycles and were carried out under air-free conditions in dry glassware. All liquid reagents were purified by distillation and dried using molecular sieves, NaH, or Na-K alloy. For all the investigated dehydrogenation systems, the substrate was mixed with the H₂ acceptor in a 4 mL sealed Schlenk pressure flask under an argon atmosphere. Then synthesized Ir pincer complexes were added to the reaction mixture with at least 1.2 equivalents of the Ir pincer complexes of KO^{*t*}-Bu when the Ir-HCl version of catalyst is used.

¹H spectra were recorded on a Varian spectrometer 400 MHz with broadband auto-tune OneProbeor or on a Bruker AV III HD 400 MHz spectrometer equipped

with a Prodigy liquid nitrogen temperature cryoprobe, and are reported in terms of chemical shift relative to residual CHCl_3 (δ 7.26).

In addition, the conversions were determined using an Agilent 6850 GC-FID equipped with a Supelco column (SPBTM-1, fused silica capillary column, 30 m x 0.25 μm film thickness) and using methods with temperature programs shown in Tables A5.1 and A5.2 and inlet program showed in Table A1.3. The obtained products were also confirmed by spiking the reaction with a commercial sample of the product.

Table A5.1 ZAS_Cyclohexene General Method Temperature Ramping Program for 1-Cyclohexene (**77**) Disproportionation

Oven Ramp	°C/min	Next °C	Hold min
Initial	-	38	1.50
Ramp 1	5.00	50	5.00
Ramp 2	10.00	100	0.00
Ramp 3	5.00	170	5.00
Ramp 4	20.00	250	0.00

Table A5.2 ZAS2 General Method Temperature Ramping Program for 4-Vinyl-1-Cyclohexene (**81**) Disproportionation

Oven Ramp	°C/min	Next °C	Hold min
Initial	-	38	1.50
Ramp 1	10.00	150	0.00
Ramp 2	20.00	250	5.00

Table A5.3 Inlet Parameters used in All Methods

Inlet	Setting
Mode	Split
Gas	He
Heater	250 °C
Pressure	9.52 psi
Total Flow	82.2
Split Ratio	100:1
Split Flow	78.5 mL/min

A5.2 Relevant Spectra

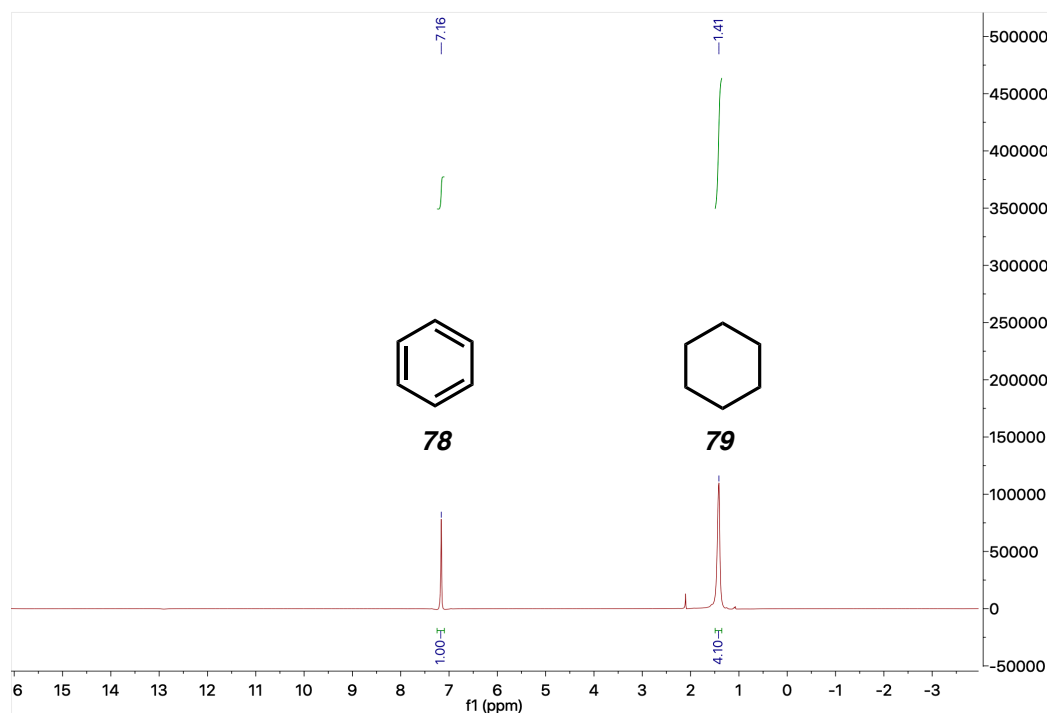


Figure A5.1 Table 3.2 Entry 3 ^1H NMR (400 MHz, Neat Reaction) of Crude Reaction Showing Full Conversion to Benzene (**78**) and Cyclohexane (**79**), Yield Calculated with Hexamethylbenzene as an Internal Standard

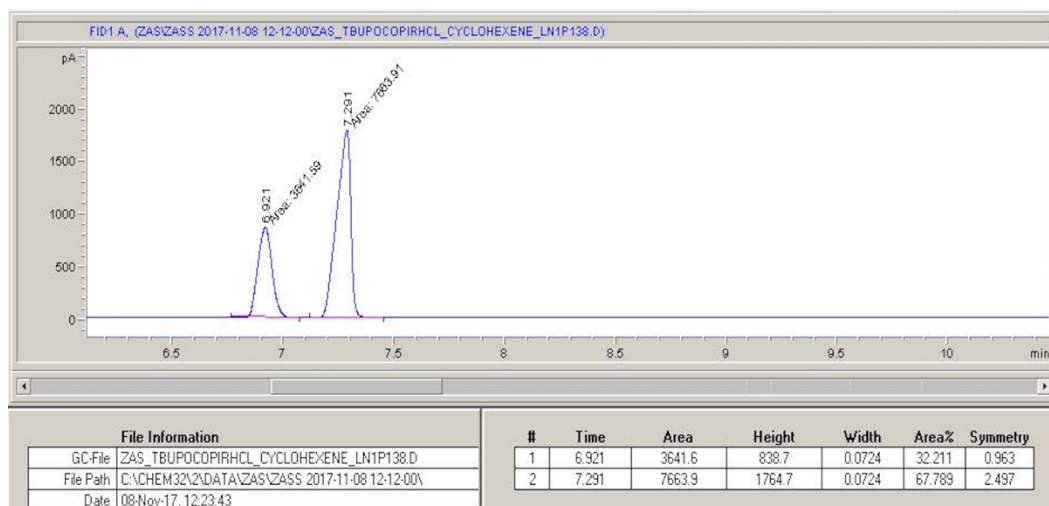


Figure A5.2 GC Spectra of **77** Crude Reaction: **78**@6.92 and **79**@7.29 Using ZAS_Cyclohexene Method in Table A5.1

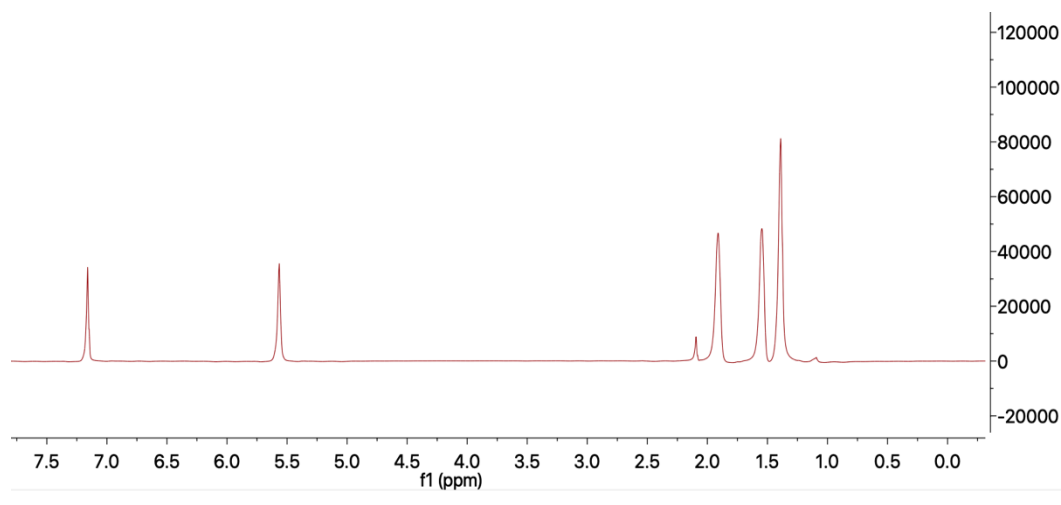


Figure A5.3 Table 3.3 Entry 1 (AVG 77 Conversion) ^1H NMR (400 MHz, Neat Reaction) of Crude Reaction, Yield Calculated with Hexamethylbenzene as an Internal Standard

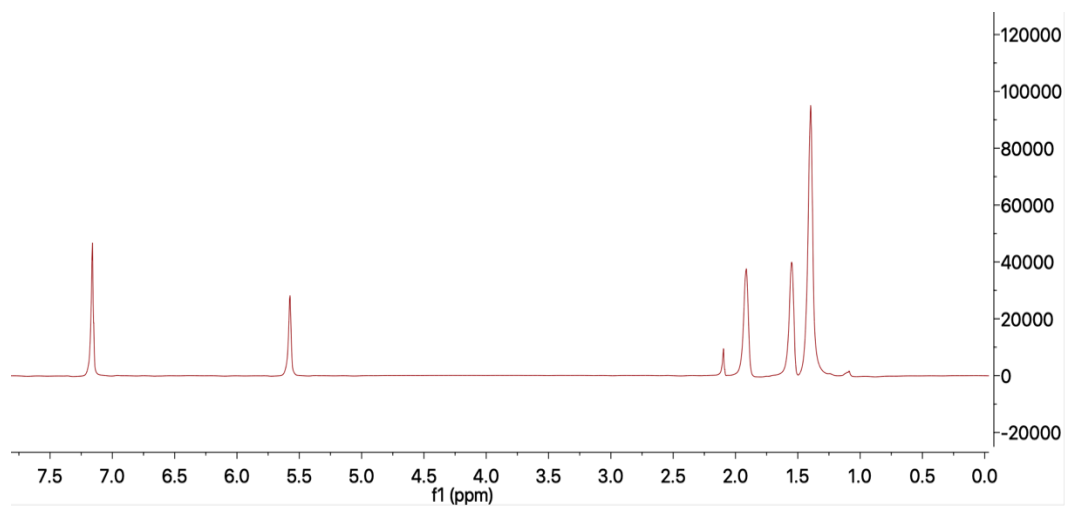


Figure A5.4 Table 3.3 Entry 2 (AVG 77 Conversion) ^1H NMR (400 MHz, Neat Reaction) of Crude Reaction, Yield Calculated with Hexamethylbenzene as an Internal Standard

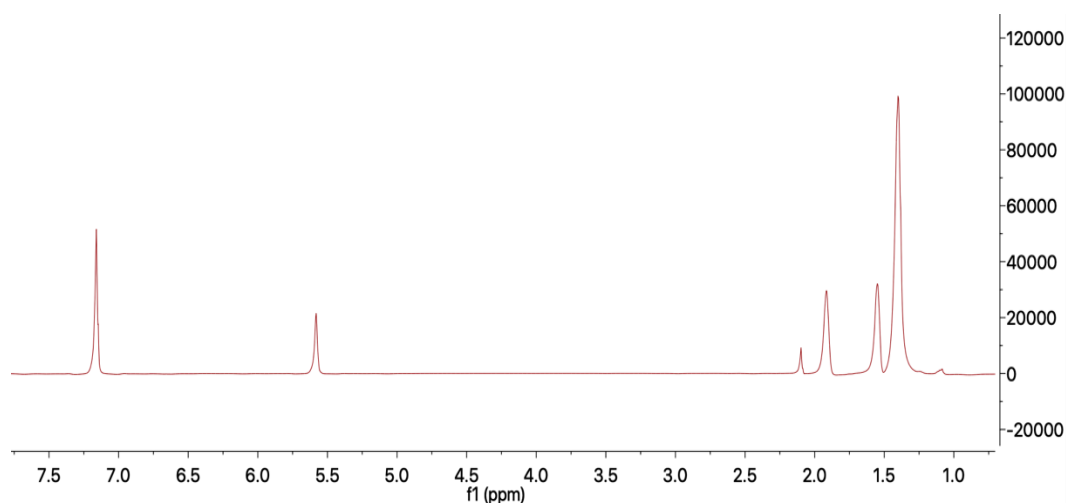


Figure A5.5 Table 3.3 Entry 3 (AVG 77 Conversion) ¹H NMR (400 MHz, Neat Reaction) of Crude Reaction, Yield Calculated with Hexamethylbenzene as an Internal Standard

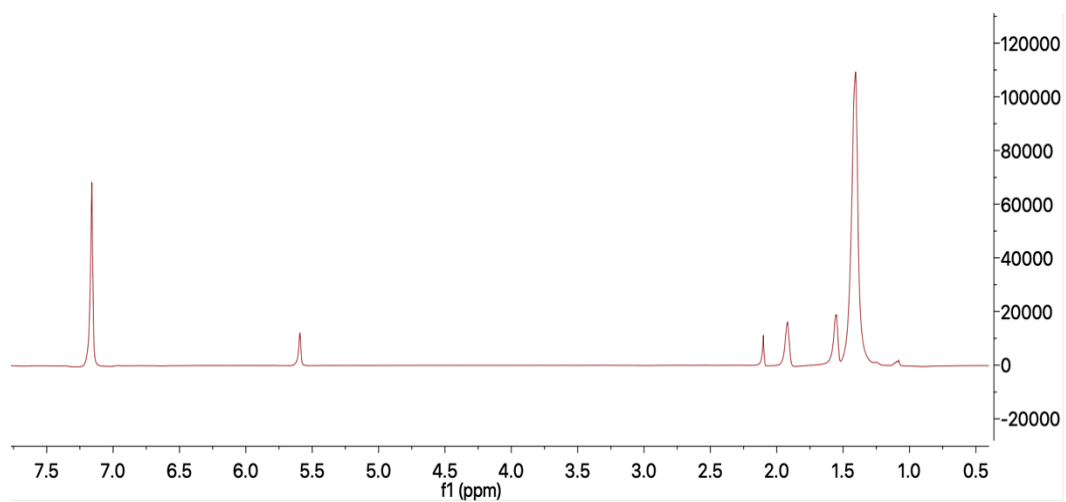


Figure A5.6 Table 3.3 Entry 4 (AVG 77 Conversion) ¹H NMR (400 MHz, Neat Reaction) of Crude Reaction, Yield Calculated with Hexamethylbenzene as an Internal Standard

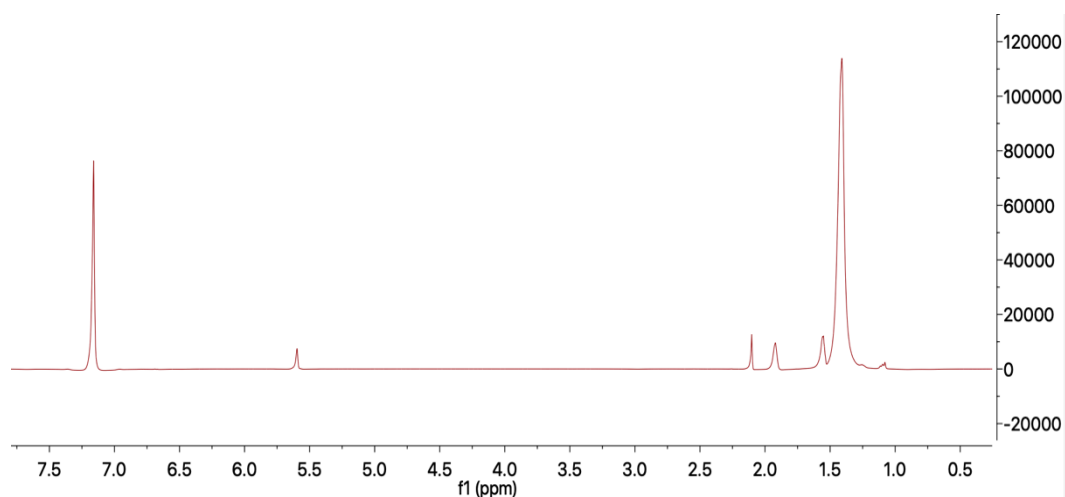


Figure A5.7 Table 3.3 Entry 5 (AVG 77 Conversion) ¹H NMR (400 MHz, Neat Reaction) of Crude Reaction, Yield Calculated with Hexamethylbenzene as an Internal Standard

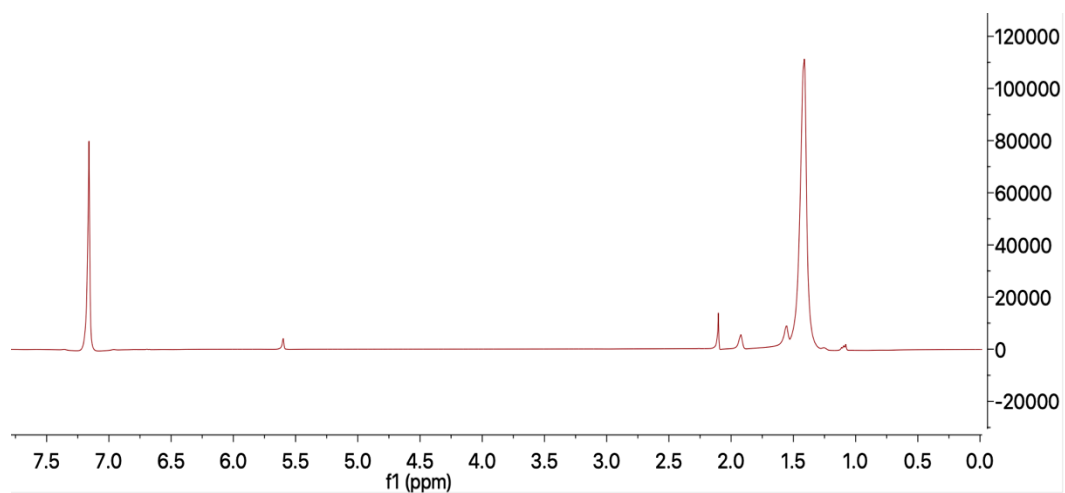


Figure A5.8 Table 3.3 Entry 6 (AVG 77 Conversion) ¹H NMR (400 MHz, Neat Reaction) of Crude Reaction, Yield Calculated with Hexamethylbenzene as an Internal Standard

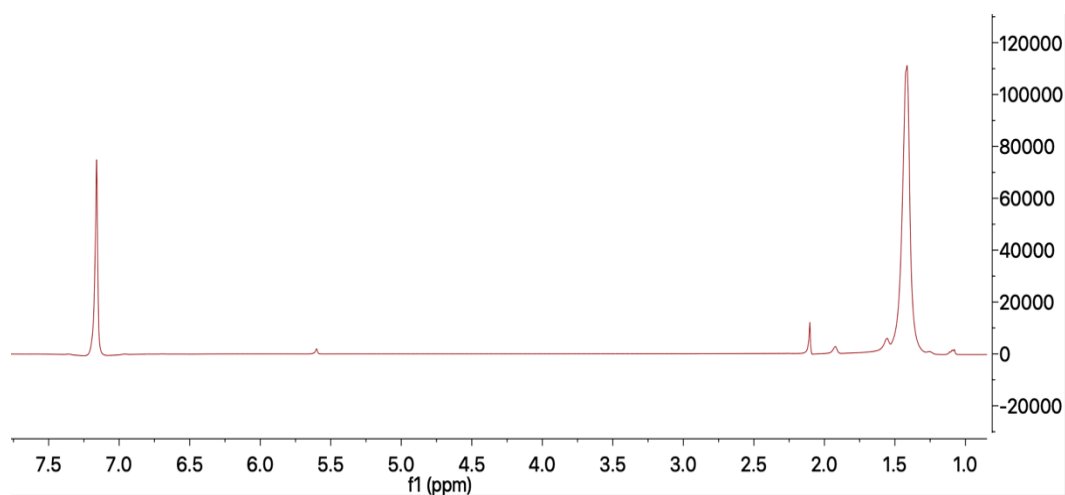


Figure A5.9 Table 3.3 Entry 7 (AVG 77 Conversion) ¹H NMR (400 MHz, Neat Reaction) of Crude Reaction, Yield Calculated with Hexamethylbenzene as an Internal Standard

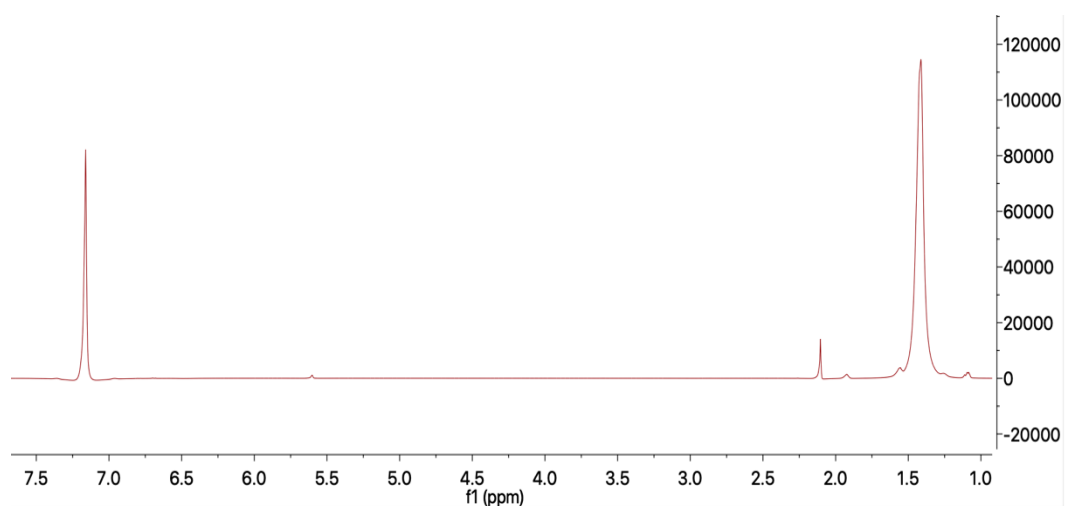


Figure A5.10 Table 3.3 Entry 8 (AVG 77 Conversion) ¹H NMR (400 MHz, Neat Reaction) of Crude Reaction, Yield Calculated with Hexamethylbenzene as an Internal Standard

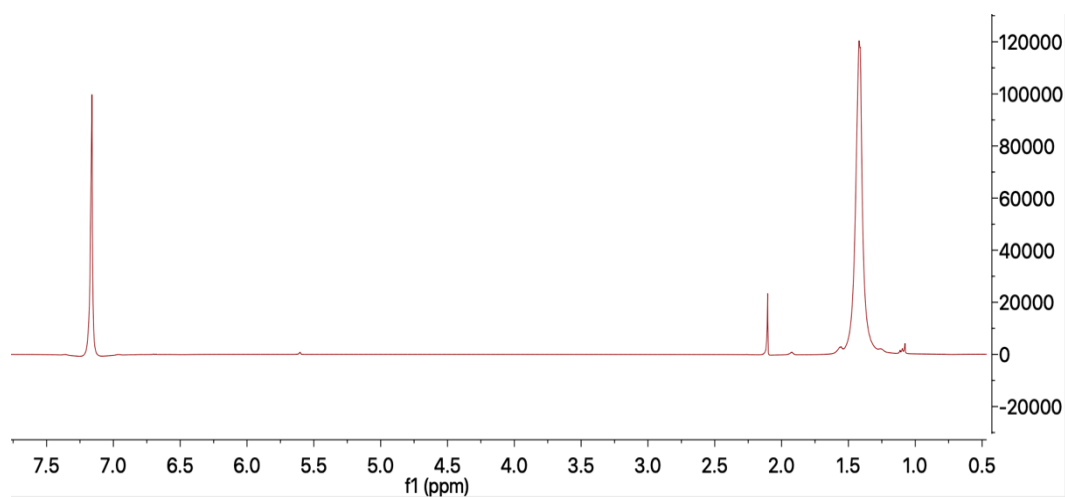


Figure A5.11 Table 3.3 Entry 9 (AVG 77 Conversion) ¹H NMR (400 MHz, Neat Reaction) of Crude Reaction, Yield Calculated with Hexamethylbenzene as an Internal Standard

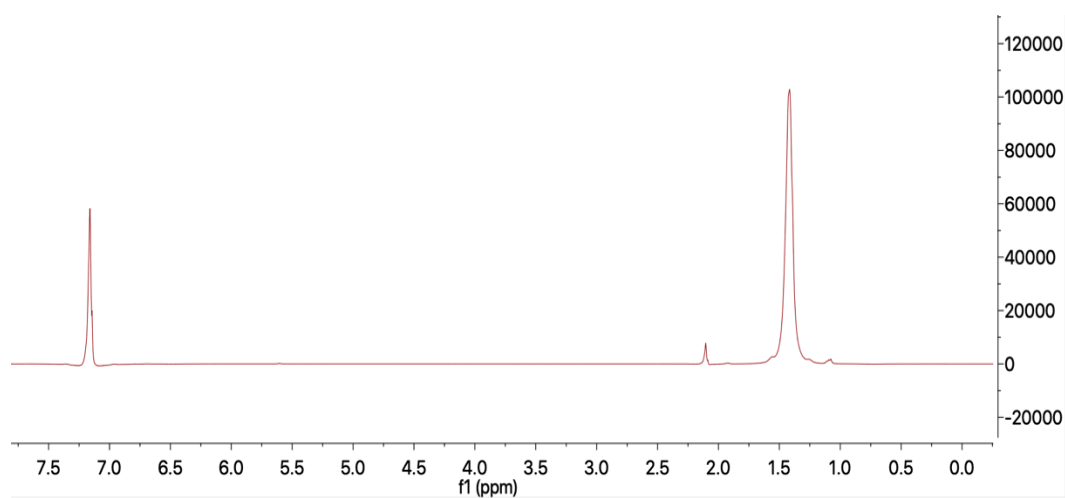


Figure A5.12 Table 3.3 Entry 10 (AVG 77 Conversion) ¹H NMR (400 MHz, Neat Reaction) of Crude Reaction, Yield Calculated with Hexamethylbenzene as an Internal Standard

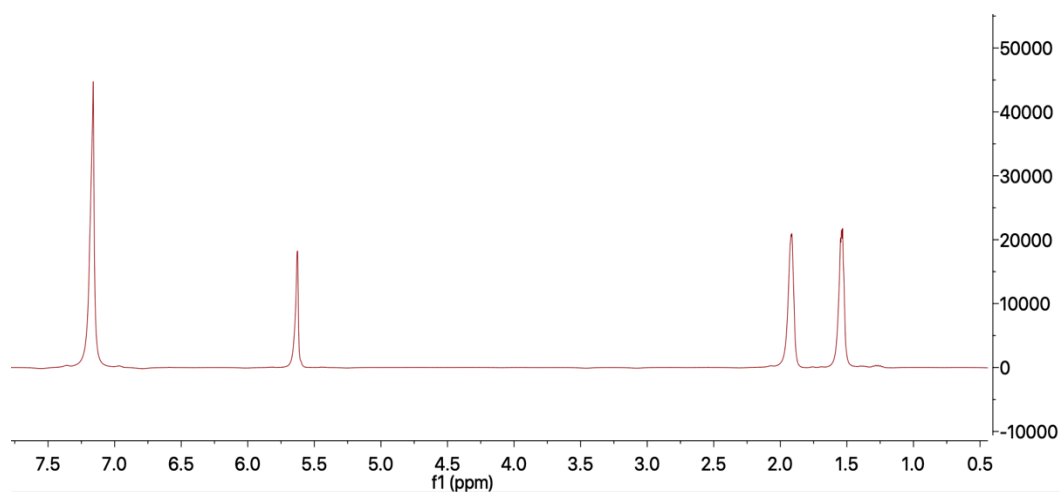


Figure A5.13 (Spiked With 50% Benzene) @ 0 Min ^1H NMR (400 MHz, Neat Reaction) of Crude Reaction, Yield Calculated with Hexamethylbenzene as an Internal Standard

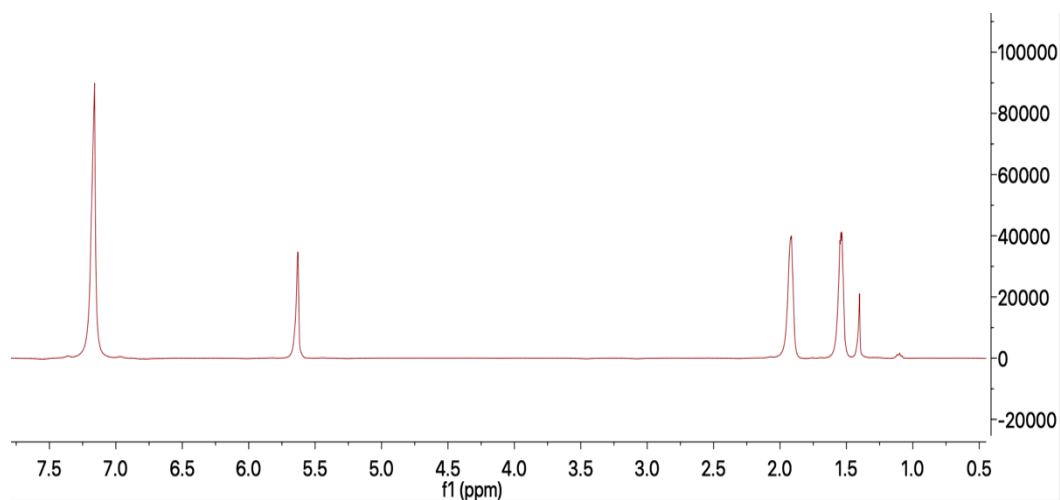


Figure A5.14 Table 3.3 Entry 1 (Spiked With 50% Benzene) ^1H NMR (400 MHz, Neat Reaction) of Crude Reaction, Yield Calculated with Hexamethylbenzene as an Internal Standard

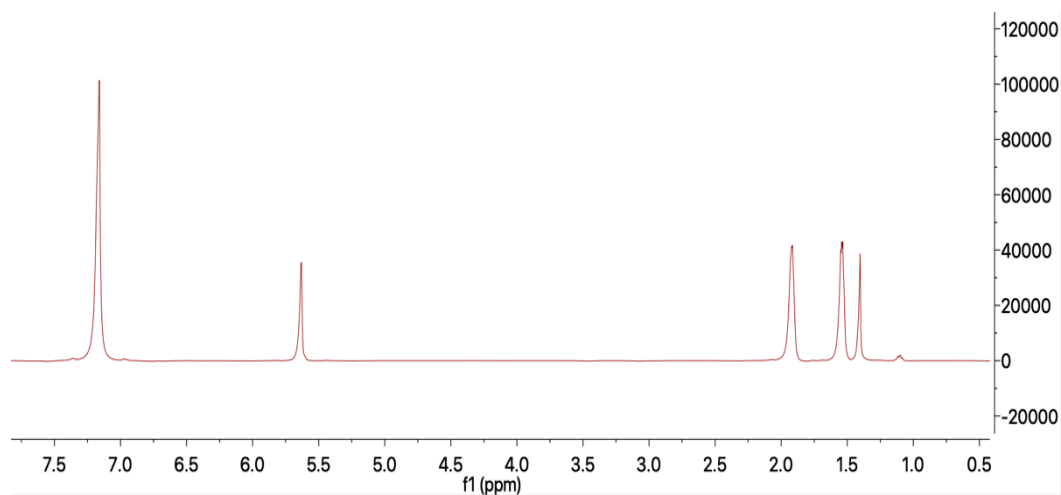


Figure A5.15 Table 3.3 Entry 2 (Spiked With 50% Benzene) ¹H NMR (400 MHz, Neat Reaction) of Crude Reaction, Yield Calculated with Hexamethylbenzene as an Internal Standard

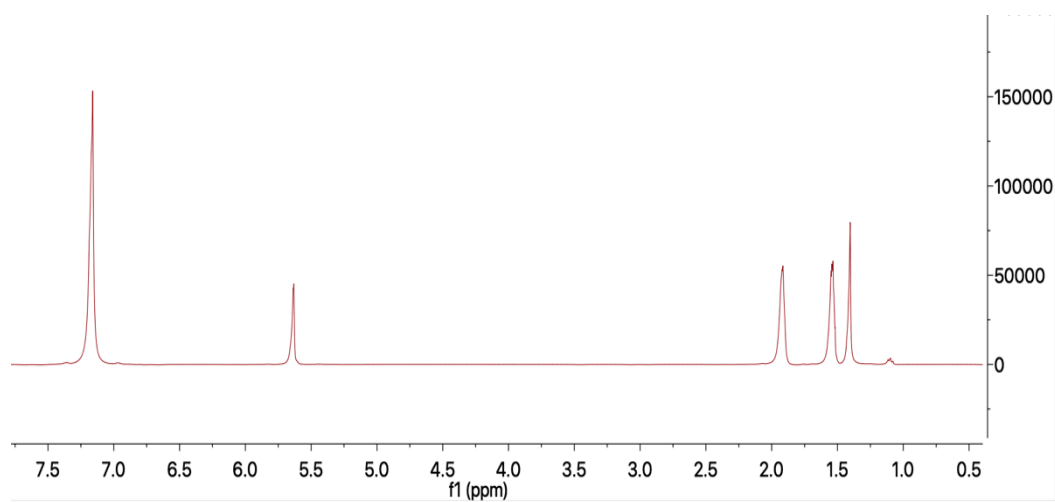


Figure A5.16 Table 3.3 Entry 3 (Spiked With 50% Benzene) ¹H NMR (400 MHz, Neat Reaction) of Crude Reaction, Yield Calculated with Hexamethylbenzene as an Internal Standard

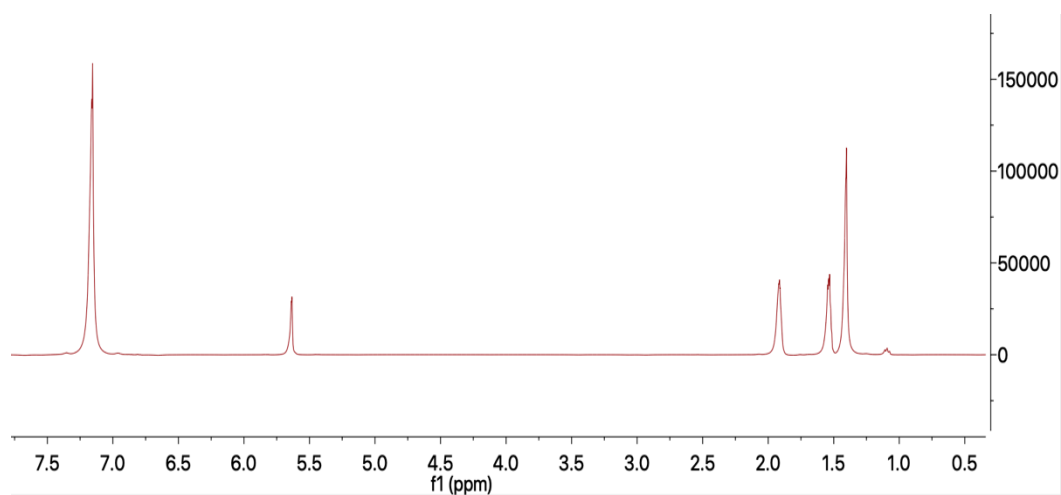


Figure A5.17 Table 3.3 Entry 4 (Spiked With 50% Benzene) ¹H NMR (400 MHz, Neat Reaction) of Crude Reaction, Yield Calculated with Hexamethylbenzene as an Internal Standard

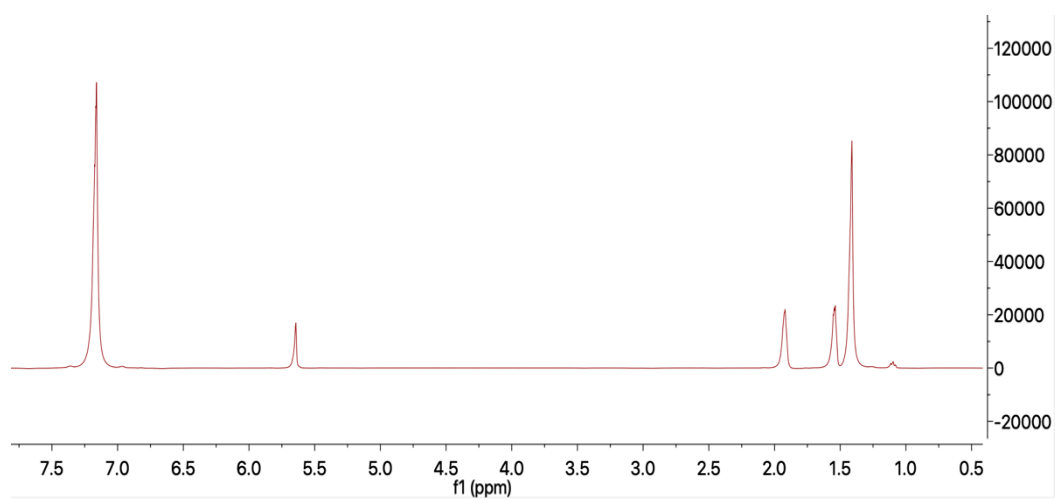


Figure A5.18 Table 3.3 Entry 5 (Spiked With 50% Benzene) ¹H NMR (400 MHz, Neat Reaction) of Crude Reaction, Yield Calculated with Hexamethylbenzene as an Internal Standard

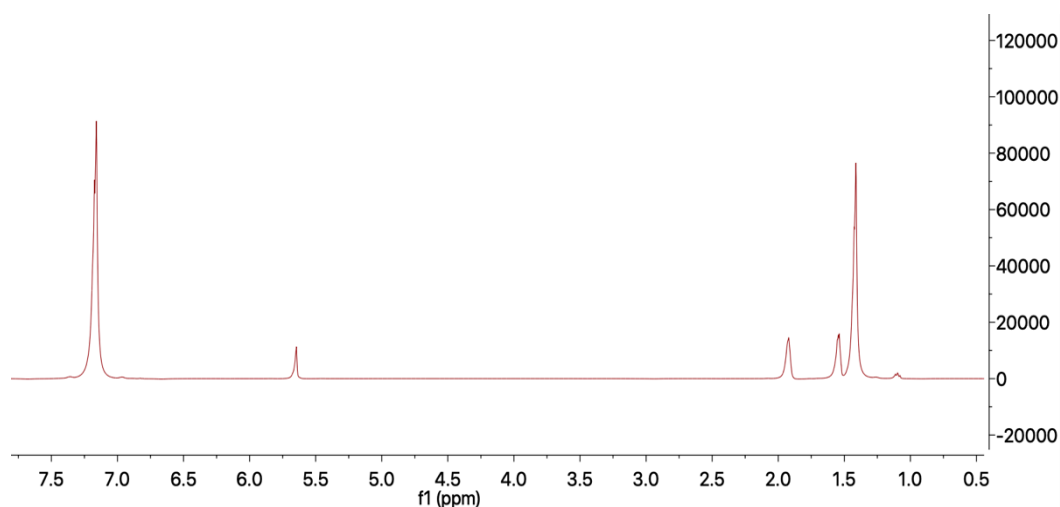


Figure A5.19 Table 3.3 Entry 6 (Spiked With 50% Benzene) ¹H NMR (400 MHz, Neat Reaction) of Crude Reaction, Yield Calculated with Hexamethylbenzene as an Internal Standard

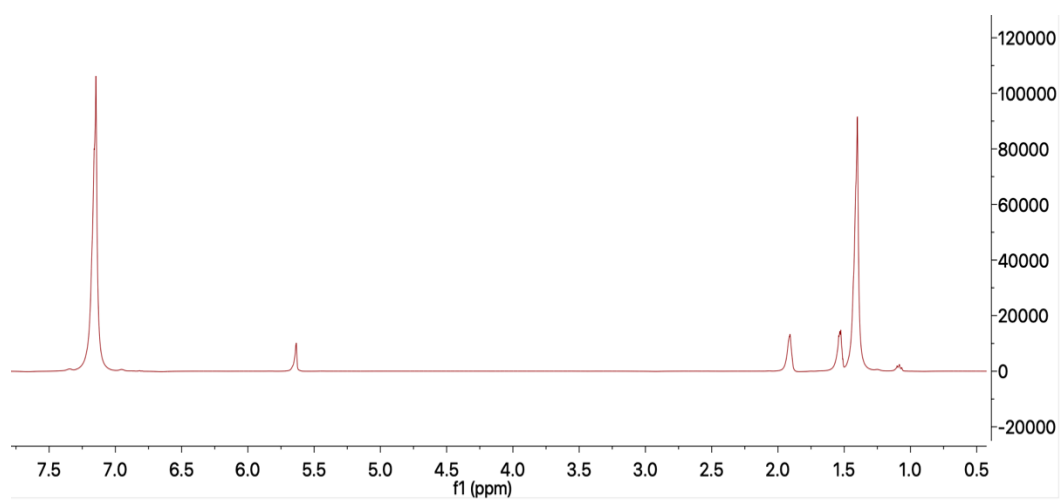


Figure A5.20 Table 3.3 Entry 7 (Spiked With 50% Benzene) ¹H NMR (400 MHz, Neat Reaction) of Crude Reaction, Yield Calculated with Hexamethylbenzene as an Internal Standard

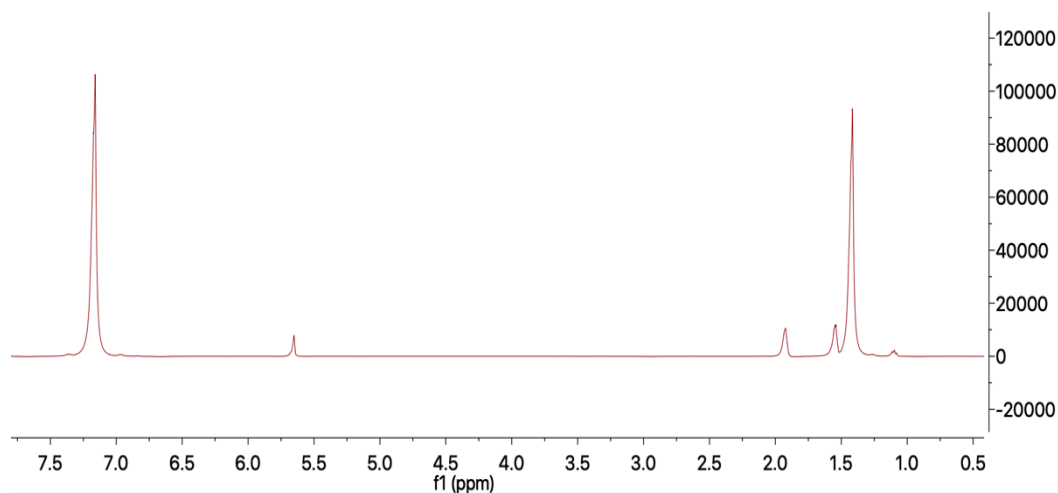


Figure A5.21 Table 3.3 Entry 8 (Spiked With 50% Benzene) ¹H NMR (400 MHz, Neat Reaction) of Crude Reaction, Yield Calculated with Hexamethylbenzene as an Internal Standard

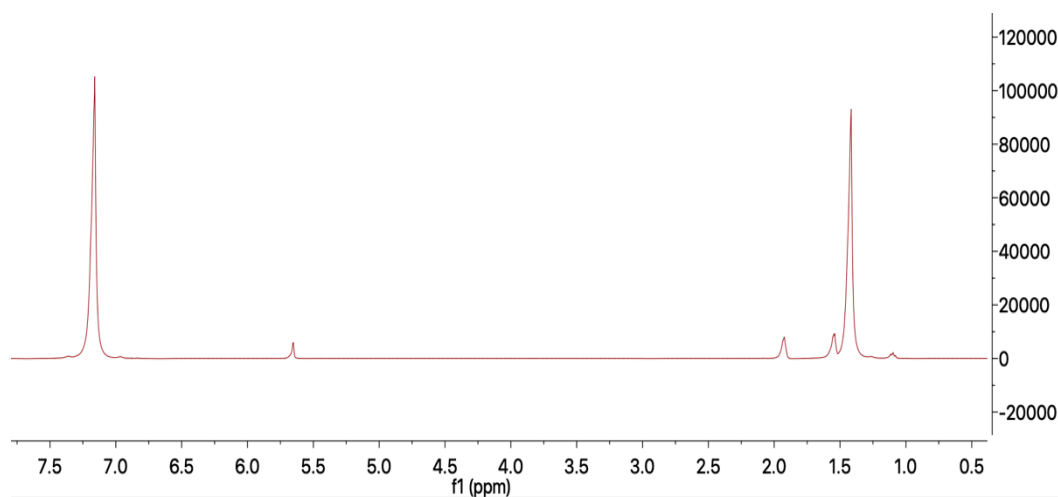


Figure A5.22 Table 3.3 Entry 9 (Spiked With 50% Benzene) ¹H NMR (400 MHz, Neat Reaction) of Crude Reaction, Yield Calculated with Hexamethylbenzene as an Internal Standard

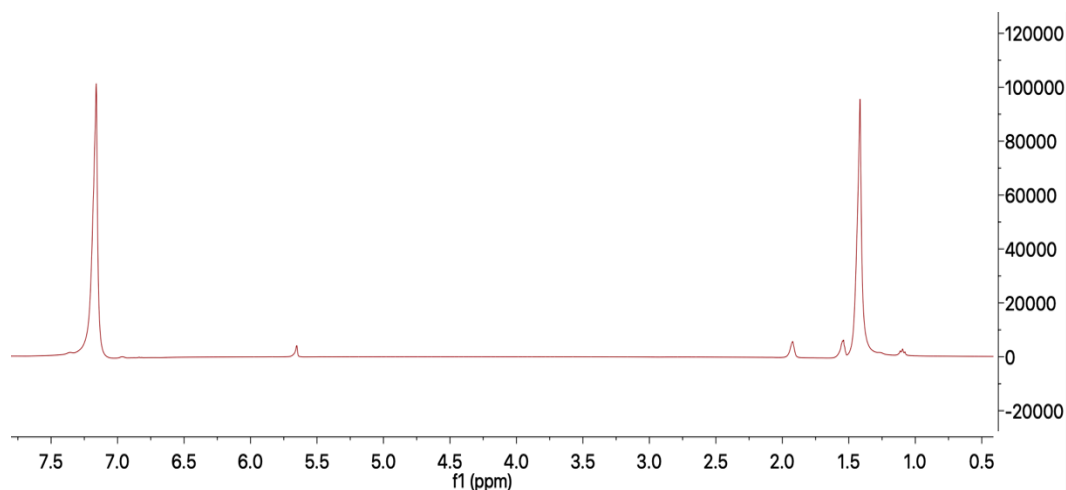


Figure A5.23 Table 3.3 Entry 10 (Spiked With 50% Benzene) ¹H NMR (400 MHz, Neat Reaction) of Crude Reaction, Yield Calculated with Hexamethylbenzene as an Internal Standard

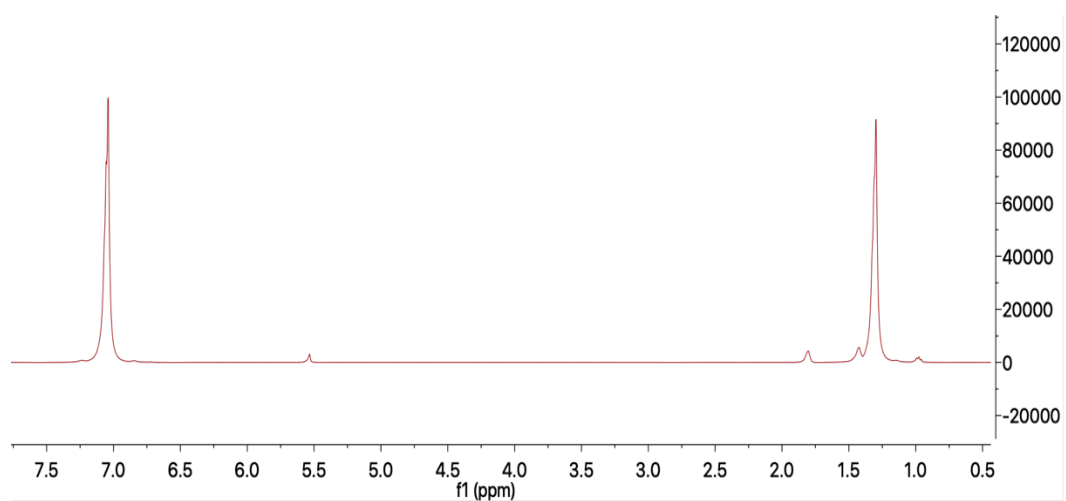


Figure A5.24 Table 3.3 Entry 11 (Spiked With 50% Benzene) ¹H NMR (400 MHz, Neat Reaction) of Crude Reaction, Yield Calculated with Hexamethylbenzene as an Internal Standard

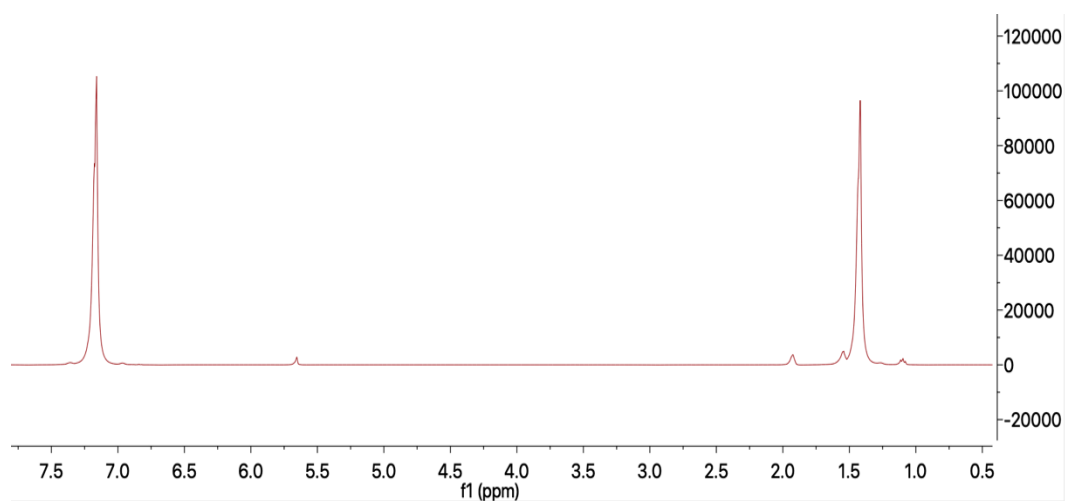


Figure A5.25 Table 3.3 Entry 12 (Spiked With 50% Benzene) ¹H NMR (400 MHz, Neat Reaction) of Crude Reaction, Yield Calculated with Hexamethylbenzene as an Internal Standard

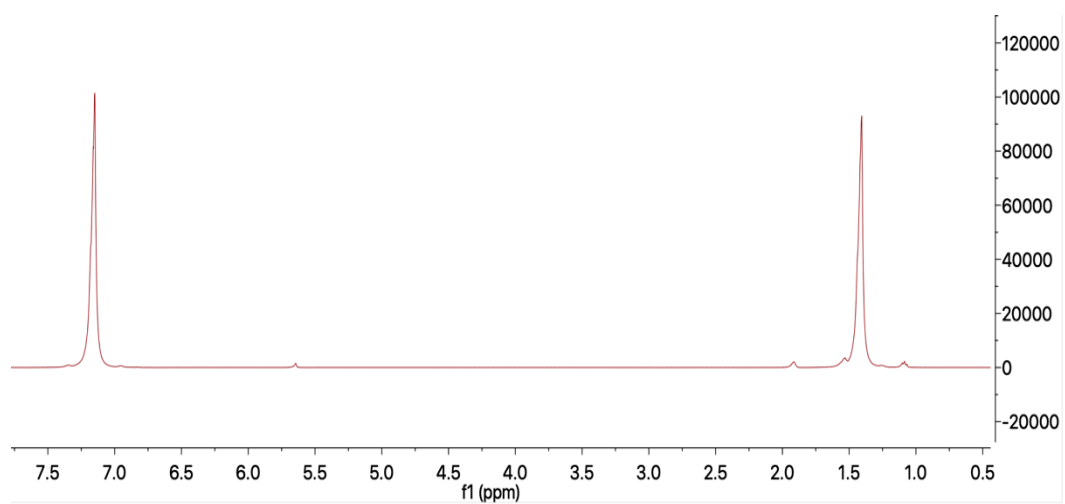


Figure A5.26 Table 3.3 Entry 13 (Spiked With 50% Benzene) ¹H NMR (400 MHz, Neat Reaction) of Crude Reaction, Yield Calculated with Hexamethylbenzene as an Internal Standard

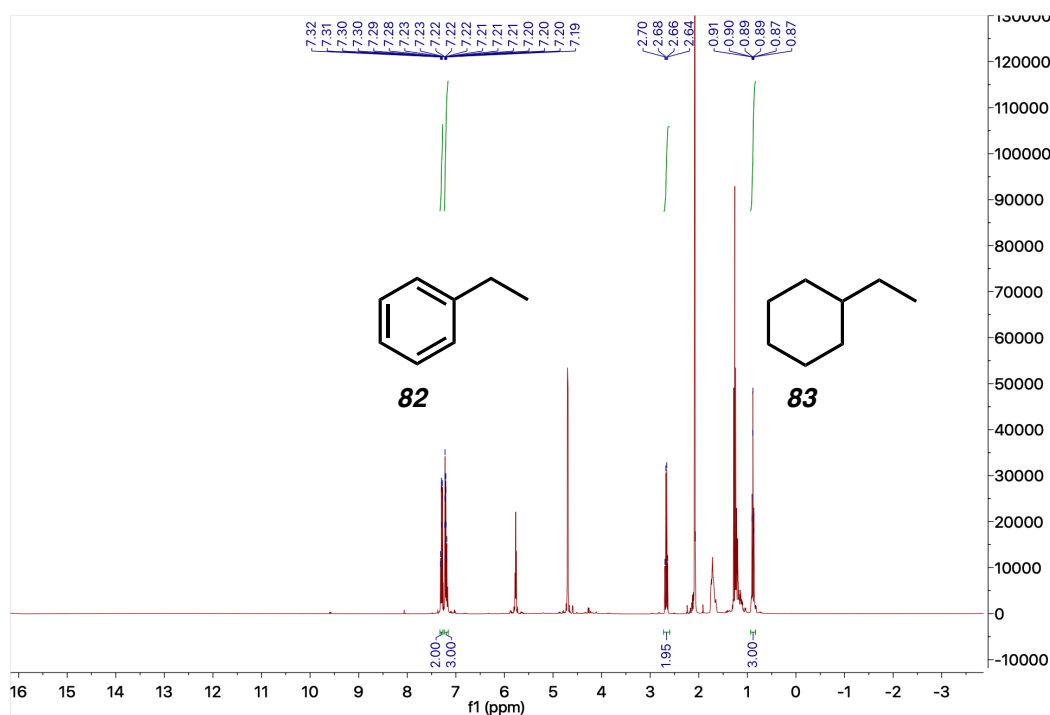


Figure A5.27 Table 3.4 Entry 3 ¹H NMR (400 MHz, Neat Reaction) of Crude Reaction Showing Full Conversion to Ethylbenzene (**82**) and Ethylcyclohexane (**83**), Yield Calculated with *Cis*-1,4-Diacetoxy-2-Butene as an Internal Standard – 97% Purity.

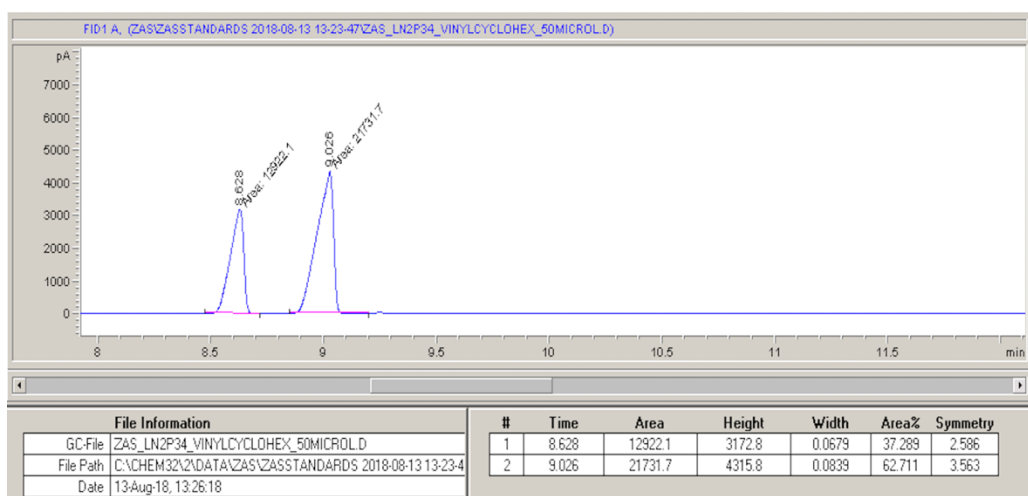


Figure A5.28 GC Spectra of **81** Crude Reaction: **83** @8.63 and **82**@9.03 Using ZAS2 Method in Table A5.2

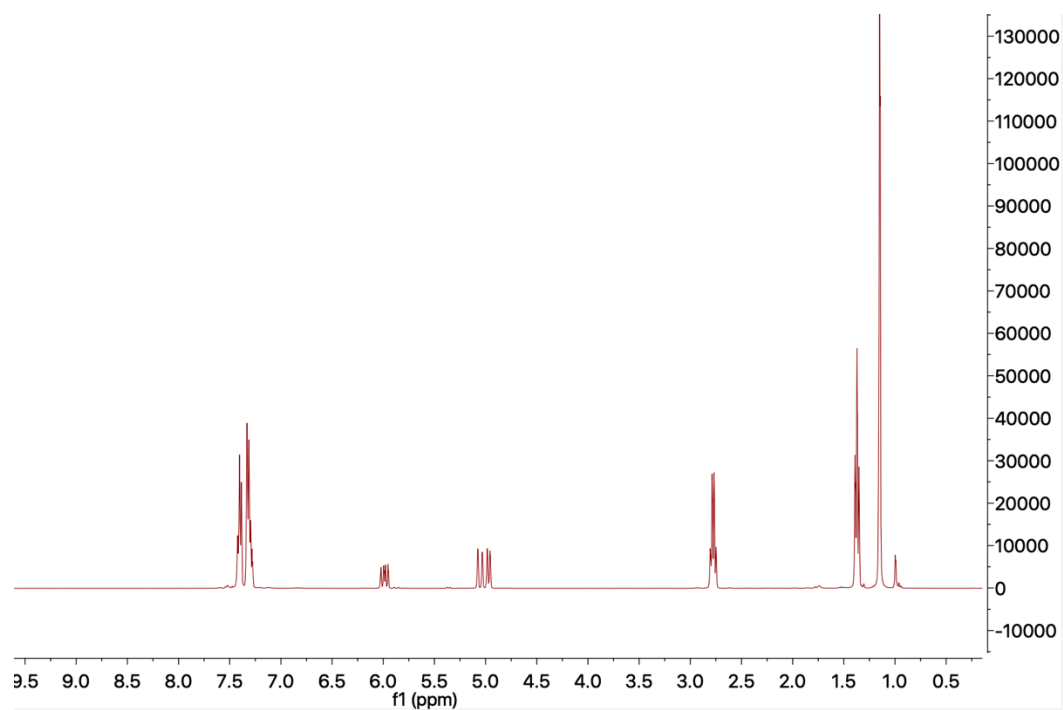


Figure A5.29 Scheme 3.7 ^1H NMR (400 MHz, Neat Reaction) of Crude Reaction Showing No Conversion

COMPREHENSIVE BIBLIOGRAPHY

1. Bischler, A.; Napieralski, B., *Berichte der deutschen chemischen Gesellschaft* **1893**, 26 (2), 1903-1908.
2. Pictet, A.; Spengler, T., *Berichte der deutschen chemischen Gesellschaft* **1911**, 44 (3), 2030-2036.
3. Franzen, H.; Kempf, H., *Berichte der deutschen chemischen Gesellschaft* **1917**, 50 (1), 101-104.
4. Anderson, A. G.; Anderson, R. G., *Journal of the American Chemical Society* **1955**, 77 (24), 6610-6611.
5. E.W. Schoeffel, D. M. B. Naphthalene. August 28, 1956.
6. Stevens Donna, G. H. H., Marshall B. Pearlman Phenols From Aromatic Sulfonic, Sulfamic, and Sulfone Compounds. April 22, 1958.
7. Black, J. W.; Crowther, A. F.; Shanks, R. G.; Smith, L. H.; Dornhorst, A. C., *The Lancet* **1964**, 283 (7342), 1080-1081.
8. Eisch, J. J. In *Adv. Heterocycl. Chem.*, Katritzky, A. R., Boulton, A. J., Eds. Academic Press: 1967; Vol. 7, pp 1-37.
9. Cantrell, T. S.; Shechter, H., *The Journal of Organic Chemistry* **1968**, 33 (1), 114-118.
10. Kaminsky, D.; Meltzer, R. I., *J. Med. Chem.* **1968**, 11 (1), 160-163.
11. Buechi, G.; Wuest, H., *The Journal of Organic Chemistry* **1971**, 36 (4), 609-610.
12. Somersall, A. C.; Guillet, J. E., *Macromolecules* **1972**, 5 (4), 410-415.

13. Kress, T. J.; Costantino, S. M., *J. Heterocycl. Chem.* **1973**, 10 (3), 409-410.
14. Moulton, C. J.; Shaw, B. L., *J. Chem. Soc., Dalton Trans.* **1976**, (11), 1020-1024.
15. Carey, F. A.; Sundberg, R. J. In *Advanced Organic Chemistry: Part A: Structure and Mechanisms*, Carey, F. A., Sundberg, R. J., Eds. Springer US: Boston, MA, 1977; pp 325-360.
16. Crabtree, R. H.; Mihelcic, J. M.; Quirk, J. M., *Journal of the American Chemical Society* **1979**, 101 (26), 7738-7740.
17. Laguerre, M.; Felix, G.; Dunogues, J.; Calas, R., *The Journal of Organic Chemistry* **1979**, 44 (24), 4275-4278.
18. Baudry, D.; Ephritikhine, M.; Felkin, H., *J. Chem. Soc., Chem. Commun.* **1980**, (24), 1243-1244.
19. Crabtree, R. H.; Demou, P. C.; Eden, D.; Mihelcic, J. M.; Parnell, C. A.; Quirk, J. M.; Morris, G. E., *Journal of the American Chemical Society* **1982**, 104 (25), 6994-7001.
20. Crabtree, R. H.; Mellea, M. F.; Mihelcic, J. M.; Quirk, J. M., *Journal of the American Chemical Society* **1982**, 104 (1), 107-113.
21. Baudry, D.; Ephritikhine, M.; Felkin, H.; Holmes-Smith, R., *J. Chem. Soc., Chem. Commun.* **1983**, (14), 788-789.
22. Shiraiwa, M.; Sakamoto, T.; Yamanaka, H., *Chem. Pharm. Bull. (Tokyo)* **1983**, 31 (7), 2275-2280.

23. Wong, D. T.; Robertson, D. W.; Bymaster, F. P.; Krushinski, J. K.; Reid, L. R., *Life Sci.* **1988**, 43 (24), 2049-2057.
24. Przybilla, K. J.; Vögtle, F., *Chem. Ber.* **1989**, 122 (2), 347-355.
25. Brown, C. E.; Ishikawa, Y.; Hackett, P. A.; Rayner, D. M., *Journal of the American Chemical Society* **1990**, 112 (7), 2530-2536.
26. Fan, Z.; Nakayama, K.; Sawanobori, T.; Hiraoka, M., *Pflügers Archiv* **1992**, 421 (5), 409-415.
27. W. M. Castor, D. H. J., *Ullmann's Encyclopedia of Industrial Chemistry*. 5th ed.; Wiley-VCH: Weinheim, 1994; p 332.
28. Gupta, M.; Hagen, C.; Flesher, R. J.; Kaska, W. C.; Jensen, C. M., *Chem. Commun.* **1996**, (17), 2083-2084.
29. Hall, C.; Perutz, R. N., *Chemical Reviews* **1996**, 96 (8), 3125-3146.
30. Nakayama, J. In *Comprehensive Heterocyclic Chemistry II*, Katritzky, A. R., Rees, C. W., Scriven, E. F. V., Eds. Pergamon: Oxford, 1996; pp 607-677.
31. Tyman, J. H. P. In *Studies in Organic Chemistry*, Elsevier: New York, 1996; Vol. 52, pp 558-661.
32. Gupta, M.; C. Kaska, W.; M. Jensen, C., *Chem. Commun.* **1997**, (5), 461-462.
33. Gupta, M.; Hagen, C.; Kaska, W. C.; Cramer, R. E.; Jensen, C. M., *Journal of the American Chemical Society* **1997**, 119 (4), 840-841.

34. Sun, X.-Z.; Grills, D. C.; Nikiforov, S. M.; Poliakoff, M.; George, M. W., *Journal of the American Chemical Society* **1997**, 119 (32), 7521-7525.
35. Foley, M.; Tilley, L., *Pharmacol. Ther.* **1998**, 79 (1), 55-87.
36. Liu, F.; S. Goldman, A., *Chem. Commun.* **1999**, (7), 655-656.
37. M. Jensen, C., *Chem. Commun.* **1999**, (24), 2443-2449.
38. Kanzelberger, M.; Singh, B.; Czerw, M.; Krogh-Jespersen, K.; Goldman, A. S., *Journal of the American Chemical Society* **2000**, 122 (44), 11017-11018.
39. Haenel, M. W.; Oevers, S.; Angermund, K.; Kaska, W. C.; Fan, H.-J.; Hall, M. B., *Angewandte Chemie International Edition* **2001**, 40 (19), 3596-3600.
40. Stork, G.; Niu, D.; Fujimoto, A.; Koft, E. R.; Balkovec, J. M.; Tata, J. R.; Dake, G. R., *Journal of the American Chemical Society* **2001**, 123 (14), 3239-3242.
41. Watson, M. D.; Fechtenkötter, A.; Müllen, K., *Chemical Reviews* **2001**, 101 (5), 1267-1300.
42. Bangcuvo, C. G.; Rampey-Vaughn, M. E.; Quan, L. T.; Angel, S. M.; Smith, M. D.; Bunz, U. H. F., *Macromolecules* **2002**, 35 (5), 1563-1568.
43. Chenier, P. J., *Survey of Industrial Chemistry*. 3 ed.; Springer US: New York, 2002; p XV, 515.
44. Klapars, A.; Huang, X.; Buchwald, S. L., *Journal of the American Chemical Society* **2002**, 124 (25), 7421-7428.

45. Bymaster, F. P.; Beedle, E. E.; Findlay, J.; Gallagher, P. T.; Krushinski, J. H.; Mitchell, S.; Robertson, D. W.; Thompson, D. C.; Wallace, L.; Wong, D. T., *Bioorg. Med. Chem. Lett.* **2003**, 13 (24), 4477-4480.
46. de Koning, C. B.; Rousseau, A. L.; van Otterlo, W. A. L., *Tetrahedron* **2003**, 59 (1), 7-36.
47. Denmark, S. E.; Fu, J., *Chemical Reviews* **2003**, 103 (8), 2763-2794.
48. Hayashi, T.; Yamasaki, K., *Chemical Reviews* **2003**, 103 (8), 2829-2844.
49. Luo, Y.-R., *Handbook of Bond Dissociation Energies in Organic Compounds*. CRC Press: Boca Raton, 2003.
50. Renkema, K. B.; Kissin, Y. V.; Goldman, A. S., *Journal of the American Chemical Society* **2003**, 125 (26), 7770-7771.
51. Zhang, X.; Fried, A.; Knapp, S.; Goldman, A. S., *Chem. Commun.* **2003**, (16), 2060-2061.
52. Göttker-Schnetmann, I.; Brookhart, M., *Journal of the American Chemical Society* **2004**, 126 (30), 9330-9338.
53. Göttker-Schnetmann, I.; White, P.; Brookhart, M., *Journal of the American Chemical Society* **2004**, 126 (6), 1804-1811.
54. Göttker-Schnetmann, I.; White, P. S.; Brookhart, M., *Organometallics* **2004**, 23 (8), 1766-1776.
55. Morales-Morales, D.; Redón, R. o.; Yung, C.; Jensen, C. M., *Inorg. Chim. Acta* **2004**, 357 (10), 2953-2956.
56. Omae, I., *Coord. Chem. Rev.* **2004**, 248 (11), 995-1023.

57. Ozerov, O. V.; Guo, C.; Papkov, V. A.; Foxman, B. M., *Journal of the American Chemical Society* **2004**, 126 (15), 4792-4793.
58. Zhu, K.; Achord, P. D.; Zhang, X.; Krogh-Jespersen, K.; Goldman, A. S., *Journal of the American Chemical Society* **2004**, 126 (40), 13044-13053.
59. Fraser, H. L.; Floyd, M. B.; Barrios Sosa, A. C. In *Prog. Heterocycl. Chem.*, Gribble, G. W., Joule, J. A., Eds. Elsevier: 2005; Vol. 17, pp 261-303.
60. Kim, J. I.; Shin, I.-S.; Kim, H.; Lee, J.-K., *Journal of the American Chemical Society* **2005**, 127 (6), 1614-1615.
61. Rossiter, S.; Péron, J.-M.; Whitfield, P. J.; Jones, K., *Bioorg. Med. Chem. Lett.* **2005**, 15 (21), 4806-4808.
62. Zhan, Z.-P.; Yang, R.-F.; Lang, K., *Tetrahedron Letters* **2005**, 46 (22), 3859-3862.
63. Bentley, K. W., *Nat. Prod. Rep.* **2006**, 23 (3), 444-463.
64. Kuklin, S. A.; Sheloumov, A. M.; Dolgushin, F. M.; Ezernitskaya, M. G.; Peregudov, A. S.; Petrovskii, P. V.; Koridze, A. A., *Organometallics* **2006**, 25 (22), 5466-5476.
65. Ranu, B. C.; Jana, R., *Eur. J. Org. Chem.* **2006**, 2006 (16), 3767-3770.
66. Anthony, J. E., *Angewandte Chemie International Edition* **2008**, 47 (3), 452-483.
67. Binder, J. B.; Raines, R. T., *Curr. Opin. Chem. Biol.* **2008**, 12 (6), 767-773.

68. Humljan, J.; Kotnik, M.; Contreras-Martel, C.; Blanot, D.; Urleb, U.; Dessen, A.; Šolmajer, T.; Gobec, S., *J. Med. Chem.* **2008**, 51 (23), 7486-7494.
69. Krohn, K.; Kouam, S. F.; Cludius-Brandt, S.; Draeger, S.; Schulz, B., *Eur. J. Org. Chem.* **2008**, 2008 (21), 3615-3618.
70. Lowell, A. N.; Fennie, M. W.; Kozlowski, M. C., *The Journal of Organic Chemistry* **2008**, 73 (5), 1911-1918.
71. Romero, P. E.; Whited, M. T.; Grubbs, R. H., *Organometallics* **2008**, 27 (14), 3422-3429.
72. Azerraf, C.; Gelman, D., *Organometallics* **2009**, 28 (22), 6578-6584.
73. Huang, Z.; Brookhart, M.; Goldman, A. S.; Kundu, S.; Ray, A.; Scott, S. L.; Vicente, B. C., *Adv. Synth. Catal.* **2009**, 351 (1-2), 188-206.
74. Jacobsen, H.; Correa, A.; Poater, A.; Costabile, C.; Cavallo, L., *Coord. Chem. Rev.* **2009**, 253 (5), 687-703.
75. Kundu, S.; Choliy, Y.; Zhuo, G.; Ahuja, R.; Emge, T. J.; Warmuth, R.; Brookhart, M.; Krogh-Jespersen, K.; Goldman, A. S., *Organometallics* **2009**, 28 (18), 5432-5444.
76. Ahuja, R.; Punji, B.; Findlater, M.; Supplee, C.; Schinski, W.; Brookhart, M.; Goldman, A. S., *Nat. Chem.* **2010**, 3, 167.
77. Brunetti, F. G.; Gong, X.; Tong, M.; Heeger, A. J.; Wudl, F., *Angewandte Chemie International Edition* **2010**, 49 (3), 532-536.
78. Crabtree, R. H., *Chemical Reviews* **2010**, 110 (2), 575-575.

79. Edwards, H. J.; Hargrave, J. D.; Penrose, S. D.; Frost, C. G., *Chemical Society Reviews* **2010**, 39 (6), 2093-2105.
80. Hebden, T. J.; Goldberg, K. I.; Heinekey, D. M.; Zhang, X.; Emge, T. J.; Goldman, A. S.; Krogh-Jespersen, K., *Inorg. Chem.* **2010**, 49 (4), 1733-1742.
81. Huang, Z.; Rolfe, E.; Carson, E. C.; Brookhart, M.; Goldman, A. S.; El-Khalafy, S. H.; MacArthur, A. H. R., *Adv. Synth. Catal.* **2010**, 352 (1), 125-135.
82. Punji, B.; Emge, T. J.; Goldman, A. S., *Organometallics* **2010**, 29 (12), 2702-2709.
83. Stabile, P.; Lamonica, A.; Ribecai, A.; Castoldi, D.; Guercio, G.; Curcuruto, O., *Tetrahedron Letters* **2010**, 51 (24), 3232-3235.
84. Chien, R.-H.; Lai, C.-T.; Hong, J.-L., *The Journal of Physical Chemistry C* **2011**, 115 (13), 5958-5965.
85. Izawa, Y.; Pun, D.; Stahl, S. S., *Science* **2011**, 333 (6039), 209.
86. Pan, M.; Lin, X.-M.; Li, G.-B.; Su, C.-Y., *Coord. Chem. Rev.* **2011**, 255 (15), 1921-1936.
87. Schultz, K. M.; Goldberg, K. I.; Gusev, D. G.; Heinekey, D. M., *Organometallics* **2011**, 30 (6), 1429-1437.
88. Zhang, X.; Wang, D. Y.; Emge, T. J.; Goldman, A. S., *Inorg. Chim. Acta* **2011**, 369 (1), 253-259.
89. Abe, M.; Eto, M.; Yamaguchi, K.; Yamasaki, M.; Misaka, J.; Yoshitake, Y.; Otsuka, M.; Harano, K., *Tetrahedron* **2012**, 68 (18), 3566-3576.

90. Biswas, S.; Huang, Z.; Choliy, Y.; Wang, D. Y.; Brookhart, M.; Krogh-Jespersen, K.; Goldman, A. S., *Journal of the American Chemical Society* **2012**, 134 (32), 13276-13295.
91. Gunnoe, B. T. In *Alkane C-H Activation Activation By Single-Site Metal Catalysis*, 1 ed.; Perez, P. J., Ed. Springer Netherlands: Dordrecht, 2012; pp 1-15.
92. Lyons, T. W.; Guironnet, D.; Findlater, M.; Brookhart, M., *Journal of the American Chemical Society* **2012**, 134 (38), 15708-15711.
93. Matano, Y.; Saito, A.; Suzuki, Y.; Miyajima, T.; Akiyama, S.; Otsubo, S.; Nakamoto, E.; Aramaki, S.; Imahori, H., *Chemistry – An Asian Journal* **2012**, 7 (10), 2305-2312.
94. Michael Findlater, J. C., Alan S. Goldman, Maurice Brookhart. In *Alkane C-H Activation Activation By Single-Site Metal Catalysis*, 1 ed.; Perez, P. J., Ed. Springer Netherlands: Dordrecht, 2012; pp 113-141.
95. Nishida, J.-i.; Tsukaguchi, S.; Yamashita, Y., *Chemistry – A European Journal* **2012**, 18 (29), 8964-8970.
96. Spadaro, A.; Frotscher, M.; Hartmann, R. W., *J. Med. Chem.* **2012**, 55 (5), 2469-2473.
97. Wang, Y.; Zhang, X.; Zhao, J.; Xie, S.; Wang, C., *J. Med. Chem.* **2012**, 55 (7), 3502-3512.
98. Wood, J. D.; Jellison, J. L.; Finke, A. D.; Wang, L.; Plunkett, K. N., *Journal of the American Chemical Society* **2012**, 134 (38), 15783-15789.

99. Cui, L.; Matusaki, Y.; Tada, N.; Miura, T.; Uno, B.; Itoh, A., *Adv. Synth. Catal.* **2013**, 355 (11-12), 2203-2207.
100. Deria, P.; Von Bargen, C. D.; Olivier, J.-H.; Kumbhar, A. S.; Saven, J. G.; Therien, M. J., *Journal of the American Chemical Society* **2013**, 135 (43), 16220-16234.
101. Dobereiner, G. E.; Yuan, J.; Schrock, R. R.; Goldman, A. S.; Hackenberg, J. D., *Journal of the American Chemical Society* **2013**, 135 (34), 12572-12575.
102. Kundu, S.; Lyons, T. W.; Brookhart, M., *ACS Catalysis* **2013**, 3 (8), 1768-1773.
103. Liu, X.; Braunstein, P., *Inorg. Chem.* **2013**, 52 (13), 7367-7379.
104. Musa, S.; Ackermann, L.; Gelman, D., *Adv. Synth. Catal.* **2013**, 355 (14-15), 3077-3080.
105. Nawara-Hultsch, A. J.; Hackenberg, J. D.; Punji, B.; Supplee, C.; Emge, T. J.; Bailey, B. C.; Schrock, R. R.; Brookhart, M.; Goldman, A. S., *ACS Catalysis* **2013**, 3 (11), 2505-2514.
106. Pho, T. V.; Toma, F. M.; Chabinyk, M. L.; Wudl, F., *Angewandte Chemie International Edition* **2013**, 52 (5), 1446-1451.
107. Romm, D. G. a. R. In *Organometallic Pincer Chemistry*, Gerard Van Koten, D. M., Ed. Springer-Verlag Berlin Heidelberg: Heidelberg, 2013; pp 289-317.
108. Shi, Y.; Suguri, T.; Dohi, C.; Yamada, H.; Kojima, S.; Yamamoto, Y., *Chemistry – A European Journal* **2013**, 19 (32), 10672-10689.

109. Zhang, H.-P.; Li, H.-Y.; Xiao, H.-F., *Journal of Chemical Research* **2013**, 37 (9), 556-558.
110. Bézier, D.; Brookhart, M., *ACS Catalysis* **2014**, 4 (10), 3411-3420.
111. Brayton, D. F.; Beaumont, P. R.; Fukushima, E. Y.; Sartain, H. T.; Morales-Morales, D.; Jensen, C. M., *Organometallics* **2014**, 33 (19), 5198-5202.
112. Dang, J.-S.; Wang, W.-W.; Zhao, X.; Nagase, S., *Org. Lett.* **2014**, 16 (1), 170-173.
113. Despiaud, C. F.; Dominey, A. P.; Harrowven, D. C.; Linclau, B., *Eur. J. Org. Chem.* **2014**, 2014 (20), 4335-4341.
114. El-Sheshtawy, H. S.; Abou Baker, A. M., *J. Mol. Struct.* **2014**, 1067, 225-232.
115. Fancelli, D.; Abate, A.; Amici, R.; Bernardi, P.; Ballarini, M.; Cappa, A.; Carenzi, G.; Colombo, A.; Contursi, C.; Di Lisa, F.; Dondio, G.; Gagliardi, S.; Milanesi, E.; Minucci, S.; Pain, G.; Pelicci, P. G.; Saccani, A.; Storto, M.; Thaler, F.; Varasi, M.; Villa, M.; Plyte, S., *J. Med. Chem.* **2014**, 57 (12), 5333-5347.
116. Jia, X.; Zhang, L.; Qin, C.; Leng, X.; Huang, Z., *Chem. Commun.* **2014**, 50 (75), 11056-11059.
117. Liu, X.; Jiang, L.; Li, J.; Wang, L.; Yu, Y.; Zhou, Q.; Lv, X.; Gong, W.; Lu, Y.; Wang, J., *Journal of the American Chemical Society* **2014**, 136 (38), 13094-13097.

118. Ouros, A.; Oberson de Souza, M.; Pastore, H., *Journal of the Brazilian Chemical Society* **2014**, 25.
119. Schmidt, R.; Griesbaum, K.; Behr, A.; Biedenkapp, D.; Voges, H.-W.; Garbe, D.; Paetz, C.; Collin, G.; Mayer, D.; Höke, H., *Ullmann's Encyclopedia of Industrial Chemistry* **2014**, 1-74.
120. Schulze, M., *Chem. Ing. Tech.* **2014**, 86 (8), 1304-1304.
121. Yao, W.; Zhang, Y.; Jia, X.; Huang, Z., *Angewandte Chemie International Edition* **2014**, 53 (5), 1390-1394.
122. Zhang, X.; Xie, T.; Cui, M.; Yang, L.; Sun, X.; Jiang, J.; Zhang, G., *ACS Appl. Mater. Interfaces* **2014**, 6 (4), 2279-2284.
123. Akshai Kumar, A. S. G. In *The Privileged Pincer-Metal Platform: Coordination Chemistry & Applications*, Gerard Van Koten, R. A. G., Ed. Springer, Cham: Cham, 2015; Vol. 54, pp 307-334.
124. Banothu, J.; Basavoju, S.; Bavantula, R., *J. Heterocycl. Chem.* **2015**, 52 (3), 853-860.
125. Chang, J.; Song, X.; Huang, W.; Zhu, D.; Wang, M., *Chem. Commun.* **2015**, 51 (84), 15362-15365.
126. DeBono, A.; Capuano, B.; Scammells, P. J., *J. Med. Chem.* **2015**, 58 (15), 5699-5727.
127. Ding, L.; Yang, C.; Su, Z.; Pei, J., *Science China Chemistry* **2015**, 58 (2), 364-369.
128. Girard, S. A.; Huang, H.; Zhou, F.; Deng, G.-J.; Li, C.-J., *Organic Chemistry Frontiers* **2015**, 2 (3), 279-287.

129. Lyons, T. W.; Bézier, D.; Brookhart, M., *Organometallics* **2015**, 34 (16), 4058-4062.
130. Ponra, S.; Vitale, M.; Michelet, V.; Ratovelomanana-Vidal, V., *Arkivoc* **2015**, 2016.
131. Zhang, Z.-H.; Zhang, H.-J.; Deng, A.-J.; Wang, B.; Li, Z.-H.; Liu, Y.; Wu, L.-Q.; Wang, W.-J.; Qin, H.-L., *J. Med. Chem.* **2015**, 58 (18), 7557-7571.
132. Costa, E. V.; Pinheiro, M. L. B.; Maia, B. H. L. N. S.; Marques, F. A.; Ruiz, A. L. T. G.; Marchetti, G. M.; Carvalho, J. E. d.; Soares, M. B. P.; Costa, C. O. S.; Galvão, A. F. C.; Lopes, N. P.; Koolen, H. H. F.; Bezerra, D. P.; Barison, A., *J. Nat. Prod.* **2016**, 79 (6), 1524-1531.
133. Ke, Z.; Tsui, G. C.; Peng, X.-S.; Yeung, Y.-Y. In *Prog. Heterocycl. Chem.*, Gribble, G. W., Joule, J. A., Eds. Elsevier: 2016; Vol. 28, pp 219-274.
134. Kwan, E. H.; Kawai, Y. J.; Kamakura, S.; Yamashita, M., *Dalton Trans.* **2016**, 45 (40), 15931-15941.
135. Li, Y.; Clevenger, R. G.; Jin, L.; Kilway, K. V.; Peng, Z., *The Journal of Physical Chemistry C* **2016**, 120 (2), 841-852.
136. Liu, J.; Zheng, H.-X.; Yao, C.-Z.; Sun, B.-F.; Kang, Y.-B., *Journal of the American Chemical Society* **2016**, 138 (10), 3294-3297.
137. Rossi, R.; Lessi, M.; Manzini, C.; Marianetti, G.; Bellina, F., *Synthesis* **2016**, 48 (22), 3821-3862.

138. Yuan, B.; Zhuang, J.; Kirmess, K. M.; Bridgmohan, C. N.; Whalley, A. C.; Wang, L.; Plunkett, K. N., *The Journal of Organic Chemistry* **2016**, 81 (18), 8312-8318.
139. Ando, H.; Kusumoto, S.; Wu, W.; Nozaki, K., *Organometallics* **2017**, 36 (12), 2317-2322.
140. Enoki, T.; Matsuo, K.; Ohshita, J.; Ooyama, Y., *Phys. Chem. Chem. Phys.* **2017**, 19 (5), 3565-3574.
141. Jana, A.; Misztal, K.; Źak, A.; Grela, K., *The Journal of Organic Chemistry* **2017**, 82 (8), 4226-4234.
142. Jayaram, V.; Sridhar, T.; Sharma, G. V. M.; Berrée, F.; Carboni, B., *The Journal of Organic Chemistry* **2017**, 82 (3), 1803-1811.
143. Kumar, A.; Bhatti, T. M.; Goldman, A. S., *Chemical Reviews* **2017**, 117 (19), 12357-12384.
144. Vardanyan, R. In *Piperidine-Based Drug Discovery*, Vardanyan, R., Ed. Elsevier: 2017; pp 299-332.
145. Wen, L.-R.; Dou, Q.; Wang, Y.-C.; Zhang, J.-W.; Guo, W.-S.; Li, M., *The Journal of Organic Chemistry* **2017**, 82 (3), 1428-1436.
146. Bizzarri, C.; Spuling, E.; Knoll, D. M.; Volz, D.; Bräse, S., *Coord. Chem. Rev.* **2018**, 373, 49-82.
147. Jayaram, V.; Sridhar, T.; Sharma, G. V. M.; Berrée, F.; Carboni, B., *The Journal of Organic Chemistry* **2018**, 83 (2), 843-853.
148. Kidonakis, M.; Mullaj, A.; Stratakis, M., *The Journal of Organic Chemistry* **2018**, 83 (24), 15553-15557.

149. Yavari, I.; Khajeh-Khezri, A., *Synthesis* **2018**, 50 (20), 3947-3973.
150. Balewski, Ł.; Sączewski, F.; Gdaniec, M.; Kornicka, A.; Cicha, K.; Jalińska, A., *Molecules (Basel, Switzerland)* **2019**, 24 (22), 4070.
151. He, X.; Zheng, Y.-W.; Lei, T.; Liu, W.-Q.; Chen, B.; Feng, K.; Tung, C.-H.; Wu, L.-Z., *Catalysis Science & Technology* **2019**, 9 (13), 3337-3341.
152. Mahato, S.; Mukherjee, A.; Santra, S.; Zyryanov, G. V.; Majee, A., *Org. Biomol. Chem.* **2019**, 17 (34), 7907-7917.
153. Matsuura, K.; Nishida, J.-i.; Ito, T.; Yokota, R.; Kitamura, C.; Kawase, T., *Tetrahedron* **2019**, 75 (2), 278-285.
154. Pahlavan, F.; Hosseinneshad, S.; Samieadel, A.; Hung, A.; Fini, E., *Industrial & Engineering Chemistry Research* **2019**, 58 (27), 11939-11953.
155. Varejão, J. O. S.; Varejão, E. V. V.; Fernandes, S. A., *Eur. J. Org. Chem.* **2019**, 2019 (27), 4273-4310.
156. Cortegiani, A.; Ingoglia, G.; Ippolito, M.; Giarratano, A.; Einav, S., *J. Crit. Care* **2020**.
157. Holshue, M. L.; DeBolt, C.; Lindquist, S.; Lofy, K. H.; Wiesman, J.; Bruce, H.; Spitters, C.; Ericson, K.; Wilkerson, S.; Tural, A.; Diaz, G.; Cohn, A.; Fox, L.; Patel, A.; Gerber, S. I.; Kim, L.; Tong, S.; Lu, X.; Lindstrom, S.; Pallansch, M. A.; Weldon, W. C.; Biggs, H. M.; Uyeki, T. M.; Pillai, S. K., *N. Engl. J. Med.* **2020**, 382 (10), 929-936.
158. Wang, M.; Cao, R.; Zhang, L.; Yang, X.; Liu, J.; Xu, M.; Shi, Z.; Hu, Z.; Zhong, W.; Xiao, G., *Cell Res.* **2020**, 30 (3), 269-271.

ABOUT THE AUTHOR

Zainab Ahmed Al-Saihati was born in Saudi Arabia on August 24th, 1989 to Huda and Ahmed Al-Saihati. She grew up in a small city called Saihat in the Eastern Province. Since a young age, she was always passionate and curious to understand the phenomena unfolding in the world at large. At this time, women in the Middle East do not have the same liberties as men. As a Saudi woman, Zainab has been inspired to defy the limiting beliefs and societal norms in regards to being a Middle Eastern woman. Fortunately, Saudi Aramco, a world-renowned chemical and energy company, opened an elite international scholarship program for aspiring young Saudi citizens including women for the first time a year before Zainab's high school graduation.

At the age of 18, Zainab was awarded a scholarship from Saudi Aramco and moved abroad on her own to attend the University of Texas at Austin. During her undergraduate studies, Zainab became interested in research and participated in several research projects. She joined Professor Katherine Willet's lab and investigated the design and synthesis of silver nanocubes, including the characterization of their shape by Scanning Electron Microscope technology. While visiting her family in Saudi Arabia during the summer, she worked as a summer intern researcher at Saudi Aramco, conducting research to find separation methods of contaminants in diesel fuels. Additionally, she studied the effect of aromatics contamination on its properties.

Zainab enjoys the outdoors, traveling, exploring diverse cultures, and building friendships with people from different backgrounds. She also enjoys participating in outreach programs and has taught science classes to elementary school kids. Although being thousands of miles away from her home and family, has not been easy, Zainab has found her journey navigating the USA on her own to be an empowering experience. Zainab believes this experience has enriched her personality, molding her into an independent, strongly motivated woman.

Upon completion of her BSc degree, she joined Saudi Aramco's R&D Department in 2012, and worked for three years as a fuels scientist. She led a variety of projects encompassing crude oil and refined products characterizations, fuels additives testing, and understanding structure-activity relationships. Zainab presented her work-related research at the 9th International Conference & Exhibition on Chemistry in Industry (ChemIndex) in 2013, where she met her future co-advisor for the first time, Professor Robert H. Grubbs. In 2015, Zainab was awarded another scholarship from her employer Saudi Aramco to continue her education and follow her dream to pursue a PhD. She chose to attend California Institute of Technology in Pasadena, California where she pursued doctoral studies under the supervision of Professors Robert H. Grubbs and Brian M. Stoltz. Zainab's PhD research has focused on developing relatively environmentally benign methods toward the synthesis of substituted and unsubstituted aromatics *via* dehydrogenation by single-site iridium pincer ligated complexes.

Upon completion of her doctoral research in May 2020, Zainab will be the first Saudi woman to obtain a PhD from Caltech. She will return to Saudi Arabia and continue her professional career at Saudi Aramco. She is interested in green chemistry and will continue to conduct research toward finding and developing methods toward the synthesis of important industrial building blocks.

One of Zainab's favorite quotes by Albert Einstein, who was a visiting professor at Caltech, is "education is not the learning of facts, but the training of the mind to think." With her PhD, she aspires to shape and change science in Saudi Arabia and create new fields of research. Her ultimate dream is to inspire and mentor women in Saudi Arabia and the Middle East, and encourage and aid those who are interested to join STEM fields.